A *metE* mutant of *Chlamydomonas reinhardtii* provides new perspectives on the evolution of vitamin B_{12} auxotrophy

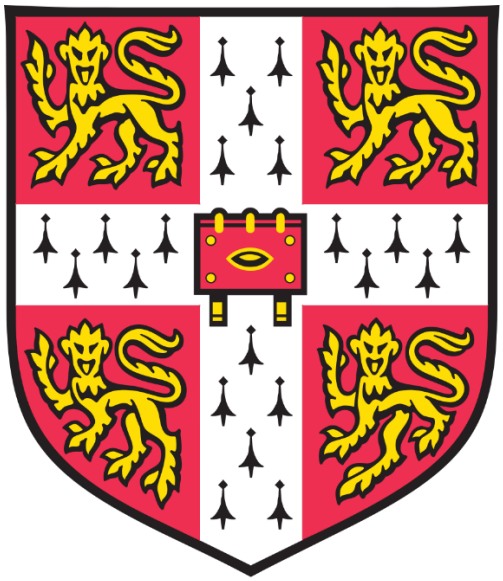

Frederick Xavier de St Pierre Bunbury

Emmanuel College

University of Cambridge

This dissertation is submitted for the Degree of Doctor of Philosophy

September 2018

Declaration

This dissertation is the result of my own work and includes nothing which is the outcome of work done in collaboration except as declared in the Preface and specified in the text.

It is not substantially the same as any that I have submitted, or, is being concurrently submitted for a degree or diploma or other qualification at the University of Cambridge or any other University or similar institution except as declared in the Preface and specified in the text. I further state that no substantial part of my dissertation has already been submitted, or, is being concurrently submitted for any such degree, diploma or other qualification at the University of Cambridge or any other University or similar institution except as declared in the Preface and specified in the text.

It does not exceed the prescribed word limit for the relevant Degree Committee.

Signed: .....

Date:.....

Acknowledgments

First of all, I must thank the sources of funding that made this research possible. The Biotechnology and Biological Sciences Research Council provided my stipend and funds to cover the cost of research consumables. Emmanuel College and the Cambridge Philosophical Society both provided grants that allowed me to attend and present at international conferences.

Professor Alison Smith has been a better supervisor than I could have hoped for. That Alison seemed to have more enthusiasm than even I myself had on some occasions for my project, while also giving me the reins to shape it as I saw fit, was very much appreciated. Alison's extensive knowledge of algal metabolism and attention to detail was also invaluable in guiding this work, and I hope that we might publish together soon! My second supervisor, Dr. Uta Paszkowski, introduced me to more sophisticated symbiotic systems that initiate in the plant rhizosphere, and helped me refocus the aims from my first-year report so that they would be more achievable.

Dr. Katherine Helliwell produced the *metE7* strain, which was the focal point of most of my research, and has maintained an interest in my findings as well as making helpful suggestions for future work. Dr. Elena Kazamia performed many coculture experiments with a similar system that informed my experiments. In my first year in the lab Dr. Vaibhav Bhardwaj was a fantastic mentor, introducing me to many of the techniques I would later go on to use countless times. Dr. Payam Mehrshahi has provided great encouragement and helped me to better understand many of my results. Similarly, I have had many interesting conversations with Dr. Maria Huete-Ortega, who provided lots of useful advice. Dr. Katrin Geisler is one of the most hard-working people I have met and has often gone out of her way to ensure that I could conduct my experiments easily and to a high standard. Sue Aspinall has also made my work much easier and safer by keeping a busy lab running smoothly. Dr. Matthew Davey taught me how to perform lipid analysis of algal samples, and it was a pleasure to co-supervise an undergraduate student with him. Both of my undergraduate students, Sam Fitzsimmons and Bradford Loh, were capable scientists who were willing to learn and enthusiastic about their projects, and whose results helped guide some of my own work. Dr. Deborah Salmon performed the amino acid and methionine cycle metabolite analysis that is presented here. I had several interesting conversations with Dr. Ottavio Croze, Dr. Francois Peaudecerf and Hannah Laeverenz Schlogelhofer relating to the mathematical modelling of algal-bacterial cocultures. Andy Sayer and Andre Holzer will continue with work most closely related to my own, and it has been very rewarding to be able to discuss our findings together. Dr. Matthew Cooper, Dr. Mark Scaife, Dr. Louisa Norman, Dr. Christian Ridley, Dr. Alex Litvinenko, Dr Johan Kudahl, Aleix Gorchs-Rovira, Iain Bower, Patrick Hickland, Marcel Llavero-Pasquina, Stefan Grossfurthner, Sam Coffin, and Dr. Gonzalo Mendoza have been great people to share a lab with and all of them have helped me along the way.

Kshitij Sabnis and Anna Gibbons did so much to make my role as Men's Captain of the Pentathlon team as easy as possible, and therefore allowed me to have a very productive final year in Cambridge both in and out of the lab. My housemate Alice Rees has gone through the same undergraduate and graduate courses as myself over the last seven years in Cambridge and it has been great to have someone to talk to who has shared so many experiences.

My brother Fabian has recently taken an increasing interest in evolutionary biology, and it has been very satisfying to have long conversations with a kindred spirit. My sisters, Madeleine and Jemima, and particularly my parents, Michael and Lotty, have been incredibly supportive, and it is still their advice that I trust more than anyone else's. Having parents that are not only unconditionally supportive, but also show a genuine interest in my work has been a real source of pride. Thinking back to over a decade ago I can now remember my father saying how interesting it was that so many animals had evolved to become dependent on vitamins. Perhaps that was the seed that set me on this journey in the first place.

Summary

Vitamin B_{12} is synthesised only by prokaryotes yet is widely required by eukaryotes as an enzyme cofactor. Roughly half of all algae require vitamin B_{12}, and the phylogenetic distribution of this trait suggests that it has evolved on multiple occasions. Previous work using artificial evolution generated a *metE* mutant of *Chlamydomonas reinhardtii* (hereafter *metE7)* that requires B_{12} for growth. Here, I use *metE7* to investigate how a newly-evolved B_{12} auxotroph might cope with B_{12} limitation and interact with B_{12}-producing bacteria.

Compared to the closely related natural B_{12} auxotroph *Lobomonas rostrata, metE7* has a higher requirement and lower binding affinity for B_{12}. B_{12} deprivation of *metE7* caused an increase in cell diameter, indicative of a decreased rate of cell division relative to growth. Other responses included an accumulation of starch and triacylglycerides at the expense of polar lipids and free fatty acids, and a decrease in photosynthetic pigments, proteins and free amino acids. This is reminiscent of nitrogen deprivation, but closer investigation revealed that B_{12} deprivation caused a substantial increase in reactive oxygen species, which preceded a rapid decline in cell viability. This might be explained by the observation that there was no induction of non-photochemical quenching, unlike under nitrogen deprivation. The metabolite S-adenosyl homocysteine, a potent inhibitor of methylation, increased substantially during B_{12} deprivation, as did the transcripts for several enzymes of one-carbon metabolism.

The rhizobial bacterium *Mesorhizobium loti* formed a commensal relationship with wild-type *C. reinhardtii*, benefiting from the alga's photosynthate. When co-cultured with *metE7* this interaction should be considered a mutualism as the alga was dependent on bacterial B_{12}. Adding B_{12} or glycerol to the coculture increased the cell density of *metE7* and *M. loti* respectively, revealing that the rate of nutrient transfer between species was the factor limiting growth. It was unsurprising therefore that when grown in triculture, the wild type soon outcompeted *metE7*, even when *M. loti* growth and B_{12} production were fuelled by added glycerol. B_{12} release was also shown to be critical for mutualism: a mutant of *E. coli* that released more B_{12} into the media was, in contrast to its parental strain, able to support *metE7*.

The mutual support of *metE7* and *M. loti* over 6 months during an artificial evolution experiment illustrates that newly-evolved B_{12} auxotrophs could survive in the presence of B_{12}-producers, but it was also demonstrated that *M. loti* could not produce sufficient B_{12} to favour the evolution of B_{12} dependence in *C. reinhardtii*. In summary, this work has provided an insight into the challenges of evolving B_{12} auxotrophy making it all the more remarkable that it is such a common trait.

Table of contents

Table of figures

List of abbreviations

BQH	Black Queen hypothesis
CFU	Colony forming units
EC_{50}	Concentration required for 50% of maximal output
EF	Ecological fitting
FAMES	Fatty acid methyl esters
FFA	Free fatty acids
FFH	Foraging to farming hypothesis
FTL1	Formate tetrahydrofolate ligase
Fv/Fm	PSII maximum efficiency
GC	Gas chromatography
Hcy	Homocysteine
HPLC	High performance liquid chromatography
Met	Methionine
METE	B_{12}-independent methionine synthase
METH	B_{12}-dependent methionine synthase
METM	S-adenosylmethionine synthetase
MS	Mass spectrometry
MTHFD	Methylenetetrahydrofolate dehydrogenase
MTHFR	Methylenetetrahydrofolate reductase
N	Nitrogen
NPQ	Non-photochemical quenching
OD	Optical density
PSII	Photosystem II
qPCR	quantitative polymerase chain reaction
ROS	Reactive oxygen species
RQH	Red Queen hypothesis
RT-qPCR	Reverse transcriptase quantitative polymerase chain reaction
SAH	S-adenosylhomocysteine
SAH1	S-adenosylhomocysteine hydrolase
SAM	S-adenosylmethionine
sd	standard deviation
SHMT2	Serine hydroxymethyltransferase 2
TAG	Triglycerides/Triacylglycerols
THF	Tetrahydrofolate
TYMS	Thymidylate synthase
WT	Wild type

Chapter 1: Introduction

1.1 The evolution of algae

The term algae may evoke images of seaweed or pond scum, but it encompasses an astoundingly diverse array of organisms. A widely agreed-upon definition is not forthcoming, but a simple and inclusive one might be that algae are a group of eukaryotes that at least at one point in their evolution were capable of photosynthesis. This definition however, would include plants while excluding what were previously called 'blue-green algae' and now termed cyanobacteria. In order to exclude plants, some definitions have specified that algae must also lack leaves, stems, and roots. Phytoplankton is a similar term to algae, but with a definition of 'photosynthetic microscopic organisms' it excludes macroalgae while including cyanobacteria. I will use the term algae to refer to eukaryotes that possess plastids but are not embryophytes (land plants).

Oxygenic photosynthesis is thought to have evolved only once in bacteria (Fischer et al., 2016), and from there been transferred to eukaryotes via endosymbiosis (McFadden, 2001). Phylogenetic studies suggest a phagotrophic protist engulfed one or more cyanobacterial cells around 900-1600 million years ago (Shih & Matzke, 2013; Yoon et al., 2004). Instead of being digested the cyanobacteria persisted within the protist cell, and perhaps as the Menage a trois hypothesis (MATH) suggests, this was with the help of a member of the *Chlamydiales* that could remodel the phagocytic membrane to produce an inclusion body protecting the cyanobacterium (Ball et al., 2013; Brodie, Ball, et al., 2017). They were able to continue to photosynthesise and divide, but with substantial gene transfer to the host nucleus the previously free-living bacterium became the wholly-dependent plastid found in eukaryotes today (Martin et al., 1998). This photosynthetic eukaryote gave rise to three divergent lineages within roughly 200 million years: the green, red, and glaucophyte algae (Dorrell & Smith, 2011). Most of algal diversity does not derive from these lineages however, instead it is due to secondary endosymbioses of these lineages by distantly related non-photosynthetic protists (Dorrell & Smith, 2011; Hong & Wilson, 2013; McFadden, 2001). Euglenids and Chlorarachniophytes arose by engulfing green algae, while most other lineages engulfed red algae (Takahashi et al., 2007; Takishita et al., 2008). There is also evidence of tertiary symbioses within the dinoflagellates as they contain chloroplasts from cryptomonads, diatoms, and haptophytes, which themselves had engulfed red algae (Imanian & Keeling, 2007; Tamura et al., 2005). Dinoflagellates are also unusual in that they possess a nuclear-encoded single subunit RuBisCO that was acquired by horizontal gene transfer from proteobacteria, and which has replaced the RuBisCO derived from the primary cyanobacterial endosymbiont (Janouskovec et al., 2010; Morse et al., 1995; Whitney et al., 1995). Comparatively, the study of another dinoflagellate, *Durinskia baltica*, and its endosymbiont, *Glenodinium foliaceum*,

used transcriptomics to find that there was no endosymbiotic gene transfer, and little functional reduction in either partner (Hehenberger et al., 2016).

Paulinella, a rather unique genus of photosynthetic eukaryotes, does not contain a normal plastid, but instead contains so-called 'chromatophores', derived from a much more recent endosymbiosis of an α cyanobacterium 90-140 million years ago (Delaye et al., 2016). The 1 Mbp chromatophore genome is five to ten times larger than most plastids (Brodie, Chan, et al., 2017; Nowack et al., 2008), which is partly a result of its relatively recent acquisition, but also likely because horizontal gene transfer from other free-living bacteria counteracts the ongoing endosymbiotic gene transfer to the nucleus (Nowack et al. 2016). Horizontal and endosymbiotic gene transfer, which are common among algae, have hindered the construction of an accurate 'tree of life' and indeed some authors have suggested 'uprooting the tree of life' perhaps replacing it with a 'ring of life' or 'web of life'. (Doolittle, 2000; Forterre, 2015; Soucy et al., 2015)

1.2 The diversity of algae

Considering the diverse evolutionary histories of algae, it should come as no surprise that they are geographically widespread and adapted to a variety of niches. *Cyanidioschyzon merolae* and *Galdieria sulphuraria* are both red algae that inhabit hot springs where temperatures can reach 56°C and pH values range from 0.05-3 (Barbier, 2005). In the laboratory *C. merolae* can resist temperatures up to 63°C by increasing expression of heat shock proteins over 1000-fold (Kobayashi et al., 2014). On the other end of the spectrum, the diatom *Fragilariopsis cylindrus* is a dominant species in the sea ice niche of polar regions, which owes some of its survival advantage to the upregulation of antifreeze proteins in response to cold stress (Bayer-Giraldi et al., 2010, 2011). Polar snow algae from Antarctica and the Arctic, such as *Chloromonas polyptera* and *Chloromonas nivalis* survive even colder temperatures by overwintering as cysts (Remias et al., 2010, 2013), although during the growing season, when the cells are photosynthetically active, the temperatures are remarkably stable around 0°C (Stibal et al. 2007).

The most visibly striking adaptation of many snow algae is the ability to change colour from green through orange to purple/red by altering the concentrations of pigments such as astaxanthin and chlorophylls over the growing season or according to their depth in the snow and hence exposure to sunlight (Stibal et al. 2007; Remias et al. 2005, 2013). These snow algal carotenoids serve a photoprotective role by dissipating absorbed light energy as heat (Bidigare et al. 1993) and have been found to significantly decrease snow surface albedo and hence increase glacier melting, which in turn provides a larger habitat for further growth, so completing a positive feedback loop (Lutz et al. 2016; Yallop et al. 2012). Another green alga naturally exposed to high light intensities is *Chlorella ohadii*, which was isolated from a biological soil crust in the Negev desert and exhibits the fastest doubling

time of any photosynthetic organism, at 1.3 hours (Ananyev et al. 2017; Treves et al. 2013). *C. ohadii* increases its photosynthetic rate with light intensity up to twice that of full sunlight without a substantial accumulation of carotenoids or energy dissipation by non-photochemical quenching (Treves et al. 2016; Ananyev et al. 2017). Some algae lack all photosynthetic pigments and survive heterotrophically, such as *Euglena longa*. *E. longa* expresses only one protein from its plastid that is not directly involved in gene expression itself (Záhonová et al. 2016), yet oddly enough, and in contrast to its close photosynthetic relative *Euglena gracilis*, plastid gene expression is essential for cell growth (Hadariová et al. 2017).

Algae also vary enormously in size from the smallest known free-living eukaryote *Ostreococcus tauri*, which at 0.8-1.3 µm is smaller than *E. coli* (Palenik et al. 2007; Marin and Birger 2014), to the macroalga *Macrocystis pyrifera*, a giant kelp which can grow at rates of 60 cm per day to lengths of 45 m (Steneck et al. 2002). Within the class to which *O. tauri* belongs there appears to be a trend towards reduced size and morphological complexity (Marin and Birger 2014), however, overall there is greater support for the idea of evolution trending towards increased size and complexity (Carroll 2001). One of the major transitions in organismal complexity is the evolution of multicellularity, a phenomenon that has occurred in algae more often than in all other eukaryotes (Niklas 2014), and relatively recently in the Volvocine algae: since the divergence of *Volvox carteri* and unicellular species such as *Chlamydomonas reinhardtii* 200 million years ago (Kirk 1999; Herron et al. 2009). Indeed, the evolution of multicellularity has happened more than once within the green lineage, since the Volvocales are not the ancestors of green macroalgae and land plants. As was noted previously, algal phenotypic diversity is to be expected from their polyphyly, but it is worth appreciating how this diversity contributes to their ubiquity.

1.3 The nutrient requirements of algae

Algae are mainly aquatic oxygenic photolithotrophs and so water and carbon, although required in the greatest quantities, rarely limit growth (Howarth 1988). Nonetheless, the low solubility and diffusivity of carbon dioxide in water and its molecular similarity to oxygen, which competes for the active site of RuBisCO, has driven the evolution of CO_2-concentrating mechanisms on multiple occasions (Badger et al., 1998; Giordano et al., 2005; Raven, 2010) After carbon, nitrogen is the next most abundant element in phytoplankton biomass (Ho et al. 2003), and is thought to limit growth in large areas of the ocean (Ryther & Dunstan, 1971; Tyrrell & Law, 1997), while phosphorus is thought to be the ultimate limiting factor (Tyrrell, 1999), particularly in fresh waters (Hecky & Kilham, 1988). Nitrate and phosphate concentrations in ocean samples show a remarkable degree of correlation at a ratio of 16:1, termed the Redfield ratio (Tyrrell, 1999). Phosphorus influx to the ocean is mainly from rivers, while the major available form of nitrogen, nitrate, is topped up via the action of nitrogen-

fixers (Tyrrell, 1999). Under low nitrate conditions nitrogen-fixers have a growth advantage and so increase the amount of fixed nitrogen in their environment (Smith, 1983), which forms a negative feedback loop maintaining the Redfield ratio. However, the optimum ratios of N:P have been estimated to vary between species and conditions from around 8 when growth is exponential to over 40 when nutrients or light limit growth and investment in resource-acquisition machinery is necessary (Klausmeier et al., 2004). Nevertheless, nitrogen fertilisation in estuarine waters was found to have a greater impact on fast-growing microalgae than macrophytes, and microalgae required a 3-fold higher nitrogen concentration per unit biomass to sustain maximal growth (Pedersen & Borum, 1996).

Nitrogen and phosphorus are not the only elements that limit phytoplankton growth, in fact in polar waters dissolved concentrations of nitrate and phosphate are high and appear underutilised (Holm-Hansen, 1985). Iron fertilisation experiments have caused reductions in dissolved nitrate and phosphate, and an increase in phytoplankton biomass and photosynthesis, indicating that iron is the factor limiting growth in many parts of the globe (Boyd et al., 2000; Martin & Fitzwater, 1988; Martin et al., 1990), including those denoted as HNLC (high nitrogen-low chlorophyll). In the tropical North Atlantic net photosynthesis was primarily nitrogen-limited, yet phosphorus and iron input from Saharan dust deposition stimulated nitrogen fixation and primary productivity indicating that nutrients are often co-limiting (Mills et al., 2004).

For many marine microalgae iron acquisition involves the binding of ferric or ferrous iron at the cell surface (Sutak et al., 2012), but the photosynthetic *Ochromonas sp.* have been shown to obtain iron by ingesting bacteria (Maranger et al., 1998). Algae can also acquire nutrients other than iron and nitrogen from bacteria, including B vitamins (Helliwell, 2017; Panzeca et al., 2006). Over 50% and 20% of algae are dependent on vitamins B_{12} and B_1 respectively (Croft et al., 2006), with even higher percentages among those contributing to harmful algal blooms (Tang et al., 2010). Large areas of the ocean are depleted of these vitamins (Panzeca et al., 2009; Sanudo-Wilhelmy et al., 2012), and dissolved B_{12} concentrations in the ocean and freshwater were found to be inversely correlated with the abundance of phytoplankton, suggestive of B_{12} uptake (Ohwada, 1973; Sañudo-Wilhelmy et al., 2006). Nutrient addition experiments have found that phytoplankton growth in the Ross Sea near Antarctica is co-limited by B_{12} and iron (Bertrand et al., 2007), and in the South Atlantic and Northeast Pacific B_{12} became limiting after nitrogen or iron addition (Browning et al., 2017; Cohen et al., 2017). It would seem therefore, that algal communities are likely to respond to their local nutrient profile in such a way as to maximise productivity, resulting in differences in nutrient limitations between species, which leads overall towards multiple nutrient colimitations of the community.

1.4 Algal responses to nutrient limitation at the cellular level

1.4.1 Storage, uptake, and recycling

Responding appropriately to nutrient limitation is essential to survival, and as such algae have evolved a variety of coping mechanisms. As *C. reinhardtii* is the most widely used alga in laboratory-based nutrient limitation studies, the examples given in this section will be restricted to this species. *C. reinhardtii* can store certain nutrients in anticipation of future limitation, for example it over-accumulates iron (Terauchi et al., 2010) but not copper (Page et al., 2009), even though that exacerbates photooxidative stress (Long & Merchant, 2008). Polyphosphate bodies or acidocalcisomes are organelles that have been found to contain high levels of phosphate, calcium, magnesium and zinc (Ruiz et al., 2001). Mutants of a polyphosphate polymerase subunit showed impaired acidocalcisome formation and were found to lose viability more quickly under nitrogen, phosphorus, or sulphur deprivation (Aksoy et al., 2014).

One of the earliest responses of *C. reinhardtii* to nutrient deprivation is an increase in the maximal rate of uptake and affinity for the limiting nutrient (Hill et al., 1996; Yildiz et al., 1994). Iron limitation leads to increases in FOX1 and FTR1 transporters (Urzica, Casero, et al., 2012), and sulphur limitation to upregulation of the plant-like H^+/SO_4^{2-} transporter SULTR2 and the animal-like Na^+/SO_4^{2-} transporters SLT1/2 (Pootakham et al., 2010). *C. reinhardtii* encodes a considerable number of nitrogen transporters: 13 putative NO_3^-/NO_2^- and 8 putative NH_4^+ transporters (Fernandez & Galvan, 2007), and under nitrogen deprivation preferentially upregulates those with fewer amino acids and hence lower nitrogen requirements, such as AMT1 (Schmollinger et al., 2014). Nutrient limitation also induces expression of periplasmic enzymes that cleave inorganic groups from organic compounds, and so make the nutrient available for uptake. Arylsulfatases, which cleave sulfate from organic compounds, are highly upregulated by sulphur limitation, (over 1000-fold at the transcript level) (González-Ballester et al., 2010; Zhang et al., 2004), while alkaline phosphatase activity was found to increase 300-fold on phosphorus deprivation (Quisel et al., 1996). Increased uptake of organic compounds containing the limiting nutrient is also thought to occur, as sulphur limitation induces expression of amino acid transporters (AOT2/4) (González-Ballester et al., 2010), and nitrogen limitation elevates transcript abundance for urea and purine transporters (Schmollinger et al., 2014).

In addition to increasing its ability to take up limiting nutrients, *C. reinhardtii* also responds to nutrient limitation by being more frugal. Under copper limitation levels of the Cu-containing apoprotein plastocyanin decrease and cytochrome c552, which can perform the same role in the plastid electron transport chain but contains Fe instead, increases (Merchant & Bogorad, 1986). One of the few transcripts that decrease under slight Fe deprivation is a chloroplast-targeted ferredoxin (FDX5) which contains a [2Fe-2S] cluster (Glaesener et al., 2013; Jacobs et al., 2009). On the other

hand, levels of an Fe-dependent plastidial superoxide dismutase (SOD) are maintained, suggesting preferential allocation of Fe. In fact under Fe limitation SOD activity overall is augmented due to a 1000-fold increase in transcripts for a plastidial Mn-dependent SOD (Page et al., 2012). During sulphur deprivation there is a decrease in transcripts for enzymes catalysing the flux from cysteine into the methionine cycle, and also for enzymes involved in the formation of the sulphur-containing cofactors thiamine and biotin (González-Ballester et al., 2010). Sulphur is also saved by reducing the sulphur content of proteins: four cell wall proteins upregulated under sulphur limitation had a cysteine + methionine content of 0.1% compared to 4-8% for the 10 most abundant cell wall proteins (González-Ballester et al., 2010; Takahashi et al., 2001). Similarly, LHCBM9, the one light harvesting complex protein of PSII with a substantially lower cysteine + methionine content than the other 8, is the only one to be upregulated under sulphur deprivation (González-Ballester et al., 2010; Nguyen et al., 2008).

1.4.2 Maintaining redox status

Responses to the deprivation of most nutrients in *C. reinhardtii* involve a downregulation of photosynthesis (Grossman, 2000; Wykoff et al., 1998). Iron limitation leads to a remodelling of photosystem I (PSI) and associated light harvesting complexes (LHCs) to optimise photosynthetic function and minimise photo-oxidative damage, without a decrease in photosystem II (PSII) (Moseley et al., 2002; Naumann et al., 2007). On the other hand, sulphur and phosphorus deprivation were shown to decrease PSII activity by 50% without affecting PSI (Wykoff et al., 1998), resulting in a reduced requirement for enzymes to detoxify superoxide produced by PSI (González-Ballester et al., 2010). A *tab2* mutant, which could not maintain PSI under nitrogen deprivation, was unable to accumulate triacylglycerides (TAGs), and upregulated photoprotective mechanisms as well as expression of enzymes required to eliminate reactive oxygen species (Gargouri et al., 2014). Maintaining the balance between NADPH and ATP generation is crucial to avoiding oxidative stress, and under nitrogen deprivation processes such as chlororespiration increase (Saroussi et al., 2016) to reduce the NADPH:ATP ratio, and power the photoprotective mechanism of non-photochemical quenching (Müller et al., 2001). Another important aspect of non-photochemical quenching is mediated via carotenoids, and although nitrogen deprivation causes chlorosis due to pigment degradation, carotenoids are preferentially maintained so as to dissipate excess absorbed light energy as heat (Philipps et al., 2012).

As well as reducing linear electron flow and so NADPH production under nutrient deprivation, *C. reinhardtii* also increases consumption of NADPH, which is still produced in excess of its requirement for cell growth, by synthesising starch and TAGs (Cakmak, Angun, Demiray, et al., 2012; Kamalanathan et al., 2016; Siaut et al., 2011). The importance of these storage molecules is emphasised by the physiology of mutants: *sta6*, a mutant incapable of producing starch, shows a

reduced rate of NADPH re-oxidation and accelerated photoinhibition under nitrogen limitation (Krishnan et al., 2015); *pgd1*, a mutant disrupted in remodelling plastid lipids into TAGs and so showing reduced TAG content on nitrogen deprivation had reduced viability unless photosynthetic electron transport was blocked (Li et al., 2012). TAG accumulation is also important for cell recovery after nutrient deprivation, and mutants such as *cht7*, compromised in the hydrolysis of TAGs, show slower and less ordered recovery from nitrogen deprivation (Tsai et al., 2017).

Of the multitude of responses to nutrient limitation, a large proportion appear to be controlled by a small number of response regulators. The copper response regulator CRR1 is a transcription factor (Kropat et al., 2005), which among other genes increases the expression of the Fe-dependent cytochrome c6 under copper limitation, and leads to the degradation of the Cu-dependent plastocyanin protein (Eriksson et al., 2004). PSR1, another transcription factor (Wykoff et al., 1999), is responsible for 65% of the changes in transcript abundances on phosphate deprivation (Moseley et al., 2006), and in a *psr1* mutant starch and TAG accumulation and the downregulation of photosynthesis were misregulated (Bajhaiya et al., 2016). Transcriptomic studies have also been used with mutants in the response to sulphur starvation (González-Ballester et al., 2010; Zhang et al., 2004). *snrk2.1* and *sac1*, a serine threonine kinase (Gonzalez-Ballester et al. 2008) and a plasma membrane sensor (Davies et al., 1996) respectively, are involved in responding to sulphur deprivation, and among other genes induce the expression of a possible transcriptional regulator ARS73a (Aksoy et al., 2013). The fact that many of these response regulator mutants have significantly lower viability on nutrient deprivation is evidence of their importance. Moreover, the near universality of starch and TAG accumulation while downregulating photosynthesis underscores the vital importance of maintaining redox status during a cessation of growth.

1.5 Vitamin B_{12}: structure, synthesis, uptake, and function.

1.5.1 Structure

The discovery of an anti-pernicious anaemia factor in liver by Whipple, Minot and Murphy in 1926 (Elders, 1926), and the elucidation of its structure (illustrated in Figure 1.1a) using X-ray crystallography in 1955 by Hodgkin and colleagues (Hodgkin et al., 1956) were the subjects of the awarding of two Nobel prizes. The anti-pernicious anaemia factor was first crystallised in 1948 and named vitamin B_{12}, but this form, (cyanocobalamin) was later found to be an artefact of the extraction process (Rickes et al., 1948). The biologically relevant vitamers of vitamin B_{12} for humans are adenosylcobalamin (AdoCbl) and methylcobalamin (meCbl), which have 5'-deoxyadenosyl and methyl groups replacing the cyano group as the upper axial ligand to the cobalt ion (Randaccio et al., 2010). The cobalt ion is further coordinated by four nitrogen atoms at the centre of a tetrapyrrole, and another nitrogen atom in the lower axial ligand dimethylbenzimidazole (DMB). Two further upper axial ligand vitamers of B_{12} have been described, hydroxocobalamin and glutathionylcobalamin.

Hydroxocobalamin, produced in large amounts by some bacteria (Perlman & Barrett, 1959), is the third most abundant form of B_{12} in human plasma (van Kapel et al., 1983) and the most UV-stable vitamer (Juzeniene & Nizauskaite, 2013). Hydroxocobalamin is converted to adenosylcobalamin in the liver (Fenton & Rosenberg, 1978), and to cyanocobalamin when used as a treatment for cyanide poisoning (Hall et al., 2007). Glutathionylcobalamin (GSCbl) is formed on cell entry of hydroxocobalamin by reacting with reduced glutathione (GSH) (Xia et al., 2004) and is thought to be an intermediate in the formation of the coenzyme vitamers MeCbl and AdoCbl (Suto et al., 2001). Others have suggested that it also has a role as an intracellular antioxidant (Birch et al., 2009), and in contrast, as a promoter of nitric oxide synthase which produces the reactive oxygen species nitric oxide during inflammation (Wheatley, 2007). The name B_{12} also encompasses other cobalt-containing corrinoids that instead of DMB as the lower axial ligand, possess alternative bases. The most well-known uses adenine (Taga & Walker, 2008). This molecule, called pseudocobalamin, is inactive in humans (Dagnelie et al., 1991) and orders or magnitude less bioavailable to many algae (Helliwell et al., 2016) but is widely produced and used by cyanobacteria such as *Arthrospira sp.* (Heal et al., 2017; Watanabe et al., 2002).

1.5.2 Synthesis

Artificial synthesis of B_{12} was achieved in 1972 after a collaborative effort involving more than 100 scientists over a 10-year period (Woodward, 1973). This large-scale effort was needed because of the complexity of the molecule. This is also reflected in the over 20 enzymatic steps required for its cellular biosynthesis in nature from the common tetrapyrrole precursor uroporphorinogen III (Warren et al., 2002). The adenosylcobalamin biosynthetic pathway, which has only been found in prokaryotes, is composed of the convergence of the corrinoid and lower axial ligand pathways (Warren et al., 2002). Both of these have aerobic and anaerobic forms, which were mainly elucidated by studies in *Pseudomonas denitrificans* (Heldt et al., 2005) and *Salmonella enterica* (Roessner & Scott, 2006) respectively. *S. enterica* does however use an aerobic pathway for DMB synthesis (Keck et al., 1998). Although eukaryotes are unable to synthesise AdoCbl de novo, several species are able to remodel pseudocobalamin to cobalamin if they are also provided with DMB (Helliwell, 2017; Helliwell et al., 2016).

1.5.3 Uptake

Because no eukaryotes and only 37% of bacteria were predicted to synthesise B_{12} according to their complement of B_{12} biosynthesis genes (Zhang et al. 2009, Kudahl 2017), many organisms have evolved mechanisms to take it up. The BtuBFCD system in Gram-negative bacteria or BtuFCD system in Gram-positive bacteria are the best characterised prokaryote B_{12} uptake systems (Rodionov

et al., 2003). BtuB is a TonB-dependent B_{12}-binding protein found exclusively in the outer membrane of Gram-negative bacteria (Shultis et al., 2006), while the periplasmic protein BtuF, and the ABC

i Figure 1.1 Structure and function of vitamin B_{12}

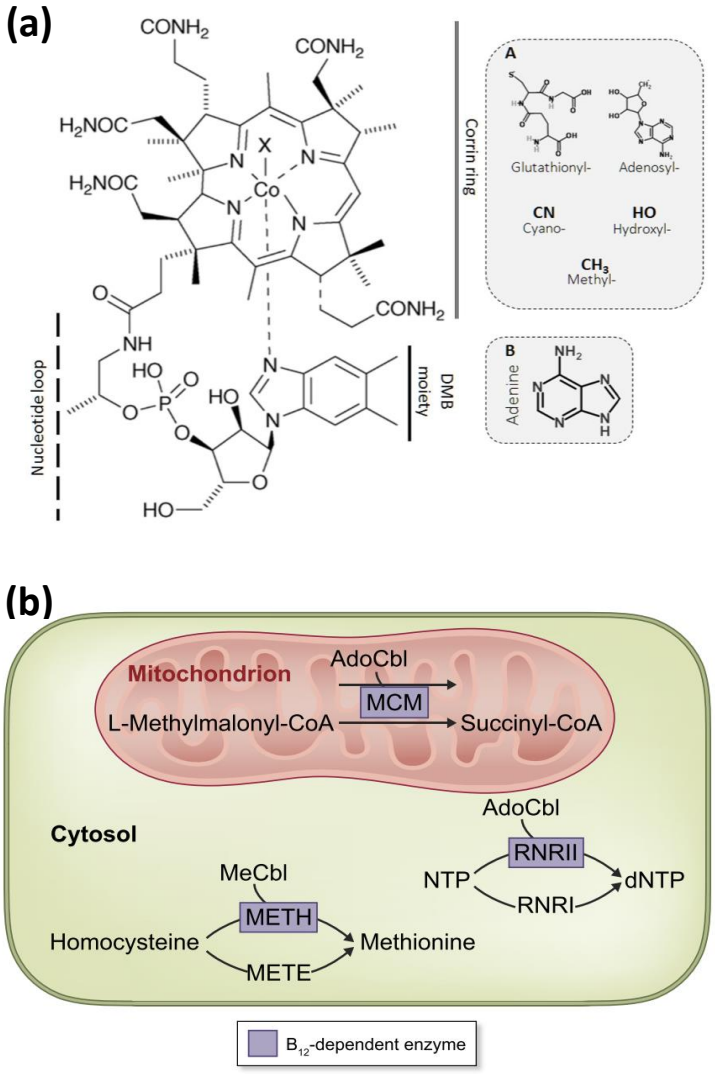

Figure 1.1 Structure and function of vitamin B_{12}. **(a)** Structure of vitamin B_{12} with corrin ring, nucleotide loop, and lower axial ligand (dimethylbenzimidazole (DMB)) labelled. In Pseudocobalamin the lower axial ligand, is replaced by adenine. There are 5 known upper axial ligands to B_{12}: glutathionyl, adenosyl, cyano, hydroxyl, and methyl. **(b)** The three eukaryotic B_{12}-dependent enzymes and the reactions they catalyse. Methylmalonyl-CoA mutase (MCM) is involved in odd-chain fatty acid metabolism, type II ribonucleotide reductase (RNRII) catalyses deoxyribose synthesis, and methionine synthase (METH) catalyses the formation of methionine and tetrahydrofolate from methyl-tetrahydrofolate and homocysteine. Panel A was taken from Cooper 2014, and Panel B was taken from Helliwell 2017, both with permission.

transporter BtuCD, are present in 90% of bacteria that take up B_{12} (Zhang et al., 2009). In the Bacteroidetes, which comprise 80% of the gut microbiome (Consortium et al., 2012), a majority of bacteria were found to encode more than one *BtuB* homolog (Degnan et al., 2014). *Bacteroides thetaiotaomicron* encodes three homologs, two of which provided a selective advantage over the other depending on the supplied corrinoids (Degnan et al., 2014). In humans, more than 15 gene products are involved in B_{12} transport or processing (Nielsen et al., 2012). B_{12} is released from food in the stomach and subsequently binds haptocorrin, which is then digested in the duodenum releasing B_{12} to be later bound by intrinsic factor and taken up by endocytosis after interacting with cubam in the plasma membrane of ileal enterocytes. B_{12} is then exported into the bloodstream by an ABC transporter MRP1 where it is bound by transcobalamin and carried to cells around the body for uptake by the plasma membrane protein CD320. Much less is known about B_{12} uptake in algae, but in *E. gracilis* it occurs in two stages, an initial rapid and passive phase, followed by a slower energy-dependent one (Sarhan et al., 1980). In *Phaeodactylum tricornutum* and *Thalassiosira pseudonana*, a plasma membrane-localised protein called CBA1 is upregulated up to 160-fold in the absence of cobalamin, and overexpression of CBA1 lead to increased rate of B_{12} uptake (Bertrand et al., 2012).

1.5.4 Function in eukaryotes

In bacteria B_{12} acts as a cofactor for over 20 enzymes catalysing reactions that fall into one of three classes: methyl transfer, isomerisation, or reductive dehalogenation (Banerjee & Ragsdale, 2003). In eukaryotes on the other hand, and considering the investment in B_{12} uptake, there are remarkably few B_{12}-dependent enzymes, with three overall and just two in animals (Figure 1.1b) (Croft et al., 2006; Marsh & Marsh, 1999). Several Protista such as *E. gracilis* encode a type II ribonucleotide reductase (RNR II) which uses the AdoCbl cofactor for the synthesis of deoxyribonucleotides from ribonucleotides, the limiting step in DNA synthesis (Elledge et al., 1993; Larsson et al., 2010). Unlike RNRI and RNRIII, which both act independently of B_{12} but are obligately aerobic and anaerobic respectively, RNR II can function in both conditions (Torrents et al., 2006). Methylmalonyl-coA mutase (MCM) is another AdoCbl-dependent isomerase (Takahashi-Iñiguez et al. 2012), and is involved in odd-chain fatty acid metabolism in mammals (Kennedy et al., 1990). Increased levels of methylmalonic acid, derived from the MCM substrate methylmalonyl-coA, is indicative of vitamin B_{12} deficiency or mutations in the MCM gene (Mcmullin et al., 2001; Van Der Meer et al., 1994). The other B_{12}-dependent enzyme in humans is methionine synthase (METH), which uses MeCbl to catalyse the methyl transfer from 5-methyltetrahydrofolate onto homocysteine to yield tetrahydrofolate and methionine (Banerjee & Matthews, 1990). An increase in serum concentration of the substrate homocysteine has been correlated with risk of cardiovascular disease and can indicate either B_{12} or folate deficiency (Jacobsen, 1998).

Plants and fungi are independent of vitamin B_{12} as they express the B_{12}-independent isoforms RNR I and METE, and do not use MCM (Kolberg et al., 2004; Smith et al., 2007). The algal species *C. reinhardtii* and *P. tricornutum* encode both isoforms of methionine synthase, but in the presence of B_{12} suppress *METE* (Bertrand et al., 2013; Helliwell et al., 2014). In *E. coli*, METE has a 50-fold lower catalytic rate than METH (Gonzalez et al., 1992), and so is required in high concentrations of up to 3-5% of total cellular protein content (Pedersen et al., 1978). METE in *C. reinhardtii* has been found to have lower thermal tolerance than METH (Xie et al., 2013), and in *E. coli* METE is sensitive to high temperature and oxidative stress (Hondorp & Matthews, 2004; Mogk et al., 1999). It seems therefore, that B_{12} dependent-isoforms of ribonucleotide reductase and methionine synthase allow a species to power metabolism more efficiently and under a greater range of environmental conditions.

1.6 Methionine synthase and One-carbon metabolism

Methionine synthase connects folate-mediated one-carbon transfers with the activated methyl (methionine) cycle (Figure 1.2). Serine, glycine, and formate provide methyl groups to tetrahydrofolate (THF) to form folates of various oxidation states from the most oxidised, 10-formyl-THF, through 5,10-methenyl-THF, 5,10-methylene-THF to the most reduced, 5-methyl-THF (Hanson & Roje, 2001). 5,10-methylene-THF contributes to thymidylate and pantothenate synthesis (Neuburger et al., 1996; Ottenhof et al., 2004), while 10-formyl-THF is used to produce purines and methionyl tRNA (Baggott & Tamura, 2015). But the major anabolic demand for one-carbon folates is of 5-methyl-THF for the synthesis of methionine and subsequently S-adenosylmethionine (SAM) (Hanson & Roje, 2001; Leung et al., 2017; Reed et al., 2006). Although serine and glycine provide large quantities of methyl groups, SAM is the most versatile methyl donor and is often termed the ‘universal methyl donor’ because histones, DNA, lipids, and various proteins are methylated by SAM-utilising methyltransferases (Chiang et al., 1996; Lieber & Packer, 2002).

1.6.1 Methionine cycle

SAM and its demethylated product S-adenosylhomocysteine (SAH) are known to regulate the expression of genes such as S-adenosylhomocysteine hydrolase (SAHH) and methionine synthase (METH) in bacteria via binding to riboswitches in the 5’UTRs of these transcripts (Corbino et al., 2005; Wang et al., 2008). In humans SAM reduces the activity of methylene tetrahydrofolate reductase (MTHFR) by feedback inhibition, and in all organisms SAH is a competitive inhibitor of multiple SAM-utilising methyltransferases (Ueland, 1982). The ratio of SAM:SAH has thus been

termed the methylation index, with low values resulting in hypomethylation of a range of compounds including DNA (Waterland, 2006). Hypermethylation of cytosines in DNA and of the lysine 9 residue of histone 3 (H3K9) are associated with heterochromatin, which contains repetitive regions or transposons that are suppressed (Johnson et al., 2002; Rose & Klose, 2014). Therefore, genome hypomethylation often relieves this suppression, leading to increased and aberrant gene expression (Jones, 2012). SAH and Homocysteine (Hcy) are interconverted by the action of the reversible enzyme SAHH which has an equilibrium constant that favours the production of SAH (Guranowski & Pawelkiewicz, 1977; Haba & Cantoni, 1958). Despite this, the flux is normally towards homocysteine formation due to its rapid removal by conversion to methionine or cystathionine (Hoffman et al., 1980). In plants, the reverse transulfuration pathway, which produces cysteine from homocysteine via cystathionine, does not exist (Datko & Mudd, 1984) but an alternative pathway unique to plants that forms part of the S-methylmethionine cycle (Ranocha et al., 2001) can regenerate methionine. This pathway, however, forms a futile cycle with no external input of methyl groups (Ranocha et al., 2001).

1.6.2 Folate metabolism

5-methyl-THF can accumulate in humans in a phenomenon known as folate trapping if B_{12} or methionine is limiting (Scott & Weir, 1981). In plants, 5-methyl-THF is consumed by a B_{12}-independent methionine synthase and can also be metabolised by a reversible reaction catalysed by MTHFR (Roje et al., 1999). Because of this, and although 5-methyl-THF is one of the most abundant folates in plants (Loizeau et al., 2007), folate trapping is unlikely to occur, and MTHFR activity is not suppressed by SAM as it is in humans (Roje et al., 1999). Serine hydroxymethyltransferase (SHMT) has several isoforms in plants which are targeted to the cytosol, plastid, and mitochondria (Besson et al., 1995). Another reversible reaction, the equilibrium position favours the C1 transfer from serine to THF to form 5,10-methylene-THF and glycine (Besson et al., 1993). Glycine can donate a further carbon to THF and release CO_2 and NH_3 in the process, a key stage of photorespiration that occurs in the mitochondria (Timm et al., 2012). Overall, in photosynthetic organisms the demand for methyl groups for methylation is mainly provided by serine through 5,10-methylene-THF, 5-methyl-THF, methionine, and finally SAM (Hanson & Roje, 2001).

ii Figure 1.2 A simplified metabolic map of the C1-cycle

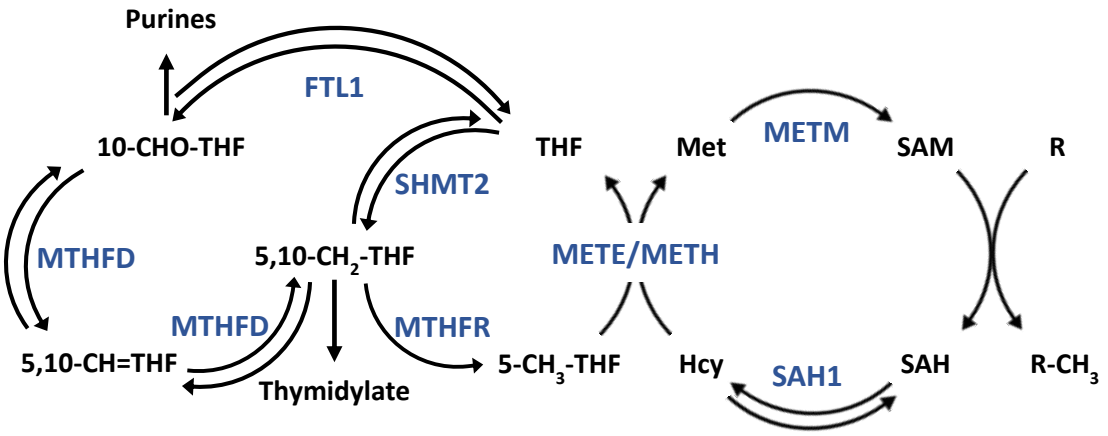

Figure 1.2 A simplified metabolic map of the C1 cycle in *C. reinhardtii*. Enzyme abbreviations are presented in blue and metabolites in black. Double arrows indicate that the enzyme can catalyse the reaction in both directions, i.e. the reaction is reversible. Enzyme abbreviations: FTL1, Formate tetrahydrofolate ligase; METE, B_{12}-independent methionine synthase; METH, B_{12}-dependent methionine synthase; METM, S-adenosylmethionine synthetase; MTHFD, Methylenetetrahydrofolate dehydrogenase; MTHFR, methylenetetrahydrofolate reductase; SAH1, S-adenosylhomocysteine hydrolase 1; SHMT2, Serine hydroxymethyltransferase 2. Metabolite abbreviations: Hcy, Homocysteine; Met, Methionine; SAH, S-adenosylhomocysteine; SAM, S-adenosylmethionine; THF, Tetrahydrofolate; 5-CH_3-THF, 5-methyltetrahydrofolate; 5,10-CH_2-THF, 5,10-Methylenetetrahydrofolate; 5,10-CH=THF, 5,10-Methenyltetrahydrofolate; 10-CHO-THF, 10-formyltetrahydrofolate.

1.6.3 Disrupting one-carbon metabolism

In humans, several single nucleotide polymorphisms (SNPs) in genes for enzymes of one-carbon metabolism, and folate metabolism in particular, have been associated with increased levels of homocysteine in the blood, including Thymidylate synthase (TYMS) (Trinh & Laird, 2002), and MTHFR (Lievers et al., 2001). Combinations of certain polymorphisms such as in methionine synthase (MTR) and MTHFR are particularly associated with higher homocysteine levels (Feix et al., 2001), but it is in patients with these SNPs that folic acid supplementation can have the greatest homocysteine-lowering effects (Qin et al., 2012). Plasma homocysteine has been shown to have a highly significant predictive effect for cardiovascular disease (Wald et al., 2002). Despite this, the lowering of homocysteine by folic acid supplementation does not reduce the risk of cardiovascular disease (Bazzano et al., 2006; Clarke et al., 2010), but there is strong evidence of reducing other diseases such as neural tube defects (Atta et al., 2016; Castillo-Lancellotti et al., 2012). Homocysteine concentrations in the blood are also negatively correlated with concentrations of vitamin B_6 and B_{12}, (Selhub et al. 1993) which are cofactors for two homocysteine-metabolising enzymes, cystathionine-β-synthase (CBS) and MTR respectively (Finkelstein, 1998).

Folate and vitamin B_6 are synthesised de novo in plants (Hanson & Jesse, 2011; Tambasco-Studart et al., 2005) and vitamin B_{12} is not necessary for metabolism (Smith et al., 2007), but the effects of disrupting one-carbon metabolism have been investigated by application of the antifolate drug methotrexate. Methotrexate inhibits growth and disrupts the methyl cycle (Loizeau et al., 2007; Wu et al., 1993) leading to a significant increase in the methylation index of *Arabidopsis thaliana*, but the plant appears to respond by prioritising nucleotide synthesis over methylation (Loizeau et al. 2008). In *A. thaliana* mutants disrupted in genes for folate synthesis (*FPGS1*), folate mediated one carbon transfer (*MTHFD1*), or the activated methyl cycle (*MAT4*), the methylation index decreases leading to lower DNA and histone (H3K9) methylation and subsequently transposon derepression (Groth et al., 2016; Meng et al., 2018; Zhou et al., 2013).

It is clear therefore that disruption of one-carbon metabolism can have significant consequences on the physiology of an organism irrespective of whether they are dependent on an exogenous source of vitamins. However, those organisms that rely on external provision of B_6, B_9, and B_{12} are perhaps particularly likely to experience changes in flux through the folate and methionine cycles and the downstream effects on DNA synthesis and methylation.

1.7 Algal symbioses

1.7.1 Parasitic interactions

Symbiosis is a term that can be used rather broadly to refer to a beneficial or harmful interaction between two unrelated organisms. Using this definition, algae engage in a multitude of symbioses spread along the parasitism to mutualism continuum. Non-photosynthetic algae such as *Plasmodium falciparum* and *Toxoplasma gondii* parasitize humans causing malaria and toxoplasmosis respectively (Baumeister et al., 2010; Fichera & Roos, 1997). Some photosynthetic algae are also parasites, such as *Cephaleuros parasiticus* which grows mainly on the leaves of tropical trees (Joubert & Rijkenberg, 1971; Vasconcelos et al., 2018). There are also several examples of the converse, algae being parasitized, for example *Emiliania huxleyi* blooms often come to an abrupt end as coccolithovirus infections rapidly spread through the population (Schroeder et al., 2003, 2002). Outdoor cultures of algal ponds are frequently infected with parasites (Carney & Lane, 2014), and one fungal species, *Amoeboaphelidium protococcarum*, was found to inject its protoplast into the cells of the alga *Scenedesmus dimorphus* (Letcher et al., 2013).

1.7.2 Interactions with multicellular hosts

It is well known that the *Symbiodinium* endosymbionts of corals provide photosynthate to their hosts (Whitehead, 2003). However, it has only been shown more recently that the nitrogen provided by the coral host to *Symbiodinium* can be derived mainly from heterotrophic diazotrophic bacterial communities, which are transferred vertically from coral parent to its larvae (Ceh et al., 2013; Lema et al., 2012). Although considered a mutualism, the coral host exerts significant control over *Symbiodinium* cell density by producing factors that induce release of photosynthate (Gates et al., 1995), limiting the provision of nitrogen (Falkowski et al., 1993), and digesting and extruding the algal cells (Titlyanov et al., 1996). In 1879 Anton de Bary first used the term symbiosis to refer to lichens (Oulhen et al., 2016), and it is now recognised that some of the most productive lichens are tripartite: composed of not only the algal photobiont and fungal mycobiont, but also a nitrogen-fixing cyanobiont (Scheidegger, 2016). Many of the algal photobionts can live freely whereas the mycobiont is more often obligately symbiotic, which is perhaps why it needs to exert greater control over the photobiont to maintain the symbiosis (Muggia et al., 2013; Richardson, 1999). In addition to these well-known lichen and coral interactions, certain algae can also form mutualisms with vertebrates, such as the green alga *Oophila amblystomatis*, which can grow intracellularly in the embryos of the salamander *Amblystoma maculatum* where it supplies oxygen and receives nitrogenous waste in return (Kerney et al., 2011). Presence of the alga is correlated with lower embryonic mortality and earlier and more synchronised hatching at a larger size and later developmental stage (Gilbert, 1942; Graham et al., 2014).

1.7.3 Physical interactions with bacteria

In most of the examples described above the algal partner resided on or within its multicellular host, but it is also the case that algae interact with bacteria attached to their surfaces or that simply occur in the same environment (Amin et al., 2012). In the oceans the average concentrations of bacteria, at 10^5-10^6 cells·ml^{-1}, are orders of magnitude lower than in sediments, the soil, or the human gut (Whitman et al., 1998). However, there is considerable heterogeneity in their distribution, with microscale patches of much higher concentration (Blackburn et al., 1998). Although the surfaces of diatoms are often free from bacterial colonisation (Droop & Elson, 1966), the profile of bacterial genera that co-occur with specific diatom species is well conserved in different geographical locations, and over long periods of cultivation in the laboratory (Amin et al., 2012; Behringer et al., 2018). Many bacteria are able to maintain this association in the open ocean using the gradient of dissolved organic matter (DOM) in the phycosphere surrounding diatoms to direct their chemotaxis (Barbara & Mitchell, 2003; Mitchell et al., 1996). Some marine bacteria, such as *Shewanella putrefasciens*, have high swimming speeds of 100 µm·s^{-1}, and can increase these in the presence of algae, allowing them to remain in the phycosphere of a motile alga (Barbara & Mitchell, 2003; Stocker et al., 2008). The importance of motility for the interactions between bacteria and diatoms was illustrated by the fact that flagella mutants of *Silicibacter sp.* or *Dinoroseobacter shibae* were less able to support the growth of the diatoms *Pfiesteria piscicida* and *Prorocentrum minimum* respectively (Miller & Belas, 2006; Wang et al., 2015).

Once the bacteria have located algae, attachment to the cell surface could considerably improve the efficiency of nutrient acquisition and transfer. In cultures of the diatom *Pseudonitschia multiseries*, bacteria were found to attach preferentially to certain locations on the frustule, which might be sites of organic matter release, and the number of epiphytic bacteria increased as the diatom cells entered stationary phase (Kaczmarska et al., 2005). Expression of genes for bacterial attachment to algae, as well as attachment itself, has also been found to increase during phytoplankton blooms (Bertrand et al., 2015; Mayali et al., 2011; Rinta-Kanto et al., 2012). In addition, bacteria that attached to the surface of *Thalassiosira weissflogii* were found to induce algal aggregation, but only if the algae were photosynthetically active (Gärdes et al., 2011). The diazotrophic cyanobacterium *Richelia intracellularis*, forms an even closer but facultative physical association with diatoms such as *Rhizosolenia clevei* and *Hemiaulus sp.* by inhabiting their perisplasmic space between the frustule and plasmalemma (Sundström, 1984; Villareal, 1990). *R. intracellularis* was also estimated to be able to produce 7.5 times as much organic nitrogen through nitrogen fixation as needed for its own growth and to transfer 97% of it to its host (Foster et al., 2011). Cyanobacteria related to *Cyanothece sp*, have become fully integrated as obligate endosymbionts of diatom species in the family *Rhopalodiaceae*, in what are termed spheroid bodies (Nakayama et al., 2011; Prechtl et al., 2004). These spheroid bodies

lack genes for photosynthesis, but retain those for nitrogen fixation, and the large proportion of pseudogenes they encode suggest they are in the midst of substantial genome reduction (Nakayama et al., 2014).

1.7.4 Chemical interactions with bacteria

Nutrient transfer is a common basis for mutualisms between bacteria and algae, with several reports of nitrogen-fixing cyanobacteria improving the growth of diatoms in the ocean (Fiore et al., 2010; Foster & Zehr, 2006; Janson et al., 1999; Turk-Kubo et al., 2017). Freshwater and terrestrial examples have also been studied, often by combining the bacteria and algae in artificial symbiotic cultures and measuring the growth promotion as well as the transfer of nitrogen and carbon using a mass spectrometry-based imaging technique called Nano-SIMS (de-Bashan et al., 2016; Hernandez et al., 2009). Many rhizobia that promote plant growth through nitrogen fixation also produce B_{12} (Palacios et al., 2014), and B_{12} production is essential for *Sinorhizobium meliloti* to be able to form a symbiosis with *Medicago sativa*, due to its role as a cofactor in DNA synthesis (Campbell et al., 2006; Taga & Walker, 2010). Vitamin B_{12} is also central to the artificial symbiosis between the soil bacterium *Mesorhizobium loti* and the freshwater alga *Lobomonas rostrata* (Kazamia et al., 2012), and *S. meliloti*, a related rhizobium, can improve the thermal tolerance of *C. reinhardtii* by providing B_{12} (Xie et al., 2013). Although many marine bacteria also produce B_{12}, a large proportion of this is pseudocobalamin, a form that is only available to certain algal species (Heal et al., 2017; Helliwell et al., 2016). However, it has been shown that some algae that take up pseudocobalamin remodel it by replacing the lower axial ligand with dimethylbenzimidazole (DMB; see section 1.5.1), and in doing so could indirectly support algae that require 'true' cobalamin (Helliwell et al., 2016). Certain species of algae provide more than an energy source to their bacterial partners: *Ostreococcus tauri* was shown to support the niacin, biotin, and p-aminobenzoic acid requirements of *Dinoroseobacter shibae* in return for thiamine and cobalamin (Cooper et al., 2019). On the other hand, other experiments have found that algae may reduce the release of organic carbon if they are nutrient replete and so do not require the presence of mutualistic bacteria, for example in the co-cultures of *L. rostrata* and *M. loti* in the presence of B_{12} (Grant et al., 2014).

Bacterial mutualists do not always synthesise the compounds required by algae, instead they can facilitate its uptake from the environment. For example, *Marinobacter sp.* increases iron uptake by the alga *Scripsiella trochoidea* by 20-fold when exposed to light, not by releasing iron but by producing a photolabile, iron-binding siderophore called vibrioferrin (Amin et al., 2009). An Antarctic ice diatom, *Amphiprora kufferathii*, is frequently found associated with epiphytic bacteria that do not appear to improve algal nutrient uptake, but instead protect it against hydrogen peroxide using the enzyme catalase, which the alga does not express (Hünken et al., 2008). Mutualistic bacteria can also provide protection to their algal hosts by preventing the settling of pathogenic organisms, for

example, *Pseudoalteromonas tunicata*, at a density of only 10^2-10^3 cells·cm^{-2}, prevents surface colonisation by various marine fungal species that infect its host, *Ulva australis* (Rao et al., 2007). *Phaeobacter gallaeciensis* is also thought to protect its algal host *E. huxleyi* by secretion of antibiotics and promote its growth by auxin production, however, on detecting p-coumaric acid, an indicator of algal senescence, *P. gallaeciensis* switches to production of roseobacticides which hasten the death of *E. huxleyi* (Seyedsayamdost et al., 2011). Algae and bacteria interact mutualistically in a multitude of ways from nutrient provision, to recycling of damaging waste products, and protection against pathogens, but as demonstrated by the last example, mutualists, sensing a better opportunity, can rapidly switch to a pathogenic lifestyle.

1.8 Artificial evolution of a B_{12}-dependent alga

Croft et al. (2005) found that over 50% of algal species are dependent upon B_{12}, that the likely reason for this dependence was the loss of the B_{12}-independent methionine synthase (METE), causing them to rely on the B_{12}-dependent METH, and that as a result they may form symbioses with B_{12}-producing bacteria in order to survive (Croft et al., 2005). The correlation between the lack of a functional copy of *METE* and a B_{12}-dependent phenotype persists across the tree of life (Figure 1.3a) (Helliwell, 2017). The evolution of B_{12} dependence amongst certain members of the Volvocine algae (Figure 1.3b), such as *V. carteri* and *Gonium pectorale*, may have been relatively recent as they still encode remnants of the *METE* gene (Helliwell et al., 2014). In another Volvocine alga, *C. reinhardtii*, *METE* transcript levels have been found to decrease rapidly to almost undetectable levels within 3 hours of addition of B_{12} at 1000 ng·l^{-1} , and protein levels also declined to a steady state after 36 hours (Helliwell et al., 2014). On the other hand, in *Coccomyxa subellipsoidea*, which lacks the B_{12}-dependent methionine synthase isoform (*METH*), no decrease in *METE* transcript was observed. The almost complete suppression of *METE* under sufficient B_{12} is likely to make its contribution to methionine synthesis and therefore the C1-cycle insignificant. This could allow mutations in the gene to occur without any decrease in fitness.

Helliwell et al. (2015) cultured *C. reinhardtii* in media containing 1000 ng·l^{-1} B_{12}, and within 500 doublings of the alga observed the evolution of a B_{12}-dependent mutant (Figure 1.4a), which was called 'S-type' due to its stunted growth on agar lacking B_{12} (Helliwell et al., 2015). S-type cells outcompeted the initial B_{12}-independent strain and were shown to have a significantly higher maximal growth rate under replete B_{12} conditions. Analysis of the *METE* gene from S-type cells revealed that a type II Gulliver-related transposable element (GR-TE) had inserted into the 9th exon (Figure 1.4b). When S-type cells were plated on agar lacking B_{12} it was observed that on rare occasions colonies with a wild-type phenotype would arise from within the stunted colony (Figure 1.4c). Analysis of the *METE* gene from these colonies with a wild-type phenotype revealed that they had lost the GR-TE

insertion. These isolates were called R-type due to their reversion to B_{12}-independence. When multiple colonies with the S-type stunted phenotype were analysed for the presence of the GR-TE, the seventh clone that was tested was found to be lacking it (Figure 1.4d). However, it did contain a nine nucleotide 'footprint' derived from the transposon (Figure 1.4e). This clone was subsequently called *metE7* and unlike S-type cells would not revert to B_{12} independence when grown in the absence of B_{12}. It was also shown that *metE7* growth in media lacking B_{12} could be rescued by the addition of three B_{12}-producing rhizobia: *Mesorhizobium loti*, *Sinorhizobium meliloti*, or *Rhizobium leguminosarum*.

iii Figure 1.3 Phylogenetic relationships between B_{12}-dependent and B_{12}-independent organisms

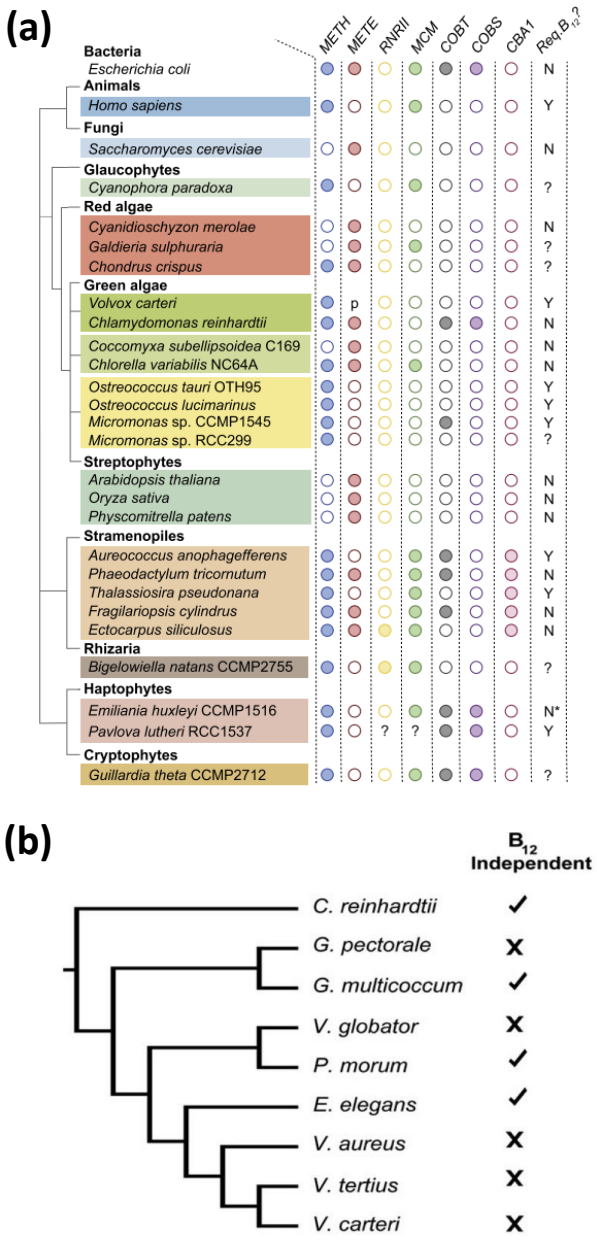

Figure 1.3 Phylogenetic relationships between B_{12}-dependent and B_{12}-independent organisms. **(a)** A schematic illustrating B_{12} requirements of various eukaryotic species (and one prokaryote) alongside their gene complements for B_{12}-related enzymes. Absence of a functional copy of *METE* is the best predictor of B_{12} requirement. **(b)** An illustration of the phylogenetic relationship between certain Volvocalean species, with those species that can grow independently of B_{12} indicated by a tick next to their name. These figures were taken from Helliwell, 2017 and Helliwell et al., 2013, with permission.

iv Figure 1.4 Laboratory evolution of a stable B_{12}-dependent *METE* mutant of *C. reinhardtii*: *metE7*

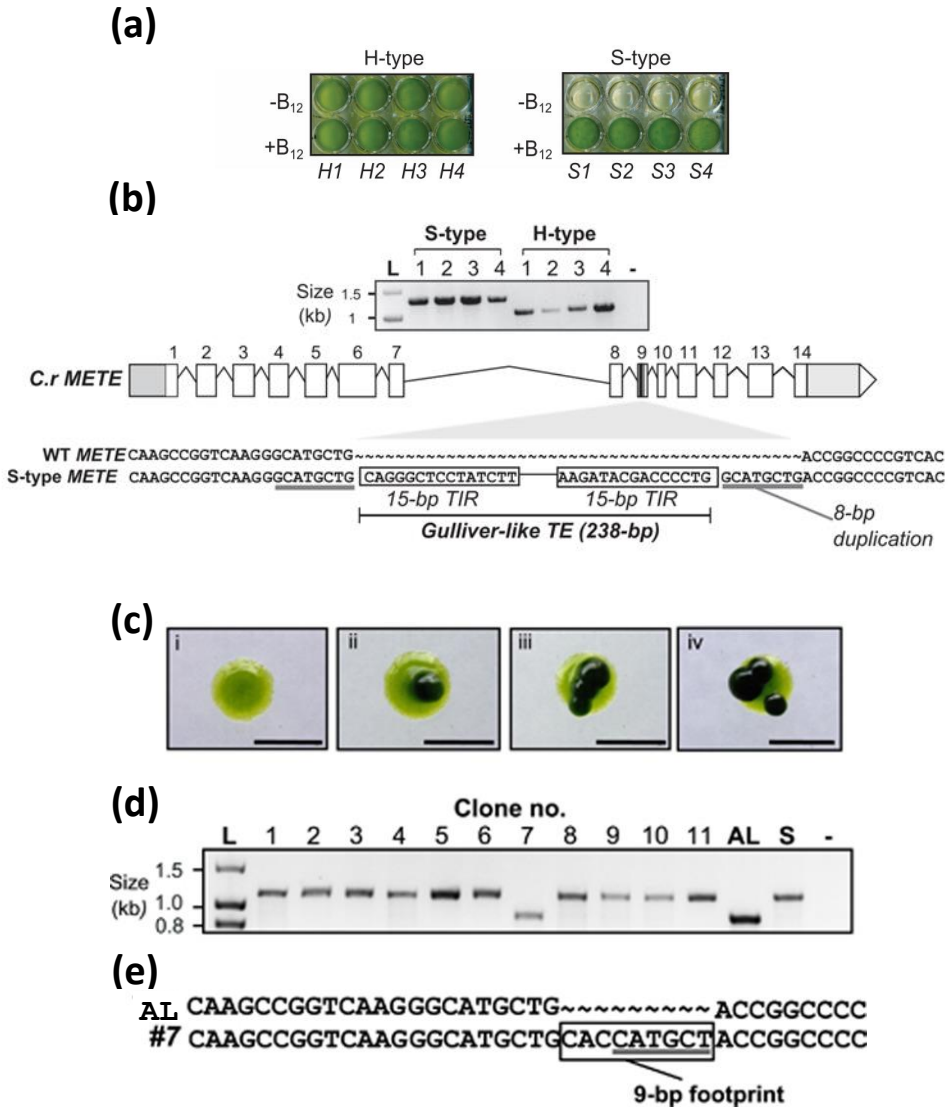

Figure 1.4 Laboratory evolution of a stable B_{12}-dependent *METE* mutant of *C. reinhardtii*: *metE7*. **(a)** Experimental evolution of *C. reinhardtii* in high levels of B_{12} produced two phenotypes in the absence of B_{12}: H-type cells maintained B_{12}-independent growth, while S-type cells were unable to grow. **(b)** DNA from S-type and H-type colonies of *C. reinhardtii* was amplified using primers that span a section of the *METE* gene that contains a Gulliver-related transposable element in S-type cells. The lower portion shows the site of insertion of the GR-TE in the 9th exon of the *METE* gene of S-type cells, and some of the GR-TE's sequence characteristics. **(c)** Photographs through a dissecting microscope of S-type colonies 11 days after plating on TAP agar without B_{12}, showing that in some cases darker H-type colonies appear to grow from single reversion events. **(d)** PCR products after amplification across the GR-TE insertion site from phenotypically S-type (stunted) colonies grown on TAP agar without B_{12}. Clone number seven (*metE7*) produces a band of similar size to the ancestral line. **(e)** Sequence alignment of ancestral line and *metE7* DNA sequences at GR-TE insertion site. *metE7* contains a 9-nucleotide footprint derived from incomplete excision of the GR-TE. All images and diagrams were taken from Helliwell et al., 2015, with permission.

1.9 Evolution of symbioses

1.9.1 The Queens of coevolution

The 'Red Queen hypothesis' (RQH) was proposed by Van Valen in 1973 as a way of explaining the finding from fossil evidence that species tended to go extinct with a constant probability (Van Valen, 1973). This was puzzling because if species A were to outcompete or simply outlive species B then it would seem that species A was better adapted and so should be less likely to go extinct. This constant probability of extinction therefore suggested varying selection pressures driven by constantly evolving antagonistic or competitive species. The hypothesis was subsequently widely used as an explanation for the evolution and maintenance of sexual reproduction, particularly in response to parasites (Hamilton, 1980; Hamilton et al., 1989; Jaenike & J., 1978; Morran et al., 2011). The inspiration for naming the hypothesis the 'Red Queen', came from Lewis Caroll's 'Through the Looking-Glass' in which the Queen of Hearts says, 'It takes all the running you can do to stay in the same place', which seemed to capture the coevolutionary arms-race between antagonistic species, such as host and parasite. The 'Black Queen hypothesis' (BQH) was devised almost four decades later and also provided a theory for coevolution of species (Morris et al., 2012). The name was also inspired by a playing card, the Queen of Spades, which in the game of Hearts is a card that players aim to get rid of due to the penalty associated with holding it at the end of the game. A 'Black Queen function' is one that is costly to perform, essential to some members of the community that do not perform it, and 'leaky', meaning that some portion of its output becomes a public good/service (Morris, 2015). Both the Red and Black Queen hypotheses display a strong element of negative frequency-dependent fitness: for the Red Queen, hosts with a rare susceptibility phenotype are fitter than those with a common phenotype because parasites with the complementary virulence factor of the common susceptibility phenotype can spread more easily, hence negatively affecting the more common host phenotype; in the BQH, those 'beneficiary' strains that depend on 'helpers' for the performance of the Black Queen function become less fit if they dominate the community, because in so doing they reduce the number of helpers. This common theme of fitness being negatively frequency-dependent provides a counterargument to the 'Competitive exclusion principle', which states that species competing for the same limiting nutrients cannot coexist (Hardin, 1960), and therefore also provides an explanation for the 'Paradox of the Plankton', which observes that plankton diversity is substantial despite a nutrient-limited environment (Hutchinson, 1961).

According to the RQH, continuous improvement or gain of functions and hence increased complexity is selected for, while under the BQH it is a race to the bottom by genome streamlining (Morris, 2015). The Red and Black Queens therefore contribute to the selective forces that regulate genome sizes (Cordero & Polz, 2014; Cuypers & Hogeweg, 2012; Katju & Bergthorsson, 2013), with genome simplification being the temporally dominant mode of evolution, punctuated by episodes of

complexification (Cuypers & Hogeweg, 2012; Wolf & Koonin, 2013). This does not provide much indication however, as to whether competitive or cooperative interactions predominate in the microbial world, but there are many proponents of the idea that competition dominates cooperation (Foster & Bell, 2012; Hibbing et al., 2010), and vice versa (Elias & Banin, 2012; Schink, 2002). Foster et al. (2012), mention that studies which propose cooperation as a dominant mode of interaction, such as those focusing on biofilms (Reisner et al. 2006; Burmølle et al. 2006), are intentionally unrepresentative (Foster & Bell, 2012). However, there is considerable evidence that positive interactions between species can facilitate the culture of the axenically 'unculturable' through, for example, iron provision by siderophores or release of short peptide signalling molecules (D'Onofrio et al., 2010; Nichols et al., 2008; Ohno et al., 1999).

The realm of the Red Queen is restricted to competitive interactions, and has been seized upon in particular to explain how sexual reproduction keeps hosts ahead of parasites, or at least in the race (Lively et al., 1990; Moritz et al., 1991). Under the Black Queen, 'helpers' tend to experience little negative impact from 'beneficiaries' (which clearly benefit), and so the hypothesis concerns the development and maintenance of commensal interactions (Morris et al., 2012, 2014). Disregarding the fact that commensalism occupies an infinitely small space on the continuum from parasitism to mutualism, and hence theoretically does not exist, it can in practice lead to prolonged association between species and hence provide the opportunity for the evolution of mutualism (Ewald, 1987; Harcombe, 2010; Lawrence et al., 2012; Morris, 2015). Indeed, the evolution of mutualism from parasitism via commensalism is favoured in cases where a parasite is vertically transmitted (Ewald, 1987; Yamamura, 1993). Although some mathematical models have found that cooperation can evolve and thrive in the presence of other symbiotic strategies (Axelrod & Hamilton, 1981), others have found that it is a poor strategy causing loss of autonomy and hence fragility, but also tends to take a form akin to mutual exploitation which reduces community productivity (Oliveira et al., 2014). Furthermore, parasites and autonomous organisms are nested within predominantly mutualistic clades suggesting breakdown of mutualism to parasitism or independence does occur (Sachs & Simms, 2006).

1.9.2 The Evolution of cooperation

For cooperation to evolve there must firstly be an advantage to cooperating relative to independence. Barker et al. (2017) suggest there are three main advantages to cooperation, 'acquisition of otherwise inaccessible goods and services, more efficient acquisition of resources, and buffering against variability' (Barker et al., 2017). The development of the legume-rhizobia symbiosis allowed plants to utilise the otherwise inaccessible N_2 as a nitrogen source, and rhizobia were able to utilise the otherwise inaccessible CO_2 as a carbon source (Long, 1989). Certain cyanobacteria with simple multicellularity compartmentalise nitrogen fixation into heterocysts, so that nitrogen fixation

and photosynthesis occur in separate cells (Kumar et al., 2010). This specialisation improves the efficiency of nitrogen acquisition because oxygen, a by-product of oxygenic photosynthesis, inhibits the nitrogenase enzyme (Wong & Burris, 1972). In general, specialisation will be favoured if the relationship between investment in a trait and its payoff is 'accelerating' (West et al., 2015) or 'convex' (Michod, 2006, 2007), i.e. if it pays to invest more specifically than widely. The phenomenon of comparative advantage can then be made use of so that after the products of specialists have been distributed, all units of the group can gain (Hoeksema & Schwartz, 2003). Cooperation can also buffer against variability and so reduce the chance that any individual falls below a crucial threshold required for survival, for example, in vampire bats reciprocal food sharing occurs as individuals fluctuate between having an excess and shortfall of food (Carter & Wilkinson, 2013). So, advantages to cooperation are widespread, but they are also often left open to exploitation by selfish individuals who do not reciprocate.

The prisoner's dilemma is a game where two rational players are presented with two options: to cooperate or to defect, and they are not allowed to alter the other player's decision in any way. This gives rise to four possible combination of options, of which one combination is both the Nash equilibrium and has the minimum total payoff value (Rapoport & Chammah, 1965). A Nash equilibrium is the outcome where switching your option while the other player sticks to theirs will cause you to lose out, and vice versa from their perspective (Nash, 1950). Hence it is a dilemma because both players are driven by selfish interests to choose the option that results in the lowest total benefit. A special case of the prisoner's dilemma, called the 'donation game', more aptly describes the barriers to cooperation within and between species (Doebeli & Knowlton, 1998). A 'cooperator' provides a benefit to the other player at a cost to themselves, where the benefit is greater than the cost. In this case, irrespective of the other player's option it is beneficial to 'defect' i.e. not cooperate. Therefore, natural selection at the level of the individual should lead to the breakdown of cooperation.

Szathmary and Maynard Smith (1995) and later West et al. (2015) argued that the evolution of complex lifeforms was not a smooth ramp, but instead was defined by major transitions in individuality (Szathmáry & Smith, 1995; West et al., 2015). Individuals that could replicate independently prior to the transition could only replicate as part of the group (which they cooperated to form) after the transition (Szathmáry & Smith, 1995). In other words, the group becomes the individual. Queller et al. (1997) distinguished two types of transition: Fraternal transitions based on cooperation between kin, and Egalitarian transitions based on cooperation between distantly related individuals (Queller, 1997). The endosymbiosis of a cyanobacterium by a heterotrophic protist is an example of well-known egalitarian transition (Queller & Strassmann, 2016), while the development of multicellularity in the *Volvocales* is a well-characterised fraternal one (Herron & Michod, 2008). Note that most mutualisms do not meet the strict requirements of an egalitarian transition as they are not obligate and horizontal transmission allows for independence of replication (West et al., 2015), for

example, interactions between legumes and rhizobia are facultative and rhizobia are not transmitted vertically with the host (Maroti & Kondorosi, 2014; Westhoek et al., 2017).

Perhaps the best-known theory to explain why cooperation persists is 'group-level selection', which posits that selection can act more strongly at the level of the group than the individual (Wright, 1945). Therefore, although defectors are fitter than co-operators, groups of co-operators are fitter than groups of defectors, and so when starting with mixed groups cooperation can be favoured under certain circumstances. If selection is weak and group splitting is rare then cooperation is favoured when B/C>1+n/m, where n is the maximum number of individuals per group and m is the number of groups (Traulsen & Nowak, 2006). Introducing migration between groups has been found to favour defectors (Traulsen & Nowak, 2006), which in essence is equivalent to the hypothesis that vertical transmission favours cooperation (Sachs et al., 2011). The 'Foraging to Farming hypothesis' (FFH) uses the example of a B_{12}-independent alga interacting with B_{12}-producing bacteria to illustrate it's point about how mutualisms might arise in phytoplankton communities (Kazamia et al., 2016). The FFH suggests that were an alga to lose *METE* and so become dependent upon B_{12}, there would be a selective advantage to 'farming' the B_{12}-producing bacteria by providing photosynthate so that a greater quantity and guarantee of B_{12} supply could be had. The FFH does not specifically address how cheating, or reducing photosynthate production, could be deterred or avoided, and so perhaps group-level selection could offer a mechanism to support the FFH. The number of hypotheses that address the paradox of why cooperation between individuals occurs at all is evidence of the broad interest in this question. Whether they are competing hypotheses, however, or simply competing metaphors is not always clear.

1.10 Thesis aims and structure

The overarching aim of this thesis was to provide some insight into the early stages after the initial evolution of vitamin B_{12} dependence in algae, a phenomenon that is predicted to have occurred multiple times (Croft et al., 2005). This approach could be compared to the study of the alga *P. chromatophora*, which has formed an endosymbiosis with a cyanobacterium relatively recently, to infer the early stages of the formation of photosynthetic organelles (Nowack et al., 2011). Perhaps there is no reason to suggest that the *metE7* mutant is any different from other mutants of *C. reinhardtii*, in which case this is a study of the function of *METE* in this alga's physiology. However, the circumstances of its generation by experimental evolution, and the fact that the underlying mechanism of its B_{12} dependence is widely shared among B_{12} auxotrophs (Helliwell, 2017; Helliwell et al., 2011), leads me to believe that study of this mutant will reveal wider evolutionary and ecological implications. By way of a visual introduction to the organisms used in this work a collection of microscope images is assembled in Figure 1.5.

In chapter three I investigate the responses of *metE7* to deprivation of vitamin B_{12}. Firstly, I compare the growth of *metE7* and the wild-type *C. reinhardtii* in different concentrations of B_{12}. To compare *metE7* to a closely related natural B_{12} auxotroph, both *metE7* and *L. rostrata* were tested for their B_{12} growth response, B_{12} uptake, and storage. I hypothesised that the most likely consequences of B_{12} deprivation in *metE7* would be an alteration in C1-cycle metabolite and enzyme transcript abundance, and so measured a subset of these in the wild type and *metE7* mutant in B_{12} replete and deplete conditions. A wider variety of cellular composition measurements were then made on *metE7* cells under B_{12} deprivation, including quantification of protein, starch, lipids, free amino acids, and fatty acids. To get a better perspective of the dynamics of the response to B_{12}, C1-cycle metabolites and enzyme transcripts were quantified at several time points over 3 days of B_{12} deprivation and for 2 days after B_{12} add-back. Physiological aspects of the response to B_{12} deprivation, including cell viability, PSII maximum efficiency (*Fv/Fm*), non-photochemical quenching, and production of reactive oxygen species were then compared in *metE7* and *L. rostrata.* To have a better idea as to whether the differences in the responses of *metE7* and *L. rostrata* might be attributed to the fact that *L. rostrata* has had time to evolve mechanisms to improve survival under B_{12} deprivation, I decided to also measure the response of *metE7* to nitrogen deprivation, a condition *C. reinhardtii* has had ample time to evolve coping mechanisms for. *metE7* was then exposed to a combination of nitrogen and B_{12} deprivation to see whether nitrogen deprivation could elicit responses that would improve survival during B_{12} deprivation. Finally, *metE7* lines were sub-cultured weekly over a period of 6 months in three different B_{12} conditions to test whether *metE7* could adapt to B_{12} auxotrophy and improve its growth and survival under limiting concentrations of B_{12}.

Over the long term, a B_{12}-dependent alga, by definition, will require a source of B_{12}, which in the natural environment will ultimately come from B_{12}-producing prokaryotes. In Chapter four I investigate how *metE7* grows in coculture with B_{12}-producing bacteria. Firstly, however, I test whether *M. loti* has any effect on wild-type *C. reinhardtii* and vice versa, because Kazamia et al. (2012) had previously found that *C. reinhardtii* would not support *M. loti* (Kazamia et al., 2012). Algal and bacterial growth and B_{12} production were then compared in cocultures of *M. loti* with *metE7* or B_{12}-independent strains of *C. reinhardtii*, and then also with *L. rostrata*. To test whether *metE7* and *M. loti* were limited in coculture by their partner's ability to provide their required nutrients, B_{12} or glycerol was added to batch and semi-continuous cocultures, and the changes in algal and bacterial cell density recorded. Grant et al., (2014) found that *M. loti* produced more B_{12} per cell when grown in coculture with *L. rostrata* (Grant et al., 2014), so to see whether the same was true of *metE7*, B_{12} concentrations in the media and cell fractions as well as *M. loti* cell densities were compared in axenic cultures and cocultures. To further investigate this, axenic cultures of *metE7* were added to axenic cultures of *M. loti* for a short incubation period before specifically removing *metE7* cells by filtration. The uptake of B_{12} from the media by *metE7* cells and any subsequent B_{12}

production by *M. loti* was then measured. Having explored *M. loti* B_{12} synthesis in cocultures I then examined the role of B_{12} release into the media, firstly with an *M. loti* mutant in a component of the B_{12} uptake system (*btuF)*, and subsequently in a *btuF* mutant of a strain of *E. coli* engineered to produce B_{12}. Finally, I investigated whether *M. loti* could produce enough B_{12} to favour the growth of a B_{12}-dependent strain of *C. reinhardtii* over a B_{12}-independent one.

In chapter five I discuss the results from the previous two chapters in a broader context and suggest experiments that could be performed to build on those results. I focus on the potential of developing *C. reinhardtii* as a model for algal C1-metabolism, how the active response to B_{12} deprivation appears rather limited and consider the conditions that might lead to the development of a highly cooperative mutualism between a newly evolved B_{12} auxotroph and B_{12}-producing bacteria.

v Figure 1.5 Microscope photographs of the green algae used in this work

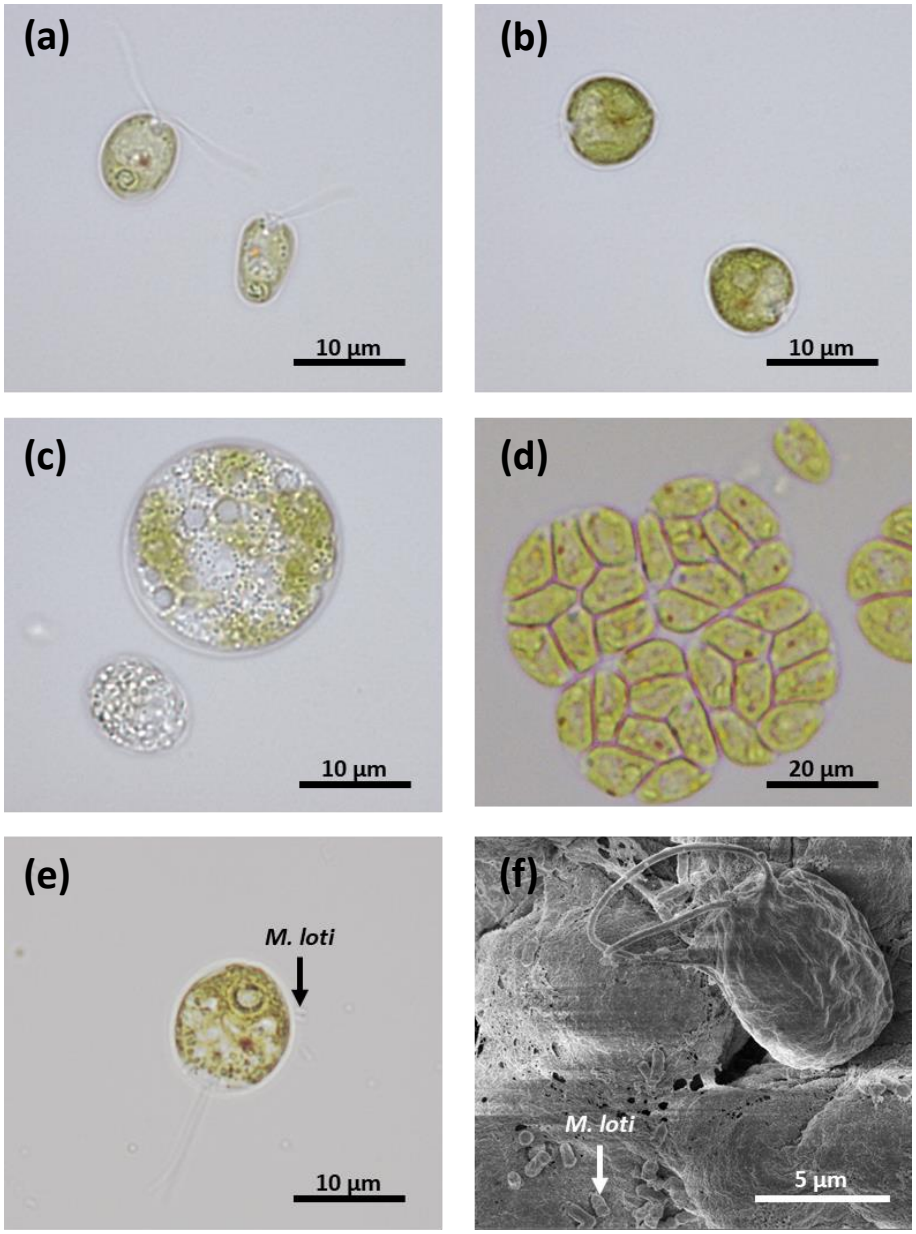

Figure 1.5 Microscope photographs of the green algae used in this work: **(a)** B_{12}-replete *C. reinhardtii metE7*; **(b)** B_{12}-replete *L. rostrata*; **(c)** B_{12}-deprived *metE7*; **(d)** Palmelloid of *metE7* cells after resupplying B_{12} to B_{12}-deprived cells; **(e)** Coculture of *metE7* and *M. loti*; **(f)** Scanning electron microscope photograph of a coculture of *metE7* and *M. loti.* In the lower two panels the location of one of the *M. loti* cells is denoted by an arrow, and in all panels the scale bars represent the length written immediately above them.

Chapter 2: Methods

2.1 Strains

Two closely related B_{12}-dependent chlorophyte algal strains were used in this study: *Lobomonas rostrata* (SAG 45/2), and *Chlamydomonas reinhardtii* (*metE7)*. *metE7* was derived from strain 12 of wild type 137c by experimental evolution: selection for rapid growth under 1000 $ng \cdot l^{-1}$ B_{12} produced a *metE* (B_{12}-independent methionine synthase) mutant via insertion of a type II transposable element, and subsequent incomplete transposition of the element left 9bp behind and produced a genetically stable B_{12}-dependent strain hereafter referred to as *metE7* (Helliwell et al., 2015).

Mesorhizobium loti, a soil dwelling rhizobium that forms facultative symbiotic relationships with legumes was used as a B_{12} producer in most coculture experiments with the B_{12}-dependent algae. Strain MAFF303099 was most commonly used, but a *btuF* and *bluB* mutant were also used. Two *Escherichia coli* coli strains, ED656 and ED662, were also used as B_{12}-producers, and were received as a gift from Dr. Evelyne Deery, University of Kent. Both strains synthesise B_{12}, but ED662 has a kanamycin resistance cassette inserted into the gene encoding *BtuF*. *Salmonella typhimurium* AR3612, a *metE* and *cysG* double mutant, was used in bioassays to determine the concentration of B_{12} in samples.

2.2 Algal and bacterial culture conditions

Algal colonies were maintained quarterly on Tris-acetate phosphate (TAP) (Kropat et al., 2011) + 1000 $ng \cdot l^{-1}$ cyanocobalamin (B_{12}) agar (1.5%) in sealed transparent plastic tubes at room temperature and ambient light. Colony transfer by spreading on the agar surface using sterile loops was performed in a laminar flow hood. To initiate liquid cultures colonies were picked and inoculated into filter-capped cell culture flasks (Nunc^{TM}, ThermoFisher), or 24 well polystyrene plates (Corning®Costar® Merck) containing TAP or Tris minimal medium at less than 60% volume capacity, and supplemented with a range of B_{12} concentrations. Cultures were grown under continuous light or a light-dark period of 16hr-8hr, at 100 $\mu E \cdot m^{-2} \cdot s^{-1}$, at a temperature of 25ºC, with rotational shaking at 120 rpm in an incubator (InforsHTMultitron; Basel, Switzerland).

For nutrient starvation experiments the pre-culture TAP media contained 200 $ng \cdot l^{-1}$ of B_{12}, and when cell densities surpassed $1*10^6$ $cells \cdot ml^{-1}$ or an OD730 nm of 0.2, cultures were washed by centrifugation at 2,000 g for 2 minutes, followed by supernatant removal and resuspension of the cell pellet in media lacking the nutrient (N or B_{12}), and the process repeated twice more. Cells were resuspended in cotton wool-stoppered 500 ml borosilicate conical flasks or nunc flasks to an OD730

nm of roughly 0.1. Cultures were grown as above for 96-120 hours with aliquots sampled for analysis daily.

Bacteria were maintained in glycerol stocks stored at -80°C. To prepare these for experiments cultures were grown to late log phase in liquid TY or LB media, centrifuged at 10,000 g for 2 minutes, the pellet resuspended in filter-sterilised 10% glycerol, and the microfuge tube dropped into liquid nitrogen for snap freezing followed by storage in a -80°C freezer. To initiate bacterial culture a small portion of the glycerol stock was removed by stabbing a pipette tip into the stock and spreading on LB and TY agar plates incubated at 37°C overnight or 28°C for 3 days for *E. coli* and *M. loti* respectively. After confirming the lack of contamination by colony morphology, colonies were picked and inoculated into nunc flasks containing Tris minimal medium with 0.1% glycerol. Axenic bacterial cultures were incubated under the same conditions as algal cultures, which are described above.

Cocultures of algae and bacteria were initiated by inoculating them into Tris minimal medium from axenic cultures where cell densities had been checked to ensure a ratio of roughly 1:20. In some cases cocultures were allowed to acclimate for several days before making a dilution based on the algal cell density and starting measurements.

2.3 Algal and bacterial growth measurements

Algal cell density and optical density at 730 and 750 nm were measured using a Z2 particle count analyser (Beckman Coulter Ltd.) with limits of 2.974-9.001 µm, and a FluoStar Optima (BMG labtech) or Thermo Spectronic UV1 spectrophotometer (ThermoFisher) respectively. Mean cell diameter was measured via image analysis of microscope photographs using a MATLAB algorithm written by Hannah Laeverenz-Schlogelhofer. These were taken at 100-200* magnification on an Olympus BX43 light microscope of 15 µl of culture between a microscope slide and cover slip. Dry mass was measured by filtering 20 ml of culture through pre-dried and weighed grade five whatmann filter paper (Sigma-Aldrich WHA1005090), drying at 70ºC for 24 hours, followed by further weighing on a Secura mass balance (Sartorius). Viability of algal cells was determined by 10-fold serial dilution of a culture aliquot in growth media and spotting 10 µl volumes on TAP + 1000 $ng \cdot l^{-1}$ B_{12} 1.5% agar plates, followed by incubation at 25ºC, 20 $\mu E \cdot m^{-2} \cdot s^{-1}$ of continuous light for 96 hours and then counting the number of single cells and colonies separately at 100* magnification. *M. loti* and *E. coli* colony forming unit (CFU) density was measured similarly but on TY or LB plates with incubation at 28ºC in the dark for 3 days or 37°C overnight respectively. *E. coli* ED662 was distinguished from ED656 by its kanamycin resistance and hence ability to grow on LB + 50 $\mu g \cdot ml^{-1}$ kanamycin plates. Single cells for all bacteria were too small to count with a light microscope. When

bacteria were grown axenically, optical density was also used as a proxy for cell density with measurements at 600 nm on a FluoStar Optima (BMG labtech) spectrophotometer.

2.4 Pigment quantification

A 1ml aliquot of algal culture with OD730 nm>0.1 was centrifuged at 2,000 g for 2 minutes, the supernatant discarded, and the cell pellet resuspended in 1 ml dimethylformamide. Pigments were extracted by vortexing for 10 minutes, centrifuging at 10,000 g for 2 minutes, and transfer of the supernatant to a 1.5 ml cuvette (Greiner Bio-one). Optical density at 480, 647 and 664.5 nm was measured using a Spectrophotometer (ThermoFisher) and using the equations by Inskeep and Bloom (Inskeep & Bloom, 1985) and Wellburn (Wellburn, 1994), chlorophyll A, chlorophyll B, and carotenoid concentrations were calculated.

$$Chl\ a = 12.70A_{664.5} - 2.79A_{647}$$

$$Chl\ b = 20.70A_{647} - 4.62A_{664.5}$$

$$Total\ Chl = 17.90A_{647} + 8.08A_{664.5}$$

$$Chl\ x + c\ (carotenoids) = \frac{1000A_{480} - 2.14Chl\ a - 70.16Chl\ b}{245}$$

2.5 Protein quantification

The cell pellet from 1 ml of culture was resuspended in 1 ml of 1 M NaOH and vortexed for 1 minute. The tube was incubated at 100ºC in a water bath for 5 minutes and left at room temperature to cool for 10 minutes. Tubes were centrifuged at 2000 g for 2 minutes and 30 µl of supernatant added to a 96 well clear microplate, followed by 270 µl of Bradford dye (Biorad), incubation at room temperature for 5 minutes, then absorption measured at 595 nm on a FluoStar Optima (BMG labtech), and compared with a standard curve of bovine serum albumin (BSA).

2.6 Amino acid analysis

10 ml of samples were centrifuged at 2,000 g for 2 minutes, supernatant removed, and cell pellet lyophilised at <-40ºC and <10 Pascals for 12-24 hours in a freeze drier (Edwards Pirani 501). The freeze-dried cell pellet was analysed by Dr. Deborah Salmon, University of Exeter, according to the protocol provided below:

5 mg of a freeze-dried sample of cultures were extracted in acetonitrile, and then re-extracted with 20% methanol spiked with an internal standard containing stable isotope-labelled amino acids (L-amino acid mix; Sigma-Aldrich). The supernatants were pooled, and amino acids were derivatised

with an AccQ•Tag Ultra derivatization kit (Waters Corp., Milford, MA, USA). HPLC-ESI-MS/MS quantitative analysis of the amino acids was performed using an Agilent 6420B triple quadrupole (QQQ) mass spectrometer (Agilent Technologies, Palo Alto, CA, USA). All ions were scanned in positive ion mode and given a dwell time of 50 ms. Data analysis was undertaken using Agilent Mass Hunter Quantitative analysis software for QQQ (v.B.07.01). Accurate quantification used the stable isotope-labelled internal standards added during sample extraction, and data were normalized to the DW of the samples.

2.7 SAM, SAH, and Methionine quantification

10ml of samples were centrifuged at 2,000 g for 2 minutes, supernatant removed, and cell pellet lyophilised at <-40ºC and <10 pascals for 12-24 hours. The freeze-dried cell pellet was analysed by Dr. Deborah Salmon, University of Exeter, according to the protocol provided below:

300 µl of 10% methanol (LC-MS grade) spiked with stable isotope-labelled amino acids (L-amino acid mix, Sigma-Aldrich, Co., St. Louis, MO, USA) was added to each sample. They were vortexed three times, every 10 min, before sonicating for 15 min in an iced water bath. After a final vortex, samples were centrifuged (16,100 x g) for 15 min at 4ºC. 150 µl of supernatant was transferred to glass MS vials. Samples were kept on ice throughout the extraction procedure, prior to being run on the LC-MS QQQ.

Quantitative analysis was performed using an Agilent 6420B triple quadrupole (QQQ) mass spectrometer (Agilent Technologies, Palo Alto, USA) coupled to a 1200 series Rapid Resolution HPLC system. 5 µl of sample extract were loaded onto a SeaQuant ZIC HILIC 100A, 3.5 µm, 2.1 x 150 mm analytical column (Merck, USA). For detection using positive ion mode, mobile phase A comprised 100% LC-MS grade acetonitrile with 0.15% formic acid and mobile phase B was 100% water (LC-MS grade) with 0.15% formic acid and 5 mM ammonium formate. The following gradient was used: 0 min – 20% B; 17 min – 80% B; 20 min – 80% B; 21 min – 20% B; followed by a 9 minute re-equilibration time. The flow rate was 0.2 ml min^{-1} and the column temperature was held at 35 °C for the duration. The QQQ source conditions for electrospray ionisation were as follows: gas temperature was 350°C with a drying gas flow rate of 11 $l \cdot min^{-1}$ and a nebuliser pressure of 35 psig. The capillary voltage was 4 kV. The fragmentor voltage and collision energies were optimised for each compound. Data analysis was undertaken using Agilent MassHunter Quantitative Analysis software (version B.01.7.01). Methionine concentrations were calculated using the spiked labelled methionine (5 µM) in each sample. Concentrations of the other compounds were calculated using calibration curves produced from standard concentration dilutions. Data was normalised to the spiked labelled glycine (50 µM) internal standard, and then to the dry weight of each sample.

2.8 Starch quantification

The cell pellet from 1 ml of sample was resuspended in 1ml acetone, vortexed for 5 minutes, pelleted by centrifugation at 10,000 g for 2 minutes, and resuspended in 1ml deionised H_2O. Total starch from this sample was quantified using a commercial amyloglucosidase enzymatic kit (starch assay kit SA-20; Sigma-Aldrich) according to the manufacturer's instructions.

2.9 Lipid analysis

All chemicals were purchased from Sigma-Aldrich, unless stated otherwise. Lipid extraction was based on a modified Bligh and Dyer method (Bligh & Dyer, 1959; Horst et al., 2012). To extract the total lipids, 10 ml of culture was centrifuged at 2000g for 2 minutes, the supernatant removed, 10 ml of chloroform-methanol (2:1, v/v) added to the pellet, and the tube was vortexed for 15 seconds and sonicated for 30 minutes in ice water. Prior to extraction, samples were spiked with 1 $mg \cdot ml^{-1}$ C15:0 pentadecanoic acid. 5 ml of deionized water was added followed by centrifugation at 1000 g for 3 minutes at 4ºC for phase separation. The lower chloroform phase was dried in a solvent evaporator (45°C; GeneVac EZ-2; SP Scientific, Ipswich, United Kingdom) and resuspended in 200 µl n-heptane (Escobar Galvis et al., 2001). Triacylglycerides, polar lipids, and free fatty acids in the crude total lipid extract were analysed by gas chromatography (GC)-flame ionization detection (FID) with a Varion Select Biodiesel for glycerides GC metal column (10 m by 0.32 mm; film thickness, 0.1 µm; part number CP9076; Agilent Technology)(Horst et al., 2012). TAGs were identified and quantified by comparison to a glyceryl tripalmitate standard.

The total lipid fractions of the samples were converted to fatty acid methyl esters (FAMEs; acid catalyzed) as described by Stephenson et al. (Stephenson et al., 2010). The FAMEs were separated and identified using gas chromatography (TraceGCUltra; Thermo Scientific) with a Zebron ZB-Wax capillary GC column (30m by 0.25 mm; film thickness, 0.25 µm; Phenomenex, United Kingdom). The injection volume was 1 µl with a 35:1 split ratio, the injector temperature was 230°C, and helium was used as the carrier gas at a constant flow rate of 1.2 ml min^{-1}. The following gradient was used: initial oven temperature, 60°C for 2 minutes and then an increase to 150°C at 15°C min^{-1} and to 230°C at 3.4°C min^{-1}. The detector temperature was 250°C. FAMEs were identified by mass spectrometry and were quantified by comparison with a methyl octadecanoate standard.

2.10 Transcript quantification

RNA extraction was performed on the liquid nitrogen frozen cell pellet from 10 ml of algal culture using the RNeasy® Plant Mini Kit (QIAGEN). Cells were initially lysed by resuspension in 450 µl buffer RLT + 1% v/v Beta-mercaptoethanol, addition of acid-washed autoclaved glass

microbeads and vortexing in 4*10 second intervals at 4ºC. Manufacturer's instructions were then followed. DNase treatment was carried out using TURBO DNA-free™ kit (Ambion), and cDNA synthesis using SuperScript®III First-Strand synthesis system for RT-PCR (Invitrogen) according to the manufacturer's instructions. RNA concentration and purity were quantified using a nanodrop spectrophotometer measuring absorbance from 230-280 nm. DNase treatment was assessed by testing whether PCR would amplify any products after DNAse treatment but before cDNA synthesis. For quantitative PCR, SYBR® Green JumpStart™ Taq ReadyMix™ was used with 0.2 µl cDNA and a final concentration of 0.5 µM of each primer in a 10 µl total reaction volume in a Rotor-Gene Q real-time PCR machine (QIAGEN). The qPCR program involved a 5 minute 95ºC initial denaturation followed by 40 cycles of 95ºC for 10 seconds, 55ºC for 15 seconds, 72ºC for 25 seconds, with a final extension at 72ºC for 90 seconds. Melt curves were generated following directly on from the final extension by increasing the temperature from 72 to 95°C in 1°C steps held for 5 seconds each. Primers (described in appendix) were designed to anneal across exon-intron boundaries where possible to prevent amplification from any remaining gDNA, and otherwise designed to anneal to separate exons so that products from gDNA would be larger than the 100-200bp expected from cDNA and so could be distinguished by gel electrophoresis. Amplification efficiency and PCR cycle at which fluorescence reached a threshold value were calculated using Rotor-Gene Q software v2.02. Amplification efficiency was also calculated using a calibration curve based on serial dilutions of cDNA and was found to be significantly higher at 1.9-1.98 than the values reported by the Rotor-Gene Q software. Therefore, although the Pfaffl method for relative quantification of transcripts was used, the default (and highest) amplification efficiency of 2.0 was used (Pfaffl, 2001). Several housekeeping genes were initially investigated, including RACK1, RPL10A, EEF1, ACTIN, H2B, UBQ, GTF5, but finally just RACK1 was selected as being representative of the others.

2.11 Reactive oxygen species quantification

2 µl of 1 mM 2',7' Dichlorofluorescein diacetate (Sigma-Aldrich) dissolved in DMSO was added to 198 µl of cell culture in a black f-bottom 96 well plate (Greiner bio-one) and incubated at room temperature in the dark for 60 minutes before recording fluorescence at 520 nm after excitation at 485 nm in a FluoStar Optima Spectrophotometer (BMG labtech). Fresh cell culture media devoid of any cells was used as a blank.

2.12 Photosynthetic parameter measurement

200 µl of cultures with an OD730 nm>0.1 were transferred to a 96 well plate which was then incubated at 25°C in the dark for 20 minutes within the CF imager (technologica). F_0 was measured prior to, and F_m during, a saturating pulse at 6172 $\mu E \cdot m^{-2} \cdot s^{-1}$. The light intensity was increased to 4

$\mu E \cdot m^{-2} \cdot s^{-1}$ and the cells allowed to acclimate for 30 seconds prior to another set of fluorescence measurements before and during a saturating pulse. This was repeated in increasing steps of light intensity: 8, 16, 32, 64, 128, 256, 512, 1024, and 2000 $\mu E \cdot m^{-2} \cdot s^{-1}$. From these fluorescence measurements the CF imager software calculated Non-photochemical quenching (*Fm/Fm'-1*), PSII maximum efficiency (*Fv'/Fm'*), and the coefficient of photochemical quenching (*Fq'/Fv'*) at each light intensity.

2.13 Vitamin B_{12} quantification

Prior to B_{12} quantification, cultures were separated into fractions. In most cases 1.15 ml of culture was centrifuged at 10,000 g for 2 minutes, 1.1 ml of the supernatant was aliquoted into a fresh tube, and 1.1 ml of fresh media was used to resuspend the cell pellet. To measure B_{12} uptake by *C. reinhardtii* and *L. rostrata* over short time periods the algae were inoculated into syringes capped with 0.4 µm filters and the filtrate (representing the media as no cells were present) collected at various time intervals.

Vitamin B_{12} was quantified by measuring the growth of a B_{12}-dependent *Salmonella typhimurium* strain AR3612 when incubated with a certain dilution of the sample of interest. AR3612 was inoculated from a glycerol stock and spread on an M9-based (Recipe in Appendix) agar plate, that was then incubated at 37°C overnight (12-24 hours). 1 ml of 0.9% NaCl solution was added to the plate, the colonies scraped into suspension and transferred to a 1.5 ml microfuge tube. The tube was centrifuged at 16,000 g for 1 minute, supernatant removed, 1 ml of 0.9% NaCl solution added to resuspend the pellet, and the process repeated twice more. Washed AR3612 cells were inoculated into 2*M9 media (Recipe in Supp. Table 1) at a 2000-fold dilution.

1.1 ml of the sample of interest was aliquoted into a microfuge tube, placed in a boiling water bath for 15 minutes, centrifuged at 16,000 g for 1 minute, and a volume of supernatant inversely proportional to its estimated B_{12} concentration added to a 24 well plate. This bioassay has optimal accuracy for solutions with B_{12} concentrations between 5 and 200 $pg \cdot ml^{-1}$ when 1ml is added to the 24 well plate. For solutions predicted to have greater concentrations, lower volumes were added and made up to 1ml with deionised water. To this 1ml solution, 1 ml of 2*M9 media inoculated with washed AR3612 was added. In parallel to this, 1 ml volumes with known B_{12} concentrations between 0 and 300 $pg \cdot ml^{-1}$ were added to a 24 well plate to create the standard. Plates were incubated at 37°C for 16 hours and optical density at 600 nm recorded. Using a logistic equation to connect the optical density and B_{12} concentration of the known solutions, the optical density of wells to which the samples had been added could be converted to a B_{12} concentration.

2.14 Artificial Evolution setup

A culture of *metE7* cells was plated on TAP +1000 ng·l^{-1} B_{12} agar, then eight colonies picked and resuspended in TAP + 200 ng·l^{-1} B_{12} in a 96 well plate. Each well was split into three wells, each in a different 96 well plate containing 200 µl of a different media: TAP +1000 ng·l^{-1} $B_{12,}$ TAP +25 ng·l^{-1} B_{12}, and Tris minimal medium. *M. loti* was prepared in a similar manner to *metE7*, except preculturing was performed in Tris min + 0.01% glycerol. *M. loti* was added to the Tris min culture containing *metE7* at a density roughly 20 times greater than the alga. The 96 well plates were incubated at 25°C, under continuous light at 100 µE·m^{-2}·s^{-1}, on a shaking platform at 120 rpm. Each week the cultures were diluted: Those in TAP +1000 ng·l^{-1} B_{12} were diluted 10,000-fold, TAP +25 ng·l^{-1} B_{12} = 100-fold, and Tris min = 5-fold. Every three weeks 10 µl of serial dilutions of each culture was also spotted onto TAP agar + Ampicillin (50 µg·ml^{-1}) and Kasugamycin (75 µg·ml^{-1}) and TAP agar + 1000 ng·l^{-1} B_{12} to check for B_{12} independent revertants, and to act as a reserve should revertants or other contamination occur later. If cultures were found to be contaminated or contain revertants, then at the next transfer they were replaced by colonies from the same well that had grown on the TAP agar plates. At two points during the 7-month evolution period all cultures were transferred to TAP agar plates where they were stored for 2 weeks during an absence from the lab, meaning that the total time in liquid culture was 6 months.

2.15 Statistics and mathematical models

Shapiro-Wilk test: Many parametric tests, such as Welch's t-test and Tukey's range test assume that the intra-group data shows a normal distribution about the mean. To satisfy this assumption of normality the Shapiro-Wilk test was used and those groups with critical p-values rejected. The significant p-value per test was adjusted using the Sidak correction to maintain the family wise error rate at 0.05. If at least one group of data was shown to differ significantly from a normal distribution, then all the data was log-transformed and the Shapiro-Wilk test repeated. The function used in R was 'shapiro.test()'.

Bartlett's test: Tukey's range test also requires the groups of data being compared to show homoscedasticity. To satisfy this assumption Bartlett's test was applied, and any data with a p-value<0.05 was log-transformed and retested. Only those data with p>0.05 were subsequently tested for a difference in means with a parametric test e.g. Tukey's range test. The function used in R was 'bartlett.test()'.

Welch's T-test: This test was used to determine if there was a significant difference in the means of two groups both containing data that was normally distributed. The function used in R was 't.test()'.

ANOVA: This test was used to determine if there was a significant difference in the means of more than two groups each containing data that was normally distributed. The function used in R was 'aov()'

Tukey's range test: When an ANOVA had reported a significant difference in the means of groups of data ($p<0.05$), Tukey's range test was used to make all pairwise comparisons between groups and report on their statistical significance. The function used in R was 'HSD.test()'.

Backward stepwise elimination: Linear models were used to explain the relationships between B_{12} concentration, *M. loti* cell density, and whether the culture contained *metE7*. Starting with a linear model where B_{12} concentration was explained by the interaction between *M. loti* density and presence of algae, the interaction term was removed first, followed by the least significant (highest p-value) of the two additive terms. The Bayesian information criterion (BIC) was calculated for each model, as was the adjusted R^2 value and ANOVA result for the difference between two models connected by the removal of one term. The model with the lowest BIC value was selected.

Verhulst equation: This was used to fit a model to the optical density data of algal cultures over time grown under different B_{12} concentrations. $N = \frac{KN_0e^{rt}}{K+N_0(e^{rt}-1)}$

Michaelis-Menten equation: This was used to fit optical density data of algae over different B_{12} concentrations. The optical density data was either used from the final timepoint of growth or was the predicted carrying capacity (K) from the Verhulst equation above. $V = \frac{V_{max}[S]}{K_m+[S]}$

4 parameter logistic equation: This was used to fit optical density data of *S. typhimurium* over different B_{12} concentrations and was found to be more accurate than the Michaelis-Menten equation. Rearranging the formula to make $[B_{12}]$ the subject allowed conversion of optical densities of the samples to B_{12} concentrations. $y = D + \frac{A-D}{1+(\frac{x}{C})^B}$ and rearranged $x = c(\frac{a-y}{y-D})^{\frac{1}{B}}$

Chapter 3: Coping with B_{12} auxotrophy in the short term

3.1 Introduction

Chlamydomonas reinhardtii is a unicellular, biflagellated, photosynthetic, soil-dwelling microalga (Merchant et al., 2007). In this environment macro and micro-nutrients can be heterogeneously distributed, and abiotic factors such as temperature and light intensity can vary dynamically and drastically over diurnal and annual cycles (Fierer, 2017). As *Chlamydomonas* is a mixotroph, with the ability to survive as a heterotroph or photoautotroph, it is considered a model system for improving our understanding of both photosynthesis and dark fermentation (Dubini et al., 2009; Rochaix, 1995). *Chlamydomonas* has also been found to have sophisticated mechanisms for acclimating to macro and micro nutrient deficiencies (Grossman, 2000). Some of these responses are specific to the limiting nutrient, such as increasing expression of high-affinity transporters, increasing the recycling of that nutrient, and reducing its use where possible (González-Ballester et al., 2010; Saroussi et al., 2017). Others however, are more general and are common to most if not all nutrient limitation responses. These include a down-regulation of photosynthesis, a decrease in growth and cell division, and an increase in storage compounds such as starch and triacylglycerides (Saroussi et al., 2017; Wykoff et al., 1998).

Chlamydomonas reinhardtii itself does not absolutely require vitamin B_{12}, but many of its close relatives in the Volvocales do, including *Volvox carteri, Gonium pectorale*, and *Lobomonas rostrata* (Helliwell et al., 2011). The metabolic reason for their B_{12} requirement is the lack of a B_{12}-independent methionine synthase (METE), which renders them reliant on B_{12} as a cofactor for the alternative methionine synthase enzyme (METH) (Helliwell et al., 2011). Despite being independent, *C. reinhardtii* still appears to respond to vitamin B_{12} by downregulating the expression of at least three proteins, METE, S-adenosylhomocysteine hydrolase (SAH1), and serine hydroxymethyltransferase 2 (SHMT2) (Helliwell et al., 2014). *Phaeodactylum tricornutum* is similar to *Chlamydomonas* in that it has the ability to use B_{12} without being dependent upon it, and was also found to show little difference in overall gene expression in the presence of B_{12} (Bertrand et al., 2012). One of the proteins that was suppressed by high levels of B_{12} however, was found to have a role in the high affinity uptake of vitamin B_{12} and therefore called cobalamin acquisition protein 1 (CBA1). No proteins involved in the uptake of vitamin B_{12} in *Chlamydomonas* are well characterised, although there is some evidence that a pherophorin in the cell wall binds B_{12} (Croft 2005).

Helliwell et al. (2015), generated a *metE* mutant of *Chlamydomonas* by artificial evolution in conditions of high vitamin B_{12} concentration (Helliwell et al., 2015). This mutant was completely

reliant on B_{12} for growth, but in the presence of the vitamin it had a slight growth advantage over its B_{12}-independent progenitor. Further characterisation of the mutant showed that it had acquired a type II Gulliver-related transposable element (GRTE) in the 9th exon of the *METE* gene. Certain isolates of the mutant were found to revert to B_{12} independence, and in all cases analysis of the *METE* gene found that the GRTE had excised completely, restoring the wild type sequence. Sequencing over the insertion site in colonies that remained B_{12}-dependent identified one (#7) that lacked most of the GRTE, but importantly retained nine nucleotides at the site of insertion, which appeared to prevent *METE* translation. This mutant, which was unable to revert to B_{12} independence, was called *metE7* and has been the focus of this thesis.

In this chapter I characterize the responses of *metE7* to various concentrations of vitamin B_{12} and compare it to the responses of its ancestral B_{12}-independent strain. I then go on to compare the mutant with a closely related B_{12} auxotroph, *Lobomonas rostrata*. During B_{12} deprivation of *metE7* I quantify changes in gene expression, cellular composition, photosynthetic activity, and viability, and contrast these with changes under nitrogen deprivation, which are known to protect against cell death. Finally, I compare strains of *metE7* that underwent a further period of experimental evolution for 6 months under three different B_{12} conditions to see whether *Chlamydomonas* can improve its survival during B_{12} deprivation within a relatively short period of time.

3.2 Results

3.2.1 Comparing a B_{12} auxotroph with its B_{12}-independent ancestor

C. reinhardtii metE7 had previously been shown to require B_{12} for growth (Helliwell et al., 2015), but to quantify this more precisely, growth under a range of B_{12} concentrations was tested to develop a dose-response curve. The maximum culture density achieved under three trophic conditions was measured for *metE7* as well as two B_{12}-independent lines: the ancestral strain and a phenotypic revertant. Tris minimal medium was used for photoautotrophic conditions and TAP media for heterotrophic and mixotrophic conditions, and cells were inoculated at approximately 100 cells·ml^{-1}. Light intensity and duration of 100 µE·m^{-2}·s^{-1} and 24 hours was used for the mixotrophic and photoautotrophic conditions; heterotrophic cultures were maintained in darkness except for 5 minutes per day for inspection and measurement of optical density. After 6 days under mixotrophic conditions or 8 days otherwise, the optical density of cultures had stopped increasing and cell density was measured. Figure 3.1 shows a clear dose-response for *metE7* where cell density is limited by B_{12} below a certain value, which is dependent on the culture condition. The concentration of B_{12} at which the cell density was half the value achieved under replete B_{12} (EC_{50}) was 11 ng·l^{-1} for both heterotrophic and photoautotrophic conditions and 95 ng·l^{-1} for mixotrophic conditions. At

concentrations of B_{12} roughly twice these values *metE7* reaches similar densities to the ancestral and revertant lines in all three media. As expected from previous studies (Moon et al., 2013), this is higher in mixotrophic culture than in either heterotrophic or photoautotrophic conditions. Across these conditions under replete B_{12} the ancestral line grew to a slightly higher density than the revertant, and *metE7* reached an intermediate level. Both the ancestral and revertant lines showed little response to vitamin B_{12} concentration, but there was a slight reduction in the densities of the revertant line by high B_{12} concentrations. Measurements of vitamin B_{12} in freshwater have shown that concentrations are usually below 15 $ng \cdot l^{-1}$, hence *metE7* would most likely be limited for vitamin B_{12} under normal environmental conditions (Daisley, 1969; Ohwada, 1973).

Figure 3.2a illustrates how the methionine and folate cycles are linked by the action of methionine synthases, or in the case of *metE7*, just the B_{12}-dependent METH isoform. B_{12} deprivation is therefore likely to limit growth of *metE7* by restricting the transfer of methyl groups from methyl-tetrahydrofolate to homocysteine. To test this hypothesis, B_{12} sufficient (200 $ng \cdot l^{-1}$) cultures of the ancestral and *metE7* strains were washed and transferred to B_{12} replete (1000 $ng \cdot l^{-1}$) and deprived (no B_{12}) conditions and incubated for 30 hours. The cultures were then pelleted by centrifugation and lyophilised overnight before being sent to Dr. Deborah Salmon at the University of Exeter who measured methionine cycle metabolites by High performance liquid chromatography coupled to mass spectrometry (HPLC/MS). Homocysteine concentrations were too low to be accurately measured, but methionine, S-adenosylhomocysteine (SAH) and S-adenosylmethionine (SAM) were quantified (Figure 3.2b). B_{12} deprivation had no effect on the metabolites in the ancestral line, where levels of all three were identical in the presence or absence of B_{12}. However, in *metE7* B_{12} deprivation increased both methionine and SAH concentrations without altering the level of SAM. This resulted in a 10-fold decrease in the SAM:SAH ratio from 32 to 3.1. The SAM:SAH ratio is often termed 'methylation potential' due to the fact that SAM is a universal methyl donor, and SAH is a competitive inhibitor of these methylation reactions (Melnyk et al., 2000). The interconversion of homocysteine and S-adenosylhomocysteine is catalysed by S-adenosylhomocysteine hydrolase, a reversible reaction with an equilibrium that favours the production of S-adenosylhomocysteine (Palmer & Abeles, 1979; Turner et al., 2000). Under normal conditions the methionine cycle operates by maintaining low levels of homocysteine, but with flux impeded at the methionine synthase step in *metE7* during B_{12} deprivation it was expected that homocysteine would accumulate and cause an increase in S-adenosylhomocysteine. Reduced flux through methionine synthase was predicted to cause the concentration of methionine and SAM to decrease, however, this was not the case and might indicate a reduced use of methionine, for example, in protein synthesis.

vi Figure 3.1 Growth of *C. reinhardtii* lines in different trophic conditions and B_{12} concentrations

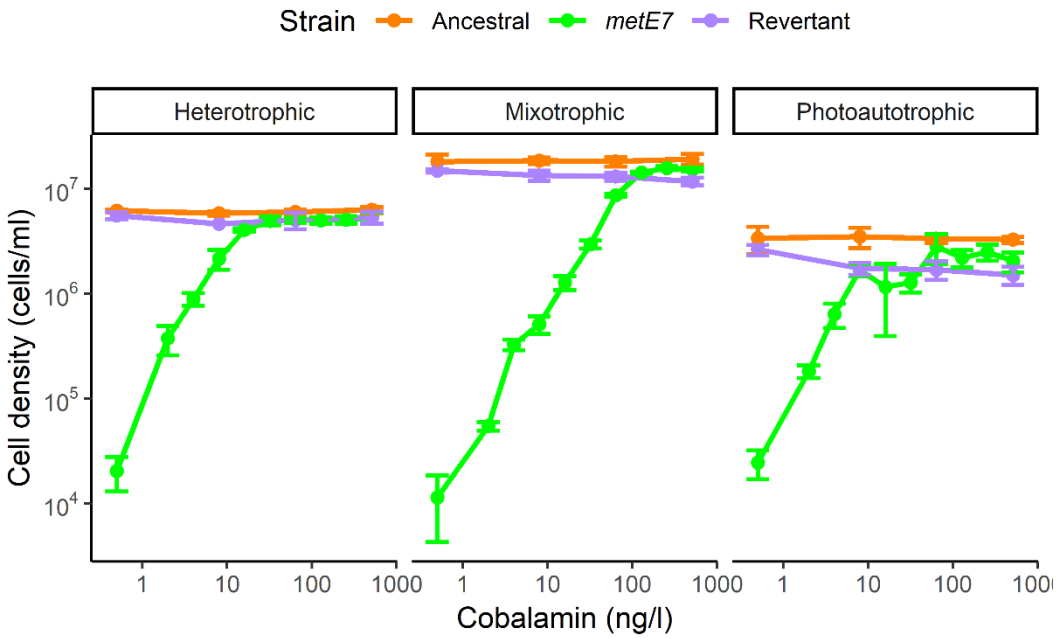

Figure 3.1. Maximum cell density achieved by three lines of *C. reinhardtii* in different trophic conditions and a range of Cobalamin (B_{12}) concentrations. The three lines include the 'ancestral' line prior to experimental evolution, '*metE7',* a stable B_{12}-dependent line, and 'revertant', a B_{12} independent line that had reverted from a B_{12}-dependent line. Cultures were grown heterotrophically (TAP medium in the dark), mixotrophically (TAP medium in continuous light), and photoautotrophically (Tris minimal medium in continuous light). B_{12} concentrations ranged from 0.5 to 512 ng·l^{-1} and precultures of the algae, which were grown with 200 ng·l^{-1} B_{12}, were washed thrice and inoculated at a density of roughly 100 cells·ml^{-1}. Cell density was measured by particle counter after 6 days of growth for mixotrophic cultures or 8 days for heterotrophic and photoautotrophic conditions. Orange = Ancestral, Green = *metE7,* Purple = Revertant, error bars = sd, n=3.

vii Figure 3.2 Metabolites and enzymes of the C1-cycle in *C. reinhardtii*

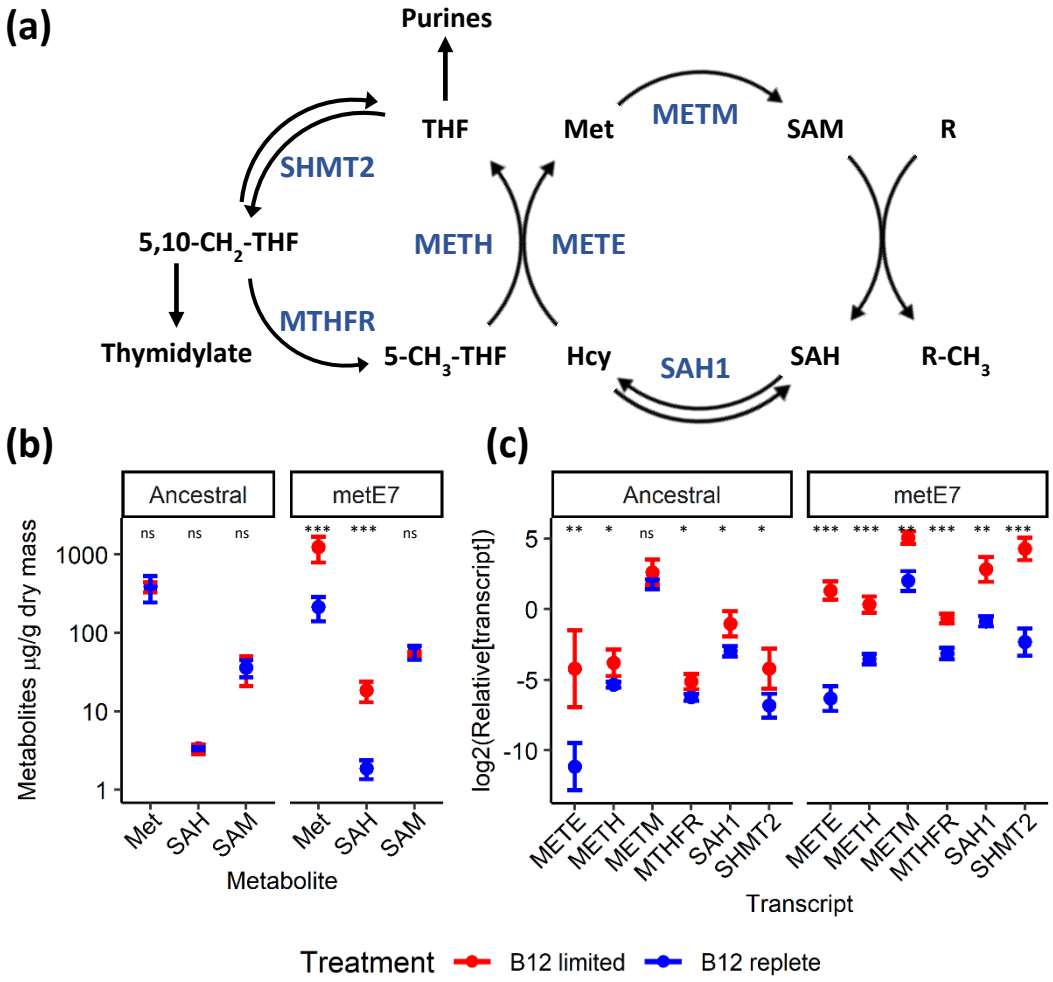

Figure 3.2 Metabolites and enzymes of the C1-cycle in *C. reinhardtii.* **(a)** Metabolic map of a portion of the C1 cycle centred around METE and METH, with enzyme abbreviations in blue, metabolite abbreviations in black, and arrows depicting enzyme-catalysed reactions. **(b)** Abundance of 3 methionine cycle metabolites measured by HPLC in the ancestral line and *metE7* in B_{12} replete (blue) and deprived (red) conditions after 30 hours of growth. **(c)** Abundance of 6 transcripts for enzymes of the C1 cycle measured by RT-qPCR on RNA extracted from the ancestral line and *metE7* in B_{12} replete (blue) and deprived (red) conditions after 30 hours of growth. Error bars = sd, n=3-4. Abbreviations: Met = Methionine, SAH = S-adenosylhomocysteine, SAM = S-adenosylmethionine, METE = B_{12}-independent methionine synthase, METH = B_{12}-dependent methionine synthase, METM = S-adenosylmethionine synthetase, MTHFR = methylenetetrahydrofolate reductase, SAH1=S-adenosylhomocysteine hydrolase, SHMT2=Serine hydroxymethyltransferase 2.

Three enzymes, METE, SAH1, and SHMT2, were found by Helliwell et al. (2014) to be downregulated in *C. reinhardtii* on addition of B_{12} (Helliwell et al., 2014). These catalyse three reactions adjacent to one another in the C1 cycle (Figure 3.2a). In addition to these, a further three enzymes that catalyse C1 cycle reactions adjacent to methionine synthase were chosen for quantification in B_{12} replete and deprived conditions. RNA was extracted from the same samples used for analysis of methionine cycle metabolites, and after reverse transcription the cDNA was used in quantitative PCR to infer transcript abundances (Figure 3.2c). These levels were normalised to the commonly used housekeeping gene RACK1. In the ancestral line, the three most upregulated transcripts under B_{12} deprivation relative to B_{12} replete conditions were the ones previously identified by Helliwell et al., METE, SHMT2, and SAH1 at 170, 7.0 and 4.4-fold respectively (Figure 3.2b). The other three, METH, MTHFR, and METM, were upregulated to a lesser extent of 3.4, 2.2 and 2.0-fold respectively. In *metE7* all six transcripts also increased under B_{12} deprivation, but the magnitude of the increase was greater for all genes except for METE, which at 190-fold was not significantly greater than the ancestral line. The upregulation of SHMT2, SAH1, MTHFR, and METM transcripts in the ancestral line under B_{12} deplete conditions might be in response to limited flux through the pathway, which would indicate that METE activity cannot fully substitute for METH activity under B_{12} replete conditions. In *metE7* this upregulation is more extreme, particularly for SHMT2 at 94-fold, but because B_{12} is clearly the limiting factor it would be ineffective in maintaining the methionine cycle.

3.2.2 Comparing a recently evolved and a natural B_{12} auxotroph

The ancestral and *metE7* line showed clear differences in their responses to B_{12} in terms of C1 cycle metabolites and transcripts, which was unsurprising considering that methionine synthesis is vital for metabolism. Perhaps a fairer comparison with *metE7* might therefore be another alga lacking *METE*. *Lobomonas rostrata* is a closely related green alga with similar physiology (Belcher & Swale, 1961; Croft et al., 2005; Helliwell et al., 2016; Kazamia et al., 2012). Previous work in our laboratory sequenced the *L. rostrata* transcriptome and comparison of the transcripts with those of sequenced algae found that it is most closely related to *C. reinhardtii* and *V. carteri*, both in the Volvocales (Helliwell et al., 2018). *metE7* and *L. rostrata* were inoculated at 10,000 cells·ml^{-1} and grown under mixotrophic conditions, i.e. TAP media in constant illumination at 100 µE·m^{-2}·s^{-1} for 5 and 9 days respectively before quantification of culture density on a spectrophotometer. Comparing the carrying capacities of each species showed that at high levels of vitamin B_{12} *metE7* grows to a higher density, while at lower levels, below 60 ng·l^{-1}, *L. rostrata* achieved the higher density (Figure 3.3a). Together these factors meant that *L. rostrata* had a considerably lower concentration required to reach half its maximum capacity (EC_{50}). This lower EC_{50} might be advantageous under the majority of environmental conditions where B_{12} is frequently below 20 ng·l^{-1} (Daisley, 1969; Daisley & Fisher,

1958; Ohwada, 1973; Ohwada & Taga, 1972; Panzeca et al., 2009; Sañudo-Wilhelmy et al., 2014), and so may reflect natural selection for increased growth at low concentrations of B_{12}.

Another way of surviving extended periods of low vitamin B_{12} might be by storing significantly more B_{12} than the minimum requirement for growth. *L. rostrata* and *metE7* were saturated with B_{12} by culturing them in TAP media with 10 $\mu g \cdot l^{-1}$ of B_{12} for 24 hours before pelleting the cells, washing them thrice, and then resuspending them in TAP media. Optical density of the cultures was then followed for 12 days with a 10-fold dilution required at day 6 to allow the culture to continue growing until it was limited by B_{12}. *metE7* grew more quickly but stopped growing after 2 days (Figure 3.3b). *L. rostrata* growth on the other hand, continued for 10 days and reached an optical density roughly 10 times greater than *metE7*. Together these results suggest that *metE7* would frequently be limited by the concentration of B_{12} in the environment and that *L. rostrata* provides one example of a natural B_{12} auxotroph which is unsurprisingly better adapted to survival under these conditions.

To investigate whether the improved growth of *L. rostrata* at low B_{12} was a product of increased uptake, B_{12} absorption from media with various starting B_{12} concentrations was measured for both *metE7* and *L. rostrata*. After incubating the algal cells at an optical density of 0.01 in 1 ml of TAP media containing known concentrations of B_{12} for 1 hour, the cells were pelleted by centrifugation and the supernatant used for measuring the remaining B_{12} concentration using the bioassay with a *metEcysG* mutant of *Salmonella typhimurium*. B_{12} uptake was subsequently calculated by subtracting the amount of B_{12} remaining in the media from the initial amount of B_{12} added. The results (Figure 3.3c) showed that although uptake varied considerably between replicates of each species, B_{12} uptake increased as its initial concentration increased and saturated at around 150 $ng \cdot l^{-1}$ B_{12}. Despite there being no statistically significant difference in B_{12} uptake at any one concentration of B_{12} between the species, the trend was for *L. rostrata* to take up more B_{12} at low concentrations and less B_{12} at high concentrations, suggestive of a higher affinity and lower capacity uptake system. Further testing with a larger number of biological replicates and under greater variety of conditions could help to identify whether this difference indeed exists. Nonetheless, there was some further evidence that B_{12} uptake differed between *metE7* and *L. rostrata*. Cultures with an optical density of 0.01 were inoculated with either 10 or 100 $ng \cdot l^{-1}$ B_{12} and maintained in suspension in syringe bodies for a 4-hour period. During this period small volumes of culture were pressed through a 0.4 µm filter at various intervals and the B_{12} concentration of this filtrate (representing cell-free media) measured as before (Figure 3.3d). When B_{12} concentrations started at 100 $ng \cdot l^{-1}$ uptake was rapid for both species with most occurring in the first 10 minutes. Uptake by *L. rostrata* was lower and saturated more quickly than for *metE7* at this higher starting concentration. However, when starting at 10 $ng \cdot l^{-1}$, uptake by *L. rostrata* was greater than that of *metE7*.

viii Figure 3.3 Comparison of the response of *metE7* and *L. rostrata* to vitamin B_{12}

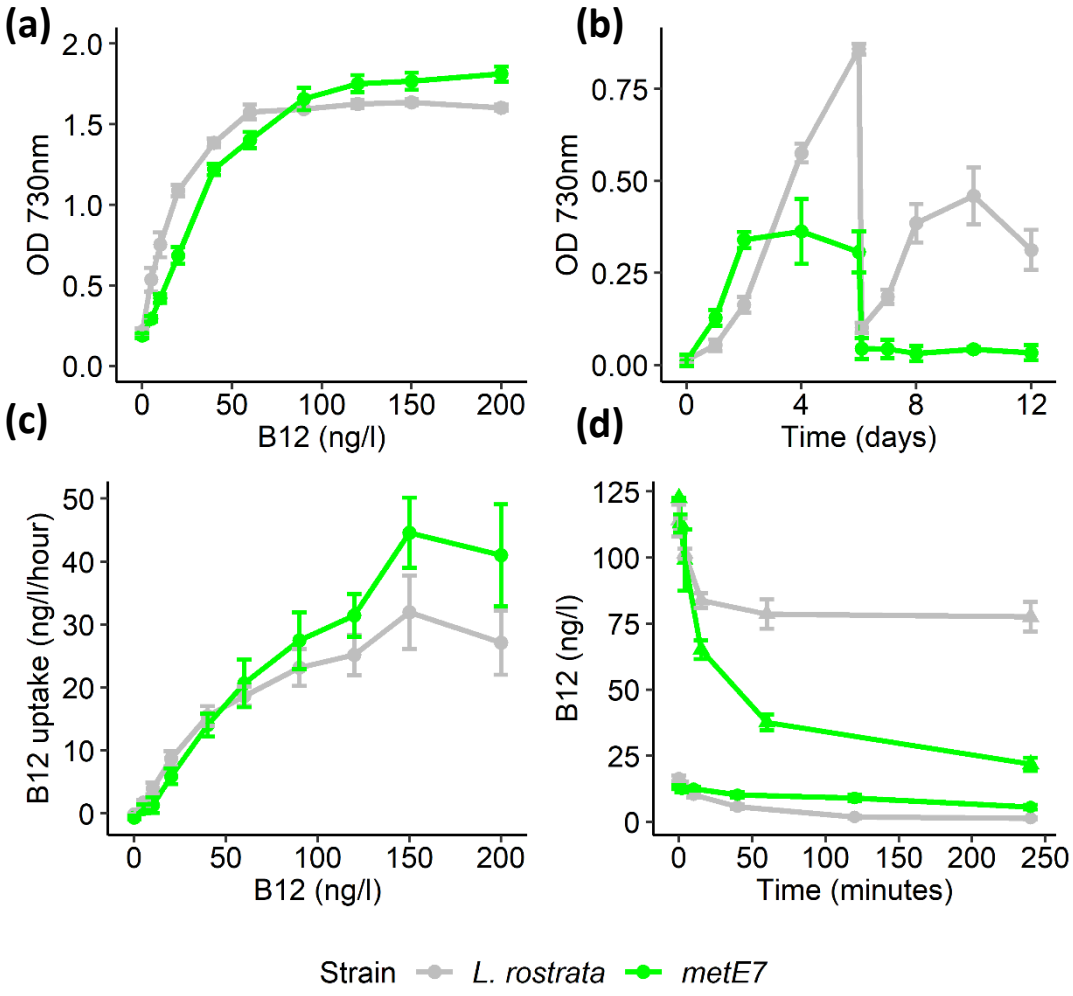

Figure 3.3 Comparison of the response of *metE7* and *L. rostrata* to vitamin B_{12}. **(a)** Cell density achieved after 5 or 9 days of growth for *metE7* or *L. rostrata* respectively in TAP media containing a range of B_{12} concentrations. **(b)** Algae saturated with vitamin B_{12} by preculturing in 10,000 ng·l^{-1} B_{12}, were washed and resuspended in TAP media lacking B_{12} and allowed to grow for 12 days, with a 10-fold dilution occurring on day six. **(c)** Vitamin B_{12} taken up from the media after inoculating algae at an optical density of 0.01 into TAP media with various B_{12} concentrations and allowing them to absorb B_{12} for 1 hour. **(d)** Vitamin B_{12} remaining in the media into which algae were inoculated at an optical density of 0.01 over a period of 4 hours, starting at either high (~100 ng·l^{-1}) or low (~10 ng·l^{-1}) concentrations of B_{12}. green = *metE7,* grey = *L. rostrata*, n>=4, error bars = sd, except for figure c for which error bars = std. error as various experimental results were combined.

3.2.3 Characterising the changes in cellular composition during B_{12} deprivation

The macromolecular composition of *C. reinhardtii* cells can change considerably under nutrient deprivation (Juergens et al., 2016). These changes are often very similar irrespective of the limiting nutrient (Grossman, 2000; Saroussi et al., 2017). Therefore, I hypothesized that B_{12} limitation would induce certain similar responses, such as an increase in energy storage compounds. *metE7* cells were precultured in TAP with sufficient B_{12} (200 $ng \cdot l^{-1}$) to reduce the subsequent carryover of stored vitamin, then washed and resuspended in TAP with or without 1000 $ng \cdot l^{-1}$ B_{12} and cultured for 4 days mixotrophically. Cultures were visually inspected by microscopy (Figure 3.4a), and cell density and diameter, which were measured daily (Figure 3.4b), were found to decrease and increase respectively on B_{12} deprivation relative to B_{12} replete conditions. The amounts of starch, proteins, pigments, triglycerides, free fatty acids, and polar lipids were measured in the middle and end of the growth period (day 2 and 4) (Figure 3.4c). Starch showed a substantial increase under B_{12} limited conditions making up roughly 30% of cell dry weight by day 2, compared to only 5% in the B_{12} replete treatment. Triglycerides had also increased to 3% and later 4.5% by day 4. Both the increase in these compounds and the relative timing of that increase, albeit the low time resolution of these measurements, were similar to those observed for *Chlamydomonas* under other nutrient deprivation conditions: Starch tends to increase earlier and more sharply than triglycerides (Juergens et al., 2016; Siaut et al., 2011). Although triglycerides increased, both polar lipids and free fatty acids decreased to such an extent that the overall lipid levels remained at roughly 8-10% of cell dry weight in both conditions. This might suggest that TAG accumulation during B_{12} deprivation is not a result of de novo fatty acid synthesis, but a result of transfer of fatty acids from membrane lipids. Protein levels declined under B_{12} deprivation to 15 and 10% of cell dry weight on days 2 and 4 respectively, while under B_{12} replete conditions they were mainly in the range of 20 to 25%. Chlorophyll levels decreased even more substantially so that after 4 days of B_{12} deprivation levels were at 0.5% of cell dry weight, 7-fold lower than in B_{12} replete conditions, although whether this was due to reduced synthesis, degradation or bleaching is uncertain. On day 4, samples were pelleted by centrifugation and lyophilised before sending them to Dr. Deborah Salmon at the University of Exeter for free amino acid quantification using HPLC. As with the protein content, amino acid concentrations were lower under B_{12}-limited conditions, but to an even greater extent (Figure 3.5a). The only amino acid which was more abundant under B_{12}-limited conditions was glutamine, but arginine, glutamic acid, and serine levels were relatively similar in both conditions. The most statistically significant decrease was in methionine, which disagrees with the result mentioned previously, although the samples were taken from cultures at different times during B_{12} deprivation and measured by a different method. Several other amino acids including isoleucine, leucine, lysine, and tryptophan decreased to an even greater extent (6-9 fold) than methionine under B_{12} deprivation. Total fatty acids were derivatised from lipid extracts taken from cell pellets sampled on day 4, then esterified and quantified using gas

chromatography-mass spectrometry (Figure 3.5b). The most abundant fatty acid was palmitic acid (C16:0) in B_{12}-limited conditions and α Linolenic acid (C18:3) in B_{12} replete conditions. The degree of fatty acid saturation was considerably higher under B_{12} limited conditions and the total level of fatty acids was also slightly higher.

In addition to those genes for which transcript abundance was tested previously, three further genes whose enzymes are also involved in one carbon metabolism were analysed on day 2 (Figure 3.5c). None of these showed a significant increase under B_{12} limitation after 48 hours relative to B_{12} replete conditions, and one, Formate-tetrahydrofolate ligase (FTL1), showed a significant decrease. The previously tested six genes all showed an increase under B_{12} limitation and hence agreed with the former results, with METE, SHMT2, and SAH1 again being the most highly upregulated.

Having concentrated on the abundance of various compounds and transcripts after a certain period of vitamin B_{12} deprivation, I decided to refocus on methionine cycle metabolites and transcripts but to improve the time resolution during B_{12} deprivation and add-back (Figure 3.6). *metE7* cells were precultured mixotrophically with sufficient B_{12} (200 $ng \cdot l^{-1}$), and then washed and transferred to media lacking B_{12}, but to which 1000 $ng \cdot l^{-1}$ was added 3 days later. Methionine, SAM, and SAH concentrations were measured as described before by Dr. Deborah Salmon at the University of Exeter (Figure 3.6a). SAH levels were found to rise considerably, by a factor of 100, during the first 24 hours of B_{12} deprivation. SAM levels also increased over this period but only by 3-fold, and then maintained that level until B_{12} was added back on day 3. SAH levels on the other hand declined considerably between day 1 and day 3, before the addition of B_{12}. After addition of B_{12}, both SAM and SAH decreased, almost to their original concentrations. Methionine levels were considerably more variable, particularly in the first 12 hours of B_{12} deprivation. Despite being the product of the limiting reaction, methionine levels were actually higher after 24 hours of B_{12} deprivation and declined steadily from thereon with relatively little impact from the addition of vitamin B_{12}.

ix Figure 3.4 Growth and macromolecular composition of *metE7* cells under B_{12} replete or limited conditions

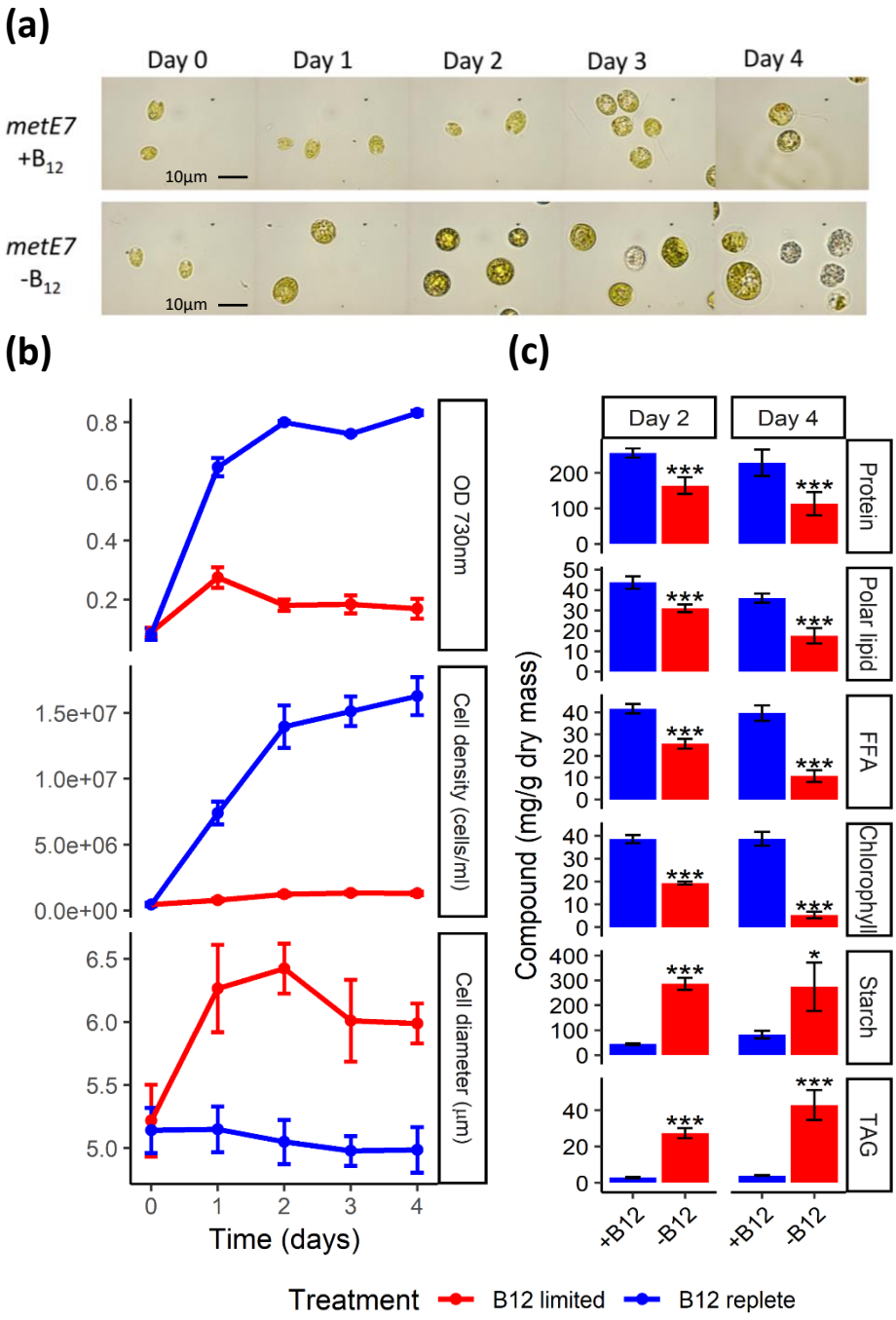

Figure 3.4 Growth and macromolecular composition of *metE7* cells under B_{12} replete or limited conditions. **(a)** Microscope photographs taken at 1000* magnification of *metE7* cells grown in TAP medium in B_{12} replete (1000 ng·l^{-1}) or B_{12} limited (0 ng·l^{-1}) conditions over a period of 4 days **(b)** Growth (optical density at 730nm and cell density) and mean cell diameter of *metE7* cells over the 4-day period. **(c)** Macromolecular composition of cells on day 2 and day 4 of the growth period expressed as mg of that compound per gram of algal dry mass. blue = B_{12} replete, red = B_{12} limited, error bars = sd, n=5, *=p<0.05, ***=p<0.001 (Welch's t test).

x Figure 3.5 Concentrations of various compounds or transcripts in *metE7* under B_{12} replete or limited conditions

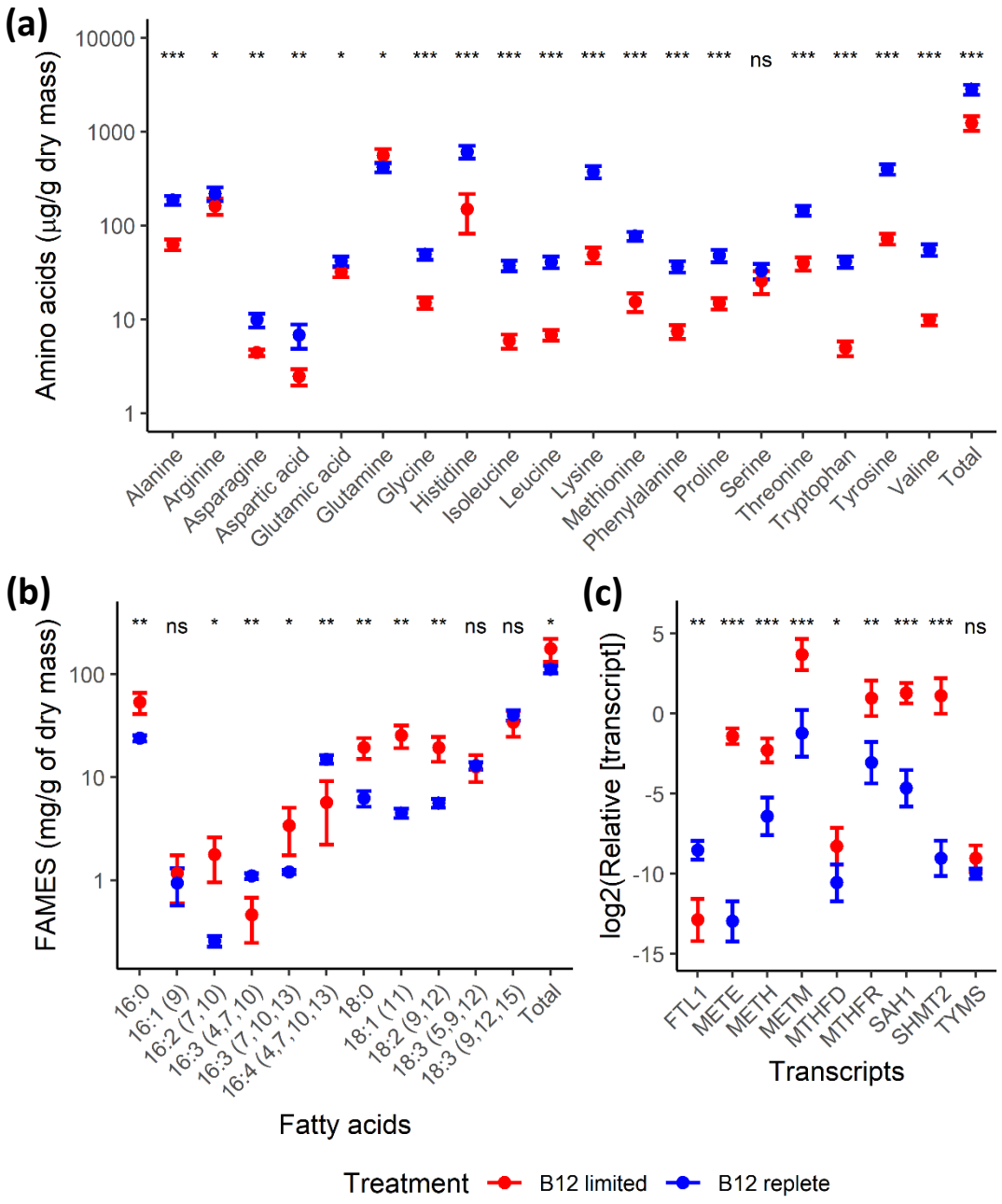

Figure 3.5 Concentrations of various compounds or transcripts in *metE7* under B_{12} replete or limited conditions. **(a)** Cell pellets sampled on day 4 of growth were lyophilised and then amino acids quantified by HPLC (Performed by Dr. Deborah Salmon, University of Exeter). **(b)** Total lipids were extracted on day 4, lipids were derivatised and fatty acids esterified before quantification by GC-MS. **(c)** RNA extracted from cell pellets frozen in liquid nitrogen on day 2 was reverse transcribed and cDNA quantified by qPCR. Most gene abbreviations are mentioned in Figure 3.2, the remaining are as follows: FTL1=Formate tetrahydrofolate ligase, METC=Cystathionine beta lyase, MTHFD=Methylenetetrahydrofolate dehydrogenase, TYMS=Thymidilate synthase. blue = B_{12} replete, red = B_{12} limited, error bars = sd, n=5, *=p<0.05, **=p<0.01, ***=p<0.001 (Welch's t test).

xi Figure 3.6 C1-cycle metabolites and enzyme transcripts during B_{12} deprivation and replenishment

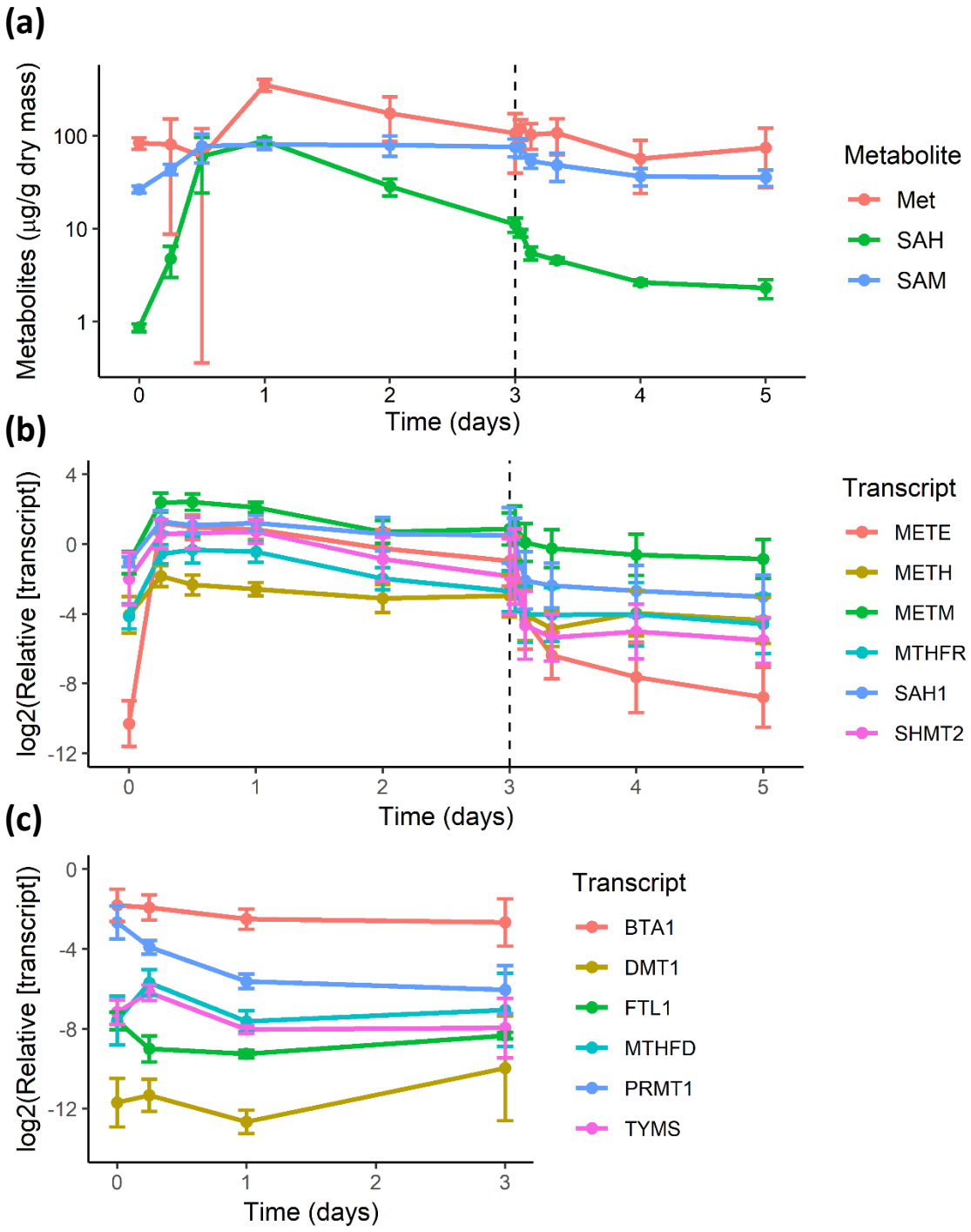

Figure 3.6 Changes in C1 cycle metabolites and enzyme transcripts during B_{12} deprivation (days 0-3), and B_{12} add-back (day 3-5). **(a)** Cell pellets were lyophilised and then C1 cycle metabolites quantified by HPLC (Performed by Dr. Deborah Salmon, University of Exeter). **(b)** and **(c)** RNA extracted from cell pellets frozen in liquid nitrogen was reverse transcribed and cDNA quantified by qPCR, with abundance normalised to the housekeeping gene RACK1. Only 6 genes in panel b were analysed throughout the 5 days, while those in panel c were only analysed during B_{12} deprivation (days 0-3). Vertical dashed line indicates the timing of B_{12} addition to a concentration of 1000 $ng{\cdot}l^{-1}$. Error bars = sd, n >= 3.

From the set of six transcripts that were shown to increase under B_{12} deprivation at 30 and 48 hours (Figure 3.2b and 3.5c), all of the increase occurred in the first 6 hours after transfer to B_{12}-free media (Figure 3.6b). These levels then declined slowly over the next 3 days until the addition of B_{12}, at which point the decline was more significant, with the majority occurring within 8 hours. three further genes involved in the C1 cycle, Methylene tetrahydrofolate dehydrogenase (MTHFD1), Thymidylate synthase (TYMS), and FTL1, which did not previously show an increase under B_{12} limitation were also tested (Figure 3.6c). As expected, there was little change in MTHFD1 and TYMS transcript abundance during B_{12} deprivation, but the changes that did occur were highly correlated with one another. The FTL1 results were also in agreement, with a decrease during B_{12} deprivation. The other three transcripts in Figure 3.6c all code for methyltransferases: Diacylglyceryl-N,N,N-trimethylhomoserine synthesis protein (BTA1), Protein-/Histone-arginine N-methyltransferase (PRMT1), and Cytosine-C5 specific DNA methyltransferase (DMT1). Only PRMT1 significantly changed from day 0 to day 3, decreasing 9-fold. Although several of the transcript abundance profiles in Figure 3.6b were somewhat similar to those for the metabolites SAM and SAH in Figure 3.6a, there are important differences, including the fact that transcript abundance increases more rapidly and earlier than metabolites. This might suggest that expression of these genes is initially controlled by B_{12} rather than C1 cycle metabolite abundance.

3.2.4 Comparing nitrogen and B_{12} deprivation in *metE7* and B_{12} deprivation in *L. rostrata*

I previously showed that *L. rostrata* has a lower requirement for vitamin B_{12} than *metE7* and so decided to investigate how different its response to B_{12} deprivation was, particularly with respect to maintaining viability. Initially both algae were cultured mixotrophically with 200 $ng \cdot l^{-1}$ B_{12}. They were both then washed and transferred to TAP media lacking B_{12} and cultured as before. As expected, *L. rostrata* continued to grow in the B_{12} deplete media, while there was no further substantial growth of *metE7* (Figure 3.7a-b). Photosystem II maximum efficiency, measured as *Fv/Fm*, and viability, measured as the proportion of cells that could form colonies on nutrient replete agar, declined in both strains over the 6-day period, however the decline was more severe in *metE7* (Figure 3.7c-d). Non-photochemical quenching in *L. rostrata* started at a higher value and declined more slowly than in *metE7*, however by day 4 the levels of NPQ was similar in both strains as they had risen in *metE7* cells from day 1 to 6 (Figure 3.7e). Reactive oxygen species, which were measured by fluorescence of dichlorodihydrofluorescein diacetate (DCFDA) and normalised to the cell density, were slightly higher in *metE7* cells and there was a trend towards an increase throughout the B_{12} deprivation period (Figure 3.7f).

The comparison with *L. rostrata* was meant as a representative example of other naturally B_{12}-dependent algae. Instead of attempting to improve the evidence for this hypothesis that *metE7* is poorly adapted to coping with B_{12} deprivation by using other closely related B_{12} auxotrophs, I instead decided to focus on how *metE7* would respond to deprivation of a nutrient for which it has had a long time to evolve acclimatory responses. As one of the best studied nutrient deprivation responses in *C. reinhardtii* is to a lack of nitrogen I decided to compare this response in *metE7* with B_{12} deprivation in *metE7* and in *L. rostrata*. Cells were precultured in sufficient B_{12} conditions (200 $ng \cdot l^{-1}$) before being washed and transferred to B_{12}-free or B_{12}-replete (1000 $ng \cdot l^{-1}$) but nitrogen-free TAP media and cultured mixotrophically for 4 days. As the cultures had been transferred early during log-phase in the precultures, *metE7* continued to grow for longer than in the other experiments reported in this chapter. Figure 3.8a shows that the initial growth rate of *metE7* under nitrogen deprivation conditions was considerably slower than the B_{12}-deprived cultures, and B_{12}-deprived *L. rostrata* growth rate was the intermediate of the three. After two days however, B_{12}-deprived *metE7* reached a maximum and declined thereafter, while *L. rostrata*, and nitrogen-deprived *metE7* growth continued throughout. B_{12}-deprived *metE7* cells also increased in diameter more quickly than nitrogen-deprived *metE7*, while *L. rostrata* cell diameter decreased over the first day, but then increased over the next 3 days so that by day 4 there was little difference between the three treatments (Figure 3.8b). Changes in cell viability, shown in Figure 3.8c, differed markedly between treatments. B_{12}-deprived *L. rostrata* maintained roughly 90% viability over the 4-day period, while B_{12}-deprived *metE7* viability declined dramatically from day 1 onwards, ending up at 7% on day 4. In nitrogen-deprived *metE7*, after a substantial decrease of more than 50% on the first day, viability then recovered to 80%. PSII maximum efficiency (*Fv/Fm*) is often used as an indicator of phytoplankton nutrient stress (Parkhill et al., 2001), so it would seem from the results in Figure 3.8d that *metE7* under both nutrient deprivation conditions was more stressed than *L. rostrata*. *Fv/Fm* declined most rapidly under nitrogen deprivation, but with a slight delay there was also a decrease under B_{12} deprivation. Although *Fv/Fm* also declined initially in *L. rostrata* it had stabilised after roughly one day at around 0.5.

xii Figure 3.7 Comparison of *L. rostrata* and *metE7* during B_{12} deprivation

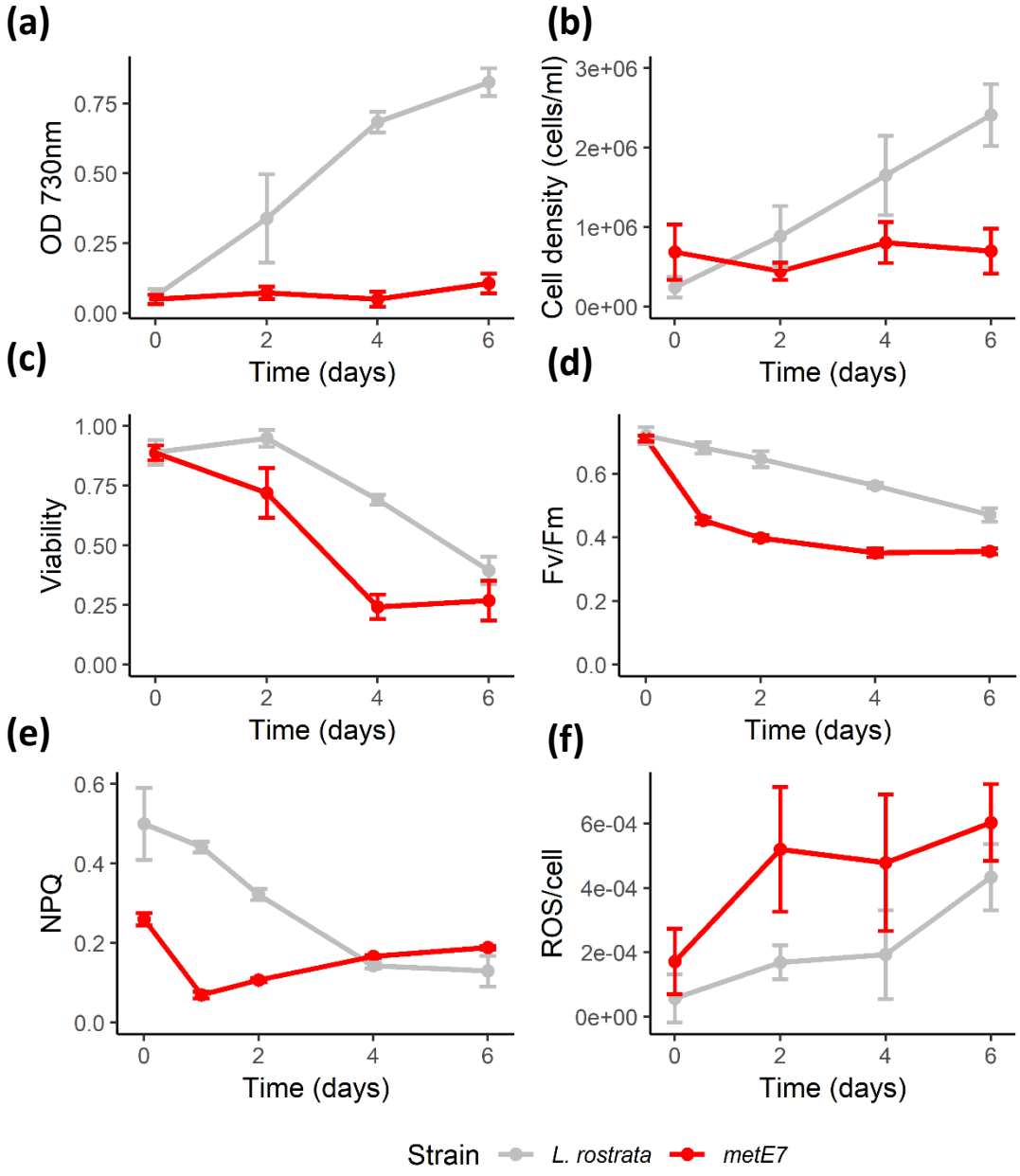

Figure 3.7 Comparison of *L. rostrata* and *metE7* during B_{12} deprivation over 6 days. **(a)** Optical density at 730 nm of cultures, **(b)** Total cell density of cultures, **(c)** Proportion of cells that could form colonies (Viability), **(d)** PSII maximum efficiency measured by chlorophyll fluorescence, **(e)** Non-photochemical quenching measured by chlorophyll fluorescence, **(f)** Reactive oxygen species measured by DCFDA fluorescence and normalised per cell. Grey = *L. rostrata,* Red = *metE7*, error bars = sd, n=6.

xiii Figure 3.8 Comparison of *metE7* under B_{12} deprivation with *metE7* under nitrogen deprivation and *L. rostrata* under B_{12} deprivation

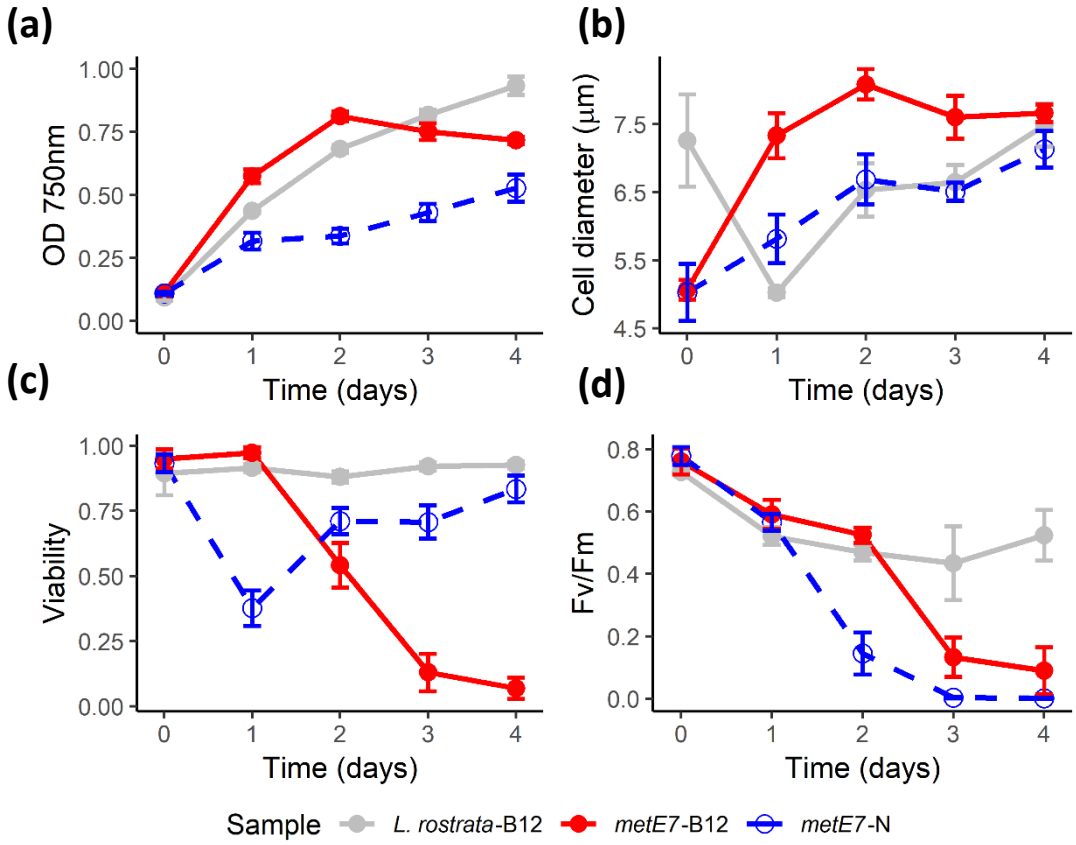

Figure 3.8 Comparison of *metE7* under B_{12} deprivation with *metE7* under nitrogen deprivation, and *L. rostrata* under B_{12} deprivation. **(a)** Optical density at 750 nm of cultures, **(b)** Mean cell diameter measured by image analysis of microscope photographs, **(c)** Proportion of cells that that could form colonies (Viability), **(d)** PSII maximum efficiency measured by chlorophyll fluorescence. Blue-dashed = *metE7* –nitrogen, red = *metE7* – B_{12}, grey = *L. rostrata* –B_{12}, error bars = sd, n=5.

xiv Figure 3.9 Comparison of *metE7* under a combination of nutrient deprivation conditions

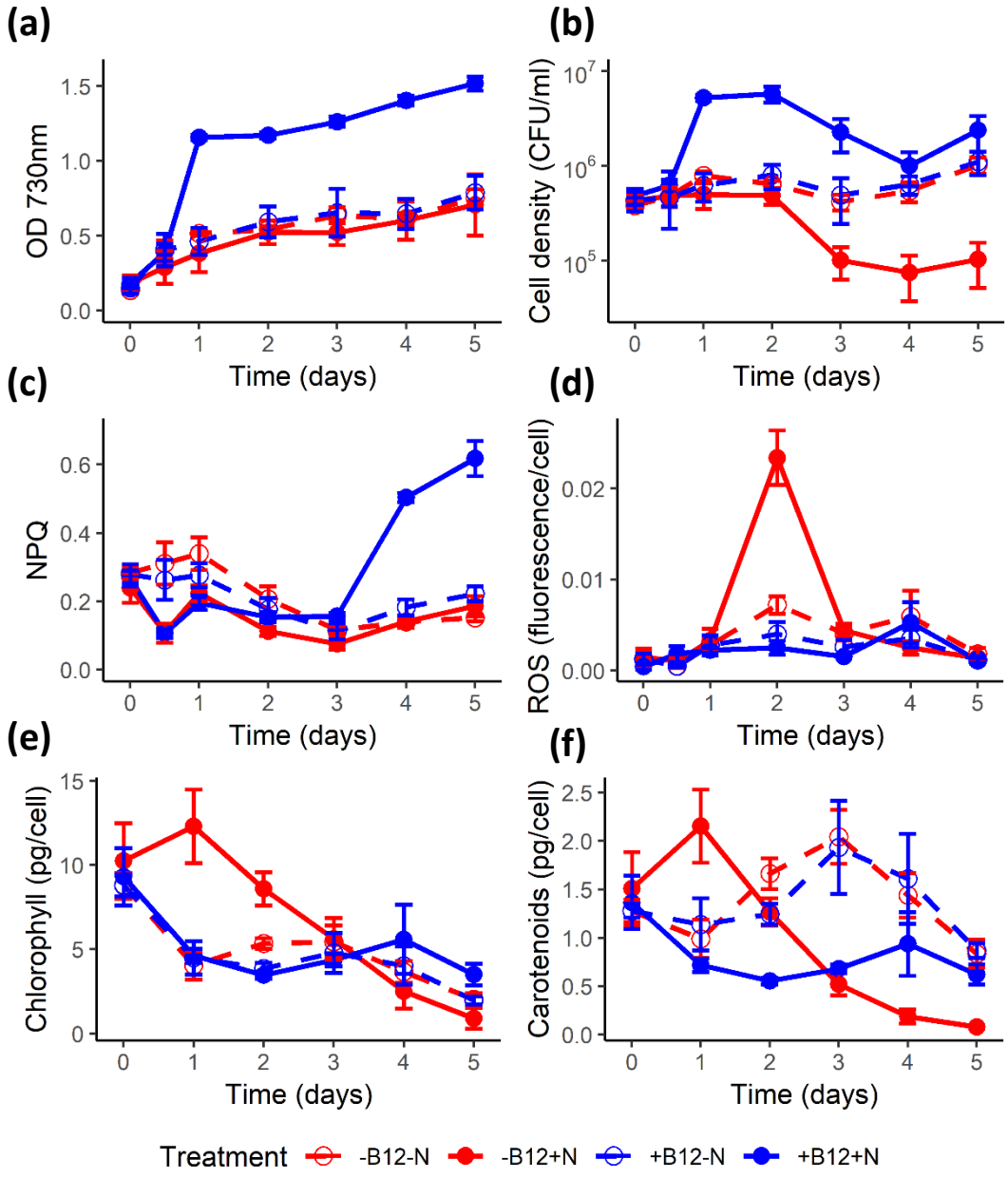

Figure 3.9 Comparison of *metE7* under a combination of nutrient deprivation conditions. **(a)** Optical density at 730nm of cultures, **(b)** Density of colony forming units (viable cells), **(c)** Non-photochemical quenching measured by chlorophyll fluorescence, **(d)** Reactive oxygen species measured by DCFDA fluorescence and normalised per cell **(e)** Total chlorophyll measured by spectrophotometer and normalised per cell, **(f)** carotenoids measured by spectrophotometer and normalised per cell. Blue solid = nutrient replete, red solid = B_{12} limited, blue dashed = nitrogen limited, red dashed = both nitrogen and B_{12} limited. Error bars = sd, n=4.

xv **Figure 3.10 Comparison of *metE7* under a combination of nutrient deprivation conditions 2**

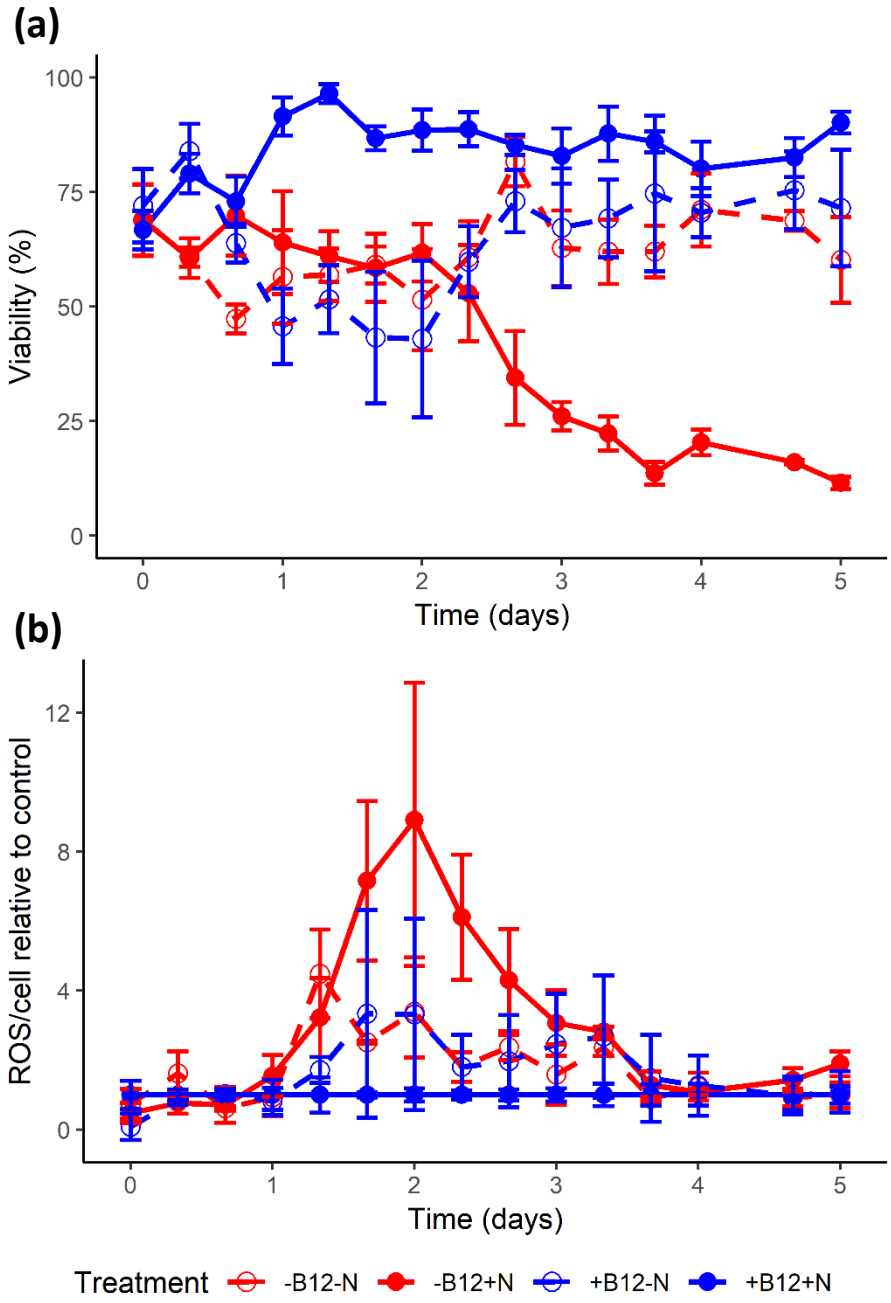

Figure 3.10 Comparison of *metE7* under a combination of nutrient deprivation conditions. **(a)** Proportion of cells that could form colonies on nutrient replete agar, **(b)** ROS measured by DCFDA fluorescence and normalised both per cell and to the nutrient replete treatment. Blue solid = nutrient replete, red solid = B_{12} limited, blue dashed = nitrogen limited, red dashed = both nitrogen and B_{12} limited. Error bars = sd, n = 4.

3.2.5 Combining B_{12} and nitrogen deprivation

metE7 had survived nitrogen deprivation better than B_{12} deprivation (Figure 3.8c), but it was unclear whether the metabolic role of B_{12} would make it make it intrinsically more difficult to cope without than a nitrogen source. To test whether this was the case, or if *C. reinhardtii* had instead evolved mechanisms to cope with nitrogen deprivation which could cross-protect against B_{12} deprivation, *metE7* cells were cultured in media lacking both nitrogen and B_{12}. As before, *metE7* cells were grown mixotrophically with 200 $ng \cdot l^{-1}$ B_{12} before being washed and resuspended in TAP media with 1000 $ng \cdot l^{-1}$ of B_{12} or media either lacking ammonium, B_{12}, or both ammonium and B_{12}. Following resuspension, growth in the three nutrient-deprived conditions was similar and considerably lower than in the nutrient replete condition (Figure 3.9a). This confirmed that the cells were indeed nutrient-deprived, and that the severity of the limitation, in terms of restricting growth, was similar for B_{12} and nitrogen. However, the number of colony forming units per ml of culture (a measure of the total number of viable cells) was significantly different between the nutrient-depleted conditions: under B_{12} deprivation alone $CFU \cdot ml^{-1}$ declined substantially after two days relative to the nitrogen deplete conditions (Figure 3.9b). The combination of nitrogen and B_{12} deprivation did not cause a similar decrease in the number of colony-forming units. Measurements of non-photochemical quenching (NPQ) showed that in the first 12 hours there was a decline under both B_{12} deplete and nutrient replete conditions, whereas under both nitrogen deplete conditions there was a temporary increase (Figure 3.9c). After 24 hours the levels of NPQ remained low in all three nutrient-deplete conditions but increased substantially in the nutrient replete conditions in parallel with the cells entering stationary phase. The levels of reactive oxygen species were reasonably similar between treatments across the whole growth period, except for on day 2 where both B_{12} depleted conditions showed an increase (Figure 3.9d). The ROS signal from B_{12} deficient conditions was also significantly higher than the treatment deficient in both nitrogen and B_{12}. The B_{12} deficient treatment was also the most obvious outlier in the measurements of chlorophyll and carotenoids (Figure 3.9e-f). In this treatment the levels of both pigment groups increased over the first 24 hours, although it is unclear to what extent this may be due to the increase in cell diameter that was previously observed under B_{12} deprivation (Figure 3.4b and 3.8b). By day 5 the levels of both pigments were lowest in the B_{12} deficient treatment, following 3 days of precipitous decline. The chlorophyll:carotenoid ratio in the nutrient replete conditions remained steady throughout, whereas under both nitrogen deficient conditions carotenoids actually increased from day 1 to day 3, and there was a continuous decrease in the chlorophyll:carotenoid ratio over the 5 days. A decrease in chlorophyll is a commonly observed phenomenon in *C. reinhardtii* under nutrient deprivation, as is the decrease in chorophyll:carotenoid ratio, which is known to protect against the excess absorption of light energy via dissipating some of it as heat. These responses can reduce the excitation of chlorophyll and hence reduce the production of singlet oxygen, a damaging reactive oxygen species (Müller et al., 2001). Therefore, it is

conceivable that these responses to nitrogen deprivation are involved in protecting against the increase in reactive oxygen species seen under B_{12} deprivation alone. To determine whether the high levels of reactive oxygen species on Day 2 of B_{12} deprivation was reflective of reality or simply an anomaly, the experiment was repeated with higher time resolution. The results, shown in Figure 3.10a-b, were in agreement that cell viability declines most substantially after 2 days of B_{12} deprivation, which coincides with the peak in reactive oxygen species per cell.

3.2.6 Artificial evolution of *metE7* under B_{12} deprived conditions

Artificial evolution has been increasingly used in the field of microbiology due to the short generation times of microbes and hence the ability to apply a severe selection pressure and to see genetic changes in a relatively short space of time (Kawecki et al., 2012). The *metE7* mutant, was generated by artificial evolution, and I decided that this approach could also be used to see how it (a newly evolved B_{12} auxotroph) would subsequently adapt to a decrease in the concentration of vitamin B_{12}. Three conditions were chosen: Condition A was the same as had been previously used (Helliwell et al., 2015), namely TAP media with 1000 $ng \cdot l^{-1}$ B_{12} cultured in continuous light; condition B was the same except for the fact that the B_{12} concentration was 25 $ng \cdot l^{-1}$ (an amount that causes B_{12} deprivation); in condition C, TAP media was replaced with Tris minimal medium with no B_{12}, but in its place a B_{12}-producing bacteria, *Mesorhizobium loti*, was inoculated. There were also differences in the dilution rates: condition A, B, and C had dilution rates of 10000, 100, and 5 times per week respectively to reflect the different growth rates and to maintain selection pressure. All the cultures were subbed once per week over a total period of seven months in which there were two periods of two weeks long each where cultures were plated out on agar and checked for contamination as well as the presence of vitamin B_{12}-independent revertants. Cultures were also plated out onto agar in parallel with the liquid cultures when wells were suspected of containing B_{12}-independent revertants. When this was confirmed to be the case genetically and phenotypically, a B_{12}-dependent colony from the same line was picked and inoculated into the liquid media to continue the artificial evolution experiment. Vitamin B_{12}-independent lines arose in or contaminated one, six, and five cultures in conditions A, B, and C respectively, and were removed as mentioned above. After the seven months under selective conditions all cultures had survived and been maintained without contamination, including the *M. loti* in condition C. Isolates from these three conditions were compared with the progenitor *metE7* line and *L. rostrata* that had both been maintained on Tris min agar, in terms of their growth response to different concentrations of B_{12} and their response to being resuspended in B_{12}-free media. This experimental evolution setup is illustrated in Figure 3.11.

Overall, the differences between the lines evolved in different conditions was small, and in many lines, growth had slowed or stopped in the lower B_{12} concentrations while it continued in the

higher B_{12} concentrations (Figure 3.12a). Non-linear regression was used to find parameters for the Verhulst equation to best fit the OD730 nm data over the growth period at different B_{12} concentrations for each of the algal lines. The estimated carrying capacity from the Verhulst equation at each B_{12} concentration was then used to fit a Michaelis-Menten equation and so calculate two parameters: carrying capacity under replete B_{12}, and the EC_{50} (concentration required for 50% of maximal growth) for B_{12}. The predicted carrying capacity under replete B_{12} conditions of all the evolved *metE7* lines was lower than the progenitor line (Figure 3.12b). *L. rostrata* had a significantly lower carrying capacity than the progenitor *metE7*, as was shown in Figure 3.3a, but it was not significantly lower than the lines evolved under limited levels of B_{12} (conditions B and C). The EC_{50} for B_{12} was significantly lower for *L. rostrata* than any *metE7* line, and all evolved lines had lower EC_{50} values than the progenitor (Figure 3.12c). In addition, the *metE7* lines evolved in the presence of *M. loti* (condition C) had a lower EC_{50} than the lines evolved in TAP with 1000 $ng \cdot l^{-1}$ B_{12} (condition A).

During B_{12} deprivation the differences were again small between lines but the order from maximal to minimal growth after resuspension was *L. rostrata*, lines C, B, A, then *metE7* (Figure 3.13a). Lines B, A and *metE7* showed no statistical difference in optical density on day 6, but were significantly lower than line C, which in turn was significantly lower than *L.* rostrata. With respect to viability on day 6, it was again *L. rostrata* which had the greatest value, but this was not significantly higher than line B (Figure 3.13b). Although line B was not statistically higher than lines C or *metE7* it was significantly higher than line A, which had the lowest value. *Fv/Fm* was also greatest on day 6 in *L. rostrata*, and the order from highest to lowest was the same as the order of culture optical density as were the statistical groupings produced by the post-hoc Tukey test. Overall, the findings are not particularly clear, however there appears to be a trade-off between growth rate and maintaining viability under B_{12} deprivation conditions, with those lines evolved in lower levels of B_{12} (axenically or in coculture) having slower maximal growth rates under replete B_{12} but improved absolute growth and survival under B_{12}-deprived conditions.

xvi Figure 3.11 Diagram for the experimental evolution setup and the experiments used to analyse the evolved lines

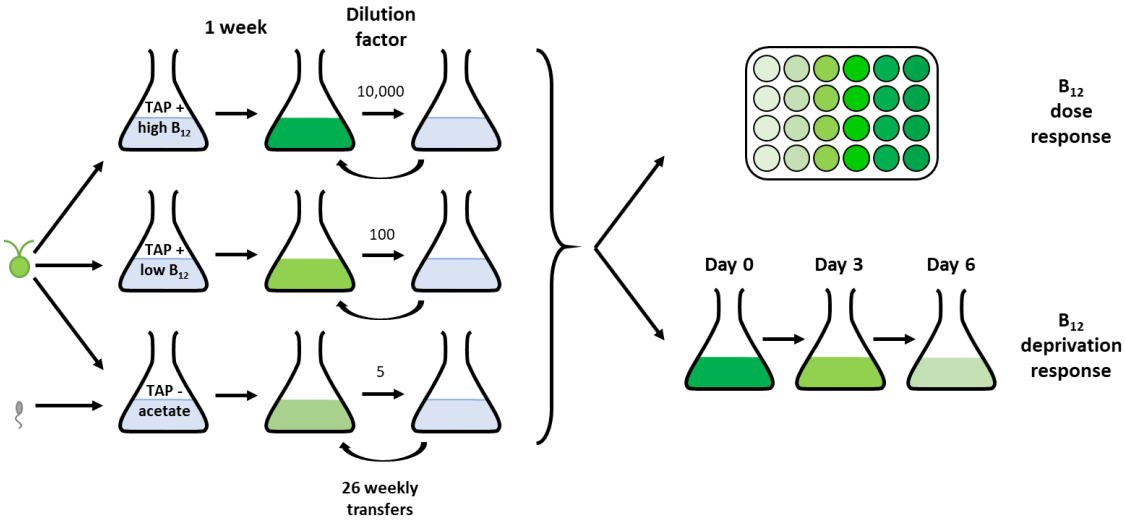

Figure 3.11 Diagram for the experimental evolution setup and the experiments used to analyse the evolved lines. *metE7* was inoculated into three different media: condition A was TAP medium + 1000 ng·l^{-1} B_{12}; condition B was TAP medium + 200 ng·l^{-1} B_{12}; condition C was Tris minimal medium. *M. loti*, a B_{12}-producing bacterium, was also inoculated into condition C. All 24 cultures (8 biological replicates in each condition) were cultured at 25 °C in continuous light at 100 µE·m^{-2}·s^{-1} with rotational shaking at 120 rpm for 1 week, after which cultures in conditions A, B, and C were diluted 10,000, 100, and 5-fold respectively into fresh medium of the same composition. This was repeated for a total of 26 weeks, or six months. The experimentally evolved lines were tested for their growth response to different concentrations of B_{12} and their response to B_{12} deprivation over a period of six days.

xvii Figure 3.12 B_{12} growth response of experimental evolution lines of *metE7* and wild type *L. rostrata*

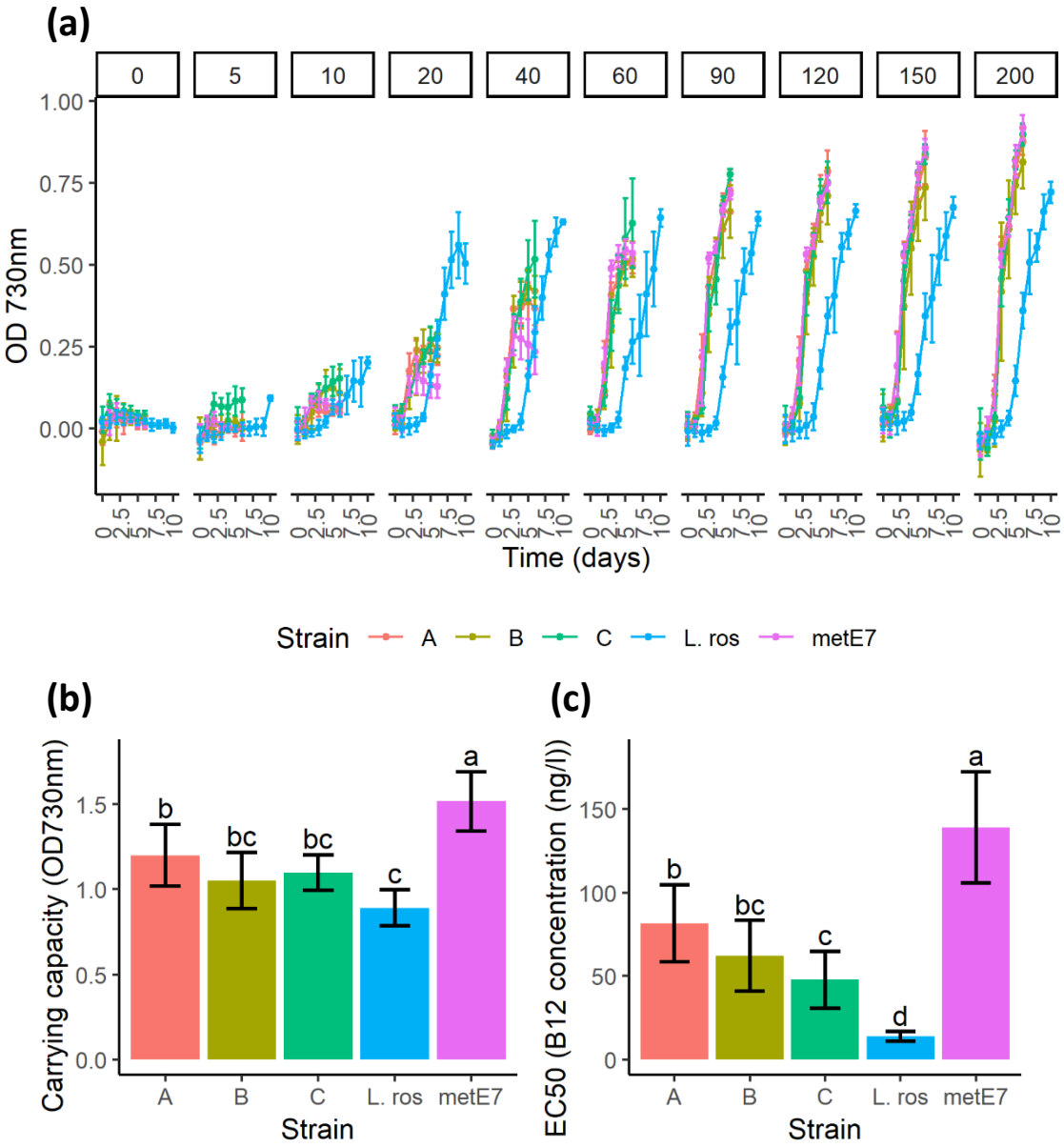

Figure 3.12 Growth under different concentrations of B_{12} of *L. rostrata*, the *metE7* progenitor strain, and its experimental evolution descendants. **(a)** Raw data of optical density at 730 nm over 10 days of different strains cultured mixotrophically in different B_{12} concentrations. **(b)** The calculated carrying capacity of cultures in replete B_{12}. **(c)** The concentration of B_{12} required to produce 50% of maximal growth (EC_{50}). Both values were calculated by using non-linear regression to first fit a Verhulst equation to the optical density data to find carrying capacities at different B_{12} concentrations, followed by a Monod equation to connect B_{12} concentration to carrying capacity. Statistical groupings were determined using Tukey's test. Line A (red)= evolution under 1000 ng·l^{-1} B_{12}, Line B (brown)= evolution under 25 ng·l^{-1} B_{12}, and Line C (green)= evolution with *M. loti* in Tris min), the progenitor *metE7* strain (purple), or *L. rostrata* (blue). Error bars = sd, n = 6.

xviii Figure 3.13 B_{12} deprivation of experimental evolution lines of *metE7* and wild type *L. rostrata*

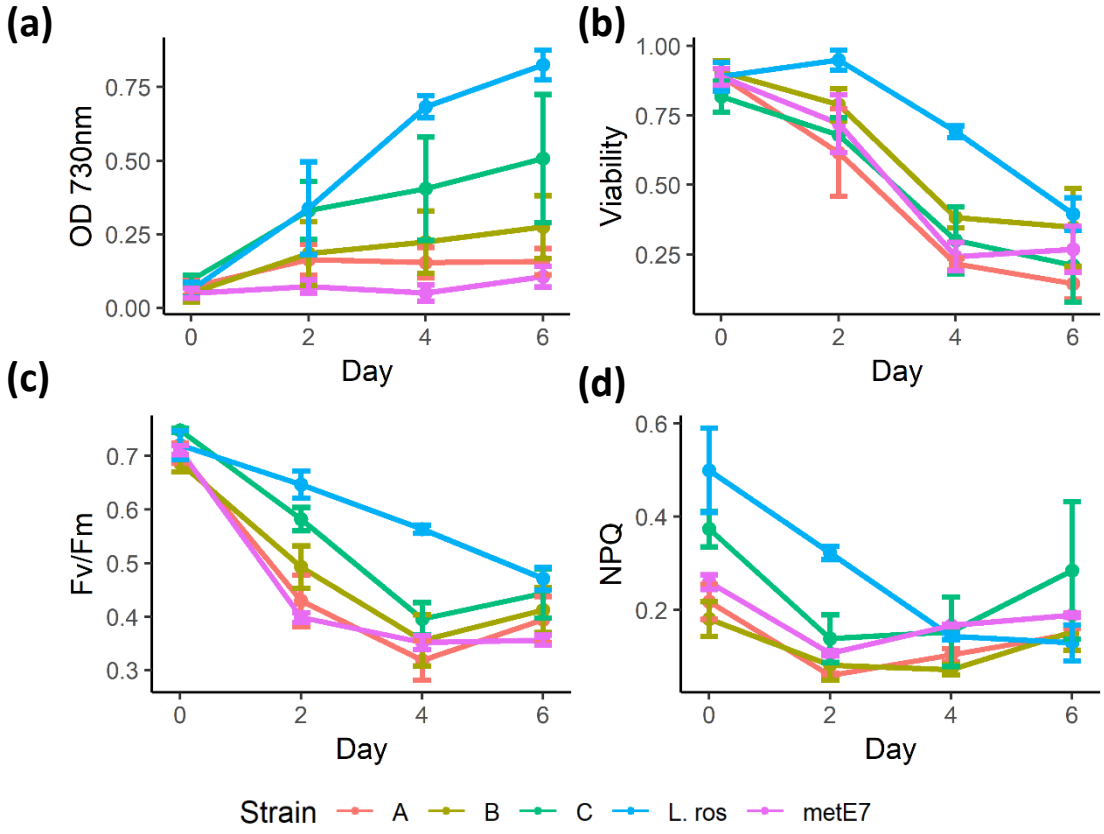

Figure 3.13 B_{12} deprivation of *L. rostrata*, the *metE7* progenitor strain, and its experimental evolution descendants. Cultures were initially grown in 200 $ng \cdot l^{-1}$ B_{12} TAP medium before washing and resuspending in B_{12}-free TAP medium **(a)** Growth measured by optical density at 730 nm, **(b)** Proportion of cells that could form colonies, **(c)** PSII maximum efficiency measured by chlorophyll fluorescence, **(d)** Non-photochemical quenching measured by chlorophyll fluorescence. Line A (red)= evolution under 1000 $ng \cdot l^{-1}$ B_{12}, Line B (brown)= evolution under 25 $ng \cdot l^{-1}$ B_{12}, and Line C (green)= evolution with *M. loti* in Tris min), the progenitor *metE7* strain (purple), or *L. rostrata* (blue). Errorbars = sd, n = 6.

3.3 Discussion

In this chapter I focussed on characterising the way a recently evolved B_{12} auxotroph (*metE7*) responds to vitamin B_{12}. To put this into context, and without simply referring to the literature, I compared *metE7* to wild type *C. reinhardtii* and *L. rostrata*, and B_{12} deprivation to nitrogen deprivation. I also compared various strains of *metE7* that underwent a period of experimental evolution with selection for ability to grow on high or low levels of B_{12} or in coculture with a B_{12}-producer, *M. loti*.

3.3.1 Growth of *metE7* is B_{12} dose-dependent

In 1905 F. F. Blackman developed the idea of limiting factors, including light and CO_2 availability, with respect to the rate of plant photosynthesis and growth (Blackman, 1903). Vitamin B_{12} is not required by plants or by wild type *C. reinhardtii* but is clearly the limiting factor in the growth of *metE7* up until a certain concentration, which itself is determined by the growth conditions. The most favourable growth conditions, where both light and a carbon source are present, requires the highest concentrations of B_{12} for it to cease to be the limiting factor. In 1913 Michaelis and Menten derived an equation linking the velocity of an enzyme-catalysed reaction to the concentration of its substrate (Michaelis & Menten, 1913), and in 1949 Monod found that an equation of the same form described the relationship between the division rate of *Escherichia coli* and glucose concentration (Monod, 1949). The connection between *metE7* final cell density and B_{12} concentration can be approximated well by an equation of the same form, but it is important to note that the dependent variable measured here was cell density not growth rate. Therefore, the B_{12} concentration at which cell density is half maximal would be more aptly denoted by the term EC_{50} rather than the half velocity constant (K_s) used in the Monod equation. The maximal cell density achieved under non-limiting B_{12} concentrations would substitute for the term μ_{max} in the Monod equation. The difference in the cell density achieved in mixotrophic and heterotrophic conditions under non-limiting B_{12} was reversed for limiting B_{12} i.e. cell density at B_{12} concentrations below 16 $ng \cdot l^{-1}$ were greater in heterotrophic conditions. This could be due to light having a detrimental effect on growth or survival when B_{12} is severely depleted. However, it might simply be an artefact of judging when carrying capacity was achieved, which was done manually using an average optical density reading across all B_{12} concentrations, whereas in fact the time required may vary considerably with B_{12} concentration and be dependent upon the presence of light or acetate. The reason for the small but consistently lower carrying capacity of the revertant line compared with the ancestral is also unclear, as is the slight negative correlation between B_{12} and carrying capacity for the revertant line. It also wasn't investigated whether very high levels of B_{12} would significantly inhibit growth of all strains, but no

adverse effects have been associated with excess B_{12} intake in humans and no tolerable upper intake level has been set even though studies have administered doses 500-2500 times the recommended daily allowance (Institute of Medicine (US), 1998).

3.3.2 B_{12} alters methionine cycle metabolites in *metE7* but not wild type *C. reinhardtii*

By many accounts one-carbon metabolism is a finely tuned set of reactions, which when disrupted has multiple significant effects on an organism's physiology (Groth et al., 2016; Hanson & Roje, 2001; Kim et al., 2015; Lucock, 2004; Moll & Davis, 2017). Within one-carbon metabolism, the metabolite S-adenosyl-L-methionine (SAM) plays a major role as the donor of methyl groups to DNA, mRNA, histones, proteins and lipids (Chiang et al., 1996). The demethylated product of these reactions, S-adenosyl-L-homocysteine, has been shown to bind with higher affinity to methyltransferases than does SAM itself, and so the ratio of SAM:SAH is termed the methylation potential (Melnyk et al., 2000). The finding that B_{12} had no effect on the concentration of methionine, SAM or SAH in the ancestral line of *C. reinhardtii* suggests that METE and METH are fully able to substitute for one another. The abundances of METE and METH protein were not measured here, however, in *P. tricornutum* METE protein levels are 60-fold higher than METH (Bertrand et al., 2013), and in *C. reinhardtii*, proteomics and RNAseq experiments found that METE was the more abundant isoform (Blaby et al., 2015; Park et al., 2015). The reason for the higher abundance of METE may be due to a lower maximal catalytic rate, as has been observed in *E. coli* (Gonzalez et al., 1992). In *metE7* the roughly 10-fold increase in SAH and resultant decrease in SAM:SAH ratio (Figure 3.2b) could substantially impact methylation, resulting perhaps in DNA hypomethylation as has been shown in humans (James et al., 2002; Yi et al., 2000). Another major SAM-consuming pathway in mammals is the trimethylation of the lipid phosphatidylethanolamine (PE) to phosphatidylcholine (PC) (Noga et al., 2003). *C. reinhardtii* lacks PC, instead containing Diacylglycerol-N,N,N-trimethylhomoserine (DGTS), which is formed from the trimethylation of diacylglycerols (Riekhof et al., 2005). Alteration in methylation potential is therefore likely to impact lipid metabolism.

Homocysteine levels were not accurately measured, however, in humans there is good evidence of a strong correlation between SAH and homocysteine levels (Yi et al., 2000), due to the reversible nature of the conversion of SAH and homocysteine by adenosylhomocysteinase (Palmer & Abeles, 1979). Therefore, it is quite plausible that homocysteine levels would have increased in *metE7* under B_{12} deprivation, especially considering that Croft et al. (2005) showed that this is the case in *L. rostrata*. The observed increase in methionine during B_{12} deprivation of *metE7* is not easily explicable. Methionine synthase deficiency, hyperhomocysteinemia, and high levels of SAH in

mammalian plasma is often associated, conversely, with low levels of methionine (Duncan et al., 2013; Engbersen et al., 1995; Watkin & Rosenblatt, 1989). This agrees with a separate set of measurements made in this chapter of methionine in B_{12} deprived and replete *metE7* cells 4 days after treatment. Therefore, it is possible that the timing or severity of B_{12} deficiency plays a role in the change in methionine concentration. Methionine levels during B_{12} deprivation in *metE7* would likely differ to some extent from humans anyway due to a different complement of methionine-generating enzymes, e.g. *C. reinhardtii* lacks betaine-homocysteine methyltransferase (BHMT), and humans lack homocysteine s-methyltransferase (HMT), which is involved in the S-methylmethionine cycle, a pathway unique to photosynthetic organisms (Hanson & Roje, 2001). Increased homocysteine methylation by HMT, or increased net protein catabolism, and a reduction in SAM synthesis might all contribute to higher methionine levels.

3.3.3 Transcripts of C1-cycle enzymes are altered by B_{12} and C1-cycle status

Analysis of various human tissues has shown that SAH and Hcy concentrations are significantly correlated with transcript abundances of several enzymes involved in methylation and one carbon metabolism (Chen et al., 2010). In bacteria some enzymes of the methionine cycle have been found to contain SAM and SAH riboswitches (Edwards et al., 2010; Wang et al., 2008), however only riboswitches responsive to Thiamine pyrophosphate (TPP) have been found in eukaryotes (Moldovan et al., 2018; Serganov & Nudler, 2013). Nonetheless, transcription of at least three genes from *C. reinhardtii* involved in one carbon metabolism are regulated by vitamin B_{12} via other mechanisms. The abundances of six transcripts involved in one carbon metabolism were measured in *metE7* and the ancestral line in B_{12}-deprived and replete conditions and showed that almost all genes in both strains were significantly upregulated under B_{12} deprivation. However, the degree of upregulation was considerably greater for all genes in *metE7* than the ancestral strain, except for METE which was similar in both strains. This suggests that B_{12} itself is likely to exert some control, whether directly or indirectly, on the expression of these enzymes at the transcript level, but that the status of one carbon metabolism might also have an impact. Under B_{12} deprivation conditions, the activity of METH would be compromised, yet in both *C. reinhardtii* strains it was upregulated. In contrast, for *P. tricornutum*, an alga that encodes *METE* and is B_{12}-independent, lack of B_{12} decreases METH protein abundance (Bertrand et al., 2013), while for *T. pseudonana*, which lacks *METE*, *METH* transcript abundance increases (Bertrand et al., 2012). The fact that *C. reinhardtii* is more similar in this respect to a B_{12} auxotroph might facilitate the acclimation to B_{12} auxotrophy. Some of the most highly upregulated transcripts in *T. pseudonana* and *P. tricornutum* under B_{12} deprivation include homologs of *METM*, *MTHFR* and *SAH1*, reflecting what was found in this work, and also by Helliwell et al., (2014) (Bertrand et al., 2012; Helliwell et al., 2014). In a study of the *C. reinhardtii* diurnal transcriptome these genes formed a cluster, which also contained *METE*, *METH*, and *SHMT2*,

whose transcripts were significantly more abundant in the day than night (Blaby et al., 2015). Under sulphur and nitrogen deprivation conditions however, these C1 cycle genes are downregulated, suggesting that their upregulation during B_{12} deprivation is not a general response to stress, but a nutrient-specific one (González-Ballester et al., 2010; Wase et al., 2014).

3.3.4 *metE7* has a higher B_{12} requirement than the natural B_{12} auxotroph *L. rostrata*

metE7 was found to have a significantly higher requirement for B_{12} than *L. rostrata*: The concentration of B_{12} required for each strain to reach half maximal density (EC_{50}) was 39 and 15 $ng \cdot l^{-1}$ respectively (Figure 3.3a). For *metE7* this translates to a minimal requirement of B_{12} of roughly 1500-2000 molecules per cell. In terms of concentration within the cell works out to be roughly 25 nM, which is within the range (0.35-590nM) reported by Tang et al., (2010) for marine B_{12} auxotrophic harmful algal bloom species (Tang et al., 2010), and similar to the average concentration in the human body at 40 nM (Hoglund et al., 1966). As a partial consequence of a higher requirement for B_{12}, *metE7* underwent fewer doublings after being saturated with B_{12} than *L. rostrata* (Figure 3.3b). When growth had ceased the population of *metE7* and *L. rostrata* cells had increased 38-fold and 160-fold respectively. The ability to rapidly take up and store large amounts of B_{12} would presumably provide a selective advantage for B_{12} auxotrophs which might compete for B_{12} produced during bacterial blooms. An alternative strategy to surviving on stored B_{12} during periods between bacterial blooms could perhaps be to have a high affinity uptake system to utilise the low concentrations produced by lower densities of bacteria or other lysed cells. The difference in B_{12} uptake between *metE7* and *L. rostrata* is not statistically significant at any initial concentration of B_{12}. It is telling nonetheless that the mean uptake for *metE7* is lower than for *L. rostrata* for all initial concentrations of B_{12} below 50 $ng \cdot l^{-1}$ and higher above 50 $ng \cdot l^{-1}$ (Figure 3.3c). In agreement with this observation is the fact that over a 4-hour period the B_{12} uptake by *metE7* is less at the low starting concentration and greater at the higher concentration (Figure 3.3d). The dynamics of uptake are reasonably similar between strains, and the fact that the majority occurs within the first 15 minutes or so is similar to the finding by Sarhan et al. (1980) that B_{12} uptake by *E. gracilis* is biphasic with a rapid, passive initial stage, followed by an energy-dependent and slower second stage (Sarhan et al., 1980). The effect of starting concentration on B_{12} uptake, although small, might indicate that the proteins that bind or transport cobalamin in *L. rostrata* have a higher affinity, but perhaps a lower turnover or abundance than in *C. reinhardtii*. B_{12} binding proteins were only recently discovered in algae: Cobalamin acquisition protein 1 (CBA1) was discovered in *P. tricornutum* and *T. pseudonana* and inferred by sequence similarity to exist in several diatoms (Bertrand et al., 2012). CBA1 was upregulated in *T. pseudonana* and to a lesser extent in *P. tricornutum* under B_{12} deprivation, and it would be interesting to see how B_{12} deprivation affects uptake in *L. rostrata* and *C. reinhardtii*.

3.3.5 Deprivation of B_{12} induces similar changes to cell composition as other nutrients

The average cell diameter of *metE7* cells was found to increase rapidly during B_{12} deprivation (Figure 3.4a-b). In many bacteria species division by binary fission restricts the variation in cell size to little over 2-fold (Taheri-Araghi et al., 2015), *C. reinhardtii* on the other hand, undergoes a multiple fission cell cycle, also referred to as palintomy (Cross & Umen, 2015). Growth happens in the light, and between one and five division cycles occur soon after the transition to darkness, resulting in the brief existence of palmelloids of up to 32 cells prior to flagellation and dissociation of the daughter cells. A culture of *C. reinhardtii* synchronised by a diurnal light period can have an average cell size significantly different from the mean, as can one affected by nutrient deprivation. Deprivation of sulphur, and to a lesser extent nitrogen, increases cell biovolume due to decreased cell division (Cakmak, Angun, Demiray, et al., 2012). One of the earliest discovered symptoms of folate and B_{12} deficiency in humans was macrocytic anaemia, an increase in mean erythrocyte volume (Zuelzer & Ogden, 1946). This is a consequence of methyl-folate trapping limiting thymidylate synthesis and hence DNA replication, which prevents progression to mitosis (Haurani, 1973; Hoffbrand & Jackson, 1993). Increased cell volume during B_{12} deprivation has also been observed in algae: In *Euglena gracilis* cell sizes take on a bimodal distribution with larger cells that appear unable to divide (Shehata.E. & Kempner, 1978). In light of this evidence, the increase in *metE7* cell size on B_{12} deprivation seems more likely a result of folate trapping and reduced DNA synthesis than a concerted downregulation of cell division, as occurs in *C. reinhardtii* when nutrients are limiting (Cakmak, Angun, Demiray, et al., 2012; Grossman, 2000).

B_{12} deprivation of *metE7* caused a slow but substantial decline in total chlorophyll (Figure 3.4c) while maintaining the ratio of chlorophyll a:b. Chlorosis is a common symptom of nutrient deficiency in *C. reinhardtii*, evident in nitrogen, sulphur, iron, and zinc limiting conditions (Kropat et al., 2011). The decrease in chlorophyll content is thought to mainly result from a cessation in synthesis while cell growth continues causing a diluting effect, but degradation may also play a role (Juergens et al., 2015; Schmollinger et al., 2014). The decrease in total protein content of *metE7* over 4 days of B_{12} deprivation occurred more slowly and was less substantial than has been reported under nitrogen and sulphur deprivation (an 80% reduction within 1 day) (Cakmak, Angun, Demiray, et al., 2012). As proteins are the major nitrogen-containing macromolecules in the cell it makes sense that nitrogen limitation would limit protein synthesis, and sulphur limitation has shown to cause a greater decrease in transcripts for proteins with a high sulphur content (González-Ballester et al., 2010). For B_{12} limitation, the reduced rate of methionine synthesis could restrict protein synthesis, but this hypothesis does not stand up to the observation that methionine levels, at least at one timepoint, were not lower in *metE7* during B_{12} deprivation. The turnover of protein may provide some of the carbon

for starch or TAG production, both of which increased under B_{12} deprivation (Msanne et al., 2012). There was no further increase in starch content between 2 and 4 days of deprivation, which is consistent with the finding that starch increases in the initial stages of nutrient limitation (Juergens et al., 2016; Siaut et al., 2011). The slight increase in starch from day 2 to 4 in B_{12}-replete conditions could suggest that as the cells enter stationary phase energy is produced in excess of that required for cell maintenance and so is diverted into the synthesis of starch (Juergens et al., 2016; Krishnan et al., 2015).

The increase in TAGs in *metE7* during B_{12} deprivation, at roughly 10-fold, is slightly higher than the change in starch, and similar to what has been observed during sulphur and nitrogen deprivation in *C. reinhardtii* (Cakmak, Angun, Ozkan, et al., 2012). What proportion of this increase is from lipid remodelling vs *de novo* fatty acid synthesis is not clear in this case, or indeed during other nutrient starvation conditions. The level of free fatty acids and polar lipids in *metE7* decrease by a roughly similar amount to the increase in TAG suggesting that perhaps there is little to no *de novo* fatty acid synthesis. During nitrogen and iron starvation in *C. reinhardtii* membrane lipids decrease drastically concomitant with the increase in TAGs (Siaut et al., 2011; Urzica et al., 2013). In addition, B_{12} deprivation causes similar shifts in fatty acid composition to N and Fe deprivation, notably the most substantial increase is in palmitic acid (16:0) and decrease is in the polyunsaturated 16:4 fatty acid (Msanne et al., 2012; Urzica et al., 2013). However, B_{12} deprivation did not cause a decrease in alpha-linolenic acid, as has been observed for the other two nutrients. In organisms as diverged as humans, *S. cerevisiae* and *A. thaliana*, disruption of one carbon metabolism causes an increase in triacylglycerides (da Silva et al., 2014; Meï et al., 2016; Visram et al., 2018). More specifically, the reduction of the methylation potential, a phenomenon also observed in this work, results in a lower phosphatidylcholine: phosphatidylethanolamine ratio, which may cause a shift in FA metabolism away from membrane lipids and towards TAGs (Malanovic et al., 2008; Visram et al., 2018). It would appear therefore that more could be learnt about the TAG accumulation effect of B_{12} deprivation on *metE7* from one carbon metabolism studies in other organisms than other nutrient deprivation studies in *C. reinhardtii*. Nevertheless, B_{12} deprivation could provide a complementary approach to understanding lipid metabolism in *C. reinhardtii*.

Abundances of the six previously studied transcripts (*METE, METH*, *METM*, *MTHFR*, *SAH1*, *SHMT2*) were in good agreement between both experiments that compared *metE7* under B_{12} replete and deprived conditions (Figure 3.2c and 3.5c). In addition to these transcripts, four further genes involved in one carbon metabolism were investigated, of which three showed no change, while *FTL1* was decreased by B_{12} deprivation. *FTL1* is related to *A. thaliana* Formate-tetrahydrofolate ligase (*THFS*), an enzyme that catalyses the reversible conversion of THF to 10-formyl THF (Hanson & Roje, 2001). *A. thaliana* and *C. reinhardtii* also encode a 10-formyl-THF deformylase which likely

catalyses the irreversible conversion of 10-formyl-THF to THF (Collakova et al., 2008; Hanson & Roje, 2001). Hence there is some reason to hypothesise that downregulation of FTL1 in *metE7* would reduce the drawdown of THF and, in parallel with the substantial increase in *SHMT2* and *MTHFR* transcript abundance, cause greater flux towards 5-CH_3-THF, the methyl donor in the production of methionine, and subsequently SAM. *MTHFR* is considered vital to balancing the folate pools used for DNA synthesis vs methylation, but it catalyses irreversible and reversible reactions in humans and plants respectively, and its nature in *C. reinhardtii* is unknown (Friso et al., 2005; Roje et al., 1999). Therefore, without further knowledge of enzyme kinetics, let alone enzyme abundances, it is very difficult to make any firm conclusions on what effect these changes in transcript abundance during B_{12} deprivation will have on folate pools.

3.3.6 B_{12} addition reverses the effects of B_{12} deprivation on the C1 cycle

A higher time resolution study of one carbon metabolism transcripts and metabolites was also generally in agreement with previous findings. Over the first 24 hours of B_{12} deprivation, SAH levels rose 100-fold, but a 3-fold increase in SAM over the same period caused a decrease in the methylation index by 34-fold (Figure 3.6a). In two *A. thaliana* mutants of one carbon metabolism (*MTHFD1* and *MAT4*) SAH levels were also found to rise, with a smaller change in SAM, resulting in an increase in methylation index of up to 20-fold (Groth et al., 2016; Meng et al., 2018). Methionine concentrations were much more variable in this work, and although the initial trend towards a decrease over the first 12 hours could be expected due to the disruption of methionine synthesis, after 24 hours methionine had substantially increased, in agreement with the measurements taken after 30 hours (Figure 3.2b). From 24 to 72 hours of B_{12} deprivation, all three metabolites decreased in abundance, the most unexpected of which was SAH. There is no evidence that plants or *C. reinhardtii* are able to metabolise homocysteine to cysteine via the reverse transulfuration pathway (Hanson & Roje, 2001), so the major route for homocysteine metabolism is via methyl transfer from 5-CH_3-THF, which in *metE7* under B_{12} deprivation is disrupted. An alternative pathway so far found only in plants is the S-methylmethionine cycle, a futile cycle composed of two reactions catalysed by methionine S-methyl transferase (*MMT*) and homocysteine S-methyltransferase (*HMT*) (Hanson & Roje, 2001). HMT converts homocysteine to methionine using SMM, or perhaps rarely SAM, as the methyl donor. *C. reinhardtii* encodes a homolog of *A. thaliana* HMT which could lower SAM and Hcy levels while replenishing methionine. A reduction in Hcy would also shift the SAH1-catalysed reaction in the direction of further Hcy synthesis causing a reduction in SAH. Addition of B_{12} after 72 hours decreased SAH, and to a lesser extent, SAM concentration. Increased flux through activated METH would consume Hcy, and indirectly SAH. Reduced competitive inhibition of methyl transfer reactions might also be the cause of declining SAM levels. Methionine, however, showed no sign of replenishment after B_{12} addition. Although flux through C1 metabolism in plants is high, indicative of

its importance to physiology, elucidation of its properties has been hindered by the difficulty in quantifying metabolites, and the relative lack of mutants (Hanson & Roje, 2001). Almost nothing is known about C1 metabolism in *C. reinhardtii*, but *metE7* could provide a useful tool for its further study.

The profiles of *METE*, *METH*, *METM*, *MTHFR*, *SAH1* and *SHMT2* were very similar to one another over the B_{12} deprivation and replenishment period, with all of the increase in transcript abundance occurring within 6 hours of resuspension in B_{12}–free media (Figure 3.6b). This dramatic initial rise occurs more quickly than the accumulation of SAH, adding to the evidence that B_{12} itself, rather than one carbon metabolites has the major control over the abundance of these transcripts. *MTHFD* and *TYMS* exhibit a similar profile to one another, but different to the previously mentioned six genes (Figure 3.6c). As both enzymes are bifunctional, and MTHFD catalyses reversible reactions it is difficult to conclude what change to metabolic flux would occur if the transcript abundance changes were reflected at the protein level. Furthermore, the overall changes over the 3-day period were minimal. The profile for *FTL1* transcript abundance was negatively correlated with the enzymes adjacent to the methionine synthesis reaction and to the concentration of SAH, lending further weight to the hypothesis that it plays a different role with respect to the methionine cycle than other enzymes of C1 metabolism.

3.3.7 *L. rostrata* survives B_{12} deprivation better than *metE7*

Considering that the EC_{50} for B_{12} was found to be lower for *L. rostrata* than *metE7*, it was unsurprising after culturing both strains with 100 $ng \cdot l^{-1}$ B_{12} and transferring them to B_{12}-free media that *L. rostrata* grew better than *metE7*. Nonetheless, by day 6 the viability of both strains was similar, showing that even an established B_{12} auxotroph is unable to survive for long in the absence of B_{12} (Figure 3.7c). Another widely reported indicator of stress in algae is derived from chlorophyll fluorescence measurements: *Fv/Fm* decreases under a number of nutrient stress conditions (Parkhill et al., 2001; White et al., 2011). The more gradual reduction in *Fv/Fm* for *L. rostrata* is reflective of the delayed decline in viability (Figure 3.7d). Nevertheless, it is important to note that *Fv/Fm* is not proportional to the percentage of viable cells: Dead cells retain some minimal fluorescence (F_0) when dark adapted, but do not exhibit an increase in fluorescence when exposed to light (Franklin et al., 2009). Hence, the measured *Fv/Fm* value is reasonably insensitive to the proportion of dead cells and, at least at low proportions, is more reflective of the *Fv/Fm* value of the live cells. With that in mind, it might be the case that during B_{12} deprivation a subpopulation of better acclimated *metE7* cells arise, which can maintain photosynthetic capacity and viability for a slightly longer period. Decrease in the value of non-photochemical quenching (NPQ) during nutrient deprivation is a commonly observed phenomenon in *C. reinhardtii*: measurements by chlorophyll fluorescence under nitrogen and sulphur

deprivation showed a gradual decline (Antal et al., 2006; Bonente et al., 2012). As NPQ dissipates excess absorbed light energy as heat it reduces the generation of singlet oxygen by excited chlorophyll and resultant oxidative damage (Müller et al., 2001). Transition to high light levels, but also to low nutrient conditions should result in light absorption in excess of utilisation and hence increased NPQ, but only under certain nutrient limiting conditions does this occur in *C. reinhardtii*, and it is more common under photoautotrophic than photoheterotrophic conditions (Saroussi et al., 2016; Terauchi et al., 2010). Perhaps therefore, NPQ would increase in *metE7* and *L. rostrata* under B_{12} deprivation had they been grown photoautotrophically. As it was, the higher starting NPQ for *L. rostrata* may have protected against the accumulation of oxidative damage, as appeared to be the case from the lower DCFDA fluorescence measurements per *L. rostrata* cell. Nonetheless, DCFDA is not considered to be the most accurate measure of ROS or oxidative damage (Kalyanaraman et al., 2012), and there are likely many other routes for ROS production and detoxification that could be altered by B_{12} deprivation.

3.3.8 *metE7* survives nitrogen deprivation better than B_{12} deprivation

Starting with the core treatment of interest, B_{12} deprivation of *metE7*, the other two treatments in Figure 3.8 substitute the alga and limiting nutrient for *L. rostrata* and nitrogen respectively. Furthermore, the connection between B_{12} deprivation of *L. rostrata* and nitrogen deprivation of *metE7* is that both are conditions that the species is likely to have encountered multiple times in its evolutionary history, and so may have developed a survival-enhancing response to. The difference in the growth profile between B_{12} and nitrogen deprivation in *metE7* suggests that under B_{12} deprivation there is no signal to reduce growth rate, and this results in unsustainable growth (Figure 3.8a). The 45% increase in mean cell diameter of B_{12}-deprived *metE7* cells over the first day, and hence 200% increase in cell volume, was substantially greater than the 45% increase in cell volume under nitrogen deprivation (Figure 3.8b). It would appear from comparison to other studies that in this way B_{12} deprivation is more similar to sulphur deprivation (Cakmak, Angun, Demiray, et al., 2012), and it is tempting to hypothesise that this may result from their shared impact on the methionine cycle (González-Ballester et al., 2010). The decrease in *L. rostrata* mean cell diameter on day one is puzzling but may be a result of the preculture conditions: as *L. rostrata* grows more slowly than *metE7* the decrease could be in response to the final resuspension in sufficient (200 $ng \cdot l^{-1}$) B_{12} (re-addition of B_{12} allows cells to resume division) prior to washing and resuspending in B_{12}-free media. Perhaps the most striking result of this experiment was the change in viability (Figure 3.8c). Nitrogen starved *C. reinhardtii* cells are known to survive for extended periods (Martin & Goodenough, 1975), yet the viability after just one day had declined by over 50%. Subsequent recovery of viability must therefore be due to the surviving cells continuing to divide to produce more viable cells despite a lower nitrogen quota, suggesting that it is the ability to acclimate to a change in nitrogen rather than

the absolute amount of nitrogen that determines survival. B_{12}-deprivation elicits no early decrease in viability, but this might be at the expense of the later and more severe decrease. Decrease in *Fv/Fm* during nitrogen deprivation may cause a decrease in the ratio of linear vs cyclic electron flow, as has been observed for sulphur and phosphorus-starved *C. reinhardtii*(Wykoff et al., 1998), or a total downregulation of photosynthesis(Schmollinger et al., 2014). B_{12} deprivation caused a delayed and less substantial decrease in *Fv/Fm* suggesting that photosynthesis continued for longer in spite of increased cell death (Figure 3.8d).

3.3.9 Nitrogen deprivation protects against B_{12} deprivation

Fv/Fm, which gives an indication of photosynthetic apparatus integrity (Schmollinger et al., 2014), and cell viability showed quite disparate responses under B_{12} and nitrogen deprivation indicating perhaps that *Fv/Fm* in these circumstances was less an indicator or stress itself than response to stress (Figure 3.8d). To investigate whether the photosynthetic and other responses to nitrogen deprivation would be sufficient to protect against B_{12} deprivation, *metE7* was cultured in media lacking both nitrogen and B_{12}, as well as media lacking each nutrient individually. The degree of growth limitation, as measured by culture optical density, was the same in all three nutrient limited conditions (Figure 3.9a). However, the lower number of viable cells in the B_{12}-limited treatment (Figure 3.9b) suggested that it was the more stressful condition. Nitrogen deprivation is a well-known prerequisite for gamete formation in *C. reinhardtii* (Beck & Acker, 1992), and cells are able to survive for many weeks under this condition (Martin & Goodenough, 1975). So, in comparison to other nutrient deprivation conditions such as sulphur or phosphorus, the loss of viability under B_{12} deprivation may not seem as drastic. The decline in viable cells in nutrient replete culture was unexpected however, and was not observed to the same extent in repeats of the experiment, but it has been found that nitrogen limitation improves survival of various phytoplankton exposed to high light (Kulk et al., 2013). That the combination of nitrogen and B_{12} deprivation improved survival relative to B_{12} deprivation alone, illustrates that nitrogen deprivation induces general survival responses that cross-protect against B_{12} deprivation. One potential and previously mentioned mechanism for protection against stress is induction of NPQ. A transient increase was observed in both nitrogen-limited conditions, however, the largest increase in NPQ was in the nutrient replete treatment following a decline in viability (Figure 3.9c). A reduction in PSII efficiency occurs in parallel with growth stagnation in *C. reinhardtii* (Grossman, 2000; Nedelcu, 2009), and an increase in the photoprotective protein LHCSR has also been observed, although this did not result in increased NPQ (Humby et al., 2013). Other mechanisms to increase light energy dissipation or reduce its initial absorption may start to dominate later in nitrogen deprivation, which could explain the transience of the NPQ rise. Indeed, under all conditions except B_{12} deprivation, total chlorophyll content per cell decreased in the first 24 hours (Figure 3.9e). The increase under B_{12} deprivation to a large extent

results from the increase in cell size, but even relative to optical density of the culture chlorophyll content was higher in this treatment. In addition to their role in NPQ, some carotenoids, including zeaxanthin and lutein, can act as antioxidants and protect against lipid peroxidation in thylakoid membranes (Müller et al., 2001; Sujak et al., 1999). After an initial decline, both nitrogen limited conditions showed an increase in carotenoids that was most clearly absent from the B_{12}-limited cultures (Figure 3.9f). B_{12} deprivation-induced loss of viability might therefore be linked to the lack of carotenoids, with their antioxidant activity as well as their effect on reducing membrane fluidity and hence penetration of thylakoid membranes by ROS (Tardy & Havaux, 1997). ROS damage was initially only measured to be highest under B_{12} deprivation at one timepoint, 48 hours (Figure 3.9d). However, subsequent measurements confirmed that 48 hours represented the midpoint and peak of a period of higher ROS damage (Figure 3.10a). This peak also coincided with the start of a decline in cell viability (Figure 3.10b). High levels of reactive oxygen species and lipid peroxidation are often found to precede cell death in plants and algae (Baroli et al., 2004; Pérez-Pérez et al., 2012; Triantaphylidès et al., 2008), and so seems likely to be cause of cell death in B_{12} deprivation. Overall, deprivation of B_{12} in *metE7* does not appear to elicit the same responses as other nutrients, which act to increase survival under suboptimal conditions.

3.3.10 Artificial evolution improves growth and survival under limiting B_{12}

The conditions chosen for experimental evolution of *metE7* were quite distinct and should have resulted in very different selection pressures. One hypothesised outcome was a difference in growth responses to a range of B_{12} concentrations, with those lines evolved under limiting B_{12} and in coculture with *M. loti* (condition B and C) having a lower requirement for B_{12} than the lines evolved under replete B_{12} conditions. Although the EC_{50} values for line B and C were lower than for line A, only the difference with line C was statistically significant, and all three evolved lines also had a significantly lower EC_{50} value than the line stored on Tris min agar during the experimental evolution period (Figure 3.12c). The predicted carrying capacity under replete B_{12} showed similar results, but there was no significant difference between any of the evolved *metE7* lines. *L. rostrata* still had the lowest EC_{50} value and carrying capacity of the strains, which was unsurprising given the relative brevity of the experimental evolution period. The differences in calculated carrying capacity and particularly in EC_{50} values may be exaggerated by the short time period over which growth was measured (within which growth at higher B_{12} concentrations had not fully saturated), and the fact that optical density declined in some strains at lower B_{12} levels.

The results of B_{12} deprivation on the evolved lines was slightly more significant in a statistical sense. *L. rostrata* had the highest optical density, viability, and PSII maximum efficiency at the end of the 6-day period, as predicted. The second highest mean value for all of these three metrics was from

either lines B or C. Line B was exposed to conditions where B_{12} was only added to a low concentration (25 $ng \cdot l^{-1}$) once per week, and so would rapidly have been taken up and become limiting again. Survival until the next addition of B_{12} may therefore have been the greatest selection pressure, and therefore caused those lines to maintain higher viability during B_{12} deprivation than those which were constantly replete (line A). Of the evolved lines, line C showed the lowest EC_{50} for B_{12} (figure 3.12c), so the fact that it reached the highest optical density and maintained the highest photosynthetic capacity during B_{12} deprivation (Figure 3.12a,c) seems to contribute to the idea that it developed the highest B_{12} use efficiency. Slow but continuous growth in the low levels of B_{12} produced by *M. loti* may have provided this selection pressure. Non-photochemical quenching does not appear to play an obvious role in maintaining viability, as *L. rostrata* and line B had some of the highest and lowest NPQ values throughout the deprivation period respectively while also both sustaining some of the highest levels of viability. Repeats of these experiments would certainly be necessary before it could be claimed with any reasonable degree of confidence that this period of experimental evolution was sufficient to make *metE7* better suited to growing in B_{12} limiting conditions. The fact that *metE7* survived the 7-month period without artificial addition of B_{12}, instead relying completely on *M. loti*, does suggest however that even a newly evolved and poorly adapted B_{12} auxotroph would have ample opportunity to adapt further.

3.4 Concluding remarks

An artificially evolved B_{12}-dependent mutant of *C. reinhardtii* (*metE7*), shows a classic dose-response to B_{12} that is not seen in the wild type. In comparison with a related B_{12} auxotroph, *L. rostrata, metE7* has a higher requirement for B_{12} with a more rapid loss of viability on B_{12} removal but similar uptake kinetics. B_{12} deprivation increases the expression of C1-cycle genes at the transcript level in both the wild type and *metE7* strain, but only causes a decrease in the methylation index (SAM:SAH ratio) in *metE7*. B_{12} deprivation of *metE7* also causes a decrease in chlorophyll, protein and amino acids, and an increase in starch, lipids and saturated fatty acids. The rapid loss of viability seen under B_{12} deprivation can be averted if the *metE7* cells are also limited for nitrogen, suggesting that it is not the lack of B_{12} per se that causes cell death, but an inability to alter metabolism. *metE7* can be supported for at least several months by a B_{12}-producing bacterium, and under these and other B_{12}-limited conditions appears to adapt by improving B_{12} use efficiency and survival under B_{12} deprivation.

Chapter 4: Coping with B_{12} auxotrophy in the long term through symbiosis

4.1 Introduction

Relationships between multicellular organisms in a community are often portrayed by food-webs, where producers and consumers are linked by the trophic flow of organic material and energy. In microbial communities, interactions based on nutrient transfer abound and bidirectional transfer or mutualism is more common (Zelezniak et al., 2015). The success of many mutualisms derives from the concept of comparative advantage: a difference in the ratio of the costs of producing two products between a pair of organisms. Often it is the case that mutualists transfer nutrients that are not just costlier for their partner to produce, but which they are incapable of producing. An example of this is the interaction between two marine microbes, the alga *Ostreococcus tauri* and bacteria *Dinoroseobacter shibae*. *O. tauri* requires vitamin B_1 and B_{12} (Palenik et al., 2007), *D. shibae* requires B_3, B_7, and B_x (Biebl et al., 2005), and each partner can produce the vitamins that the other requires, so supporting one another when grown in coculture with no added vitamins (Cooper et al., 2019).

The concentration of dissolved vitamin B_{12} varies considerably in marine and fresh waters, depending on depth, season, abundance of phytoplankton, and proximity to the coast from values as high as 83 $ng \cdot l^{-1}$ in bay areas to 0.3 $ng \cdot l^{-1}$ in the open ocean (Cowey, 1956; Daisley, 1969; Daisley & Fisher, 1958; Ohwada, 1973; Ohwada & Taga, 1972; Panzeca et al., 2009). It has been known for some time that a large number of algae require B_{12} for growth (Carlucci & Silbernagel, 1969; Croft et al., 2005; Droop, 1974), and heterotrophic bacteria have been shown to stimulate algal growth by B_{12} provision (Croft et al., 2005; Haines & Guillard, 1974; Kazamia et al., 2012; Xie et al., 2013), although there is debate as to whether this interaction is better termed symbiosis or scavenging (Croft et al., 2005; Droop, 2007). In this chapter I shall use the terms symbiosis and mutualism rather than scavenging and direct reciprocity, but only in the loosest sense to mean some interaction between organisms.

Bacteria from the Oceanospirillaceae were found to be dominant B_{12}-producers in the Southern Ocean near the sea ice edge, and to express organic-matter-acquisition and cell-surface-attachment genes, suggestive of mutualistic interactions with phytoplankton (Bertrand et al., 2015). A marine phytoplankton, *Prorocentrum minimum*, auxotrophic for vitamin B_1 and B_{12}, was supported by the addition of the B_{12}-producer *D. shibae* (Wagner-Döbler et al., 2010), and the growth of several B_{12} auxotrophic diatoms was rescued by inoculating cultures with B_{12}-producing bacteria (Haines & Guillard, 1974). There are several other examples using these approaches of environmental sampling or pairing of species in the laboratory which together suggest that interactions involving the transfer

of B_{12} are widespread. However, the dynamics of these interactions are less clear, for example, *Thalassiosira pseudonana* and an unknown B_{12}-producing bacterium supported one another with growth occurring in parallel initially, but in later growth stages the abundance of both species showed roughly antiphase oscillations (Haines & Guillard, 1974). The authors suggested this indicated that algal cell death nourished the growth of the bacteria, which then produced more B_{12} and reversed the algal decline. On the other hand, in a symbiosis between the freshwater alga *Lobomonas rostrata* and the rhizobial bacterium *Mesorhizobium loti*, mathematical modelling of the transfer of nutrients suggested that B_{12} was made available to the alga not by bacterial lysis but by some mechanism of regulated release (Grant et al., 2014). In both the marine and freshwater example mentioned above addition of B_{12} to the coculture increased algal cell density indicating that B_{12} supply by the bacteria limited algal growth. Addition of a carbon source to the *M. loti-L. rostrata* coculture increased bacterial growth without concomitant increases in algal density, suggesting decreased B_{12} synthesis per bacterium (Grant et al., 2014). In contrast, cultures of *Halomonas sp.*, which formed a symbiotic interaction with *Porphyridium purpureum* via provision of B_{12}, increased production of B_{12} per cell when the algal carbon source fucoidan was added (Croft et al., 2005). These examples suggest there is considerable variety among interactions involving B_{12} transfer that makes them worth investigating individually.

C. reinhardtii can use B_{12} as a cofactor in the synthesis of methionine, but under normal conditions grows equally well without it. At high temperatures however, in the absence of B_{12} reduced activity of the B_{12}-independent methionine synthase (METE) leads to chlorosis and cell death (Xie et al., 2013). Addition of B_{12} and hence activation of the alternative methionine synthase (METH), which is more robust to high temperatures, reduces chlorosis, as does coculturing *C. reinhardtii* with the B_{12}-producer *S. meliloti* (Xie et al., 2013). In our laboratory, experimental evolution of *C. reinhardtii* in the presence of high levels of vitamin B_{12} gave rise to a B_{12} auxotrophic mutant that outcompeted the ancestral strain (Helliwell et al., 2015). A stable B_{12}-dependent variant (*metE7*) of this evolved strain could be supported in coculture separately with three rhizobia species, including *S. meliloti*, but at a lower growth rate than when B_{12} was added to the medium. Although these mutualistic partnerships were established in the laboratory, they provide insight into a possible mechanism for long term survival in the natural environment that is available to a newly evolved B_{12} auxotroph.

In this chapter I will firstly compare how *metE7* and the ancestral *C. reinhardtii* strain grow with *M. loti* in coculture, effectively a mutualistic and commensal interaction respectively. Two mutualisms with *M. loti* will then be compared: one involving the newly evolved B_{12} auxotroph *metE7*, and the other a related but more established auxotroph *L. rostrata*. I will discuss the direct and indirect impacts of nutrient addition on cocultures of *M. loti* and *metE7*, and whether it indicates any regulation of nutrient release. By correlating *M. loti* density and B_{12} concentration in axenic culture

and cocultures, as well as by adding *metE7* cells to *M. loti* cultures I investigate whether bacterial B_{12} production is induced by the presence of algae. Using an *E. coli* mutant that releases a larger proportion of its synthesised B_{12} into the media, the importance of 'leakiness' for symbiosis is examined. Finally, I test whether *M. loti* can support the evolution of B_{12} auxotrophy by competing a B_{12}-dependent and a B_{12}-independent strain of *C. reinhardtii* against one another in the bacteria's presence.

4.2 Results

4.2.1 Comparing a mutualistic and commensal interaction

Many B_{12}-producers are heterotrophic and so ultimately rely on photoautotrophs for their fixed carbon (Heal et al., 2017). These B_{12}-producers may not have provided any benefit to the B_{12}-independent ancestors of algae, but to co-occur over long periods of time one might hypothesise that they did not have a negative impact either, i.e. were commensal. Here I have tested what the effect of *M. loti* is on the B_{12}-independent ancestral line of *C. reinhardtii* and vice versa when they are grown in media which lacks a carbon source and B_{12}. *C. reinhardtii* and *M. loti* were precultured separately by inoculating individual colonies into 50 ml nunc flasks containing 20 ml of Tris minimal medium with either 100 $ng \cdot l^{-1}$ B_{12} or 0.01% glycerol respectively. These cultures were incubated on a shaking platform at 120 rpm, 25°C, 100 $\mu E \cdot m^{-2} \cdot s^{-1}$, with a light:dark period of 16:8 hours. *C. reinhardtii* and *M. loti* were then inoculated at roughly 10,000 and 200,000 $cells \cdot ml^{-1}$ respectively in Tris minimal medium (with neither B_{12} nor a carbon source) to produce two sets of axenic cultures and one of cocultures. Measurements of the density of *C. reinhardtii* and *M. loti*, as well as the concentration of B_{12} were taken every 2-3 days over a 24-day period.

Figure 4.1a illustrates that the growth of the ancestral line of *C. reinhardtii* is not affected by the presence of *M. loti*. Figure 4.1b however, shows that there is a significant improvement in the growth of *M. loti* in the presence of *C. reinhardtii*. After 2 days of similar growth rates in axenic or coculture conditions, *M. loti* growth stops abruptly under axenic conditions, presumably as the carbon source (glycerol) from the preculture conditions is exhausted. In the coculture, *M. loti* appears to transition to the metabolism of organic compounds produced by *C. reinhardtii,* which might be secreted or be part of the algal cell itself. It is likely that any algal biomass would only be available for metabolism by *M. loti* after cell death as *M. loti* has no negative impact on *C. reinhardtii* growth.

Figure 4.2a compares the growth of the ancestral and revertant strains of *C. reinhardtii* (both B_{12}-independent) and that of *metE7* in coculture with *M. loti*. The growth of the latter is reduced

slightly compared to the B_{12}-independent strains, as is the carrying capacity reached after 20 days. This is presumably because of B_{12} limitation. Despite this, *M. loti* growth is similar whichever *C. reinhardtii* strain it is cocultured with (Figure 4.2b). Since at any one time point there are fewer *metE7* cells, this suggests that *metE7* cells provide a larger quantity of organic compounds that can be metabolised by *M. loti*. Alternatively, the differences in the ratio of bacteria to algae (Figure 4.2c) could be explained by the fact that *M. loti* growth is limited by something other than organic compound concentration. By the end of the growth period, B_{12} concentration and *M. loti* density are similar across the cultures (Figure 4.2d and 4.2b), while *metE7* density still lags behind that of the other *C. reinhardtii* strains, indicating that the B_{12} available per algal cell is likely greatest for *metE7*.

xix Figure 4.1 Growth of ancestral strain of *C. reinhardtii* and *M. loti* in axenic culture or coculture

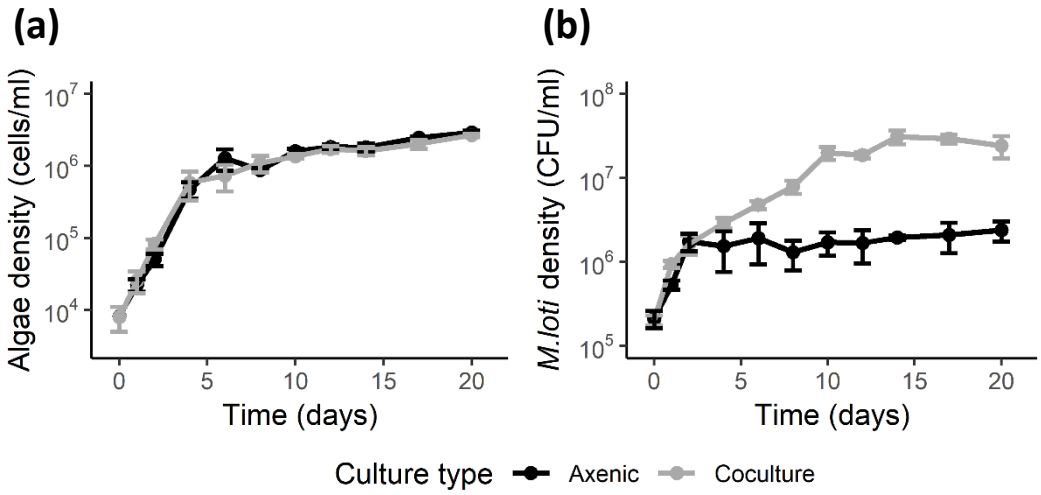

Figure 4.1 Growth of ancestral strain of *C. reinhardtii* and *M. loti* in axenic culture or coculture. Cultures were grown over a 20-day period in Tris minimal medium with illumination in a 16:8 hour period at 100 µE·m^{-2}·s^{-1} at 25°C with circular shaking at 120 rpm. **(a)** Algal cell density measured by particle counter for particles > 3 µm in diameter. **(b)** *M. loti* cell density measured as colony forming units (CFU) when serial dilutions were plated on TY agar. Black = axenic culture (either Ancestral *C. reinhardtii* or *M. loti* cultured separately), grey=coculture of ancestral *C. reinhardtii* + *M. loti*. Error bars = sd, n=4.

xx Figure 4.2 Growth of *C. reinhardtii* strains in coculture with *M. loti*

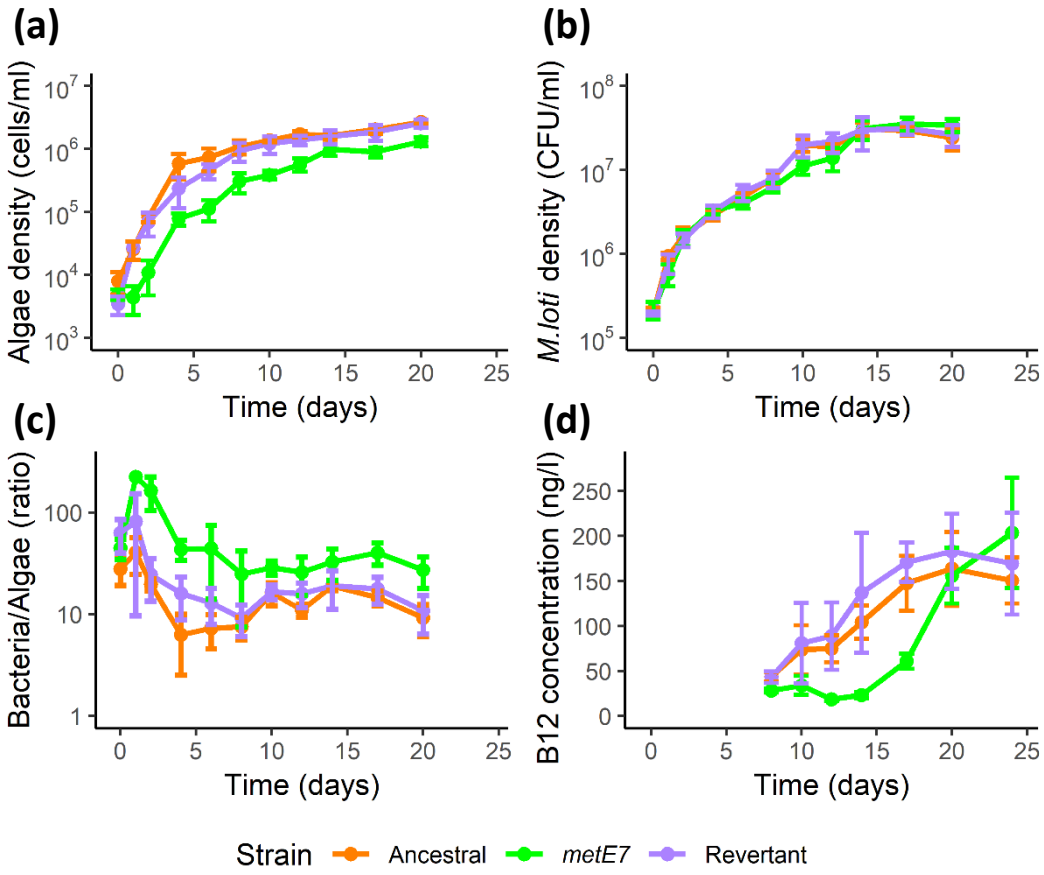

Figure 4.2 Growth of *C. reinhardtii* strains in coculture with *M. loti* over a 25-day period. Cultures were grown over a 25-day period in Tris minimal medium with illumination in a 16:8 hour period at 100 $\mu E \cdot m^{-2} \cdot s^{-1}$ at 25°C with circular shaking at 120 rpm. **(a)** Algal cell density measured by particle counter for particles > 3µm in diameter. **(b)** *M. loti* cell density measured as colony forming units (CFU) when serial dilutions were plated on TY agar. **(c)** The calculated ratio of *M. loti* CFU to algal cells. **(d)** Total B_{12} concentration in the culture measured by bioassay from day 8 onwards. Orange = Ancestral strain, green = metE7 strain, purple = Revertant. Error bars = sd, n=4.

4.2.2 Comparing a natural and newly-evolved B_{12} auxotroph

As with the previous chapter, it is useful to not only compare *metE7* with the wild type of the same species, but also with another related alga that lacks *METE*, such as *L. rostrata*. Any phenotypic differences between these species might just reflect the random mutations that have accumulated since their divergence, however they might also reflect the different selection pressures that are imposed on a B_{12}-dependent and B_{12}-independent alga. Cocultures of both *metE7* and *L. rostrata* were initially prepared as described above, however, they were allowed to equilibrate for several days prior to resuspending them at an algal cell density of roughly 10,000 cells·ml^{-1} to start algal, bacterial, and B_{12} measurements. *L. rostrata* has a slower maximal growth rate under optimal conditions than *metE7* (as shown previously in Figure 3.3b), but in coculture with *M. loti*, *L. rostrata* grows more quickly (Figure 4.3a). *M. loti* density remains higher throughout the growth period in coculture with *metE7* (Figure 4.3b), resulting in a significantly higher ratio of bacteria to algae for *metE7* than *L. rostrata* (Figure 4.3c). This appears similar to the comparison with wild type *C. reinhardtii*, and although *L. rostrata* clearly requires B_{12}, the concentration needed to support its growth is lower than that of *metE7* (Figure 3.3a). The concentration of B_{12} in the media is higher towards the end of the growth period of the *L. rostrata* coculture despite a similar or lower density of *M. loti* (Figure 4.3d). This might be due to a reduced uptake of B_{12} by *L. rostrata* or could be due to *L. rostrata* causing *M. loti* to produce more B_{12}, as has been previously suggested by Kazamia et al. (2012). Indeed, Figure 3.3e shows that for the same density of *M. loti* cells, cocultures containing *L. rostrata* have a higher concentration of B_{12} than those with *metE7* ($p<0.001$). Relative to algal cells however, to some extent the opposite appears to be true: there is more B_{12} per algal cell, particularly at higher cell densities, in cocultures containing *metE7* than *L. rostrata* (Figure 3.3f). Overall, there are minor but consistent differences between cocultures of *L. rostrata* and *metE7* that seem in part to be explained by their differences in B_{12} requirement, but perhaps are also due to their interactions with *M. loti*.

xxi Figure 4.3 Growth of *metE7* and *L. rostrata* in coculture with *M. loti*

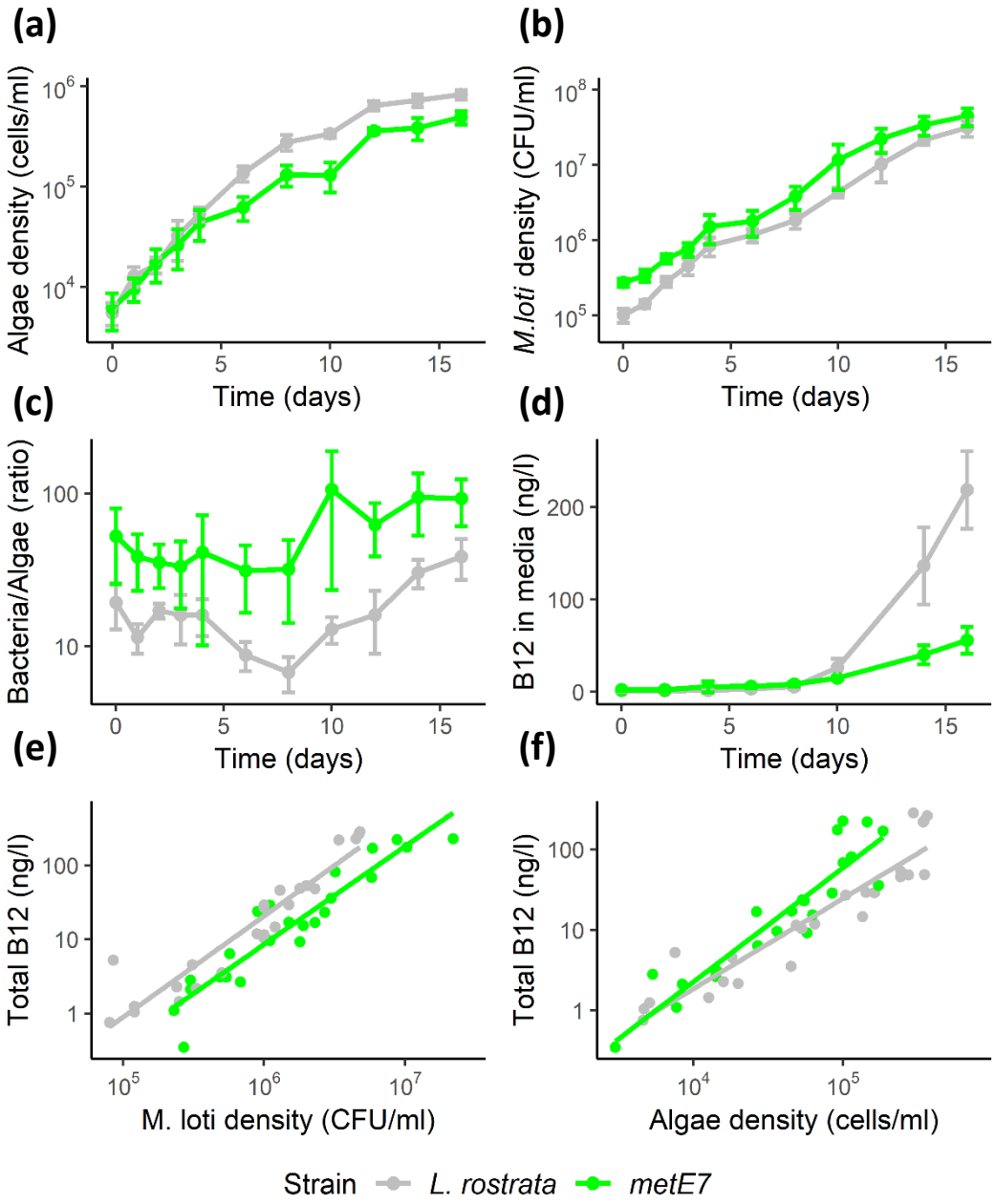

Figure 4.3 Growth of *metE7* and *L. rostrata* in coculture with *M. loti* over a 16-day period. Cultures were grown over a 16-day period in Tris minimal medium with illumination in a 16:8 hour period at 100 µE·m^{-2}·s^{-1} at 25°C with circular shaking at 120 rpm **(a)** Algal cell density measured by particle counter for particles > 3 µm in diameter. **(b)** *M. loti* cell density measured as colony forming units (CFU) when serial dilutions were plated on TY agar. **(c)** The calculated ratio of *M. loti* CFU to algal cells. **(d)** B_{12} concentration in supernatant of centrifuged culture measured by bioassay. **(e)** Correlation between total B_{12} concentration and *M. loti* CFU density. **(f)** Correlation between total B_{12} concentration and algal cell density. Green = *metE7* strain, grey = *L. rostrata*. Error bars = sd, n=4.

4.2.3 Growth limitations of *metE7* and *M. loti* in coculture

The mutualistic, or at least syntrophic, interaction between *metE7* and *M. loti* cocultured in minimal medium is highly unlikely to recreate conditions that would be optimal for the growth of each species individually. Still, the success of mutualisms more generally is because environmental conditions tend to be far from optimal from the perspective of any one species. I will describe two similar experiments that were performed to investigate the impact of adding either a carbon source or B_{12} to cocultures, both directly on the species that requires the nutrient, and indirectly on the other species. As before, cocultures were incubated in photoautotrophic conditions in Tris minimal medium on a shaking platform at 120 rpm, 25°C, 100 $\mu E \cdot m^{-2} \cdot s^{-1}$, with a period of 16:8 hours of light and dark. *M. loti* and *metE7* densities were monitored, and after the cocultures had been maintained for several days they were split into three treatments: a control where no changes were made; addition of B_{12} to a concentration of 200 $ng \cdot l^{-1}$; addition of glycerol to a concentration of 0.02 % (v/v). In the batch experiment no media was replaced after sampling, but in the semi-continuous experiment 10% of the total volume was removed for sampling and replaced with fresh media daily (containing B_{12} or glycerol where appropriate).

In Figure 4.4 day 0 denotes the day that nutrients were added, and shortly afterwards there is a divergence in the densities of *metE7* or *M. loti*. In both batch and semi-continuous conditions cobalamin addition causes an increase in *metE7* density after 1 day (Figure 4.4a). There appears to be no effect on *M. loti* density however, which remains similar to the control throughout the 6-day growth period (Figure 4.4b). Glycerol addition causes an increase in the *M. loti* density in batch and semi-continuous conditions within 1 day, but in the batch conditions the *M. loti* density peaks on day 2, after which cell death returns the cell density to the same level as the other two conditions by day 6 (Figure 4.4b). Glycerol addition also induces an increase in *metE7* density, although this occurs with a delay of roughly 1 day relative to cobalamin addition (Figure 4.4a). Combining *metE7* and *M. loti* cell density data to produce a ratio between the two exemplifies the significant change in the cocultures, and in opposite directions, elicited by nutrient addition (Figure 4.4c). For 2 days after cobalamin or glycerol addition the ratios of *M. loti*:*metE7* diverge to almost 1000-fold, but following this they converge again to differing extents. In the batch culture the convergence is completed by a substantial decline in the *M. loti:metE7* ratio two days after glycerol addition. In both batch and semi-continuous culture, glycerol addition eventually results in the ratio of *M. loti:metE7* being no different or lower than the ratio in the control conditions, even though temporarily the ratio was considerably higher.

In the semi-continuous cultures, which were performed after the batch experiment, B_{12} was also measured in the whole culture and the supernatant after centrifuging to pellet cells (Figure 4.5a-b). Algal cells with diameters from 3-9 µm and those above 9 µm were also quantified, with the

seemingly arbitrary 3-9 µm range being relevant because almost 100% of *C. reinhardtii* cells are within this range when growing in nutrient replete conditions, while cell diameters increase significantly on B_{12} deprivation (Figure 3.4a-b). The total amount of B_{12} increased by a roughly similar amount 1 day after addition of B_{12} itself or glycerol, but after that the increase in B_{12} concentration following glycerol addition was much more substantial (Figure 4.5a). Although on day 1 the B_{12} concentration was lower in the control coculture than the one to which B_{12} was added, as was to be expected, this difference had disappeared by 5-6 days, presumably due to a higher level of B_{12} synthesis in the control coculture. B_{12} was added to cultures immediately after sampling them on day 0, and yet B_{12} measured in the media 24 hours later was not any higher than the control cultures, indicating that all the added B_{12} had been taken up (Figure 4.5b). The level in the cultures with glycerol addition was, however, higher from 2 days onward. Within the first day after B_{12} addition *metE7* cell density increased, with a concomitant increase in the number of cells with diameters from 3-9 µm and decrease in those >9 µm. In the glycerol-added cultures the proportion of cells with diameters from 3-9 µm increased only after a 2-day delay. As *M. loti* density was the first factor to respond to glycerol addition, followed by an increase in B_{12} concentration, and then *metE7* cell density, it seems likely that B_{12} rather than organic carbon was limiting *metE7* growth. Together the data suggests that both *M. loti* and *metE7* are limited in coculture, for fixed carbon and B_{12} respectively, and that although glycerol addition can indirectly benefit *metE7*, B_{12} addition does not indirectly lead to increased growth of *M. loti*.

xxii Figure 4.4 Growth of *metE7* with *M. loti* and added nutrients

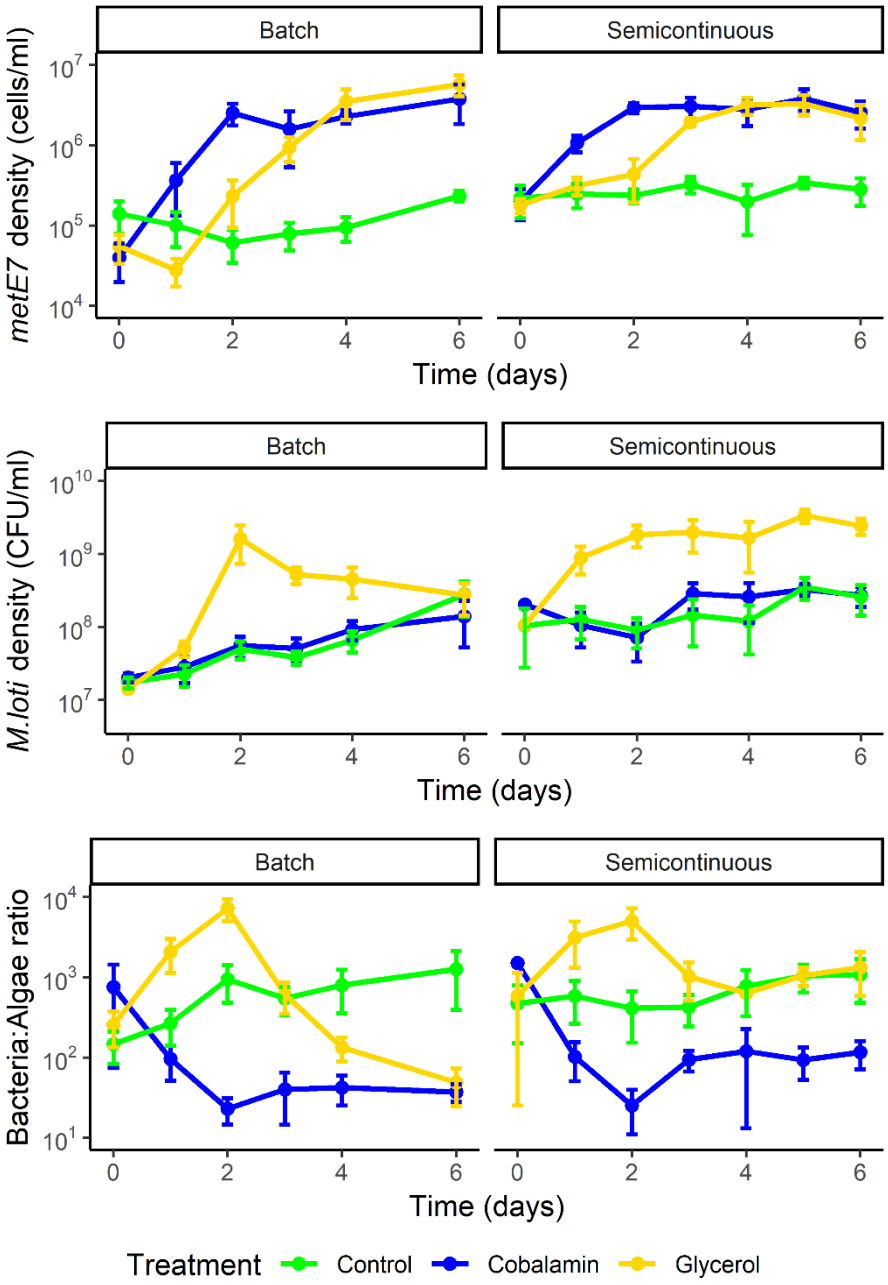

Figure 4.4 Growth of *metE7* in coculture with *M. loti* with added nutrients. Cultures were grown over a 6-day period in Tris minimal media with illumination in a 16:8 hour period at 100 $\mu E \cdot m^{-2} \cdot s^{-1}$ at 25°C with circular shaking at 120 rpm. Glycerol or cobalamin were added to established cocultures on day 0. Semi-continuous cultures were diluted with a volumetric replacement of 10% per day. **(a)** Algal cell density measured by particle counter for particles > 3 µm in diameter. **(b)** *M. loti* cell density measured as colony forming units (CFU) when serial dilutions were plated on TY agar. **(c)** The calculated ratio of *M. loti* CFU to algal cells. Green = control coculture with no nutrients added, yellow = glycerol added to 0.02% (v/v), blue = B_{12} added to 200 $ng \cdot l^{-1}$. Error bars=sd, n>=4.

xxiii Figure 4.5 Growth of *metE7* with *M. loti* and added nutrients 2

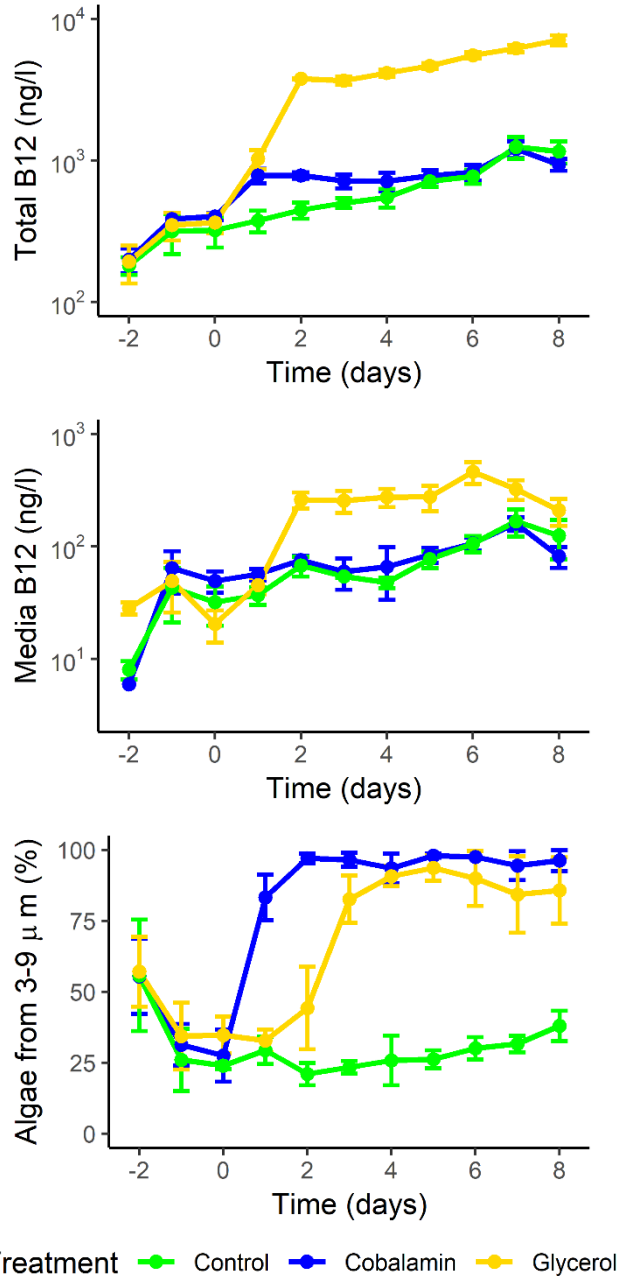

Figure 4.5 Growth of *metE7* in coculture with *M. loti* with added nutrients. Cultures were grown over a 6-day period in Tris minimal media with illumination in a 16:8 hour period at 100 $\mu E \cdot m^{-2} \cdot s^{-1}$ at 25°C with circular shaking at 120 rpm. Glycerol or cobalamin were added to established cocultures on day 0. Semi-continuous cultures were diluted with a volumetric replacement of 10 % per day. **(a)** B_{12} concentration in total culture measured by bioassay **(b)** B_{12} concentration in supernatant of centrifuged culture measured by bioassay. **(c)** Proportion of particles >3µm that were also <9µm, i.e. [3-9µm]/[>3µm]. When *C. reinhardtii* cells are in exponential phase in optimal growth conditions almost 100% are 3-9µm in diameter. Green = control coculture with no nutrients added, yellow = glycerol added to 0.02% (v/v), blue = B_{12} added to 200 $ng \cdot l^{-1}$. Error bars=sd, n=4.

4.2.4 *M. loti* B_{12} production when grown axenically and in coculture with *metE7*

Grant et al. (2014) observed that the amount of B_{12} normalised to *M. loti* cell density was higher when *M. loti* was grown in coculture with *L. rostrata* than when grown axenically (Grant et al., 2014). Several experiments similar in form to those presented in Figures 3.1-3.3 were performed primarily to provide data to aid parameter estimation for a mathematical model describing the interaction between a B_{12}-dependent alga and a B_{12}-producing bacterium (Peaudecerf et al., 2018). Here, some of the data from those experiments is used to determine whether *M. loti* also produces more B_{12} in the presence of *metE7*. The requirements for inclusion in this analysis were: the cultures were either composed of *M. loti* alone or *M. loti* in coculture with *metE7*; The cultures were incubated in Tris minimal medium with no additional amendments on a shaking platform at 120 rpm, 25°C, 100 $\mu E \cdot m^{-2} \cdot s^{-1}$, with a light:dark period of 16:8 hours; *M. loti* $CFU \cdot ml^{-1}$, and B_{12} concentration ($ng \cdot l^{-1}$) in the media and cell fraction were all quantified. To separate the cells and media, the culture was centrifuged at 16,000g for 2 minutes, and the supernatant removed as the media fraction, whilst the cell pellet was resuspended in the same volume of B_{12}-free media. The total fraction was an uncentrifuged sample, or the sum of the cell and media fractions. The values in the different fractions are shown in Figure 4.6a-c. A strong ($R^2=0.78$) and highly significant ($p<2*10^{-16}$) correlation was found between log-transformed *M. loti* density and log-transformed total B_{12} concentration. In addition, a significant effect of culture type was found ($p=2.3*10^{-11}$), where axenic cultures had an 80% higher total B_{12} concentration for a given *M. loti* density than cocultures. The gradient of the relationship between log(*M. loti* density) and log([B_{12}]) was substantially lower than 1, meaning that B_{12} per *M. loti* cell decreased as *M. loti* density increased. For B_{12} in the media fraction the interaction between *M. loti* density and culture type was highly significant ($p=1.8*10^{-11}$), indicating that in cocultures B_{12} in the media increased at a slower rate as *M. loti* density increased than in axenic cultures (Figure 4.6b). This could be explained by the fact that B_{12} is taken up by *metE7* in cocultures, but at low *M. loti* densities the concentration of B_{12} in the media may be at the limit of the affinity of the algal B_{12} uptake system. The strongest correlation was observed between B_{12} in the cell pellet and *M. loti* density, with an $R^2=0.85$, and a small (30%) but significantly ($p=0.00064$) higher concentration of B_{12} per *M. loti* cell in cocultures (Figure 4.6c). This result is not particularly surprising given that B_{12} in the cells in coculture is from both *metE7* and *M. loti* cells, however, it is in spite of a much higher total amount of B_{12} per *M. loti* cell in axenic cultures. Overall, it appears that *metE7* cells can take up B_{12} produced by *M. loti* and hence move B_{12} from the media fraction to the cell fraction but cannot increase the total B_{12} production by *M. loti*.

xxiv Figure 4.6 Correlation between *M. loti* density and B_{12} concentration in various fractions

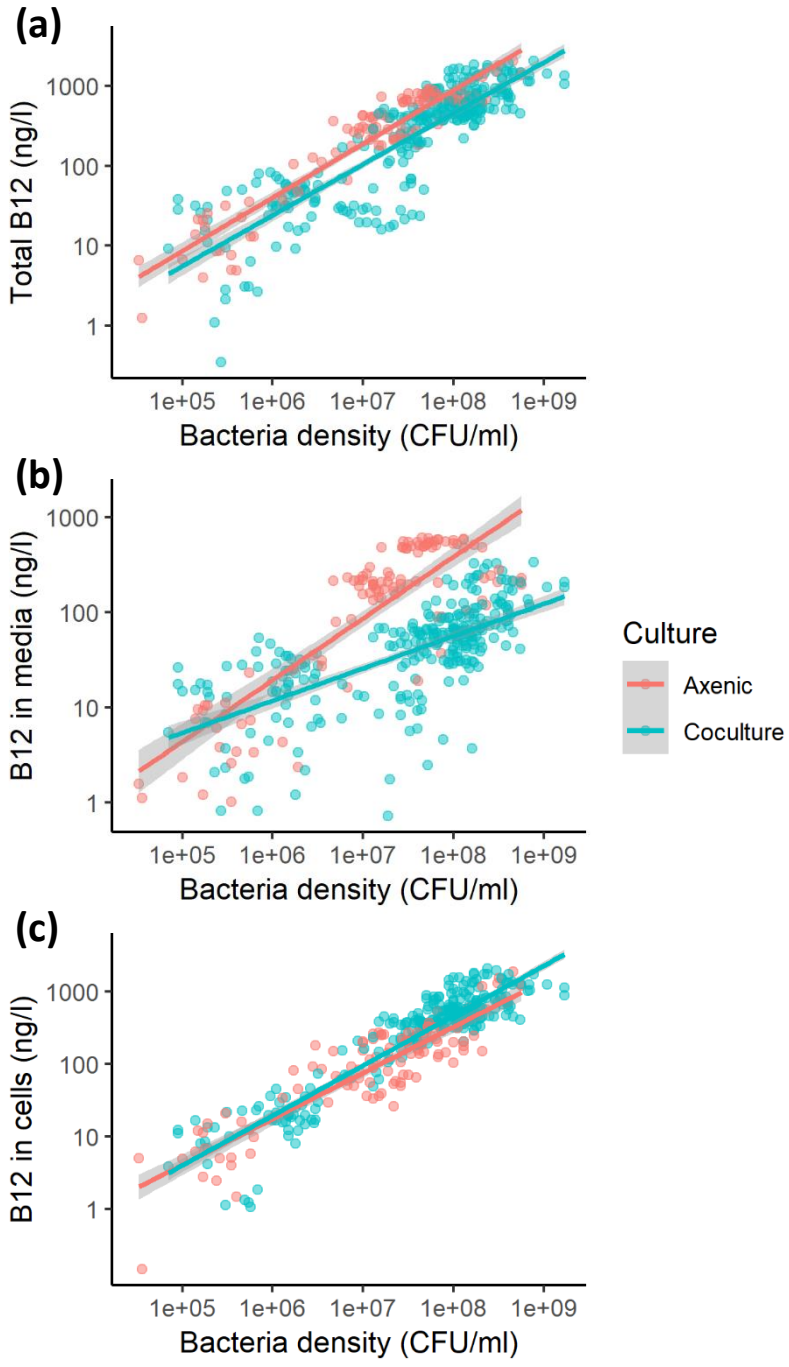

Figure 4.6 Correlation between B_{12} in various fractions of the culture and *M. loti* density. Combination of data from various experiments on axenic *M. loti* cultures, or cocultures of *metE7* and *M. loti* where both bacterial densities and B_{12} concentrations were measured. **(a)** Total B_{12} in the culture, **(b)** B_{12} in the supernatant after centrifuging an aliquot of the sample, **(c)** B_{12} in the pellet after centrifuging an aliquot of the sample. Points indicate individual measurements, lines indicate least squares best fit linear models, and shaded areas indicate 95% confidence intervals for those linear models. Pink = Axenic *M. loti* cultures, Blue = Cocultures of *M. loti* and *metE7*.

4.2.5 Does *metE7* increase B_{12} synthesis in *M. loti* by acting as a sink for the vitamin?

The correlations discussed above showed that B_{12} concentration per *M. loti* cell was higher in axenic culture than coculture, which is contrary to the findings by Grant et al. (2014) for *M. loti* coculture with *L. rostrata* (Grant et al., 2014). Nonetheless, the differences in the growth profile of *M. loti* varied substantially from batch axenic culture, where the carbon source is provided in its entirety at the beginning, to coculture where organic carbon production is continuous and dependent upon *metE7* photosynthesis. A hypothetical mechanism by which *metE7* might increase *M. loti* B_{12} production could be by reducing the concentration of B_{12} in the media, which might reduce bacterial intracellular levels of B_{12} and hence relieve suppression on B_{12} riboswitch-controlled B_{12} biosynthesis operons (Nahvi et al., 2004). Therefore, I decided to test the effect of removing B_{12} from the media of *M. loti* cultures either by replacing the media entirely or using *metE7* to take up dissolved B_{12}.

The setup of this experiment is illustrated in Figure 4.7a. Firstly, *metE7* cells were cultured in Tris minimal medium as before with 100 $ng \cdot l^{-1}$ B_{12} and then washed and transferred to fresh media containing either no B_{12} or 10,000 $ng \cdot l^{-1}$ B_{12} for a 24-hour incubation. Both sets of *metE7* cells were then washed and transferred at equal cell densities to axenic cultures of *M. loti* which had reached carrying capacity in Tris min with 0.01% glycerol. Two sets of axenic *M. loti* cultures and the two sets of cocultures with B_{12}-saturated and B_{12}-deprived *metE7* cells were then incubated for 4 hours before each culture was passed through a 5 µm filter and collected. The 5 µm pore size had previously been shown to allow *M. loti* cells to pass through freely, while preventing the passage of any intact *metE7* cells. All the cultures therefore once again only contained *M. loti*. All four sets of cultures were centrifuged at 16,000g for 2 minutes, and in one set of cultures that had never been exposed to *metE7* cells, the supernatant was removed, and fresh Tris min added. All four sets of *M. loti* cultures (Control, exposed to B_{12}-limited *metE7*, exposed to B_{12}-saturated *metE7*, and fresh media replacement) were then incubated under the previously described conditions for 3 days with measurements of *M. loti* $CFU \cdot ml^{-1}$ and B_{12} concentration in the media and cell pellet made daily. The data are shown in Figure 4.7b-e.

xxv Figure 4.7 Effect of B_{12} removal on *M. loti* B_{12} production

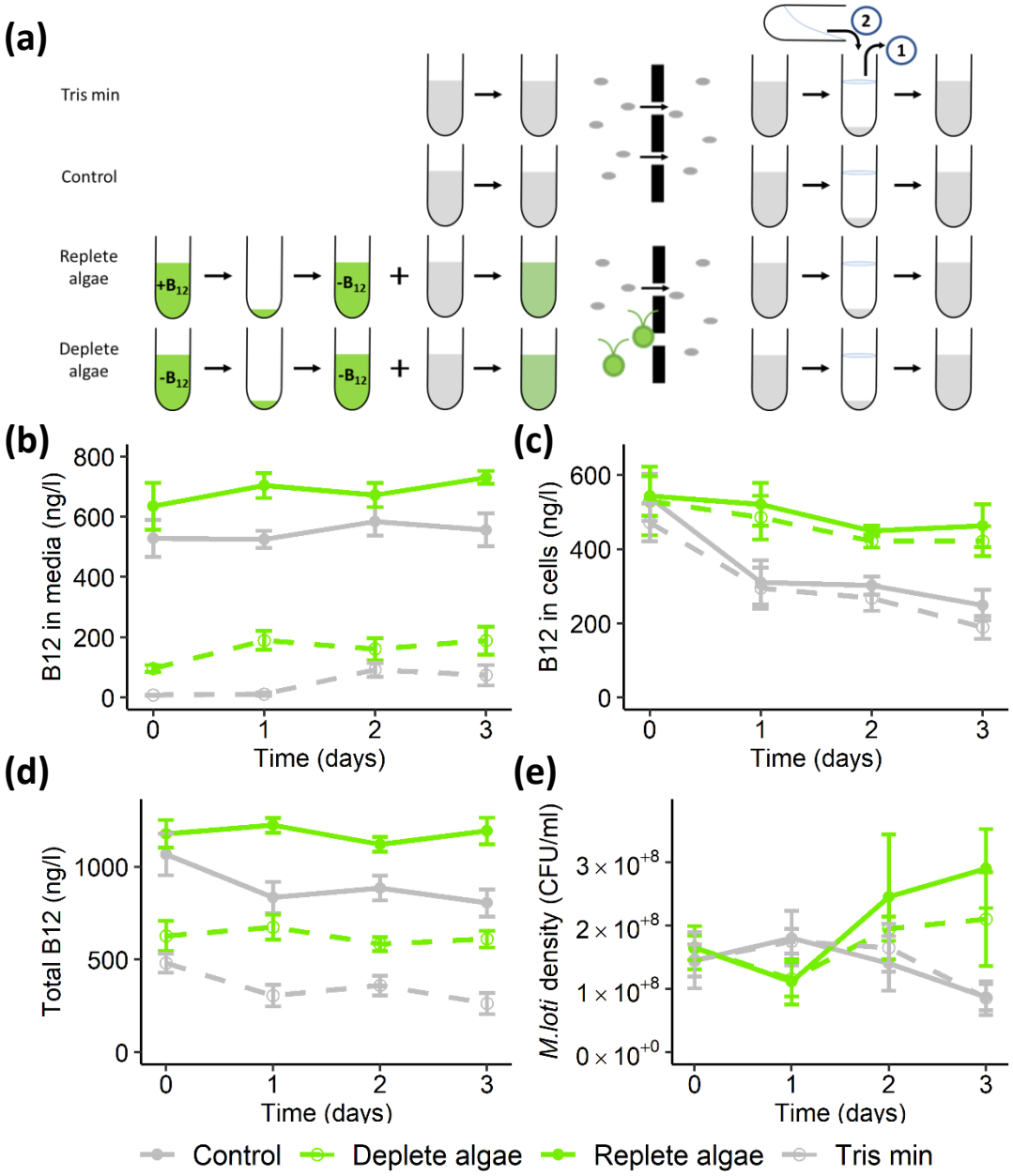

Figure 4.7 Testing whether *M. loti* alters its growth or B_{12} production if B_{12} is removed from the media. **(a)** Experimental setup: Two sets of axenic *M. loti* cultures (grey) were inoculated with *metE7* cells that were either saturated with or starved of B_{12}. All 4 cultures were then passed through a 5 µm filter, removing all *metE7* cells but not *M. loti*. These *M. loti* cultures were centrifuged, and the supernatant replaced with fresh Tris-min media in treatment 'Tris min', or otherwise resuspended without replacing the supernatant. The resuspended, newly axenic *M. loti* cultures were grown for 3 days with illumination in a 16:8 hour period at 100 $\mu E \cdot m^{-2} \cdot s^{-1}$ and 25°C with rotational shaking at 120 rpm. **(b)** B_{12} in the supernatant after centrifuging an aliquot of the sample, **(c)** B_{12} in the cell pellet **(d)** Total B_{12} in the culture **(e)** Bacterial density measured as colony forming units (CFU) plated on TY agar. Grey solid = Control *M. loti* axenic culture, Green dashed = *M. loti* exposed to B_{12}-starved *metE7*, Green solid = *M. loti* exposed to B_{12}-saturated *metE7*, Grey dashed = *M. loti* culture from which the media was replaced with Tris min. Error bars = sd, n=4.

The B_{12} concentration in the media of the *M. loti* culture that had been incubated with B_{12}-deplete *metE7* cells was significantly reduced, suggesting adsorption or absorption by *metE7* (Figure 4.7b). This did not occur in the B_{12}-replete *metE7* cells, presumably because no further B_{12} uptake was possible. A slight increase in B_{12} concentration in the media from day 0 to day 3 for all lines might be accounted for by part of the decrease in cellular B_{12} (Figure 4.7c), perhaps due to cell lysis. The control axenic cultures and those where the media had been replaced by fresh Tris min showed a decrease in total B_{12} concentration and *M. loti* density (Figure 4.7c and 4.7d). On the other hand, both cultures which had *metE7* added experienced a slight increase in *M. loti* density and a maintenance of total B_{12} concentration (Figure 4.7d and 4.7c). Concerning the original hypothesis, it appears that removing B_{12} from the media, whether by using *metE7* as a sponge or replacing the media entirely, does not result in *M. loti* increasing B_{12} synthesis.

4.2.6 Do bacterial mutants impaired in B_{12} uptake release a larger amount of B_{12}?

The total B_{12} production by a bacterium may be a relevant factor in the consideration of whether it could effectively support a B_{12}-dependent alga, but the fraction of B_{12} that is released is equally as important. If B_{12} is released from cells, whether by cell lysis, passive loss from viable cells, or active secretion, and can be reabsorbed by bacteria, the proportion of B_{12} in the media is likely to be low. Therefore, the hypothesis was that in cultures of bacterial B_{12} uptake mutants the proportion of B_{12} in the media would be higher. BtuF is a periplasmic protein of Gram-negative bacteria thought to be involved in the transport of B_{12} across the double membrane and BluB is involved in B_{12} biosynthesis (Cadieux et al., 2002; Campbell et al., 2006). Three strains of *M. loti*, the wild type sequenced strain MAFF303099 and two mutants, Δ*btuF* and Δ*bluB* were used to investigate the effect of B_{12} uptake and production on the amount of B_{12} occurring in the cellular and media fractions of cultures. The cells were grown in Tris min media as before, but with various concentrations of glycerol ranging from 0.0002 % to 0.2 % and allowed to reach carrying capacity before measurements of optical density and B_{12} concentration in the media and cell fraction were made. The optical density of Δ*bluB* was lower than Δ*btuF* and WT, which were very similar to one another (Figure 4.8a), indicating reduced growth. As expected, B_{12} concentration was lower in the culture of Δ*bluB* than either Δ*btuF* or WT, even when adjusted for the lower optical density (Figure 4.8b). Both total B_{12} and the proportion of B_{12} that was in the media were very similar in Δ*btuF* and WT (Figure 4.8b-c) suggesting that BtuF does not have a large effect on B_{12} release or uptake in *M. loti*.

E. coli does not naturally synthesise B_{12}, nor does it have an absolute requirement for it, but *E. coli* will take up and use B_{12} as a cofactor when it is available (Baker et al., 1960; Beck, 1982; Kisliuk & Woods, 1960). Deery et al., (2012) reconstituted the B_{12} biosynthesis pathway in *E. coli* by cloning in *cob* genes from various B_{12}-producing bacteria (Deery et al., 2012). By knocking out *btuF*

they found that a larger proportion of the synthesised B_{12} ended up being released (personal communication). Here, the *btuF::Kan* strain (ED662) and its background strain (ED656) were cultured in M9 and Tris minimal medium to determine whether the observation of the difference in B_{12} release between strains could be replicated. ED656 and ED662 were inoculated at 10^7 cells·ml^{-1} into M9 media with 0.1% glycerol and cultured for 12 hours at 37°C with rotational shaking at 120 rpm. To test whether these *E. coli* strains would also grow and produce B_{12} in conditions in which *C. reinhardtii* could grow, they were also inoculated at 10^7 cells·ml^{-1} into Tris minimal medium with 0.1% glycerol and cultured for 96 hours at 25°C with rotational shaking at 120 rpm. As the B_{12} biosynthetic enzymes were arranged in an operon under the control of the lac promoter, IPTG was added to half of the samples in both conditions to a concentration of 400 µM. At the end of the growth period, *E. coli* density and B_{12} concentration in the cells and media fractions were determined (Figure 4.9).

Growth of ED656 and ED662 were not significantly different from one another in both growth conditions, whether in the presence or absence of IPTG (Figure 4.9a). Figure 4.9b show the amount of B_{12} measured in the cell pellet, which also was not significantly different between strains, except for in Tris min media + IPTG where ED662 cultures had a slightly higher value (15%, $p<0.05$). IPTG addition only caused a significant increase in B_{12} production in Tris minimal medium (90% increase in both strains, $p<0.001$). Figure 4.9c shows that the B_{12} measured in the media fraction of the culture was higher for ED662 than ED656 in all four conditions, but particularly in Tris minimal medium where B_{12} concentration was 2.9 and 2.5-fold higher with or without IPTG respectively ($p<0.001$). As with the cell fraction, IPTG only seemed to increase B_{12} in the media when added to Tris min (45-60% increase, $p<0.001$).

To determine whether there was any difference in the growth rates of ED656 and ED662, a more robust and sensitive method was required. As ED662 contains a kanamycin resistance cassette, a mixed culture of ED662 and ED656 could be distinguished by the formation of colonies on LB agar (both strains) and LB agar + 50 µg·ml^{-1} kanamycin (ED662 only). The axenic cultures were mixed in five ratios: 24:1, 4:1, 1:1, 1:4 and 1:24, i.e. 4%, 20%, 50%, 80%, and 96%, and cultured in Tris min media with 0.1% glycerol, and were diluted 10,000-fold after 3, 6, and 9 days of growth. After 0, 3, 6, 9, and 15 days the numbers of colonies were determined (Figure 4.10). It was clear that the proportion of ED662 declined substantially in all cultures, indicating that ED656 had a higher growth rate under these conditions. Thus it can be concluded that ED662 (*btuf::Kan*) released more B_{12} into the media and grew more slowly than its parental strain (ED656) when cultured in Tris min media.

xxvi Figure 4.8 B_{12} production and release by *M. loti* mutants

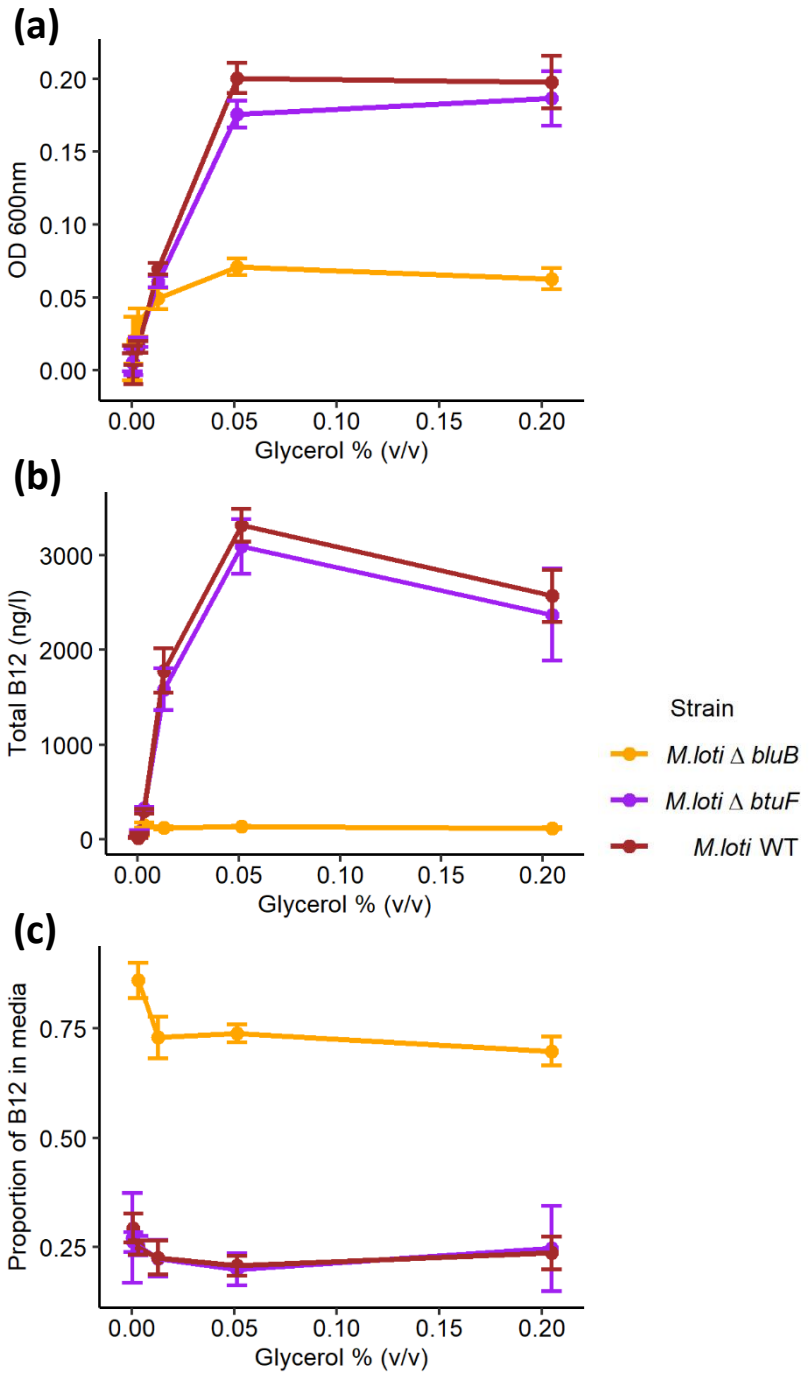

Figure 4.8 Carrying capacity and B_{12} production of *M. loti* WT and 2 mutants with different concentrations of glycerol. BluB is involved in B_{12} biosynthesis, and BtuF is involved in B_{12} transport across the plasma membranes. **(a)** Optical density of cultures at carrying capacity measured by spectrophotometer at 600nm, **(b)** Total B_{12} in the cultures measured by bioassay, **(c)** Proportion of the B_{12} found in the media, calculated by dividing the amount in the media by the total amount. Yellow = *M. loti ΔbluB* mutant, Purple = *M. loti ΔbtuF* mutant, Brown = *M. loti* WT. error bars = sd, n=4.

xxvii Figure 4.9 Growth, B_{12} production and release by two engineered *E. coli* strains

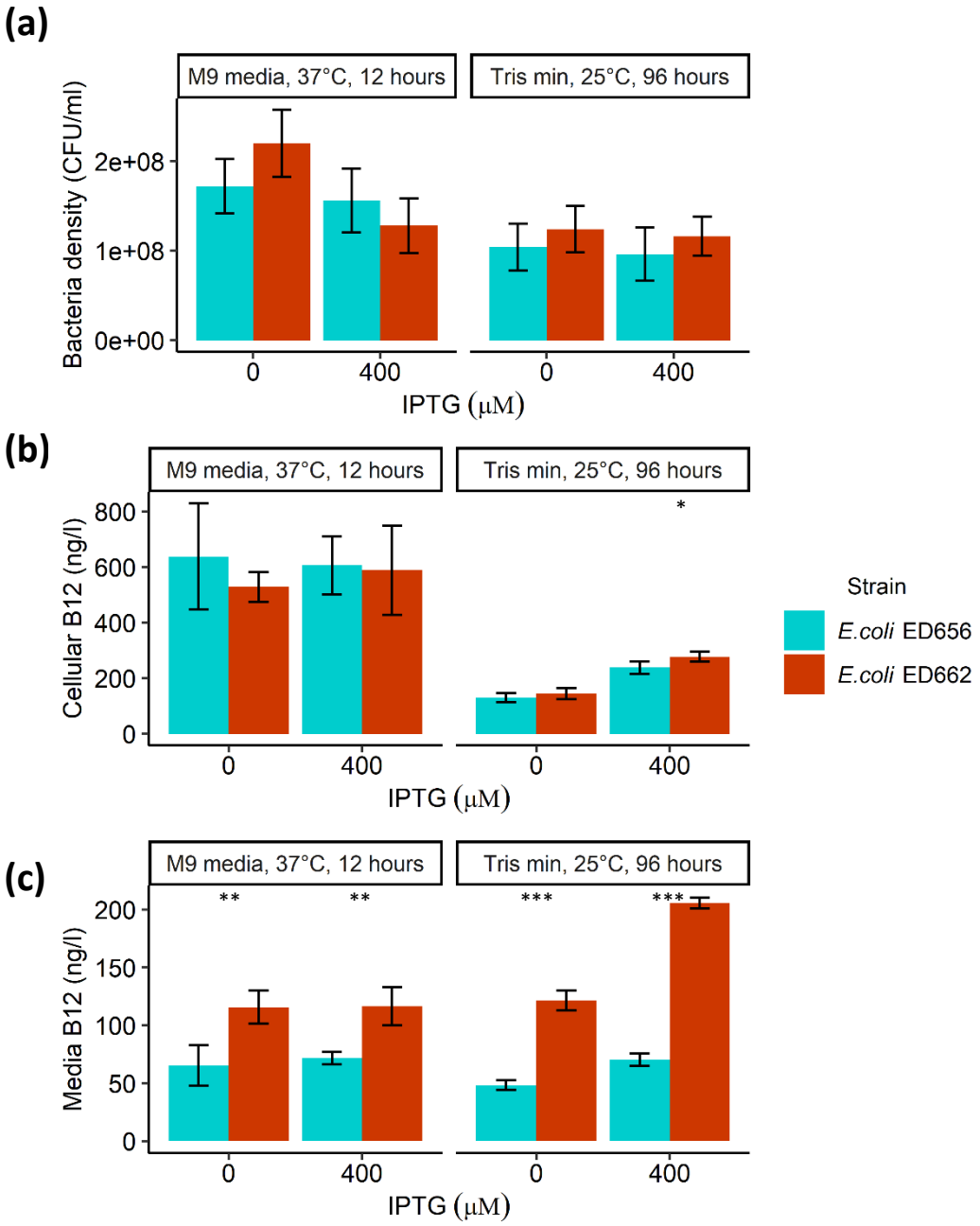

Figure 4.9 Cell density and B_{12} production of two *E. coli* strains engineered to synthesise vitamin B_{12}. ED656 expresses BtuF, a protein involved in B_{12} uptake, while ED662 is a BtuF knockout. *E. coli* cells were inoculated at 10^7 cells·ml^{-1} and grown in one of two conditions: 1) 12 hours in M9 media with 0.1% glycerol (w/w), at 25°C, and no illumination; 2) 4 days in Tris min media with 0.1% glycerol (w/w), at 25°C, and with illumination for a 16:8 hour light:dark period at 100 µE·m^{-2}·s^{-1}. **(a)** *E. coli* cell density measured as colony forming units on LB agar. **(b)** B_{12} measured in the pelleted fraction of the culture after centrifugation. **(c)** B_{12} measured in the supernatant fraction of the culture after centrifugation. Blue = ED656, Red = ED662. Error bars = sd, n=5, asterisks denote differences between ED656 and ED662, *=p<0.05,**=p<0.01, ***=p<0.001 (Welch's t test).

xxviii Figure 4.10 Growth competition between *E. coli* strains ED656 and ED662

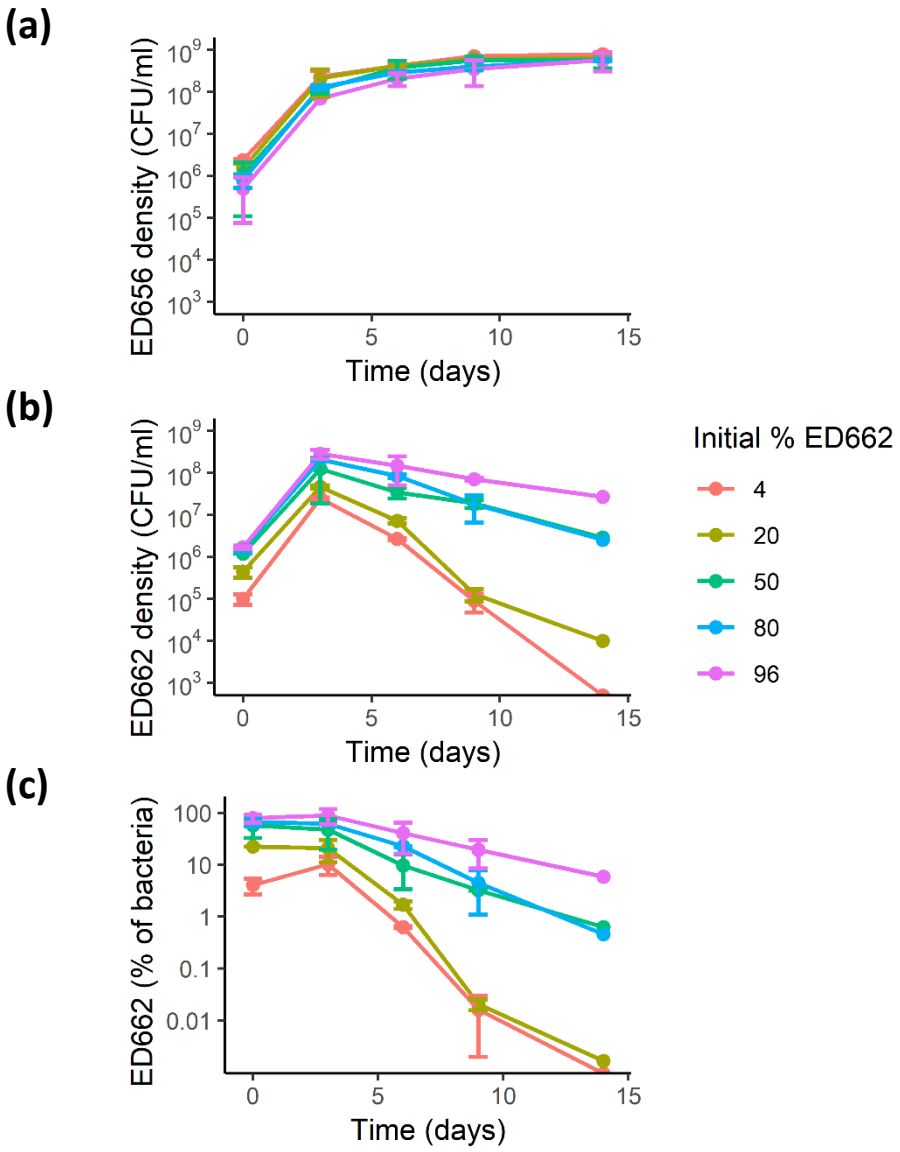

Figure 4.10 Growth of cultures consisting of a mixture of ED656 and ED662 *E. coli* at different starting ratios from 24:1 to 1:24 i.e. 4% to 96% ED662. Cultures were grown for 15 days in Tris min media at 25°C with constant illumination at 100 µE·m^{-2}·s^{-1} and were diluted 10,000 fold on day 3, 6, and 9 after measuring cell density. Colony forming units were measured by plating serial dilutions on LB and LB + kanamycin (50 µg·ml^{-1}) plates. **(a)** ED656 density calculated by subtracting CFU·ml^{-1} on LB + kanamycin plates from CFU·ml^{-1} on LB plates **(b)** ED662 density measured by CFU·ml^{-1} on LB + kanamycin plates (ED662 is resistant to kanamycin). **(c)** Calculated percentage of ED662 CFU·ml^{-1} to total *E. coli* CFU·ml^{-1} (ED656 + ED662). Error bars = sd, n=2.

4.2.7 Does increased release of B_{12} by producers lead to improved growth of *metE7*?

Although ED662 had a slight reduction in fitness relative to ED656 it seemed likely that its higher release of B_{12} into the media would allow it to better support the growth of *metE7*. Firstly, a range of different mixtures of M9 and Tris min media were made to test the growth response of *metE7*, ED656, and ED662, axenically, and in coculture (*metE7*+ED656 and *metE7*+ED662). ED656 and ED662 were inoculated at 10^6 cells·ml^{-1}, and *metE7* at 10^4 cells·ml^{-1}. 1000 ng·l^{-1} B_{12} was added to axenic *metE7* cultures, and 0.1% glycerol to axenic *E. coli* cultures, with no addition to cocultures. All cultures were then incubated at 25°C with continuous illumination at 100 µE·m^{-2}·s^{-1} and rotational shaking at 120 rpm, and after 72 hours algal and bacterial density was quantified (Figure 4.11a-b). Figure 4.11a shows that ED656 and ED662, which both grew to a similar extent, displayed improved growth at higher percentages of M9 media when cultured axenically with glycerol as a carbon source. In coculture with *metE7*, both *E. coli* strains grew poorly in all media formulations, although ED662 grew slightly better. Figure 4.11b illustrates that axenic cultures of *metE7* grew considerably worse as the percentage of M9 media increased. *metE7* grew poorly in coculture with ED656 in all media formulations, but its growth was substantially higher in cocultures with ED662 at the low M9 (high Tris min) percentages.

To further test whether *metE7* was better supported by ED662 than ED665, tricultures were made containing all three strains, but with different starting percentages of ED656 and ED662. Like the experiment displayed in Figure 4.10, ED656 and ED662 were mixed such that ED656 made up 4, 20, 50, 80, or 96% of the bacteria, and so that the total bacterial density was 10^6 cells·ml^{-1}. *metE7* was then inoculated to 10^3 cells·ml^{-1} and the cultures were incubated as described above, with algal and bacterial densities measured after 72 hours. In Figure 4.11c the density of ED656 is negatively correlated with *metE7* cell density, while in Figure 4.11d ED662 and *metE7* cell density are positively correlated. These result in an even stronger correlation between *metE7* density and the percentage of bacteria that are ED662 (Figure 4.11e). Note that the negative correlation between ED662 and *metE7* does not necessarily imply a negative physiological impact, because under these circumstances ED656 and ED662 cell densities were negatively correlated from the start, and so a high ED656 density likely implies a low ED662 density.

xxix Figure 4.11 Growth of *E. coli* strains ED656 and ED662 and *metE7* in coculture

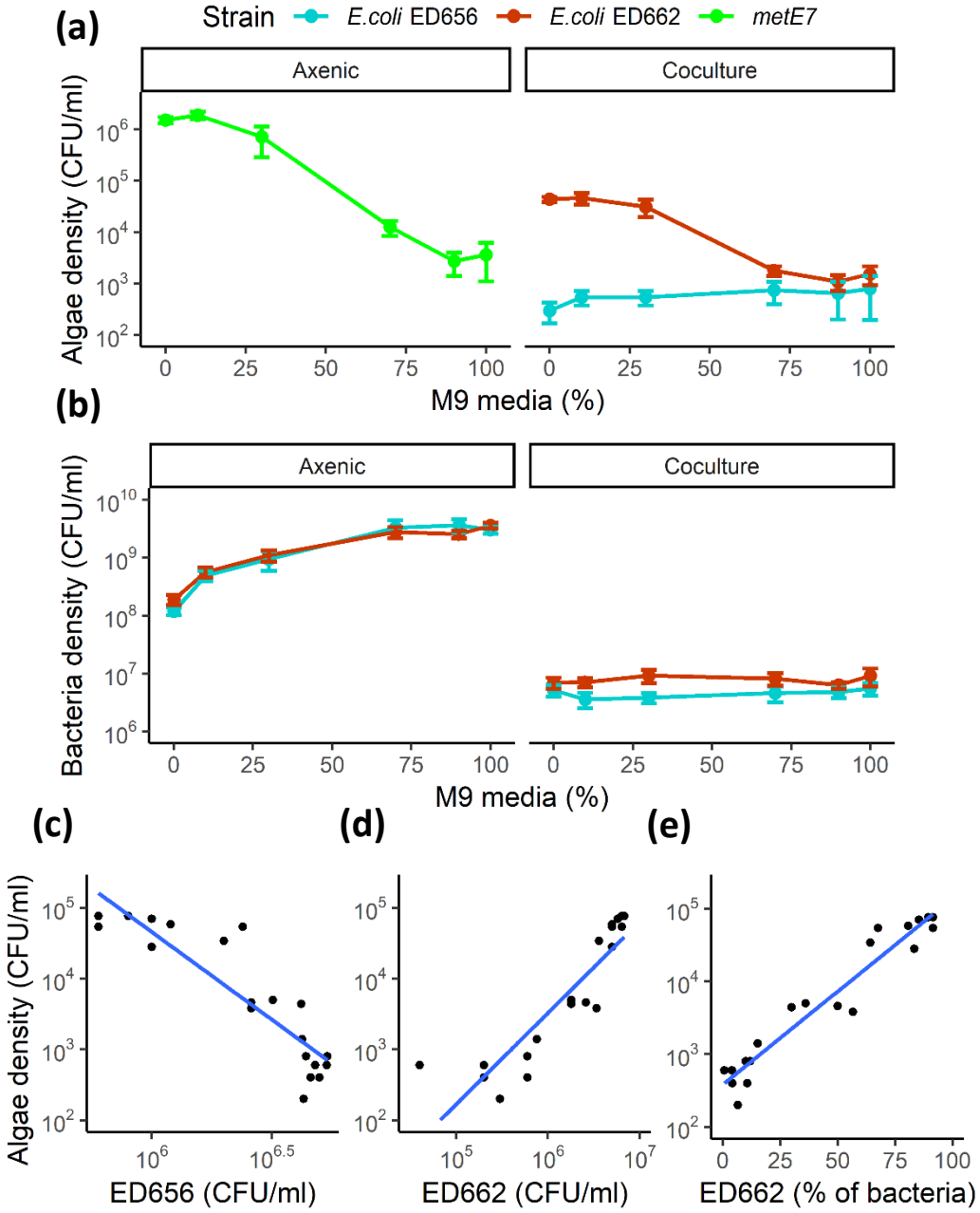

Figure 4.11 Growth of cocultures composed of *metE7* and either ED656 or ED662, or tricultures of all three. All cultures were grown for 3 days at 25°C with shaking at 120 rpm and constant illumination at 100 $\mu E \cdot m^{-2} \cdot s^{-1}$. Experiments in panel (a) and (b) tested the effect of media composition on the growth of axenic cultures and cocultures of *metE7* and either ED656 or ED662. M9 media and Tris minimal media were mixed at 0, 10, 30, 70, 90, and 100% M9, and therefore vice versa for Tris min. Axenic *metE7* was provided with 1000 $ng \cdot l^{-1}$ B_{12}, and axenic *E. coli* cultures with 0.1% glycerol (w/w). **(a)** *E. coli* density in $CFU \cdot ml^{-1}$ measured by plating on LB agar. **(b)** *metE7* $CFU \cdot ml^{-1}$ measured by plating on TAP agar with ampicillin (50 $\mu g \cdot ml^{-1}$) and kasugamycin (75$\mu g \cdot ml^{-1}$). In panels (c),(d),(e) *E. coli* ED656 and ED662 were inoculated at various starting percentages from 4% to 96%, similar to Figure 4.10. *metE7* was inoculated at 10^4 $cells \cdot ml^{-1}$, and after 3 days of growth *metE7*, ED656, and ED662 densities were measured. Correlations are displayed between **(c)** *metE7* and ED656, **(d)** *metE7* and ED662, **(e)** *metE7* and % of bacteria that are ED662.

4.2.8 Could bacteria provide sufficient B_{12} to cause the evolution and dominance of an algal B_{12} auxotroph?

ED662 could successfully support *metE7*, but preliminary data suggested that this did not persist for long after initiating cocultures, perhaps because the organic compounds produced by *metE7* were not easily metabolised by *E. coli*. Helliwell et al. (2015), showed that high levels of B_{12}, when supplied artificially, led to the evolution and dominance of the B_{12}-dependent strain S-type from a culture of the B_{12}-independent wild type *C. reinhardtii* (Helliwell et al., 2015). With the ultimate source of B_{12} being prokaryotes, I decided to investigate what the relative fitness of a B_{12}-dependent and B_{12} independent (revertant) *C. reinhardtii* would be in various conditions, including coculture with *M. loti*. S-type was used instead of *metE7* because the presence of the 246 nucleotide Gulliver-related transposable element (GRTE) allowed it to be distinguished from the revertant strain using PCR with one primer pair and gel electrophoresis. Some of the results discussed above suggested that *metE7* is limited considerably in its growth by the low supply of B_{12} released by *M. loti*. However, addition of glycerol to cocultures caused a large increase in B_{12} concentration, an increase in growth of *metE7*, and from Kazamia et al. (2012), a reduction in the expression of *METE* (performed on wild type *C. reinhardtii*) (Kazamia et al., 2012). Although glycerol addition itself is not reflective of environmental conditions, it might be considered a substitute for the fixed carbon production by other, and perhaps B_{12}-independent, phototrophs.

Mixed cultures of S-type and the revertant strain were grown for 4 days in Tris min media at 25°C under constant illumination at 100 $\mu E \cdot m^{-2} \cdot s^{-1}$ and were diluted 10-fold daily. Samples were taken each day and serial dilutions made before plating on B_{12}-free TAP agar + Ampicillin (50 $\mu g \cdot ml^{-1}$) and Kasugamycin (75 $\mu g \cdot ml^{-1}$). After 8 days of growth on the agar the colonies of S-type and revertant were clearly distinguishable as S-type colonies were both smaller and lighter in colour. On day 4 PCR was performed on an aliquot of the cultures and PCR products were separated by gel electrophoresis before quantification of the two bands (larger band for S-type) using ImageJ. As shown in Figure 4.12a, in all conditions except for with added B_{12} there was a marked decrease in the proportion of S-type over time (measured by CFU). Nonetheless, the addition of *M. loti*, particularly in the presence of glycerol, did slightly slow the decline of S-type. PCR analysis over the region of transposon insertion (which disrupted *METE* in S-type), was generally in agreement with the phenotypic screen, and also indicated that glycerol addition slowed the dominance of the revertant strain further than *M. loti* addition alone (Figure 4.12b). The measurements of S-type and revertant cell density by phenotypic and genotypic screening were generally in agreement, even though there are several reasons why they might not be. Firstly, the phenotypic screen will only detect viable cells, while PCR would likely detect cells that had recently died, but before DNA was degraded. The PCR results were also reported simply as band intensity, which would be affected by DNA size, and PCR

amplification efficiency. Thirdly, it is possible that imprecise excision of the GRTE would leave behind a short nucleotide sequence (as in the case of *metE7*) that could not be distinguished from a 'true' revertant even though the *METE* gene might still be disrupted, resulting in a B_{12}-dependent phenotype. This limited data therefore does not provide an example of bacteria favouring the evolution of B_{12} auxotrophy in algae, nevertheless it does not preclude it, and several modifications could be made to the set up to improve B_{12} production, and hence the relative fitness of this B_{12}-dependent alga.

xxx Figure 4.12 Competition between B_{12}-dependent and independent lines of *C. reinhardtii*

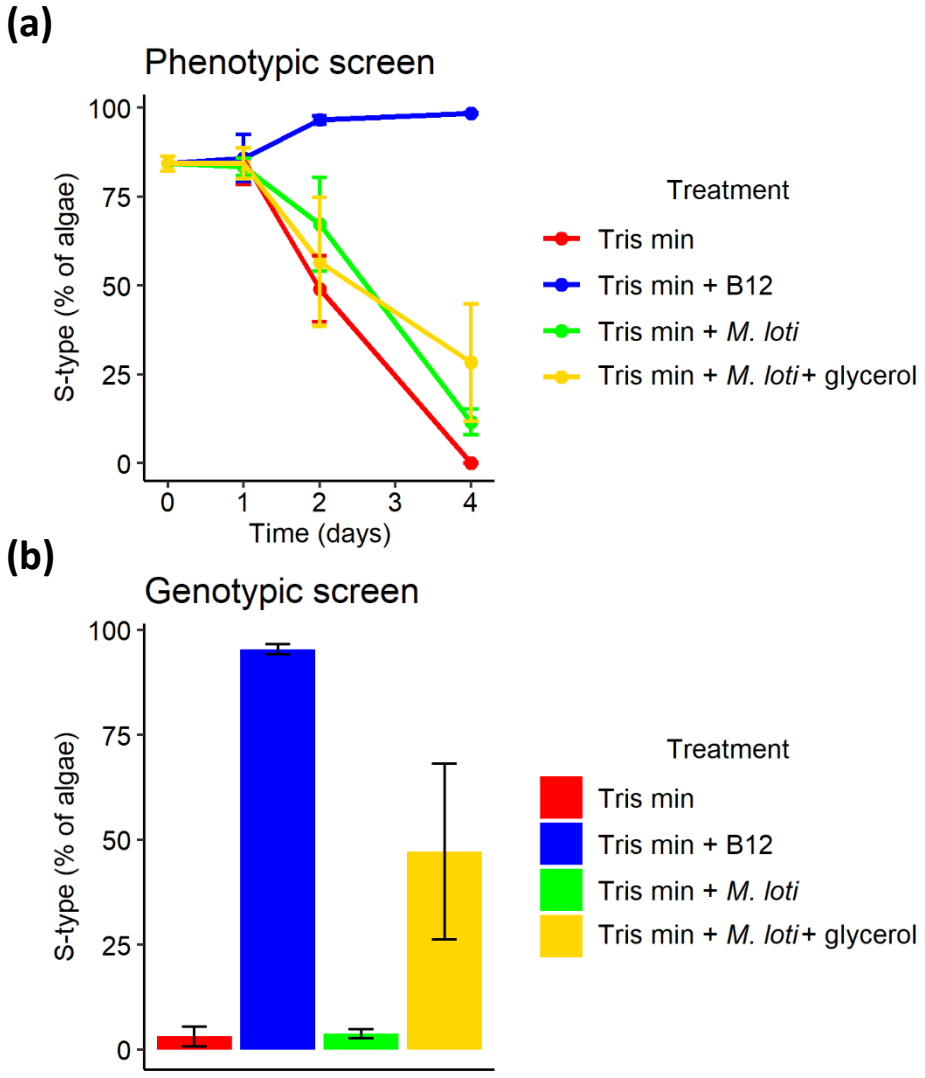

Figure 4.12 Growth of cultures consisting of a mixture of the unstable, B_{12}-dependent line of *C. reinhardtii*, and a B_{12}-independent revertant line. Cultures were grown for 4 days in Tris min media at 30°C with constant illumination at 100 $\mu E \cdot m^{2} \cdot s^{-1}$ and were diluted 10-fold on day 1, 2, and 3. **(a)** Proportion of the algae that belong to the unstable (S-type) line. This was measured by serial dilution of the culture and plating on TAP agar + Ampicillin (50 $\mu g \cdot ml^{-1}$) and Kasugamycin (75 $\mu g \cdot ml^{-1}$) and differentiating between stunted B_{12}-dependent and healthy or B_{12} independent colonies. **(b)** Proportion of the algae that belong to the unstable (S-type) line quantified on day 4 by PCR over the GRTE insert region and comparing fluorescence intensity of the two PCR product bands (larger band=S-type, smaller band = revertant). Red = algae cultured in Tris min, Blue = Tris min + 1000ngl^{-1} B_{12}, Green = Tris min + *M. loti*, Yellow = Tris min + *M. loti* + 0.1% glycerol. Error bars = sd, n=4.

4.3 Discussion

4.3.1 The interaction between wild type *C. reinhardtii* and *M. loti* is commensal

Helliwell et al. (2015) showed that the B_{12}-dependent *C. reinhardtii* strain *metE7* could be supported in coculture with three different B_{12}-producing rhizobia (Helliwell et al., 2015). Coculturing one of those bacteria, *M. loti*, with the ancestral *C. reinhardtii* strain was carried out to determine if *M. loti* had any growth-promoting effects in addition to B_{12} provision, or conversely, whether it had any inhibitory effects. The non-significant difference in ancestral line growth rates suggested that B_{12} production is the only benefit provided by *M. loti* to *metE7*. Previous studies have shown a growth promoting effect of rhizobia on *C. reinhardtii*. Xie et al. (2013) found that *S. meliloti*, which can also produce B_{12}, promoted the growth of *C. reinhardtii*, but only at temperatures well above the optimum for growth. They concluded that this was essentially due to the reduced thermal tolerance of METE relative to the B_{12}-dependent METH, hence causing *C. reinhardtii* to become increasingly reliant on B_{12} at high temperatures (Xie et al., 2013). However, Kim et al. (2014) found a growth promoting effect of various rhizobia on *C. reinhardtii* cultured at 30°C (Kim et al., 2014), which is only slightly above the optimal temperature and hence unlikely to significantly increase the reliance of *C. reinhardtii* on B_{12} (Vítová et al., 2011). Under less optimal growth conditions, such as in municipal or agricultural wastewater, it is also clear that bacteria, including rhizobia, can improve the growth of *C. reinhardtii*, and vice versa (Toyama et al., 2018). The best-known growth-promoting effect of rhizobia is on plants via supplying fixed nitrogen in root nodules (Long, 1989). Nitrogen fixation genes are only induced in *M. loti* under microaerobic conditions (Uchiumi et al., 2004), which are unlikely to occur in a photosynthesising culture of *C. reinhardtii*, but if they did, nitrogen fixation would have little effect on a nitrogen replete culture. The fact that no growth promotion of *C. reinhardtii* was observed in this work, might suggest that B_{12} production, or other services provided by rhizobia, only have an impact when conditions are suboptimal.

M. loti was shown here to derive benefit from the presence of *C. reinhardtii*, without impacting the growth of the alga, therefore the relationship might be considered commensal (Newton et al., 2010). These results disagree with those previously reported by Kazamia et al. (2012) which showed that *C. reinhardtii* was unable to support *M. loti* (Kazamia et al., 2012). The organic carbon compounds that *M. loti* utilises are not known, but research in this area could help to determine whether the relationship is commensal in the stricter sense, or saprophytic. Commensal relationships have traditionally been thought of as more stable than parasitic ones, and also provide a platform for the development of mutualisms (Ewald, 1987). Nonetheless, the positive feedback loop intrinsic to mutualisms could make them less robust to environmental shocks than commensalisms, and artificial

mutualisms have been found to evolve higher productivity and stability in parallel with reduced cooperation (Hansen et al., 2007; Hillesland & Stahl, 2010; Rozen et al., 2009). If *M. loti* were able to provide sufficient B_{12} for complete suppression of *METE* in *C. reinhardtii*, it seems reasonable that both species could coexist for long enough to allow the evolution of B_{12} dependence and hence the transition from commensalism to mutualism.

4.3.2 A mutualistic interaction has lower fecundity than a commensal one

metE7 grew less well in coculture with *M. loti* than the revertant and ancestral lines, indicating that B_{12} availability was the limiting factor (Figure 4.2a). In comparison, the growth of *M. loti* was much more similar in coculture with the three *C. reinhardtii* strains (Figure 4.2b). The ratio of *M. loti* to *C. reinhardtii* cells was therefore significantly higher for *metE7* (Figure 4.2c). This could be because *metE7* cells were able to support a greater number of *M. loti* cells. On the other hand, while *metE7* was dependent on and so limited by *M. loti*, the revertant and ancestral strains were not, and so *M. loti* growth would lag behind algal growth in the B_{12}-independent lines. As B_{12} deprivation causes an increase in cell size (Figure 3.4a-b), it might be that the biomass of *metE7* was more similar to the other strains than the cell density would suggest. Alternatively, a larger proportion of the photosynthate produced by *metE7* might be available to *M. loti*. It could be that due to B_{12} deprivation there is a metabolic shift towards more triacylglycerol and starch production (Figure 3.4c), which when released, is more readily metabolised by *M. loti*. Cell death is also increased by B_{12} deprivation (Figure 3.10a), and dead cells could provide a better nutrient source to *M. loti*. Seyedsayamdost et al. (2011) showed that *Phaeobacter gallaeciencis* interacts with *Emiliania huxleyi* in a growth-phase-dependent manner by initially secreting the growth-stimulant auxin before switching to algaecides on detecting compounds associated with algal senescence (Seyedsayamdost et al., 2011). Cocultures of *C. reinhardtii* and *M. loti* were not maintained for long periods, so it is unclear how *M. loti* would respond to algal senescence. However, if *M. loti* does not specifically reduce B_{12} production and release during *metE7* cell death, then the increase in B_{12} concentration resulting from increased bacterial growth, would only serve to rescue *metE7*. Oscillations in the cell densities of *T. pseudonana* and a B_{12} producing bacterium, when grown in coculture, were hypothesised to be the result of this process (Haines & Guillard, 1974). So, these negative feedback loops may be widespread and add a degree of stability to an interaction that is otherwise dominated by a mutualistic positive feedback loop. However, if the only way that *M. loti* can acquire carbon in these cocultures is from dead *metE7* cells then this interaction could not strictly be considered a symbiosis.

4.3.3 *L. rostrata* grows better than *metE7* when cocultured with *M. loti*

In axenic culture *L. rostrata* was found to have a slower growth rate than *metE7* at almost all B_{12} concentrations (Figure 3.12a), yet in coculture *L. rostrata* has the faster growth rate (Figure 4.3a). The dynamics of algal growth in axenic culture and in coculture are quite different because of the differences in B_{12} supply. In batch axenic culture the total B_{12} is present at the beginning of the growth period and is depleted from the media as it is taken up. In coculture the uptake of B_{12} is limited, at least initially, by B_{12} synthesis, which ensures that B_{12} levels in the media are kept low. At these low levels of B_{12} *L. rostrata* may be able to absorb a greater proportion from the media than *metE7* (Figure 3.3c-d), and due to its lower EC_{50} use the B_{12} to facilitate a higher growth rate. Towards the latter stages of the growth period, the concentration of B_{12} in the media increased in the *L. rostrata* and, to a lesser extent, *metE7* coculture. This could suggest that algal growth is starting to be limited by factors other than B_{12}, and that B_{12} is therefore able to accumulate in the media. In support of this, the ratio of bacteria to algae increases, particularly for the *L. rostrata* coculture from day 8, which is when B_{12} accumulates more rapidly in the media. That the ratio of bacteria to algae in the *L. rostrata* coculture is lower, yet the B_{12} in the media higher seems to agree with the finding that *L. rostrata* has a lower requirement for, and saturable uptake of B_{12}. Grant et al. (2014) showed that the B_{12} concentration per *M. loti* cell was higher in coculture with *L. rostrata* than when *M. loti* was cultured axenically (Grant et al., 2014), and here (Figure 4.3e) it was found that B_{12} per *M. loti* cell was higher in coculture with *L. rostrata* than with *metE7*. Therefore, *L. rostrata* may be able to induce higher B_{12} production from *M. loti*, perhaps by the type or proportion of photosynthate that it releases.

4.3.4 *metE7* growth in coculture is improved by increasing B_{12} addition or synthesis

Addition of nutrients to cocultures of *metE7* and *M. loti* revealed that both species were clearly limited by their partner's ability to supply the nutrients for which they are auxotrophic. This is not at all surprising considering the energetic requirements of photosynthesis and B_{12} biosynthesis, and hence the fitness costs that would be incurred by producing these compounds in excess of the cell's own needs and releasing them into the media. Plants, for comparison, are thought to release around 5-20% of their photosynthate into the rhizosphere to support mutualists (Turner et al., 2013). The proportion of *metE7* photosynthate that is available to *M. loti* is not known, but the only carbon source available to *M. loti* in this setup is derived from *metE7* photosynthesis. With an average volume around 100 μm^3 (calculated from cell diameter measurements), a *C. reinhardtii* cell has roughly 150 times the volume of an *M. loti* cell, but a ratio anywhere from around 20 to 1000 *M. loti* to *metE7* cells would mean that a large proportion of the organic carbon in coculture is in the bacterial fraction.

A major difference between the addition of glycerol and cobalamin to the coculture was the effect on the non-requirer. After a delay, glycerol addition caused an increase in the density of *metE7* cells, but cobalamin addition did not significantly improve *M. loti* growth. This could suggest that when *metE7* cells are B_{12}-replete a smaller proportion of photosynthate becomes available to *M. loti*. Indeed, it was suggested by Kazamia et al. (2012) that a facultative and regulated interaction between *L. rostrata* and *M. loti* was likely to exist where *L. rostrata* releases less fixed carbon when it is B_{12}-replete (Kazamia et al., 2012). As for the increase in *metE7* cell density on glycerol addition, it would seem that *M. loti* does not substantially reduce its B_{12} production and release when supplied with glycerol in the presence of *C. reinhardtii*, a result that differs from those found by Kazamia et al. (2012) in the presence of *L. rostrata*.

In semi-continuous culture the first change to occur after glycerol addition was the increase in *M. loti* cell density, then B_{12} concentration, and finally *metE7* cell density, which forms a highly probable causal chain of events. The increase in B_{12} concentration after glycerol addition was much greater than on addition of 200 $ng \cdot l^{-1}$ of B_{12} itself, but the growth of *metE7* was similar in both instances. As the B_{12} in the media was no higher 24 hours after B_{12} addition than in the control culture, *metE7* cells had probably taken up all the added B_{12}. The concentration of B_{12} in the media of the glycerol-added culture did increase however, which as was mentioned before, might indicate that the *metE7* cells were B_{12} replete and could not take up any more B_{12}. On the other hand, the size range of *metE7* cells, which under these conditions is a reasonable indicator of B_{12} status (Figure 3.4a), did not suggest that B_{12}-added cultures were more B_{12}-limited than the glycerol-added cultures. Within 2 days of B_{12} addition, over 95% of cells were between 3 and 9 µm in diameter, a size range that >98% of *C. reinhardtii* cells are within when grown continuously in nutrient replete conditions. The proportion of *metE7* cells in that same size range after glycerol addition was always slightly lower, at roughly 80-90%. To reconcile these observations, it could be that not all the B_{12} in the media (or supernatant) fraction is available to *metE7*. Perhaps a large proportion of B_{12} measured in the media, particularly in the glycerol-added cocultures, remains bound by proteins released into suspension on lysis of bacterial or algal cells. Only after boiling the samples prior to use in the B_{12} bioassay might the B_{12} be released into solution by protein denaturation and hence be available for uptake (Schjonsby, 1989).

4.3.5 *metE7* does not increase *M. loti* B_{12} biosynthesis

B_{12} concentration per *M. loti* cell was higher in axenic culture than coculture with *metE7* at all *M. loti* densities (Figure 4.6a). This incongruity with the results described by Grant et al. (2014) for *M. loti* and *L. rostrata*, where B_{12} per bacterial cell was higher in coculture, might simply be due to the difference in the species of algae. In this work, *M. loti* cocultures with *L. rostrata* had higher B_{12} contents per bacteria than those with *metE7*, and so it seems plausible that *L. rostrata*, but not *metE7*

can increase B_{12} production by *M. loti*. On the other hand, this work also showed that B_{12} concentration per *M. loti* cell decreases with increasing cell density, as had been previously shown for *R. leguminosarum* (Kazamia 2012). Axenic *M. loti* provided with 0.1% glycerol grows to a higher density than in coculture with *L. rostrata,* and so the lower B_{12} per *M. loti* cell in axenic culture reported by Grant et al. (2014) may simply be a result of its higher cell density.

It is important to note that the gradient of a linear model connecting the natural logarithms of two variables which theoretically show direct proportionality is often less than one. This is due to a statistical phenomenon known as 'regression to the mean'. Regression to the mean however, would also make it likely that the gradient of the linear model of the inverse relationship was also less than one. As this is not the case here it seems that B_{12} concentration per *M. loti* cell really does decrease with cell density. Feedback inhibition of B_{12} biosynthesis via B_{12} binding to riboswitches upstream of biosynthetic gene operons has long been known in bacteria, and overcoming this has led to higher yields of B_{12} in industrial settings (Fang et al., 2017; Moore et al., 2014). In *M. loti* the two larger cobalamin biosynthesis operons, for which the proximal genes are cobW and cobL, have a vitamin B_{12} riboswitch upstream of the start codon, and B_{12} addition suppresses the expression of some of these genes (Bhardwaj 2016). It is possible therefore that an accumulation of B_{12} in the media as cell density increases would cause a decrease in B_{12} biosynthesis.

The correlation coefficient between *M. loti* density and B_{12} content of the cellular fraction was greater than for total B_{12}. This might be explained by the fact that *M. loti* density was measured as $CFU \cdot ml^{-1}$ of culture. When cell lysis occurs, the number of $CFU \cdot ml^{-1}$ would decline, while B_{12}, because of its stability, would persist and be measured in the media fraction, causing the total B_{12} per bacterial cell to increase. The per cell B_{12} concentration in the cellular fraction on the other hand, would be unaltered. As for the B_{12} in the media, it is clear that *metE7* can take up B_{12} (Figure 3.3c-d), and so should decrease the amount remaining in the media of cocultures. At lower *M. loti* densities though, the amount of B_{12} in the media is similar for axenic and cocultures. Perhaps the affinity of *C. reinhardtii* B_{12} uptake is sufficiently low so that only at higher B_{12} concentrations can it have a significant impact. Alternatively, the higher *M. loti* densities are also likely to be correlated with later time points when a greater proportion of the B_{12} measured in the media fraction might be free in solution and so available for uptake.

Results regarding B_{12} concentration and *M. loti* density did not lend themselves well to making clear and meaningful conclusions, but the idea that algae might be able to induce greater B_{12} production from bacteria, suggested by Grant et al. (2014), was intriguing enough for me to embark upon another, methodologically more convoluted experiment. Another PhD student in the laboratory obtained results that suggested B_{12} biosynthesis genes in *M. loti* were suppressed by B_{12} addition (Bhardwaj 2016). It seemed plausible therefore that removal of B_{12} from the media could induce B_{12}

synthesis, and hence by extension B_{12} uptake by *metE7* could do the same. Addition of B_{12}-deprived *metE7* cells to an *M. loti* culture did remove roughly 80% of the B_{12} from the media (Figure 4.7b). Following this though, the increase in media B_{12} was reflected by a reduction in the cellular fraction, so that total B_{12} did not change (Figure 4.7d). In many ways the responses of the four samples illustrated in Figure 4.7 could more easily be summarised by grouping them according whether *metE7* cells were added or not, rather than whether B_{12} had been removed from the media. By the final timepoint, the cultures to which *metE7* had been temporarily added saw an increase in *M. loti* density relative to the other two cultures, suggesting that algal photosynthate had prevented bacterial starvation and cell death. However, *metE7* addition did not increase total B_{12}, and so in the culture to which B_{12}-saturated *metE7* cells had been added the B_{12} per *M. loti* cell actually decreased. Overall therefore, these results agree with those previously discussed: although *metE7* can absorb B_{12} produced by *M. loti*, it is not capable of inducing *M. loti* to synthesise more B_{12}.

Considering the results discussed so far in this chapter, there is no good reason to believe that the interaction between *metE7* and *M. loti* is any more than syntrophy, where one species utilises compounds that are released passively by the other.

4.3.6 A *btuF* mutant of *E. coli*, but not *M. loti*, releases more B_{12} and better supports *metE7*

B_{12} production alone is insufficient for supporting a B_{12} auxotroph: the B_{12} must also be released from the producer so that it is available to the auxotroph. The mechanism by which B_{12} is released from *M. loti* is not known, and it may well be as simple as cell lysis. However, if *M. loti* could take up B_{12} from the media it would compete with *metE7*. BtuF is a periplasmic B_{12}-binding protein found in Gram-negative bacteria which acts concertedly with outer and inner membrane B_{12} binding proteins to transport B_{12} from the environment into the cell (Cadieux et al., 2002; Schauer et al., 2008). *btuF* mutants show reduced B_{12} uptake relative to the wild type but greater uptake than *btuB* mutants in both *E. coli* and *S. typhimurium* (Cadieux et al., 2002; Van Bibber et al., 1999). *M. loti btuF* mutants on the other hand, produced the same amount of B_{12} and released the same proportion of it into the media as the wild type strain (Figure 4.8b-c). An *M. loti bluB* mutant, which should be unable to produce B_{12} (Campbell et al., 2006), was also tested, and found to grow less well than the other two strains and produced significantly less B_{12}. The fact that some B_{12} was measured by the bioassay could be the result of the bacteria used in the bioassay (*S. typhimurium*) being able to take up the corrinoids produced by *M. loti* and complete the synthesis of B_{12} by providing the lower ligand, dimethylbenzimidazole (Raux et al., 1996). Although the amount of B_{12} or B_{12} precursors released into the media by *M. loti bluB* was lower than the other two strains, as a proportion of the total B_{12} it was greater. It is possible that intermediates of B_{12} biosynthesis would be more easily released or less easily reabsorbed than B_{12} itself, particularly if they accumulated as a consequence of

a lack of feedback inhibition by B_{12}. Alternatively, decreased fitness due to the reliance on B_{12}-independent isoforms such as *metE* may have increased cell death, lysis, and hence release of corrinoids.

As the *M. loti btuF* mutant released an equal amount of B_{12} as the wild type, a *btuF* mutant of *E. coli* was investigated instead. This *btuF* knockout strain (ED662) did release more B_{12} into the media than its parental strain (ED656), particularly when cultured in Tris min media (Figure 4.9c). The amount of B_{12} in the cell fraction was very similar for both strains, and so the total amount of B_{12} per *E. coli* cell was higher for ED662. It is possible that this is because only the B_{12} within the cell can cause repression of B_{12} biosynthesis, and so release of B_{12} into the media could reduce this repression. The proportion of B_{12} released into the media by both strains was significantly higher when they were cultured in Tris min media at 25°C for 96 hours than in M9 at 37°C for 12 hours. Because so many variables were changed between these two treatments it is difficult to determine which might have caused or contributed most significantly to this. Nevertheless, the higher release of B_{12} in conditions favourable to *C. reinhardtii* growth suggested that these strains might support *metE7*.

The growth rate of both *E. coli* strains was very similar, and so to more accurately distinguish any small difference they were competed against one another in mixed cultures. The decline of the *btuF* mutant showed that it had the lower fitness, but whether this was caused by disruption to BtuF or the cost associated with expressing the kanamycin resistance gene is unclear. Furthermore, it is possible that ED662 might have lost kanamycin resistance and so been counted as ED656 cells instead, however, axenic cultures of ED662 were never found to have lost kanamycin resistance.

Although much work has been done to optimise the composition of growth media for individual species such as *C. reinhardtii* and *E. coli*, there has understandably been only limited interest in optimising growth media for cocultures (Hom & Murray, 2014; Kropat et al., 2011; Lee, 1996; Yee & Blanch, 1993). Here, a range of mixtures of M9 and Tris min media were tested for their ability to support the growth of *E. coli* and *metE7* axenically and in coculture (Figure 4.11a-b). Both *E. coli* strains grew less well in coculture with *metE7* in all media mixtures than they did in every axenic condition. This suggested that *E. coli* was either not able to easily metabolise the carbon sources provided by *metE7* or was negatively impacted by the alga. On the other hand, *metE7* was supported in coculture at high Tris min percentages by ED662, but not by ED656. ED662 presumably still produced B_{12} at the higher M9 percentages but judging by the axenic cultures of *metE7* it would seem that the factor limiting *metE7* growth in coculture with ED662 switched from B_{12} at high Tris min percentages, to other components of the media as the percentage of M9 was increased.

Mixed cultures containing different ratios of ED656 and ED662 had substantially different effects on the growth of *metE7*: the higher the proportion of ED662 cells the better the growth of the alga. The most likely explanation for this result follows on from the finding that ED662 cells release

more B_{12}. Although ED656 cells also release B_{12}, the amount seemed to be insufficient to fully support *metE7* growth, and instead cell death due to B_{12} deprivation is likely to have dominated leading to a decline in viable cells. That a relatively small change in the amount of B_{12} released to the media can have such a significant change in the viability of a B_{12} auxotroph has interesting implications for microbial syntrophy and the evolution of auxotrophy. Bacteria that release more B_{12} would presumably incur some fitness cost relative to those that do not because of the metabolic costs of B_{12} synthesis. However, in an environment containing photosynthetic B_{12} auxotrophs, B_{12} release could ensure greater provision of photosynthate. In this example *E. coli* strains were not cultured with *metE7* for a long enough period to determine whether they were able to metabolise the photosynthate, but if they had been then a coculture of ED662 and *metE7* would likely be much more productive than one with ED656.

4.3.7 *M. loti* does not provide sufficient B_{12} to favour the evolution of B_{12} dependence in *C. reinhardtii*

The precise nature of the competitive advantage that *C. reinhardtii metE* mutants have over the wild type strain when B_{12} replete is unclear. It is unlikely that the *metE7* strain expresses a functional METE protein under any circumstances (Helliwell et al., 2015), and in replete B_{12} conditions the transcript abundance of *METE* is so low anyway that the fitness cost of METE protein synthesis would be minimal. The competitive advantage was confirmed nonetheless in this work, and under phototrophic conditions, as opposed to the mixotrophic conditions used previously (Helliwell et al., 2015). In the axenic treatments, within 4 days the culture was dominated by the S-type in the B_{12}-replete conditions, and revertant in the B_{12}-free cultures, albeit from a culture starting with a higher proportion of S-type cells (Figure 4.12a). The decline of S-type cells in the coculture with *M. loti* was expected as the coculture perturbation by nutrient addition experiments had shown that *metE7* was B_{12}-limited in coculture (Figure 4.4a). Even the addition of glycerol did not prevent the revertant strain from starting to outcompete S-type. Glycerol addition to cocultures increased the B_{12} content of the media to roughly 200 $ng \cdot l^{-1}$ (Figure 4.5a), which should be high enough to impose no growth limitation on *metE7* (Figure 3.1 and 3.3a), and which was shown to be sufficient to favour S-type over a B_{12}-independent line grown in TAP media (Helliwell et al., 2015). However, B_{12} was not measured in this experiment (Figure 4.11) and may have been considerably lower than in the coculture perturbation by nutrient addition experiment (Figure 4.4), as the culture dilution rate was substantially higher: 10-fold per day rather than 10% (1.11 fold). To improve the likelihood of providing an example where bacteria could support the evolution of B_{12} auxotrophy in *C. reinhardtii*, bacteria with higher B_{12} production rates than *M. loti* could be selected and cultivated continuously in turbidostats to maintain a higher density of bacteria and hence B_{12} concentration.

4.4 Concluding remarks

M. loti, a B_{12}-producing rhizobium, forms a commensal relationship with wild type *C. reinhardtii* and a mutualistic one with the B_{12}-dependent strain *metE7*. Addition of B_{12} or a carbon source to the *M. loti-metE7* coculture results in increased growth of the alga and bacterium respectively, indicating that both are limited by the cross-fed nutrient(s). B_{12}-limited *metE7* cells support a greater number of *M. loti* than wild type *C. reinhardtii* or *L. rostrata*, and addition of B_{12} decreases this number suggesting that B_{12} limitation of *metE7* improves the quality or quantity of organic compounds available to *M. loti*. There is no evidence that *M. loti* increases B_{12} production in the presence of *metE7*, but it does decrease production as its own cell density increases. An *E. coli btuF* mutant releases more B_{12} into the media and better supports *metE7*, despite a growth disadvantage relative to its parental strain. Even in the presence of an artificial carbon source, *M. loti* cannot provide enough B_{12} to favour the growth of *metE7* over a B_{12}-independent *C. reinhardtii* strain. Other bacterial species that produce higher levels of B_{12} could be tested for their ability to be cocultured with *metE7* and by extension provide an environment with a stable and high level of B_{12} which could favour the evolution of B_{12} auxotrophy.

Chapter 5: Discussion and Future work

Throughout this thesis the potential value of studying the *metE7* mutant of *C. reinhardtii* was considered from two main angles. Firstly, METE has a crucial role in connecting the folate and methionine cycles, and secondly, B_{12} auxotrophy among algae – a trait found in over 50% of all microalgal species surveyed, and without phylogenetic relationships - is highly correlated with the lack of *METE*. I shall discuss how my findings relate to these two viewpoints and suggest what further work would most effectively build upon what has already been achieved.

5.1 A model for studying One-carbon metabolism

From one perspective, this work has essentially been a study into the function of the *METE* gene through the physiology of the *metE7* mutant under B_{12} deprivation. The upregulation of C1-cycle enzyme transcripts was considerably greater under B_{12} deprivation in *metE7* than in the ancestral line (Figure 3.3), suggesting that perhaps the concentrations of both B_{12} *and* the C1-cycle metabolites regulated gene expression. In many bacteria the expression of several C1-cycle enzymes is regulated by riboswitches responsive to SAM and SAH, and in humans allosteric regulation and posttranslational modifications mediated by SAM play a significant role in regulating the flux through the C1-cycle (Banerjee et al., 2003; Wang et al., 2008; Yamada et al., 2005). Therefore, as in all systems, and especially eukaryotes, transcript abundances alone do not paint a full picture, and hence it was important to measure metabolites to determine what happened to SAH/SAM levels when the C1-cycle was limited by B_{12} deprivation.

Whilst SAM levels were essentially unaltered, SAH levels were 10-fold higher in B_{12} deprived relative to B_{12} replete conditions (Figure 3.3). Furthermore, the metabolite data suggests that the upregulation of enzyme expression under B_{12} deprivation did not increase flux, but rather was a response to decreased flux. Homocysteine was not quantified in this study, however, Croft et al. (2005) found that it increased 3-fold in *L. rostrata* under B_{12} deprivation, and studies of *A. thaliana* mutants of the C1-cycle found that levels were elevated in line with but to a greater extent than SAH (Croft et al., 2005; Groth et al., 2016). In humans there is also a high correlation between SAH and Hcy levels measured in the blood due to the reversibility of the conversion of SAH to Hcy by S-adenosylhomocysteine hydrolase (SAHH) (Yi et al., 2000). These results from other organisms might imply that Hcy levels would also be raised under B_{12} deprivation of *metE7*, but because of significant differences in the C1-cycle enzymes of different organisms it would be prudent to measure

homocysteine.

As methionine synthase links the methionine and folate cycles, B_{12} deprivation of *metE7* is likely to impact the concentration of folates. More countries have mandatory fortification of cereals, such as wheat, rice and maize, with folate than any other vitamin, yet there is still a high prevalence of diseases caused by folate deficiency (Arth et al., 2016). In parallel with fortification at the point of food processing, there is also considerable interest in biofortification of food crops with folate (Bekaert et al., 2008; Strobbe & Van Der Straeten, 2017). Exposure of *C. reinhardtii metE7* mutants to different concentrations of B_{12}, and determination of levels of folates would improve our understanding of the role that methionine synthase plays in algal and perhaps plant folate metabolism.

Folates are also essential for the production of nucleotides: thymidylate from 5,10-CH_2-THF and purines from 10-formyl-THF (Hanson & Roje, 2001). One of the symptoms of folate and vitamin B_{12} deficiency in humans is macrocytic anaemia, which is characterised by an enlargement of red blood cells caused by a defect in DNA synthesis (Aslinia et al., 2006). B_{12} deprivation of *E. gracilis* also causes an increase in mean cell size, which is paralleled by an almost complete disappearance of deoxynucleotide triphosphates (dNTPs) (Carell & Goetz, 1976). Application of the antifolate drug methotrexate to *A. thaliana* caused changes in gene expression suggestive of perturbed nucleotide homeostasis, but which also indicated a prioritisation of purine and thymidylate synthesis at the expense of SAM synthesis (Loizeau et al., 2008). Therefore, DNA synthesis in B_{12}-deprived *metE7* cells should be investigated as it will provide information on how the C1 cycle responds to reduced methionine synthase activity, and also the stage in the cell cycle at which growth is arrested.

B_{12} deprivation of *metE7* resulted in a 30-fold decrease in the methylation index (SAM:SAH ratio) within 24 hours (Figure 3.6a). Such a substantial change is likely to inhibit the action of methyltransferases, which methylate a variety of compounds from lipids to histones and DNA (Mentch & Locasale, 2016; Stead et al., 2006). H3K9 (histone) and DNA cytosine methylation were found to decrease considerably in C1-cycle enzyme mutants of Arabidopsis (Groth et al., 2016; Meng et al., 2018). Studies concerning the effect of B_{12} or folate status on genome methylation in humans however, have been less conclusive: although there is some consensus that folate is positively correlated with genome methylation, the results for B_{12} have been mixed (Anderson et al., 2012; Ba et al., 2011; Christensen et al., 2010; Fang et al., 2017; Kok et al., 2015; McKay et al., 2012; Pufulete et al., 2005; Rampersaud et al., 2000; Vineis et al., 2011). Therefore, it is unclear what effect a reduced methylation index would have on *C. reinhardtii* DNA methylation, but because *C. reinhardtii* has relatively low DNA methylation levels, it might be more productive to analyse previously identified hypermethylated loci (Lopez et al., 2015). On the other hand, *C. reinhardtii* has quite high levels of histone methylation (Waterborg et al., 1995), so it is possible that these marks would be more responsive to changes in the methylation index. Differential methylation of both histones and DNA

will likely impact gene expression, and perhaps expression of transposons in particular, which may lead to increased rate of genomic change under B_{12} deprivation.

In humans, the membrane phospholipid phosphatidylethanolamine (PE) is a major acceptor of methyl groups from S-adenosylmethionine during the formation of phosphatidylcholine (PC) (Noga et al., 2003). It is thought that hypomethylation of PE, which is associated with hyperhomocysteinemia causes changes in lipid metabolism that increase triglycerides (Obeid & Herrmann, 2009), and indeed epidemiological data suggests a strong positive correlation between homocysteine and triglycerides (Momin et al., 2017). In *S. cerevisiae*, homocysteine supplementation caused a decrease in PC and an increase in triglycerides, and further study found that homocysteine mediated this effect through increasing SAH (Visram et al., 2018). In this work it was found that SAH levels increased by 100-fold in the first 24 hours of B_{12} deprivation of *metE7* (Figure 3.6), and that triglyceride levels rose by 9.5-fold after 48 hours (Figure 3.4). *C. reinhardtii* lacks PC, but contains another abundant trimethylated membrane lipid, DGTS, which is thought to functionally substitute for PC (Sakurai et al., 2014). Methylation, or lack thereof, of diacylglyceride (DAG) to DGTS may therefore be the missing link between SAH and triglycerides. Although excessive production and storage of triglycerides is clearly a problem in humans, it is one of the major aims of the algal biodiesel industry (Griffiths & Harrison, 2009). It is possible therefore, that an improved understanding of the C1 cycle in *C. reinhardtii* will allow engineering of higher TAG-accumulating algal strains.

The generation of *metE7* by experimental evolution (Helliwell et al, 2015) was somewhat serendipitous, however, our lab has recently achieved targeted genome editing using CRISPR/Cpf1 technology, and a possible knockout target to further our understanding of methionine synthesis and one carbon metabolism would be *METH*. A *metH* mutant is unlikely to grow in the presence of replete B_{12}, because in these conditions the remaining methionine synthase (*METE*) would be repressed, resulting in an inability to synthesise methionine. A *metH* mutant would be a useful counterbalance to *metE7* to disentangle the effects of B_{12} and a disrupted methionine cycle on the physiology of *C. reinhardtii*. Responses to a disruption in the C1 cycle should be observed in the absence of B_{12} for *metE7* and the presence of B_{12} for *metH* but be absent from the other two permutations. These two mutants should facilitate robust investigation of the C1-cycle, and *C. reinhardtii* may become a useful model for the study of methylation, including its involvement in modifying the epigenome.

5.2 Coping with a novel nutrient limitation

C. reinhardtii exhibits a range of nutrient deprivation responses which aid survival, from inducing high affinity uptake systems for improved nutrient acquisition to downregulating

photosynthesis and increasing starch synthesis to control redox status (Saroussi et al., 2017). Compared with nitrogen deprivation, B_{12} deprivation caused a much greater decline in *metE7* viability (Figure 3.9b). Prior to and during this decline there was a marked increase in the fluorescence of the ROS-sensitive dye H_2DCFDA (Figure 3.9a). The type of ROS released was not determined here, and would require the use of more specific probes to distinguish H_2O_2, $^1O_2$, or O_2^- (Gomes et al., 2005). Other measures, such as the level of lipid peroxidation, or the activity of antioxidant enzymes, have been found to be a better indicator of stress in *C. reinhardtii* than the levels of ROS themselves (Drummen et al., 2002; Elbaz et al., 2010; Pillai et al., 2014; Urzica, Adler, et al., 2012). Taking measurements of these indicators in *metE7* under B_{12} deprivation, but also in coculture with *M. loti*, should indicate the extent and possibly the management of physiological stress.

In addition to large cells becoming more prevalent during B_{12} deprivation of *metE7*, which is also frequently observed during sulphur deprivation (Cakmak, Angun, Ozkan, et al., 2012), it was noted that palmelloids (clusters of cells that did not separate after cytokinesis), appeared to become more common. This was not quantified statistically in this work, but it would be a relatively simple phenomenon to investigate by microscopy. The formation of palmelloids has been observed in response to a range of stressors, including high concentrations of NaCl where they are thought to protect naïve daughter cells from the saline environment by producing a thick exopolysaccharide matrix (Khona et al., 2016). B_{12} deprivation would seem to pose the opposite challenge, but perhaps cells in palmelloids grow more slowly than single cells and so are less likely to lose viability (Olsen et al., 1983).

The fact that nitrogen deprivation was found to protect *metE7* against B_{12} deprivation begs the question of whether deprivation of other nutrients also provoke a general protective response. Carotenoids, which are involved in non-photochemical quenching, decreased more than chlorophyll during B_{12} deprivation, but under most other nutrient deprivation conditions, such as for sulphur, there is a relative increase in carotenoids, and this may be sufficient to provide mild protection (Cakmak, Angun, Ozkan, et al., 2012). It may be possible and revealing to induce these nutrient starvation responses while the nutrient is still replete by placing for example a global regulator of sulphur starvation, *SNRK2.1* (Gonzalez-Ballester et al., 2008), under the control of the *METE* promoter. Sulphur starvation responses might then be elicited by a lack of B_{12} and may provide protection against B_{12} deprivation-induced cell death. Indeed, in *L. rostrata* one of the most upregulated transcripts during coculture with *M. loti* relative to B_{12}-replete axenic conditions was *SNRK2.1*, suggesting it may play a role in the response to B_{12} deprivation (Kudahl 2017). As sulphur deprivation also leads to a decrease in methionine cycle metabolites (González-Ballester et al., 2010), it is tempting to hypothesise that exaptation of *SNRK2.1* to act as a B_{12} starvation response regulator would be a relatively quick fix following the evolution of B_{12} auxotrophy.

Deprivation of B_{12} was found to cause accumulation of TAGs (Figure 3.4), a phenomenon that is frequently observed under nitrogen deprivation. However, these similar outcomes may well be mediated by different mechanisms. In *A. thaliana* treated with methotrexate, total lipid levels were found to increase, due mainly to TAG accumulation, while nitrogen deprivation did not cause an overall increase in lipids, but there was a shift from membrane lipids to TAGs (Meï et al., 2016). It would therefore be worth testing if the combination of B_{12} and nitrogen deprivation has an additive effect on TAG accumulation in *metE7.* As B_{12} deprivation was also found to increase cell size, the sedimentation of these cells ought to be greater, reducing the energy required for dewatering, which is an important factor in the economic procurement of low value compounds such as TAGs for biodiesel production (Uduman et al., 2010).

Investigating the responses of *C. reinhardtii* to nutrient deprivation is increasingly reliant on 'omics' approaches such as RNA-seq technology (Blaby et al., 2015; González-Ballester et al., 2010; Juergens et al., 2015; Schmollinger et al., 2014). Nonetheless, its relatively high cost prohibits the testing of multiple different conditions, and hence it is advisable to conduct preliminary research to decide on the degree of nutrient deprivation or timepoint during deprivation that is most relevant to your research questions. This work has shown that during B_{12} deprivation the transcripts for many C1-cycle enzymes increase within 6 hours, while SAH accumulates over 24 hours, starch content increases before 48 hours, and most chlorophyll bleaching and cell death occurs after 48 hours. RNA-seq of *metE7* and wild-type *C. reinhardtii* cells cultured in B_{12}-free and B_{12}-replete media for 24 hours might therefore provide the best insight into the effects of disrupted one-carbon metabolism while avoiding differential expression of genes associated with autophagy and cell death. Using wild-type *C. reinhardtii* would ensure that the genes regulated directly in response to B_{12} were distinguishable from those impacted by disrupted one-carbon metabolism. If that group of genes is found to be particularly small, it suggests that using B_{12} to regulate transgene expression in *C. reinhardtii* would have little effect on the transcriptome.

5.3 Investigating other algae and bacteria

L. rostrata was used as an example of a related natural B_{12} auxotroph to compare with the artificially evolved *metE7* strain. *L. rostrata* had lower growth and B_{12} uptake in replete B_{12} conditions than *metE7*, but higher growth and uptake under limiting levels (Figure 3.2). *L. rostrata* also grew faster than *metE7* in coculture with *M. loti*, which might be explained by the higher B_{12} production by *M. loti* in the presence of *L. rostrata* than *metE7* (Figure 4.3). However, results from *L. rostrata* cannot be assumed to be representative of all algal B_{12} auxotrophs. There are several B_{12} auxotrophs in the Volvocales, such as *G. pectorale, V. carteri*, as well as the unrelated *E. gracilis* or the marine species *O. tauri, Amphidinium carterae,* and *T. pseudonana*. It would be of interest to measure EC_{50}

and uptake rate of B_{12}, or survival time without B_{12} in order to make comparisons to *metE7* and determine to what extent this newly evolved mutant differs from species that have adapted to the trait. Similarly, measuring the algal, bacterial, and B_{12} concentrations of cocultures containing *M. loti* and some of the freshwater algae mentioned above should provide insight into whether natural B_{12} auxotrophs are any better than *metE7* at growing in coculture with bacteria.

E. gracilis, has been used widely as a B_{12} bioassay organism (Ross, 1952), but in this work a *metE,cysG* mutant of *S. typhimurium* was used, and several B_{12} dose-response curves for *metE7* were also generated (Figure 3.1). It may be beneficial to compare a B_{12} bioassay using *metE7* to these other two organisms because *metE7* has a higher growth rate than *E. gracilis* (Marian Cramer & Myers, 1952), can reach a higher optical density than was observed for *S. typhimurium*, and may have a greater specificity for B_{12} than either species. Furthermore, if a *metH* mutant (which should show decreasing growth as B_{12} is increased) was used in parallel with *metE7*, then B_{12} measurements are likely to be more statistically accurate and robust to any inhibitory compounds in the sample.

M. loti was unable to provide sufficient B_{12} to S-type (unstable *metE* mutant) for it to outcompete the ancestral *C. reinhardtii* strain, even when provided with an exogenous carbon source (Figure 4.12). However, there may be other bacteria that would be able to. *S. meliloti* is probably a good candidate as it is a relative of *M. loti*, supports *L. rostrata* (Bhardwaj 2016), enhances the thermal tolerance of *C. reinhardtii* by provision of B_{12} (Xie et al., 2013), and some strains produce as much as 150 $mg \cdot l^{-1}$ of B_{12} (Cai et al., 2018). If *S. meliloti*, or another environmentally relevant bacterium, can be shown to provide sufficient B_{12} to favour the growth of a B_{12}-dependent *C. reinhardtii* strain over an independent one, this would provide some evidence to support the idea that B_{12}-producing bacteria drove the evolution of algal B_{12} auxotrophy.

In a completely artificial co-culture, *metE7* was grown with two *E. coli* lines engineered to synthesise adenosylcobalamin. Release of B_{12} into the media was found to be an important indicator of how well *E. coli* would support *metE7*, but it was unclear how well *E. coli* was supported in return (Figure 4.11a). The parental strain ED656 outcompeted the *btuf::Kan* mutant ED662 when they were cocultured together (Figure 4.10c), but when each bacterial strain was separately cocultured with *metE7*, ED662 performed slightly better (Figure 4.11a), suggesting perhaps that it improved the growth of *metE7*, and benefited in return. If *E. coli* and *metE7* are found not to mutually support one another particularly well, an alternative bacterium to test might be *Pseudomonas putida*. *P. putida* was found to provide additional support to *L. rostrata* when added to a coculture with *M. loti* (Ridley 2016), yet did not enhance the thermal tolerance of *C. reinhardtii* by B_{12} supply (Xie et al., 2013). This might be explained by the small proportion of B_{12} released into the media (Bhardwaj 2016). Unlike *M. loti*, *P. putida* encodes *btuB*, the outer membrane protein which when mutated abolishes B_{12} uptake in *E. coli* (Cadieux et al., 2002). Therefore, a *btuB* knockout of *P. putida* may release

substantially more B_{12} into the media as a result of not taking up the B_{12} that does get out of the cell, and hence support *metE7* to a greater extent.

5.4 Investigating nutrient transfer between *metE7* and bacteria

The growth of *M. loti* was not improved after B_{12} addition to the coculture with *metE7* despite a substantial increase in algal cell density (Figure 4.4b), suggesting that when algal cells become B_{12} replete they provide a lower quantity of organic compounds or a profile that is less easily metabolized by *M. loti*. The observation that the ratio of *M. loti* to algae in coculture was lower for B_{12}-independent strains than *metE7* appears to agree with this hypothesis (Figure 4.2). As B_{12}-deprived *metE7* cells are larger than replete cells, it would be important to measure the impact that a certain dry weight of *metE7* cells has on *M. loti* growth and also whether the viability of the *metE7* cells has an impact. Attachment of *M. loti* and *metE7* is unnecessary for mutual support, nonetheless it does occur (Bhardwaj 2016), and it is reasonable to assume that it would improve the efficiency of nutrient transfer. One method of testing whether B_{12} status affects bacterial attachment would be to prepare cocultures with various concentrations of B_{12} and chemically fix the samples prior to preparation for scanning electron microscopy.

Transfer of organic compounds from *metE7* to *M. loti* has recently been demonstrated using Nanoscale Secondary Ion Mass Spectrometry (Nano-SIMS) (H. Laeverenz Schlogelhofer, personal communication). The same technique was also used to show transfer of carbon and nitrogen in another synthetic mutualism from the plant-growth promoting bacterium *Azospirillum brasilense* to the green alga *Chlorella sorokiniana* (de-Bashan et al., 2016). However, this technique does not determine the chemical identity of the transferred compounds. HPLC/MS should provide a method for determining the abundance of specific metabolites in mixed cultures. Those metabolites in the media that decrease most after *M. loti* is added to an axenic culture of *metE7* are likely to be taken up by *M. loti*.

I briefly investigated mathematical models based on Lotka-Volterra equations as a way of rapidly running experiments *in silico* to generate testable hypotheses and guide the design of more laborious *in vivo* coculture experiments. A similar but more complex model was applied to the mutualism between *L. rostrata* and *M. loti* where each species was grown in separate flasks connected by a tube filled with polyacrylamide which only allowed the diffusion of B_{12} and small organic molecules, but not entire cells (Peaudecerf et al., 2018). In the case of well mixed cocultures of *metE7* and *M. loti* most of this added complexity would not be needed. Instead additional parameters that might improve the model include terms for the regulation of B_{12} or organic carbon release by the bacteria and alga respectively according to their growth or death rate.

Total B_{12} concentration was found to be higher in cocultures of *M. loti* with *L. rostrata* than *M. loti* with *metE7*, for all densities of *M. loti* (Figure 4.3f). This suggests that *L. rostrata* might be capable of inducing *M. loti* to produce more B_{12}. However, B_{12} per *M. loti* cell was even higher in axenic *M. loti* cultures (Figure 4.6a), indicating that the carbon source provided to *M. loti* may be the main determinant of B_{12} production, rather than the presence or absence of algae. Therefore, increasing the amount and altering the type of photosynthate released might be the best option available to algae to increase the number of bacteria in their surroundings. Dinoflagellates for example, are known to produce dimethylsulphoniopropionate (DMSP), a compound which is mainly utilised by certain clades of bacteria, such as the Roseobacter, a large proportion of which are found in the phycosphere and produce B_{12} (Kudahl 2017) (Bullock et al., 2017).

5.5 Evolution of mutualism

The Black Queen hypothesis (BQH) provides some insight into the evolution of B_{12} dependence in algae in so far as it offers a mechanism for the 'evolution of dependencies through adaptive gene loss' (Morris et al., 2012). However, Morris et al. (2012) specifically state that it is the extended phenotype of one organism that drives the loss of the gene/s responsible for that same phenotype in another organism. Uptake of methionine from the environment is unlikely to drive the loss of *METE* because in the absence of B_{12} it would not ameliorate the problem of homocysteine accumulation or the trapping of folates. Therefore, the BQH does not strictly apply because we hypothesise that it is B_{12} (which is clearly not a product of METE) that is responsible for driving the loss of *METE* in algae. On the other hand, the BQH can apply to the situation in the eubacterial lineages, where whole genome analysis identified bacteria that are dependent on B_{12} (by virtue of having only METH not METE, or only the RNRII isoform) yet do not have the full pathway to synthesise it, and therefore presumably lost elements of the pathway in the past (Kudahl 2017) (Zhang et al., 2009).

Another hypothesis, called the 'Foraging to Farming hypothesis' (FFH) was developed in our group to explain the specific example of microalgae such as *C. reinhardtii* becoming dependent on B_{12} producers. The most succinct definition is that 'mutualism can evolve as an accidental consequence of metabolic exchange'(Kazamia et al., 2016). This may not seem to be very different from the BQH, however, the BQH seeks to explain the evolution of dependencies by adaptive gene loss, while the FFH goes a step further in seeking to explain the evolution of mutualisms. The FFH posits that once the alga is dependent on the B_{12} producer it may change its behaviour to farm the bacterium, by providing photosynthate for example. In a follow-up paper to the BQH, Morris et al. (2015) propose that after Black Queen evolution causes the loss of a gene and therefore dependence of one organism on another, the coexistence of both species might provide time for the reciprocal

Black Queen evolution to occur i.e. the 'helper' to become a 'beneficiary' of a different nutrient (Morris, 2015). This is therefore a route to mutualism via two loss of function mutations in a pair of organisms that can complement one another. The FFH suggests that the 'beneficiary', such as the alga that requires B_{12}, would gain a selective advantage were it to provide something in return to its helper, such as photosynthate, because this would ensure a source of B_{12}.

When Helliwell et al. (2015) initially cocultured *metE7* with three different rhizobia they were all found to support its growth, and in this work, it was shown that the wild type *C. reinhardtii* and *metE7* both supported *M. loti* (Helliwell et al., 2015). 'Ecological fitting' (EF) includes the process whereby organisms can form novel associations by relying on traits they already possessed at the time of encounter (Agosta & Klemens, 2008). Therefore, EF provides an explanation for how synthetic mutualisms are able to function, such as between *C. reinhardtii* and *S. cerevisiae* (Hom & Murray, 2014), *C. vulgaris* and *A. brasilense* (de-Bashan et al., 2016), or indeed between *metE7* and *M. loti*. From this rather simplistic or primitive mutualism would something more sophisticated and mutually beneficial develop, such as 'farming' of one organism by the other? In this work *metE7* was cocultured with *M. loti* for a period of 6 months (condition C), at the end of which it was found to have a lower B_{12} requirement than the progenitor *metE7* strain (Figure 3.12c). This line provides the opportunity to test the FFH because the selection pressure in coculture was simply for increased growth, and the FFH predicts that this might occur by the alga releasing more photosynthate. Therefore, it would be interesting to test whether those lines in condition C do in fact release more photosynthate than lines kept under different conditions or the progenitor *metE7*.

Both the FFH and BQH offer useful insights into the evolution of symbioses and package them within memorable analogies. However, neither really tackles the problem posed by the prisoner's dilemma, which states that if it is beneficial to defect (not cooperate), then evolution will cause mutualisms to breakdown rather than strengthen, even if that leads to a worse outcome for both individuals. Is it possible both to acknowledge the existence of the prisoner's dilemma in a situation and to overcome it? A well-known hypothesis supporting the evolution of cooperation is called group selection. Traulsen and Nowak (2006) suggest that within individuals of the same species, for group-level selection to be favoured over individual-level selection, the benefits from cooperation must be much greater than the cost of cooperating, and the size of the group must be small while the number of interacting groups must be large (Traulsen & Nowak, 2006).

To test group selection, it is useful to have a clear distinction between the individuals that cooperate and those that defect, and unfortunately this work did not identify B_{12}-dependent *C. reinhardtii* strains that released large (cooperate) or small (defect) amounts of photosynthate. Note that the cooperation that might result here is not with other *C. reinhardtii* cells but with B_{12}-producing heterotrophic bacteria. On the other hand, it was found that *E. coli* ED662 released more B_{12} than

ED656, and that ED662 was better able to support the growth of *metE7*, while also exhibiting a lower growth rate than ED656. Therefore, in a triculture of ED656, ED662, and *metE7* one might expect ED656 to outcompete ED662, and this would then lead to the collapse of the coculture. However, if the groups are both small enough and numerous enough then it might be the case that during one subculture no ED656 cells are transferred, but some ED662 cells are. Then the coculture of ED662 and *metE7* should grow better than the other mixed tricultures. It is also likely that the less productive cultures that have higher proportions of ED656 will go extinct first. Therefore, if there is a process of replacing lines that have gone extinct with those that are still growing it is likely that cultures with high proportions of ED656 (prior to extinction) will be replaced by those with high proportions of ED662. ED656 will always outcompete ED662 at an individual level, but groups of ED662 will outcompete those dominated by ED656.

In nature there are no nicely separated flasks or wells on a microwell plate to represent groups, but nor is the ocean or any other aquatic environment for that matter just one big homogeneous mix of metabolites and organisms. Microscale patches of algae and bacteria can also be considered a 'group', just one that has porous boundaries. At an even smaller scale, if bacteria were able to attach to the surface of algal cells and increase their chances of being transferred to algal daughter cells, then the bacteria associated with the phycosphere, along with the algal cell, should be considered as one group. The alga and its associated bacteria will now metaphorically sink or swim depending on the extent to which the bacteria and alga cooperate with one another. When that association becomes so tight that one organism actually resides inside the other and is vertically transmitted during host division, such as a cyanobacterium within a protist, we no longer consider it a group, and a transition in individuality has occurred. Although physical attachment provides a nice way of defining a group with clear boundaries, groups can be collections of individuals that are not physically associated, but the more porous the boundaries of the group the less likely group level selection is to occur. Overall therefore, group-level selection more precisely specifies the conditions required to achieve the same outcome that the FFH predicts may occur between mutually dependent algae and bacteria.

5.6 Concluding remarks

The responses of *metE7* to B_{12} deprivation has provided several insights into one-carbon metabolism in *C. reinhardtii*, and the combination of *metE* and *metH* mutants may offer a more robust platform for its further elucidation. Considering *metE7* is evolutionarily naïve to B_{12} dependence it was unsurprising that B_{12} deprivation caused substantial loss of viability, but the fact that nitrogen deprivation responses improved survival during B_{12} deprivation indicates there is the potential for the

transition to B_{12} auxotrophy to be facilitated by exaptation. One life strategy for improving growth in the environment over the long term might be for the B_{12} auxotroph to form an association with a B_{12} producer, and algae like *C. reinhardtii* may already have a commensal relationship with bacteria like *M. loti* in place prior to the loss of *METE*. From a mutualism formed by ecological fitting, increasing the transfer of fixed carbon and B_{12} should lead to improved growth of both partners, but to achieve this requires a method to reduce the relative fitness of cheaters, and group selection may offer the simplest solution.

6. Bibliography

Agosta, S. J., & Klemens, J. A. (2008). Ecological fitting by phenotypically flexible genotypes: implications for species associations, community assembly and evolution. *Ecology Letters*, *11*(11), 1123–1134. https://doi.org/10.1111/j.1461-0248.2008.01237.x

Aksoy, M., Pootakham, W., & Grossman, A. R. (2014). Critical function of a Chlamydomonas reinhardtii putative polyphosphate polymerase subunit during nutrient deprivation. *The Plant Cell*, *26*(10), 4214–4229. https://doi.org/10.1105/tpc.114.129270

Aksoy, M., Pootakham, W., Pollock, S. V, Moseley, J. L., Gonzalez-Ballester, D., & Grossman, A. R. (2013). Tiered Regulation of Sulfur Deprivation Responses in Chlamydomonas reinhardtii and Identification of an Associated Regulatory Factor. *Plant Physiology*, *162*(1), 195–211. https://doi.org/10.1104/pp.113.214593

Amin, S. A., Green, D. H., Hart, M. C., Kupper, F. C., Sunda, W. G., & Carrano, C. J. (2009). Photolysis of iron-siderophore chelates promotes bacterial-algal mutualism. *Proceedings of the National Academy of Sciences*, *106*(40), 17071–17076. https://doi.org/10.1073/pnas.0905512106

Amin, S. a, Parker, M. S., & Armbrust, E. V. (2012). Interactions between diatoms and bacteria. *Microbiology and Molecular Biology Reviews*, *76*(3), 667–684. https://doi.org/10.1128/MMBR.00007-12

Ananyev, G., Gates, C., Kaplan, A., & Dismukes, G. C. (2017). Photosystem II-cyclic electron flow powers exceptional photoprotection and record growth in the microalga Chlorella ohadii. *Biochimica et Biophysica Acta - Bioenergetics*, *1858*(11), 873–883. https://doi.org/10.1016/j.bbabio.2017.07.001

Anderson, O. S., Sant, K. E., & Dolinoy, D. C. (2012). Nutrition and epigenetics: an interplay of dietary methyl donors, one-carbon metabolism and DNA methylation. *Journal of Nutritional Biochemistry*, *23*, 853–859. https://doi.org/10.1016/j.jnutbio.2012.03.003

Antal, T. K., Volgusheva, A. A., Kukarskih, G. P., Bulychev, A. A., Krendeleva, T. E., & Rubin, A. B. (2006). Effects of sulfur limitation on photosystem II functioning in Chlamydomonas reinhardtii as probed by chlorophyll a fluorescence. *Physiologia Plantarum*, *128*(2), 360–367. https://doi.org/10.1111/j.1399-3054.2006.00734.x

Arth, A., Kancherla, V., Pachn, H., Zimmerman, S., Johnson, Q., & Oakley, G. P. (2016). A 2015 global update on folic acid-preventable spina bifida and anencephaly. *Birth Defects Research Part A: Clinical and Molecular Teratology*, *106*(7), 520–529. https://doi.org/10.1002/bdra.23529

Aslinia, F., Mazza, J. J., & Yale, S. H. (2006). Megaloblastic anemia and other causes of macrocytosis. *Clinical Medicine & Research*, *4*(3), 236–241. Retrieved from http://www.ncbi.nlm.nih.gov/pubmed/16988104

Atta, C. A. M., Fiest, K. M., Frolkis, A. D., Jette, N., Pringsheim, T., St Germaine-Smith, C., … Metcalfe, A. (2016). Global Birth Prevalence of Spina Bifida by Folic Acid Fortification Status: A Systematic Review and Meta-Analysis. *American Journal of Public Health*, *106*(1), e24-34. https://doi.org/10.2105/AJPH.2015.302902

Axelrod, R., & Hamilton, W. D. (1981). The evolution of cooperation. *Science*, *211*(4489), 1390–1396. https://doi.org/10.1126/SCIENCE.7466396

Ba, Y., Yu, H., Liu, F., Geng, X., Zhu, C., Zhu, Q., … Zhang, Y. (2011). Relationship of folate, vitamin B12 and methylation of insulin-like growth factor-II in maternal and cord blood. *European Journal of*

Clinical Nutrition, *65*(4), 480–485. https://doi.org/10.1038/ejcn.2010.294

Badger, M. R., John Andrews, T., Whitney, S., Ludwig, M., Yellowlees, D. C., Leggat, W., … Yellowlees, D. (1998). The diversity and coevolution of Rubisco, plastids, pyrenoids, and chloroplast-based CO 2-concentrating mechanisms in algae. *Canadian Journal of Botany*, *76*, 1052–1071. https://doi.org/https://doi.org/10.1139/b98-074

Baggott, J. E., & Tamura, T. (2015). Folate-Dependent Purine Nucleotide Biosynthesis in Humans. *Advances in Nutrition (Bethesda, Md.)*, *6*(5), 564–571. https://doi.org/10.3945/an.115.008300

Bajhaiya, A. K., Dean, A. P., Zeef, L. A. H., Webster, R. E., & Pittman, J. K. (2016). PSR1 Is a Global Transcriptional Regulator of Phosphorus Deficiency Responses and Carbon Storage Metabolism in Chlamydomonas reinhardtii. *Plant Physiology*, *170*(3), 1216–1234. https://doi.org/10.1104/pp.15.01907

Baker, H., Frank, O., Pasher, I., Sobotka, H., Nathan, H. A., Hutner, S. H., & Aaronson, S. (1960). Elaboration of vitamin B12 by Escherichia coli. *Experientia*, *16*(5), 187. https://doi.org/10.1007/BF02178977

Ball, S. G., Subtil, A., Bhattacharya, D., Moustafa, A., Weber, A. P. M., Gehre, L., … Dauvillée, D. (2013). Metabolic Effectors Secreted by Bacterial Pathogens: Essential Facilitators of Plastid Endosymbiosis? W OA. *The Plant Cell*, *25*, 7–21. https://doi.org/10.1105/tpc.112.101329

Banerjee, R., Evande, R., Mer Kabil, O. ¨, Ojha, S., & Taoka, S. (2003). Reaction mechanism and regulation of cystathionine beta-synthase. *Biochimica et Biophysica Acta*, *1647*, 30–35. https://doi.org/10.1016/S1570-9639(03)00044-X

Banerjee, R., & Ragsdale, S. W. (2003). The Many Faces of Vitamin B 12 : Catalysis by Cobalamin-Dependent Enzymes. *Annual Review of Biochemistry*, *72*(1), 209–247. https://doi.org/10.1146/annurev.biochem.72.121801.161828

Banerjee, R. V, & Matthews, R. G. (1990). Cobalamin-dependent methionine synthase. *FASEB*, *4*, 1450–1459. https://doi.org/https://doi.org/10.1096/fasebj.4.5.2407589

Barbara, G. M., & Mitchell, J. G. (2003). Bacterial tracking of motile algae. *FEMS Microbiology Ecology*, *44*(1), 79–87. https://doi.org/10.1111/j.1574-6941.2003.tb01092.x

Barbier, G. (2005). Comparative Genomics of Two Closely Related Unicellular Thermo-Acidophilic Red Algae, Galdieria sulphuraria and Cyanidioschyzon merolae, Reveals the Molecular Basis of the Metabolic Flexibility of Galdieria sulphuraria and Significant Differences in Carbo. *Plant Physiology*, *137*(2), 460–474. https://doi.org/10.1104/pp.104.051169

Barker, J. L., Bronstein, J. L., Friesen, M. L., Jones, E. I., Reeve, H. K., Zink, A. G., & Frederickson, M. E. (2017). Synthesizing perspectives on the evolution of cooperation within and between species. *Evolution*, *71*(4), 814–825. https://doi.org/10.1111/evo.13174

Baroli, I., Gutman, B. L., Ledford, H. K., Shin, J. W., Chin, B. L., Havaux, M., & Niyogi, K. K. (2004). Photo-oxidative stress in a xanthophyll-deficient mutant of Chlamydomonas. *The Journal of Biological Chemistry*, *279*(8), 6337–6344. https://doi.org/10.1074/jbc.M312919200

Baumeister, S., Winterberg, M., Przyborski, J. M., & Lingelbach, K. (2010). The malaria parasite Plasmodium falciparum: cell biological peculiarities and nutritional consequences. *Protoplasma*, *240*, 3–12. https://doi.org/10.1007/s00709-009-0090-3

Bayer-Giraldi, M., Uhlig, C., John, U., Mock, T., & Valentin, K. (2010). Antifreeze proteins in polar sea ice diatoms: diversity and gene expression in the genus Fragilariopsis. *Environmental Microbiology*, *12*(4), 1041–1052. https://doi.org/10.1111/j.1462-2920.2009.02149.x

Bayer-Giraldi, M., Weikusat, I., Besir, H., & Dieckmann, G. (2011). Characterization of an antifreeze protein from the polar diatom Fragilariopsis cylindrus and its relevance in sea ice. *Cryobiology*, *63*(3), 210–219. https://doi.org/10.1016/J.CRYOBIOL.2011.08.006

Bazzano, L. A., Reynolds, K., Holder, K. N., & He, J. (2006). Effect of Folic Acid Supplementation on Risk of Cardiovascular Diseases. *JAMA*, *296*(22), 2720. https://doi.org/10.1001/jama.296.22.2720

Beck, C. F., & Acker, A. (1992). Gametic Differentiation of Chlamydomonas reinhardtii: Control by Nitrogen and Light. *Plant Physiology*, *98*(3), 822–826. https://doi.org/10.1104/PP.98.3.822

Beck, W. S. (1982). *Biological and medical aspects of vitamin B 12*. *D. Dolphin (ed.)* (Vol. 1). Retrieved from http://www.daviddolphin.com/books/book13-contents.pdf

Behringer, G., Ochsenkühn, M. A., Fei, C., Fanning, J., Koester, J. A., & Amin, S. A. (2018). Bacterial Communities of Diatoms Display Strong Conservation Across Strains and Time. *Frontiers in Microbiology*, *9*, 659. https://doi.org/10.3389/fmicb.2018.00659

Bekaert, S., Storozhenko, S., Mehrshahi, P., Bennett, M. J., Lambert, W., Gregory, J. F., … Hanson, A. D. (2008). Folate biofortification in food plants. *Trends in Plant Science*, *13*(1), 28–35. https://doi.org/10.1016/j.tplants.2007.11.001

Belcher, J. H., & Swale, E. M. F. (1961). Some new and uncommon British volvocales. *British Phycological Bulletin*, *2*(2), 56–62. https://doi.org/10.1080/00071616100650031org/10.1080/00071616100650031

Bertrand, E. M., Allen, A. E., Dupont, C. L., Norden-Krichmar, T. M., Bai, J., Valas, R. E., & Saito, M. a. (2012). Influence of cobalamin scarcity on diatom molecular physiology and identification of a cobalamin acquisition protein. *Proceedings of the National Academy of Sciences*, *109*(26), E1762-71. https://doi.org/10.1073/pnas.1201731109

Bertrand, E. M., McCrow, J. P., Moustafa, A., Zheng, H., McQuaid, J. B., Delmont, T. O., … Allen, A. E. (2015). Phytoplankton-bacterial interactions mediate micronutrient colimitation at the coastal Antarctic sea ice edge. *Proceedings of the National Academy of Sciences*, *112*(32), 9938–9943. https://doi.org/10.1073/pnas.1501615112

Bertrand, E. M., Moran, D. M., Mcilvin, M. R., Hoffman, J. M., Allen, A. E., & Saito, M. A. (2013). Methionine synthase interreplacement in diatom cultures and communities : Implications for the persistence of B 12 use by eukaryotic phytoplankton, *58*(4), 1431–1450. https://doi.org/10.4319/lo.2013.58.4.1431

Bertrand, E. M., Saito, M. A., Rose, J. M., Riesselman, C. R., Lohan, M. C., Noble, A. E., … DiTullio, G. R. (2007). Vitamin B12 and iron colimitation of phytoplankton growth in the Ross Sea. *Limnology and Oceanography*, *52*(3), 1079–1093. https://doi.org/10.4319/lo.2007.52.3.1079

Besson, V., Neuburger, M., Rebeille, F., & Douce, R. (1995). Evidence for three serine hydroxymethyltransferases in green leaf cells. Purification and characterization of the mitochondrial and chloroplastic isoforms. *Plant Physiology and Biochemistry*, *33*(6), 665–673. Retrieved from http://agris.fao.org/agris-search/search.do?recordID=FR9600081

Besson, V., Rebeille, F., Neuburger, M., Douce, R., & Cossins, E. A. (1993). Effects of tetrahydrofolate polyglutamates on the kinetic parameters of serine hydroxymethyltransferase and glycine decarboxylase from pea leaf mitochondria. *The Biochemical Journal*, *292*(Pt 2), 425–430. https://doi.org/10.1042/bj2920425

Biebl, H., Allgaier, M., Tindall, B. J., Koblizek, M., Lünsdorf, H., Pukall, R., & Wagner-Döbler, I. (2005). Dinoroseobacter shibae gen. nov., sp. nov., a new aerobic phototrophic bacterium isolated

from dinoflagellates. *International Journal of Systematic and Evolutionary Microbiology*, *55*(3), 1089–1096. https://doi.org/10.1099/ijs.0.63511-0

Birch, C. S., Brasch, N. E., McCaddon, A., & Williams, J. H. H. (2009). A novel role for vitamin B12: Cobalamins are intracellular antioxidants in vitro. *Free Radical Biology and Medicine*, *47*(2), 184–188. https://doi.org/10.1016/j.freeradbiomed.2009.04.023

Blaby, I. K., Blaby-Haas, C. E., Pérez-Pérez, M. E., Schmollinger, S., Fitz-Gibbon, S., Lemaire, S. D., & Merchant, S. S. (2015). Genome-wide analysis on Chlamydomonas reinhardtii reveals the impact of hydrogen peroxide on protein stress responses and overlap with other stress transcriptomes. *The Plant Journal : For Cell and Molecular Biology*, *84*(5), 974–988. https://doi.org/10.1111/tpj.13053

Blackburn, N., Fenchel, T., & Mitchell, J. (1998). Microscale Nutrient Patches in Planktonic Habitats Shown by Chemotactic Bacteria. *Science*, *282*(5397), 2254–2256. https://doi.org/10.1126/science.282.5397.2254

Blackman, F. F. (1903). Optima and Limiting Factors. *Annals of Botany*, *19*(2), 281–296. https://doi.org/https://doi.org/10.1093/oxfordjournals.aob.a089000

Bligh, E., & Dyer, W. (1959). A rapid method of total lipid extraction and purification. *Can. J. Biochem. Physiol.*, *37*(8), 911–917. https://doi.org/https://doi.org/10.1139/o59-099

Bonente, G., Pippa, S., Castellano, S., Bassi, R., & Ballottari, M. (2012). Acclimation of Chlamydomonas reinhardtii to different growth irradiances. *The Journal of Biological Chemistry*, *287*(8), 5833–5847. https://doi.org/10.1074/jbc.M111.304279

Boyd, P. W., Watson, A. J., Law, C. S., Abraham, E. R., Trull, T., Murdoch, R., … Zeldis, J. (2000). A mesoscale phytoplankton bloom in the polar Southern Ocean stimulated by iron fertilization. *Nature*, *407*(6805), 695–702. https://doi.org/10.1038/35037500

Brodie, J., Ball, S. G., Bouget, F. Y., Chan, C. X., De Clerck, O., Cock, J. M., … Bhattacharya, D. (2017). Biotic interactions as drivers of algal origin and evolution. *The New Phytologist*, *216*(3), 670–681. https://doi.org/10.1111/nph.14760

Brodie, J., Chan, C. X., De Clerck, O., Cock, J. M., Coelho, S. M., Gachon, C., … Bhattacharya, D. (2017). The Algal Revolution. *Trends in Plant Science*, *22*(8), 726–738. https://doi.org/10.1016/j.tplants.2017.05.005

Browning, T. J., Achterberg, E. P., Rapp, I., Engel, A., Bertrand, E. M., Tagliabue, A., & Moore, C. M. (2017). Nutrient co-limitation at the boundary of an oceanic gyre. *Nature*, *551*(7679), 242. https://doi.org/10.1038/nature24063

Bullock, H. A., Luo, H., & Whitman, W. B. (2017). Evolution of dimethylsulfoniopropionate metabolism in marine phytoplankton and bacteria. *Frontiers in Microbiology*, *8*(APR), 637. https://doi.org/10.3389/fmicb.2017.00637

Burmølle, M., Webb, J. S., Rao, D., Hansen, L. H., Sørensen, S. J., & Kjelleberg, S. (2006). Enhanced biofilm formation and increased resistance to antimicrobial agents and bacterial invasion are caused by synergistic interactions in multispecies biofilms. *Applied and Environmental Microbiology*, *72*(6), 3916–3923. https://doi.org/10.1128/AEM.03022-05

Cadieux, N., Bradbeer, C., Reeger-Schneider, E., Köster, W., Mohanty, A. K., Wiener, M. C., & Kadner, R. J. (2002). Identification of the periplasmic cobalamin-binding protein BtuF of Escherichia coli. *Journal of Bacteriology*, *184*(3), 706–717. https://doi.org/10.1128/JB.184.3.706-717.2002

Cai, Y., Xia, M., Dong, H., Qian, Y., Zhang, T., Zhu, B., … Zhang, D. (2018). Engineering a vitamin B12

high-throughput screening system by riboswitch sensor in Sinorhizobium meliloti. *BMC Biotechnology*, *18*(1), 18–27. https://doi.org/10.1186/s12896-018-0441-2

Cakmak, T., Angun, P., Demiray, Y. E., Ozkan, A. D., Elibol, Z., & Tekinay, T. (2012). Differential effects of nitrogen and sulfur deprivation on growth and biodiesel feedstock production of Chlamydomonas reinhardtii. *Biotechnology and Bioengineering*, *109*(8), 1947–1957. https://doi.org/10.1002/bit.24474

Cakmak, T., Angun, P., Ozkan, A. D., Cakmak, Z., Olmez, T. T., & Tekinay, T. (2012). Nitrogen and sulfur deprivation differentiate lipid accumulation targets of Chlamydomonas reinhardtii. *Bioengineered*, *3*(6), 343–346. https://doi.org/10.4161/bioe.21427

Campbell, G. R. O., Taga, M. E., Mistry, K., Lloret, J., Anderson, P. J., Roth, J. R., & Walker, G. C. (2006). Sinorhizobium meliloti bluB is necessary for production of 5,6-dimethylbenzimidazole, the lower ligand of B12. *Proceedings of the National Academy of Sciences*, *103*(12), 4634–4639. https://doi.org/10.1103/PhysRevA.64.022504

Carell, E. F., & Goetz, G. H. (1976). Deoxyribonucleoside triphosphate pools in Vitamin B12 deficient Euglena gracilis. *Biochem. J*, *156*(2), 473–475. Retrieved from https://www.jacobinmag.com/2015/05/social-movements-fight-for-15-occupy-civil-rights/

Carlucci, A. F., & Silbernagel, S. B. (1969). Effect of vitamin concentrations on growth and development of vitamin-requiring algae. *Journal of Phycology*, *5*(1), 64–67. https://doi.org/10.1111/j.1529-8817.1969.tb02578.x

Carney, L. T., & Lane, T. W. (2014). Parasites in algae mass culture. *Frontiers in Microbiology*, *5*, 278. https://doi.org/10.3389/fmicb.2014.00278

Carroll, S. B. (2001). Chance and necessity: The evolution of morphological complexity and diversity. *Nature*, *409*(6823), 1102–1109. https://doi.org/10.1038/35059227

Carter, G. G., & Wilkinson, G. S. (2013). Food sharing in vampire bats: reciprocal help predicts donations more than relatedness or harassment. *Proceedings of the Royal Society B*, *280*, 1–6. https://doi.org/10.1098/rspb.2012.2573

Castillo-Lancellotti, C., Tur, J. A., & Uauy, R. (2012). Impact of folic acid fortification of flour on neural tube defects: a systematic review. *Public Health Nutrition*, *16*(5), 901–911. https://doi.org/10.1017/S1368980012003576

Ceh, J., Kilburn, M. R., Cliff, J. B., Raina, J.-B., van Keulen, M., & Bourne, D. G. (2013). Nutrient cycling in early coral life stages: *Pocillopora damicornis* larvae provide their algal symbiont (*Symbiodinium*) with nitrogen acquired from bacterial associates. *Ecology and Evolution*, *3*(8), 2393–2400. https://doi.org/10.1002/ece3.642

Chen, N. C., Yang, F., Capecci, L. M., Gu, Z., Schafer, A. I., Durante, W., … Wang, H. (2010). Regulation of homocysteine metabolism and methylation in human and mouse tissues. *FASEB Journal : Official Publication of the Federation of American Societies for Experimental Biology*, *24*(8), 2804–2817. https://doi.org/10.1096/fj.09-143651

Chiang, P. K., Gordon, R. K., Tal, J., Zeng, G. C., Doctor, B. P., Pardhasaradhi, K., & Mccann, P. P. (1996). S-Adenosylmethionine and methylation. *FASEB*, *10*, 471–480. https://doi.org/https://doi.org/10.1096/fasebj.10.4.8647346

Christensen, B. C., Kelsey, K. T., Zheng, S., Houseman, E. A., Marsit, C. J., Wrensch, M. R., … Wiencke, J. K. (2010). Breast Cancer DNA Methylation Profiles Are Associated with Tumor Size and Alcohol and Folate Intake. *PLoS Genetics*, *6*(7), e1001043. https://doi.org/10.1371/journal.pgen.1001043

Clarke, R., Halsey, J., Lewington, S., Lonn, E., Armitage, J., Manson, J. A. E., … Collins, R. (2010). Effects of lowering homocysteine levels with B vitamins on cardiovascular disease, cancer, and cause-specific mortality: Meta-analysis of 8 randomized trials involving 37 485 individuals. *Archives of Internal Medicine*, *170*(18), 1622–1631. https://doi.org/10.1001/archinternmed.2010.348

Cohen, N. R., A. Ellis, K., Burns, W. G., Lampe, R. H., Schuback, N., Johnson, Z., … Marchetti, A. (2017). Iron and vitamin interactions in marine diatom isolates and natural assemblages of the Northeast Pacific Ocean. *Limnology and Oceanography*, *62*(5), 2076–2096. https://doi.org/10.1002/lno.10552

Collakova, E., Goyer, A., Naponelli, V., Krassovskaya, I., Gregory, J. F., Hanson, A. D., … Shachar-Hill, Y. (2008). Arabidopsis 10-formyl tetrahydrofolate deformylases are essential for photorespiration. *The Plant Cell*, *20*(7), 1818–1832. https://doi.org/10.1105/tpc.108.058701

Consortium, T. H. M. P., Huttenhower, C., Gevers, D., Knight, R., Abubucker, S., Badger, J. H., … White, O. (2012). Structure, function and diversity of the healthy human microbiome. *Nature*, *486*(7402), 207–214. https://doi.org/10.1038/nature11234

Cooper, M. B., Kazamia, E., Helliwell, K. E., Kudahl, U. J., Sayer, A., Wheeler, G. L., & Smith, A. G. (2019). Cross-exchange of B-vitamins underpins a mutualistic interaction between Ostreococcus tauri and Dinoroseobacter shibae. *The ISME Journal*, *13*(2), 334–345. https://doi.org/10.1038/s41396-018-0274-y

Corbino, K. A. K., Barrick, J. E., Lim, J., Welz, R., Tucker, B. B. J., Puskarz, I., … Breaker, R. R. (2005). Evidence for a second class of S-adenosylmethionine riboswitches and other regulatory RNA motifs in alpha-proteobacteria. *Genome Biology*, *6*(8), R70. https://doi.org/10.1186/gb-2005-6-8-r70

Cordero, O. X., & Polz, M. F. (2014). Explaining microbial genomic diversity in light of evolutionary ecology. *Nature Reviews Microbiology*, *12*(4), 263–273. https://doi.org/10.1038/nrmicro3218

Cowey, C. B. (1956). A preliminary investigation of the variation of vitamin B12 in oceanic and coastal waters. *Journal of the Marine Biological Association of the United Kingdom*, *35*(3), 609–620. https://doi.org/10.1017/S0025315400010456

Croft, M. T., Lawrence, A. D., Raux-Deery, E., Warren, M. J., & Smith, A. G. (2005). Algae acquire vitamin B12 through a symbiotic relationship with bacteria. *Nature*, *438*(7064), 90–93. https://doi.org/10.1038/nature04056

Croft, M. T., Warren, M. J., & Smith, A. G. (2006). Algae need their vitamins. *Eukaryotic Cell*, *5*(8), 1175–1183. https://doi.org/10.1128/EC.00097-06

Cross, F. R., & Umen, J. G. (2015). The *Chlamydomonas* cell cycle. *The Plant Journal*, *82*(3), 370–392. https://doi.org/10.1111/tpj.12795

Cuypers, T. D., & Hogeweg, P. (2012). Virtual Genomes in Flux: An Interplay of Neutrality and Adaptability Explains Genome Expansion and Streamlining. *Genome Biology and Evolution*, *4*(3), 212–229. https://doi.org/10.1093/gbe/evr141

D'Onofrio, A., Crawford, J. M., Stewart, E. J., Witt, K., Gavrish, E., Epstein, S., … Lewis, K. (2010). Siderophores from neighboring organisms promote the growth of uncultured bacteria. *Chemistry & Biology*, *17*(3), 254–264. https://doi.org/10.1016/j.chembiol.2010.02.010

da Silva, R. P., Kelly, K. B., Al Rajabi, A., & Jacobs, R. L. (2014). Novel insights on interactions between folate and lipid metabolism. *BioFactors*, *40*(3), 277–283. https://doi.org/10.1002/biof.1154

Dagnelie, P. C., van Staveren, W. A., & van den Berg, H. (1991). Vitamin B-12 from algae appears not to be bioavailable. *The American Journal of Clinical Nutrition*, *53*(3), 695–697. https://doi.org/10.1093/ajcn/53.3.695

Daisley, K. W. (1969). Monthly Survey of Vitamin B12 Concentrations in some waters of the English Lake District. *Association for the Sciences of Limnology and Oceanography*, *14*(2), 224–228.

Daisley, K. W., & Fisher, L. R. (1958). Vertical distribution of vitamin B12in the sea. *Journal of the Marine Biological Association of the United Kingdom*, *37*(3), 683–686. https://doi.org/10.1111/j.1471-6402.1981.tb00583.x

Datko, A. H., & Mudd, S. H. (1984). Responses of Sulfur-Containing Compounds in Lemna paucicostata Hegelm. 6746 to Changes in Availability of Sulfur Sources. *Plant Physiology*, *75*(2), 474–479. Retrieved from https://www.jstor.org/stable/pdf/4268701.pdf?refreqid=excelsior%3A6716c1dd295eaa237d0b6ded21677962

Davies, J. P., Yildiz, F. H., & Grossman, A. (1996). Sac1, a putative regulator that is critical for survival of Chlamydomonas reinhardtii during sulfur deprivation. *The EMBO Journal*, *15*(9), 2150–2159. https://doi.org/https://doi.org/10.1002/j.1460-2075.1996.tb00568.x

de-Bashan, L. E., Mayali, X., Bebout, B. M., Weber, P. K., Detweiler, A. M., Hernandez, J. P., … Bashan, Y. (2016). Establishment of stable synthetic mutualism without co-evolution between microalgae and bacteria demonstrated by mutual transfer of metabolites (NanoSIMS isotopic imaging) and persistent physical association (Fluorescent in situ hybridization). *Algal Research*, *15*, 179–186. https://doi.org/10.1016/j.algal.2016.02.019

Deery, E., Schroeder, S., Lawrence, A. D., Taylor, S. L., Seyedarabi, A., Waterman, J., … Warren, M. J. (2012). An enzyme-trap approach allows isolation of intermediates in cobalamin biosynthesis. *Nature Chemical Biology*, *8*(11), 933–940. https://doi.org/10.1038/nchembio.1086

Degnan, P. H., Barry, N. A., Mok, K. C., Taga, M. E., & Goodman, A. L. (2014). Human Gut Microbes Use Multiple Transporters to Distinguish Vitamin B12 Analogs and Compete in the Gut. *Cell Host & Microbe*, *15*(1), 47–57. https://doi.org/10.1016/J.CHOM.2013.12.007

Delaye, L., Valadez-cano, C., & Pérez-zamorano, B. (2016). How really ancient is Paulinella Chromatophora? *PLoS Currents*, 1–12. https://doi.org/10.1371/currents.tol.e68a099364bb1a1e129a17b4e06b0c6b

Doebeli, M., & Knowlton, N. (1998). The evolution of interspecific mutualisms. *Proceedings of the National Academy of Sciences*, *95*(15), 8676–8680. https://doi.org/10.1073/pnas.95.15.8676

Doolittle, W. F. (2000). Evolution, Uprooting the Tree of Life. *Scientific American*, *282*(2), 90–95. https://doi.org/https://www.jstor.org/stable/26058605

Dorrell, R. G., & Smith, A. G. (2011). Do red and green make brown?: perspectives on plastid acquisitions within chromalveolates. *Eukaryotic Cell*, *10*(7), 856–868. https://doi.org/10.1128/EC.00326-10

Droop, M. R. (1974). The nutrient status of algal cells in continuous culture. *Journal of the Marine Biological Association of the United Kingdom*, *54*(4), 825–855. https://doi.org/10.1017/S002531540005760X

Droop, M. R. (2007). Vitamins, phytoplankton and bacteria: symbiosis or scavenging? *Journal of Plankton Research*, *29*(2), 107–113. https://doi.org/10.1093/plankt/fbm009

Droop, M. R., & Elson, K. G. R. (1966). Are Pelagic Diatoms Free from Bacteria? *Nature*, *211*(5053),

1096–1097. https://doi.org/10.1038/2111096a0

Drummen, G. P. ., van Liebergen, L. C. ., Op den Kamp, J. A. ., & Post, J. A. (2002). C11-BODIPY581/591, an oxidation-sensitive fluorescent lipid peroxidation probe: (micro)spectroscopic characterization and validation of methodology. *Free Radical Biology and Medicine*, *33*(4), 473–490. https://doi.org/10.1016/S0891-5849(02)00848-1

Dubini, A., Mus, F., Seibert, M., Grossman, A. R., & Posewitz, M. C. (2009). Flexibility in anaerobic metabolism as revealed in a mutant of chlamydomonas reinhardtii lacking hydrogenase activity. *Journal of Biological Chemistry*, *284*(11), 7201–7213. https://doi.org/10.1074/jbc.M803917200

Duncan, T. M., Reed, M. C., & Nijhout, H. F. (2013). The relationship between intracellular and plasma levels of folate and metabolites in the methionine cycle: a model. *Molecular Nutrition & Food Research*, *57*(4), 628–636. https://doi.org/10.1002/mnfr.201200125

Edwards, A. L., Reyes, F. E., Héroux, A., & Batey, R. T. (2010). Structural basis for recognition of S-adenosylhomocysteine by riboswitches. *RNA*, *16*(11), 2144–2155. https://doi.org/10.1261/rna.2341610

Elbaz, A., Wei, Y. Y., Meng, Q., Zheng, Q., & Yang, Z. M. (2010). Mercury-induced oxidative stress and impact on antioxidant enzymes in Chlamydomonas reinhardtii. *Ecotoxicology*, *19*(7), 1285–1293. https://doi.org/10.1007/s10646-010-0514-z

Elders, C. (1926). Treatment of pernicious anemia by a special diet. *Journal of the American Medical Association*, *87*(20), 1666. https://doi.org/10.1001/jama.1926.02680200066028

Elias, S., & Banin, E. (2012). Multi-species biofilms: living with friendly neighbors. *FEMS Microbiology Reviews*, *36*(5), 990–1004. https://doi.org/10.1111/j.1574-6976.2012.00325.x

Elledge, S. J., Zhou, Z., Allen, J. B., & Navas, T. A. (1993). DNA damage and cell cycle regulation of ribonucleotide reductase. *BioEssays*, *15*(5), 333–339. https://doi.org/10.1002/bies.950150507

Engbersen, A. M. T., Franken, D. G., Boers, G. H. J., Stevens, E. M. B., Trijbels, F. J. M., & Blom, H. J. (1995). Thermolabile 5,10-Methylenetetrahydrofolate reductase as a cause of mild hyperhomocysteinemia. *American Journal of Human Genetics*, *56*(1981), 142–150. Retrieved from https://www.ncbi.nlm.nih.gov/pmc/articles/PMC1801334/pdf/ajhg00027-0150.pdf

Eriksson, M., Moseley, J. L., Tottey, S., Del Campo, J. A., Quinn, J., Kim, Y., & Merchant, S. (2004). Genetic dissection of nutritional copper signaling in chlamydomonas distinguishes regulatory and target genes. *Genetics*, *168*(2), 795–807. https://doi.org/10.1534/genetics.104.030460

Escobar Galvis, M. L., Marttila, S., Håkansson, G., Forsberg, J., & Knorpp, C. (2001). Heat stress response in pea involves interaction of mitochondrial nucleoside diphosphate kinase with a novel 86-kilodalton protein. *Plant Physiology*, *126*(1), 69–77. https://doi.org/10.1104/pp.126.1.69

Ewald, P. W. (1987). Transmission Modes and Evolution of the Parasitism-Mutualism Continuum. *Annals of the New York Academy of Sciences*, *503*(1), 295–306. https://doi.org/10.1111/j.1749-6632.1987.tb40616.x

Falkowski, P. G., Dubinsky, Z., Muscatine, L., & McCloskey, L. (1993). Population Control in Symbiotic Corals. *BioScience*, *43*(9), 606–611. https://doi.org/10.2307/1312147

Fang, H., Kang, J., & Zhang, D. (2017). Microbial production of vitamin B12: A review and future perspectives. *Microbial Cell Factories*, *16*(1), 57–67. https://doi.org/10.1186/s12934-017-0631-y

Feix, A., Fritsche-Polanz, R., Kletzmayr, J., Vychytil, A., Hö rl, W. H., Sunder-Plassmann, G., & Fö dinger, M. (2001). Increased Prevalence of Combined MTR and MTHFR Genotypes Among Individuals With Severely Elevated Total Homocysteine Plasma Levels. *American Journal of Kidney Diseases*, *38*, 956–964. https://doi.org/10.1053/ajkd.2001.28581

Fenton, W. A., & Rosenberg, L. E. (1978). Mitochondrial metabolism of hydroxocobalamin: Synthesis of adenosylcobalamin by intact rat liver mitochondria. *Archives of Biochemistry and Biophysics*, *189*(2), 441–447. https://doi.org/10.1016/0003-9861(78)90232-1

Fernandez, E., & Galvan, A. (2007). Inorganic nitrogen assimilation in Chlamydomonas. *Journal of Experimental Botany*, *58*(9), 2279–2287. https://doi.org/10.1093/jxb/erm106

Fichera, M. E., & Roos, D. S. (1997). A plastid organelle as a drug target in apicomplexan parasites. *Nature*, 407–409. https://doi.org/10.1038/37132

Fierer, N. (2017). Embracing the unknown: disentangling the complexities of the soil microbiome. *Nature Reviews Microbiology*, *15*(10), 579–590. https://doi.org/10.1038/nrmicro.2017.87

Finkelstein, J. D. (1998). The metabolism of homocysteine: pathways and regulation. *European Journal of Pediatrics*, *157*(S2), S40–S44. https://doi.org/10.1007/PL00014300

Fiore, C. L., Jarett, J. K., Olson, N. D., & Lesser, M. P. (2010). Nitrogen fixation and nitrogen transformations in marine symbioses. *Trends in Microbiology*, *18*, 455–463. https://doi.org/10.1016/j.tim.2010.07.001

Fischer, W. W., Hemp, J., & Johnson, J. E. (2016). Evolution of Oxygenic Photosynthesis. *Annual Review of Earth and Planetary Sciences*, *44*(1), 647–683. https://doi.org/10.1146/annurev-earth-060313-054810

Forterre, P. (2015). The universal tree of life: An update. *Frontiers in Microbiology*, *6*(JUN), 717. https://doi.org/10.3389/fmicb.2015.00717

Foster, K. R., & Bell, T. (2012). Competition, Not Cooperation, Dominates Interactions among Culturable Microbial Species. *Current Biology*, *22*(19), 1845–1850. https://doi.org/10.1016/J.CUB.2012.08.005

Foster, R. A., Kuypers, M. M. M., Vagner, T., Paerl, R. W., Musat, N., & Zehr, J. P. (2011). Nitrogen fixation and transfer in open ocean diatom–cyanobacterial symbioses. *The ISME Journal*, *5*(9), 1484–1493. https://doi.org/10.1038/ismej.2011.26

Foster, R. A., & Zehr, J. P. (2006). Characterization of diatom–cyanobacteria symbioses on the basis of nifH, hetR and 16S rRNA sequences. *Environmental Microbiology*, *8*(11), 1913–1925. https://doi.org/10.1111/j.1462-2920.2006.01068.x

Franklin, D. J., Choi, C. J., Hughes, C., Malin, G., & Berges, J. A. (2009). Effect of dead phytoplankton cells on the apparent efficiency of photosystem II. *Marine Ecology Progress Series*, *382*, 35–40. https://doi.org/10.3354/meps07967

Friso, S., Girelli, D., Trabetti, E., Olivieri, O., Guarini, P., Pignatti, P. F., … Choi, S. W. (2005). The MTHFR 1298A>C polymorphism and genomic DNA methylation in human lymphocytes. *Cancer Epidemiology Biomarkers and Prevention*, *14*(4), 938–943. https://doi.org/10.1158/1055-9965.EPI-04-0601

Gärdes, A., Iversen, M. H., Grossart, H.-P., Passow, U., & Ullrich, M. S. (2011). Diatom-associated bacteria are required for aggregation of Thalassiosira weissflogii. *The ISME Journal*, *5*(3), 436–445. https://doi.org/10.1038/ismej.2010.145

Gargouri, M., Bates, P. D., Park, J.-J., Kirchhoff, H., & Gang, D. R. (2014). Functional photosystem I

maintains proper energy balance during nitrogen depletion in Chlamydomonas reinhardtii, promoting triacylglycerol accumulation. *The Plant Journal*, *77*(3), 404–417. https://doi.org/10.1111/tpj.12392

Gates, R. D., Hoegh-Guldberg, O., McFall-Ngai, M. J., Bil, K. Y., & Muscatine, L. (1995). Free amino acids exhibit anthozoan "host factor" activity: they induce the release of photosynthate from symbiotic dinoflagellates in vitro. *Proceedings of the National Academy of Sciences*, *92*(16), 7430–7434. https://doi.org/10.1073/pnas.92.16.7430

Gilbert, P. W. (1942). Observations on the Eggs of Ambystoma Maculatum with Especial Reference to the Green Algae Found Within the Egg Envelopes. *Ecology*, *23*(2), 215–227. https://doi.org/10.2307/1931088

Giordano, M., Beardall, J., & Raven, J. A. (2005). CO 2 Concentrating Mechanisms in Algae: Mechanisms, Environmental Modulation, and Evolution. *Annu. Rev. Plant Biol*, *56*, 99–131. https://doi.org/10.1146/

Glaesener, A. G., Merchant, S. S., & Blaby-Haas, C. E. (2013). Iron economy in Chlamydomonas reinhardtii. *Frontiers in Plant Science*, *4*, 1–12. https://doi.org/10.3389/fpls.2013.00337

Gomes, A., Fernandes, E., & Lima, J. L. F. C. (2005). Fluorescence probes used for detection of reactive oxygen species. *Journal of Biochemical and Biophysical Methods*, *65*(2–3), 45–80. https://doi.org/10.1016/J.JBBM.2005.10.003

González-Ballester, D., Casero, D., Cokus, S., Pellegrini, M., Merchant, S. S., & Grossman, A. R. (2010). RNA-Seq Analysis of Sulfur-Deprived *Chlamydomonas* Cells Reveals Aspects of Acclimation Critical for Cell Survival. *The Plant Cell*, *22*(6), 2058–2084. https://doi.org/10.1105/tpc.109.071167

Gonzalez-Ballester, D., Pollock, S. V, Pootakham, W., & Grossman, A. R. (2008). The central role of a SNRK2 kinase in sulfur deprivation responses. *Plant Physiology*, *147*(1), 216–227. https://doi.org/10.1104/pp.108.116137

Gonzalez, J. C., Banerjee, R. V, Huang, S., Sumner, J. S., & Matthews, R. G. (1992). Comparison of Cobalamin-Independent and Cobalamin-Dependent Methionine Synthases from Escherichia coli. *Biochemistry*, (31), 6045–6056.

Graham, E. R., McKie-Krisberg, Z. M., & Sanders, R. W. (2014). Photosynthetic carbon from algal symbionts peaks during the latter stages of embryonic development in the salamander Ambystoma maculatum. *BMC Research Notes*, *7*(1), 764. https://doi.org/10.1186/1756-0500-7-764

Grant, M., Kazamia, E., Cicuta, P., & Smith, A. G. (2014). Direct exchange of vitamin B12 is demonstrated by modelling the growth dynamics of algal-bacterial cocultures. *The ISME Journal*, *8*(7), 1418–1427. https://doi.org/10.1038/ismej.2014.9

Griffiths, M. J., & Harrison, S. T. L. (2009). Lipid productivity as a key characteristic for choosing algal species for biodiesel production. *Journal of Applied Phycology*, *21*, 493–507. https://doi.org/10.1007/s10811-008-9392-7

Grossman, A. (2000). Acclimation of Chamydomonas reinhardtii to its Nutrient environment. *Protist*, *151*(3), 201–224. Retrieved from https://ac.els-cdn.com/S1434461004700206/1-s2.0-S1434461004700206-main.pdf?_tid=ba9aac7c-26a6-4c4b-a290-f0179ab4cb65&acdnat=1526920017_5ed235567a5bd3d0ed9483ec6a8ba2b1

Groth, M., Moissiard, G., Wirtz, M., Wang, H., Garcia-Salinas, C., Ramos-Parra, P. A., … Jacobsen, S. E. (2016). MTHFD1 controls DNA methylation in Arabidopsis. *Nature Communications*, *7*, 11640.

https://doi.org/10.1038/ncomms11640

Guranowski, A., & Pawelkiewicz, J. (1977). Adenosylhomocysteinase from Yellow Lupin Seeds. Purification and Properties. *European Journal of Biochemistry*, *80*(2), 517–523. https://doi.org/10.1111/j.1432-1033.1977.tb11907.x

Haba, G. D. la, & Cantoni, G. L. (1958). The Enzymatic Synthesis of S-adenosyl-L-homocysteine from Adenosine and Homocysteine. *J. Biol. Chem.*, *234*(3), 603–608. Retrieved from http://www.jbc.org/

Hadariová, L., Vesteg, M., Birčák, E., Schwartzbach, S. D., & Krajčovič, J. (2017). An intact plastid genome is essential for the survival of colorless Euglena longa but not Euglena gracilis. *Current Genetics*, *63*(2), 331–341. https://doi.org/10.1007/s00294-016-0641-z

Haines, K. C., & Guillard, R. R. L. (1974). Growth of vitamin B12-requiring marine diatoms in mixed laboratory cultures with vitamin B12 producing marine bacteria. *Journal of Phycology*, *10*(3), 245–252. https://doi.org/10.1111/j.1529-8817.1974.tb02709.x

Hall, A. H., Dart, R., & Bogdan, G. (2007). Sodium Thiosulfate or Hydroxocobalamin for the Empiric Treatment of Cyanide Poisoning? *Ann Emerg Med*, *49*, 806–813. https://doi.org/10.1016/j.annemergmed.2006.09.021

Hamilton, W. D. (1980). Sex versus Non-Sex versus Parasite. *Oikos*, *35*(2), 282. https://doi.org/10.2307/3544435

Hamilton, W. D., Axelrod, R., & Tanese, R. (1989). Sexual reproduction as an adaptation to resist parasites. *Proceedings of the National Academy of Sciences*, *87*(5), 3566–3573. https://doi.org/10.4014/jmb.1601.01032

Hansen, S. K., Rainey, P. B., Haagensen, J. A. J., & Molin, S. (2007). Evolution of species interactions in a biofilm community. *Nature*, *445*(7127), 533–536. https://doi.org/10.1038/nature05514

Hanson, A. D., & Jesse, F. G. (2011). Folate Biosynthesis, Turnover, and Transport in Plants. *Annual Review of Plant Biology*, *62*, 105–125. https://doi.org/10.1146/annurev-arplant-042110-103819

Hanson, A. D., & Roje, S. (2001). one-carbon metabolism in higher plants. *Annual Review of Plant Physiology and Plant Molecular Biology*, *52*, 119–137. https://doi.org/10.1146/annurev.arplant.52.1.119

Harcombe, W. (2010). Novel cooperation experimentally evolved between species. *Evolution*, *64*(7), 2166–2172. https://doi.org/10.1111/j.1558-5646.2010.00959.x

Hardin, G. (1960). The Competitive Exclusion Principle. *Science*, *131*(3409), 1292–1297. https://doi.org/10.1126/science.130.3374.477

Haurani, F. I. (1973). Vitamin B12 and the megaloblastic development. *Science*, *182*(4107), 78–79. https://doi.org/10.1126/science.182.4107.78

Heal, K. R., Qin, W., Ribalet, F., Bertagnolli, A. D., Coyote-Maestas, W., Hmelo, L. R., … Ingalls, A. E. (2017). Two distinct pools of B 12 analogs reveal community interdependencies in the ocean. *Proceedings of the National Academy of Sciences*, *114*(2), 364–369. https://doi.org/10.1073/pnas.1608462114

Hecky, R. E., & Kilham, P. (1988). Nutrient limitation of phytoplankton in freshwater and marine environments: A review of recent evidence on the effects of enrichment. *Limnology and Oceanography*, *33*(4part2), 796–822. https://doi.org/10.4319/lo.1988.33.4part2.0796

Hehenberger, E., Burki, F., Kolisko, M., & Keeling, P. J. (2016). Functional Relationship between a

Dinoflagellate Host and Its Diatom Endosymbiont. *Molecular Biology and Evolution*, *33*(9), 2376–2390. https://doi.org/10.1093/molbev/msw109

Heldt, D., Lawrence, A. D., Lindenmeyer, M., Deery, E., Heathcote, P., Rigby, S. E., & Warren, M. J. (2005). Aerobic synthesis of vitamin B12: ring contraction and cobalt chelation. *Biochemical Society Transactions*, *33*(Pt 4), 815–819. https://doi.org/10.1042/BST0330815

Helliwell, K. E. (2017). The roles of B vitamins in phytoplankton nutrition: new perspectives and prospects. *New Phytologist*, *216*(1), 62–68. https://doi.org/10.1111/nph.14669

Helliwell, K. E., Collins, S., Kazamia, E., Purton, S., Wheeler, G. L., & Smith, A. G. (2015). Fundamental shift in vitamin B12 eco-physiology of a model alga demonstrated by experimental evolution. *The ISME Journal*, *12*, 1–10. https://doi.org/10.1038/ismej.2014.230

Helliwell, K. E., Lawrence, A. D., Holzer, A., Scanlan, D. J., Warren, M. J., & Smith, A. G. (2016). Cyanobacteria and Eukaryotic Algae Use Different Chemical Variants of Vitamin B 12. *Current Biology*, *26*, 1–10. https://doi.org/10.1016/j.cub.2016.02.041

Helliwell, K. E., Pandhal, J., Cooper, M. B., Longworth, J., Kudahl, U. J., Russo, D. A., … Smith, A. G. (2018). Quantitative proteomics of a B12-dependent alga grown in coculture with bacteria reveals metabolic tradeoffs required for mutualism. *New Phytologist*, *217*(2), 599–612. https://doi.org/10.1111/nph.14832

Helliwell, K. E., Scaife, M. a., Sasso, S., Araujo, a. P. U., Purton, S., & Smith, a. G. (2014). Unraveling Vitamin B12-Responsive Gene Regulation in Algae. *Plant Physiology*, *165*(1), 388–397. https://doi.org/10.1104/pp.113.234369

Helliwell, K. E., Wheeler, G. L., Leptos, K. C., Goldstein, R. E., & Smith, A. G. (2011). Insights into the evolution of vitamin B12 auxotrophy from sequenced algal genomes. *Molecular Biology and Evolution*, *28*(10), 2921–2933. https://doi.org/10.1093/molbev/msr124

Hernandez, J. P., De-Bashan, L. E., Rodriguez, D. J., Rodriguez, Y., & Bashan, Y. (2009). Growth promotion of the freshwater microalga Chlorella vulgaris by the nitrogen-fixing, plant growth-promoting bacterium Bacillus pumilus from arid zone soils. *European Journal of Soil Biology*, *45*(1), 88–93. https://doi.org/10.1016/j.ejsobi.2008.08.004

Herron, M. D., Hackett, J. D., Aylward, F. O., & Michod, R. E. (2009). Triassic origin and early radiation of multicellular volvocine algae. *Proceedings of the National Academy of Sciences*, *106*(9), 3254–3258. https://doi.org/10.1073/pnas.0811205106

Herron, M. D., & Michod, R. E. (2008). Evolution of complexity in the volvocine algae: Transitions in individuality through Darwin's eye. *Evolution*, *62*(2), 436–451. https://doi.org/10.1111/j.1558-5646.2007.00304.x

Hibbing, M. E., Fuqua, C., Parsek, M. R., & Peterson, S. B. (2010). Bacterial competition: surviving and thriving in the microbial jungle. *Nature Reviews. Microbiology*, *8*(1), 15–25. https://doi.org/10.1038/nrmicro2259

Hill, K. L., Hassett, R., Kosman, D., & Merchant, S. (1996). Regulated copper uptake in Chlamydomonas reinhardtii in response to copper availability. *Plant Physiology*, *112*(2), 697–704. https://doi.org/10.1104/pp.112.2.697

Hillesland, K. L., & Stahl, D. A. (2010). Rapid evolution of stability and productivity at the origin of a microbial mutualism. *Proceedings of the National Academy of Sciences*, *107*(5), 2124–2129. https://doi.org/10.1073/pnas.0908456107

Ho, T. Y., Quigg, A., Finkel, Z. V., Milligan, A. J., Wyman, K., Falkowski, P. G., & Morel, F. M. M. (2003).

The elemental composition of some marine phytoplankton. *Journal of Phycology*, *39*(6), 1145–1159. https://doi.org/10.1111/j.0022-3646.2003.03-090.x

Hodgkin, D. C., Kamper, J., Mackay, M., Pickworth, J., Trueblood, K. N., & White, J. G. (1956). Structure of Vitamin B12. *Nature*, *178*(4524), 64–66. https://doi.org/10.1038/178064a0

Hoeksema, J. D., & Schwartz, M. W. (2003). Expanding comparative-advantage biological market models: Contingency of mutualism on partners' resource requirements and acquisition trade-offs. *Proceedings of the Royal Society B: Biological Sciences*, *270*(1518), 913–919. https://doi.org/10.1098/rspb.2002.2312

Hoffbrand, A. V., & Jackson, B. F. A. (1993). Correction of the DNA synthesis defect in vitamin B12 deficiency by tetrahydrofolate: evidence in favour of the methyl-folate trap hypothesis as the cause of megaloblastic anaemia in vitamin B_{12} deficiency. *British Journal of Haematology*, *83*(4), 643–647. https://doi.org/10.1111/j.1365-2141.1993.tb04704.x

Hoffman, D. R., Marion, D. W., Cornatzer, W. E., & Duerre, J. A. (1980). S-Adenosylmethionine and S-Adenosylhomocysteine Metabolism in Isolated Rat Liver. *The Journal of Biological Chemistry*, *255*(22), 10822–10827. Retrieved from http://www.jbc.org/content/255/22/10822.full.pdf

Hoglund, S., Dehshiri, K., Reizenstein -, P., Boddy, K., Will, G., Holmes -, B. M., … E Matthews, C. M. (1966). *Vitamin B 12 Kinetics in Man. Physics in Medicine & Biology* (Vol. 11). Retrieved from http://iopscience.iop.org/article/10.1088/0031-9155/11/2/309/pdf

Holm-Hansen, O. (1985). Nutrient Cycles in Antarctic Marine Ecosystems. In *Antarctic Nutrient Cycles and Food Webs* (pp. 6–10). Berlin, Heidelberg: Springer Berlin Heidelberg. https://doi.org/10.1007/978-3-642-82275-9_2

Hom, E. F. Y., & Murray, A. W. (2014). Niche engineering demonstrates latent capacity for fungal-algal mutualism. *Science*, *345*(6192), 94–98. https://doi.org/10.1126/science.1251487

Hondorp, E. R., & Matthews, R. G. (2004). Oxidative stress inactivates cobalamin-independent methionine synthase (MetE) in Escherichia coli. *PLoS Biology*, *2*(11), e336. https://doi.org/10.1371/journal.pbio.0020336

Hong, E. J., & Wilson, R. I. (2013). Olfactory neuroscience: Normalization is the norm. *Current Biology*, *23*(24), R1093–R1096. https://doi.org/10.1016/j.cub.2013.10.056

Horst, I., Parker, B. M., Dennis, J. S., Howe, C. J., Scott, S. A., & Smith, A. G. (2012). Treatment of Phaeodactylum tricornutum cells with papain facilitates lipid extraction. *Journal of Biotechnology*, *162*, 40–49. https://doi.org/10.1016/j.jbiotec.2012.06.033

Howarth, R. W. (1988). Nutrient Limitation of Net Primary Production in Marine Ecosystems. *Annual Review of Ecology and Systematics*, *19*(1), 89–110. https://doi.org/10.1146/annurev.es.19.110188.000513

Humby, P. L., Snyder, E. C. R., & Durnford, D. G. (2013). Conditional senescence in *Chlamydomonas reinhardtii* (Chlorophyceae). *Journal of Phycology*, *49*(2), 389–400. https://doi.org/10.1111/jpy.12049

Hünken, M., Harder, J., & Kirst, G. O. (2008). Epiphytic bacteria on the Antarctic ice diatom Amphiprora kufferathii Manguin cleave hydrogen peroxide produced during algal photosynthesis. *Plant Biology*, *10*(4), 519–526. https://doi.org/10.1111/j.1438-8677.2008.00040.x

Hutchinson, G. E. (1961). The Paradox of the Plankton. *The American Naturalist*, *95*(882), 137–145. Retrieved from

https://www.jstor.org/stable/pdf/2458386.pdf?refreqid=excelsior%3A5751416b5982b0e7eef367ffe67d0d09

Imanian, B., & Keeling, P. J. (2007). The dinoflagellates Durinskia baltica and Kryptoperidinium foliaceum retain functionally overlapping mitochondria from two evolutionarily distinct lineages. *BMC Evolutionary Biology*, *7*(1), 172. https://doi.org/10.1186/1471-2148-7-172

Inskeep, W. P., & Bloom, P. R. (1985). Extinction Coefficients of Chlorophyll a and b in N,N-Dimethylformamide and 80% Acetone. *Plant Physiology*, *77*(2), 483–485. https://doi.org/10.1104/pp.77.2.483

Institute of Medicine (US) Standing Committee on the Scientific Evaluation of Dietary Reference Intakes and its Panel on Folate, O. B. V. and C. (1998). Vitamin B12. Retrieved from https://www.ncbi.nlm.nih.gov/books/NBK114302/#ch9.s64

Jacobs, J., Pudollek, S., Hemschemeier, A., & Happe, T. (2009). A novel, anaerobically induced ferredoxin in *Chlamydomonas reinhardtii*. *FEBS Letters*, *583*(2), 325–329. https://doi.org/10.1016/j.febslet.2008.12.018

Jacobsen, D. W. (1998). Homocysteine and vitamins in cardiovascular disease. *Clinical Chemistry*, *44*(8(B)), 1833–1843. Retrieved from http://clinchem.aaccjnls.org/content/clinchem/44/8/1833.full.pdf

Jaenike, & J. (1978). A hypothesis to account for the maintenance of sex within populations. *Evol. Theory*, *3*, 191–194. Retrieved from https://ci.nii.ac.jp/naid/10003762411/

James, S. J., Melnyk, S., Pogribna, M., Pogribny, I. P., & Caudill, M. A. (2002). Elevation in S-Adenosylhomocysteine and DNA Hypomethylation: Potential Epigenetic Mechanism for Homocysteine-Related Pathology. *The Journal of Nutrition*, *132*(8), 2361S–2366S. https://doi.org/10.1093/jn/132.8.2361S

Janouskovec, J., Horák, A., Oborník, M., Lukes, J., & Keeling, P. J. (2010). A common red algal origin of the apicomplexan, dinoflagellate, and heterokont plastids. *Proceedings of the National Academy of Sciences*, *107*(24), 10949–10954. https://doi.org/10.1073/pnas.1003335107

Janson, Wouters, Bergman, & Carpenter. (1999). Host specificity in the Richelia-diatom symbiosis revealed by hetR gene sequence analysis. *Environmental Microbiology*, *1*(5), 431–438. https://doi.org/10.1046/j.1462-2920.1999.00053.x

Johnson, L. M., Cao, X., & Jacobsen, S. E. (2002). Interplay Between Two Epigenetic Marks: DNA methylationan and Histone H3 Lysine 9 Methylation. *Current Biology*, *12*(16), 1360–1367. https://doi.org/10.1016/S0960-9822(02)00976-4

Jones, P. A. (2012). Functions of DNA methylation: islands, start sites, gene bodies and beyond. *Nature Reviews Genetics*, *13*(7), 484–492. https://doi.org/10.1038/nrg3230

Joubert, J. J., & Rijkenberg, F. H. J. (1971). Parasitic Green Algae. *Annual Review of Phytopathology*, *9*(1), 45–64. https://doi.org/10.1146/annurev.py.09.090171.000401

Juergens, M. T., Deshpande, R. R., Lucker, B. F., Park, J.-J., Wang, H., Gargouri, M., … Shachar-Hill, Y. (2015). The regulation of photosynthetic structure and function during nitrogen deprivation in Chlamydomonas reinhardtii. *Plant Physiology*, *167*(2), 558–573. https://doi.org/10.1104/pp.114.250530

Juergens, M. T., Disbrow, B., & Shachar-Hill, Y. (2016). The Relationship of Triacylglycerol and Starch Accumulation to Carbon and Energy Flows during Nutrient Deprivation in Chlamydomonas reinhardtii. *Plant Physiology*, *171*(4), 2445–2457. https://doi.org/10.1104/pp.16.00761

Juzeniene, A., & Nizauskaite, Z. (2013). Photodegradation of cobalamins in aqueous solutions and in human blood. *Journal of Photochemistry & Photobiology, B: Biology*, *122*, 7–14. https://doi.org/10.1016/j.jphotobiol.2013.03.001

Kaczmarska, I., Ehrman, J. M., Bates, S. S., Green, D. H., Léger, C., & Harris, J. (2005). Diversity and distribution of epibiotic bacteria on Pseudo-nitzschia multiseries (Bacillariophyceae) in culture, and comparison with those on diatoms in native seawater. *Harmful Algae*, *4*, 725–741. https://doi.org/10.1016/j.hal.2004.10.001

Kalyanaraman, B., Darley-Usmar, V., Davies, K. J. A., Dennery, P. A., Forman, H. J., Grisham, M. B., … Ischiropoulos, H. (2012). Measuring reactive oxygen and nitrogen species with fluorescent probes: challenges and limitations. *Free Radical Biology & Medicine*, *52*(1), 1–6. https://doi.org/10.1016/j.freeradbiomed.2011.09.030

Kamalanathan, M., Pierangelini, M., Shearman, L. A., Gleadow, R., & Beardall, J. (2016). Impacts of nitrogen and phosphorus starvation on the physiology of Chlamydomonas reinhardtii. *Journal of Applied Phycology*, *28*(3), 1509–1520. https://doi.org/10.1007/s10811-015-0726-y

Katju, V., & Bergthorsson, U. (2013). Copy-number changes in evolution: rates, fitness effects and adaptive significance. *Frontiers in Genetics*, *4*, 273. https://doi.org/10.3389/fgene.2013.00273

Kawecki, T. J., Lenski, R. E., Ebert, D., Hollis, B., Olivieri, I., & Whitlock, M. C. (2012). Experimental evolution. *Trends in Ecology & Evolution*, *27*(10), 547–560. https://doi.org/10.1016/j.tree.2012.06.001

Kazamia, E., Czesnick, H., Nguyen, T. T. Van, Croft, M. T., Sherwood, E., Sasso, S., … Smith, A. G. (2012). Mutualistic interactions between vitamin B12 -dependent algae and heterotrophic bacteria exhibit regulation. *Environmental Microbiology*, *14*(6), 1466–1476. https://doi.org/10.1111/j.1462-2920.2012.02733.x

Kazamia, E., Helliwell, K. E., Purton, S., & Smith, A. G. (2016). How mutualisms arise in phytoplankton communities: building eco-evolutionary principles for aquatic microbes. *Ecology Letters*, *19*(7), 810–822. https://doi.org/10.1111/ele.12615

Keck, B., Munder, M., & Renz, P. (1998). *Biosynthesis of cobalamin in Salmonella typhimurium: transformation of riboflavin into the 5,6-dimethylbenzimidazole moiety*. Retrieved from https://link.springer.com/content/pdf/10.1007%2Fs002030050679.pdf

Kennedy, D., Cannavan, A., Molloy, A., Taylor, S. M., & D W J Blanchflower, A. N. (1990). Methylmalonyl-CoA mutase (EC 5.4.99.2) and methionine synthetase (EC 2.1.1.13) in the tissues of cobalt-vitamin B12 deficient sheep. *British Journal of Nutrition*, *64*, 721–732. https://doi.org/10.1079/BJN19900074

Kerney, R., Kim, E., Hangarter, R. P., Heiss, A. A., Bishop, C. D., & Hall, B. K. (2011). Intracellular invasion of green algae in a salamander host. *Proceedings of the National Academy of Sciences*, *108*(16), 6497–6502. https://doi.org/10.1073/pnas.1018259108

Khona, D. K., Shirolikar, S. M., Gawde, K. K., Hom, E., Deodhar, M. A., & D'Souza, J. S. (2016). Characterization of salt stress-induced palmelloids in the green alga, Chlamydomonas reinhardtii. *Algal Research*, *16*, 434–448. https://doi.org/10.1016/j.algal.2016.03.035

Kim, B.-H., Ramanan, R., Cho, D.-H., Oh, H.-M., & Kim, H.-S. (2014). Role of Rhizobium, a plant growth promoting bacterium, in enhancing algal biomass through mutualistic interaction. *Biomass and Bioenergy*, *69*, 95–105. https://doi.org/10.1016/j.biombioe.2014.07.015

Kim, P. B., Nelson, J. W., & Breaker, R. R. (2015). An Ancient Riboswitch Class in Bacteria Regulates Purine Biosynthesis and One-Carbon Metabolism. *Molecular Cell*, *57*(2), 317–328.

https://doi.org/10.1016/j.molcel.2015.01.001

Kirk, D. L. (1999). Evolution of multicellularity in the volvocine algae. *Current Opinion in Plant Biology*, *2*(6), 496–501. Retrieved from http://www.ncbi.nlm.nih.gov/pubmed/10607653

Kisliuk, R. ., & Woods, D. . (1960). Interrelationships between Folic Acid and Cobalamin in the Synthesis of Methionine by Extracts of Escherichia coli. *Biochem. J*, *75*, 467. Retrieved from https://www.ncbi.nlm.nih.gov/pmc/articles/PMC1204495/pdf/biochemj01012-0054.pdf

Klausmeier, C. A., Litchman, E., Daufresne, T., & Levin, S. A. (2004). Optimal nitrogen-to-phosphorus stoichiometry of phytoplankton. *Nature*, *429*(6988), 171–174. https://doi.org/10.1038/nature02454

Kobayashi, Y., Harada, N., Nishimura, Y., Saito, T., Nakamura, M., Fujiwara, T., … Misumi, O. (2014). Algae Sense Exact Temperatures: Small Heat Shock Proteins Are Expressed at the Survival Threshold Temperature in Cyanidioschyzon merolae and Chlamydomonas reinhardtii. *Genome Biology and Evolution*, *6*(10), 2731–2740. https://doi.org/10.1093/gbe/evu216

Kok, D. E. G., Dhonukshe-Rutten, R. A. M., Lute, C., Heil, S. G., Uitterlinden, A. G., van der Velde, N., … Steegenga, W. T. (2015). The effects of long-term daily folic acid and vitamin B12 supplementation on genome-wide DNA methylation in elderly subjects. *Clinical Epigenetics*, *7*, 121. https://doi.org/10.1186/s13148-015-0154-5

Kolberg, M., Strand, K. R., Graff, P., & Andersson, K. K. (2004). Structure, function, and mechanism of ribonucleotide reductases. *Biochimica et Biophysica Acta*, *1699*(1–2), 1–34. https://doi.org/10.1016/S1570-9639(04)00054-8

Krishnan, A., Kumaraswamy, G. K., Vinyard, D. J., Gu, H., Ananyev, G., Posewitz, M. C., & Dismukes, G. C. (2015). Metabolic and photosynthetic consequences of blocking starch biosynthesis in the green alga *Chlamydomonas reinhardtii sta6* mutant. *The Plant Journal*, *81*(6), 947–960. https://doi.org/10.1111/tpj.12783

Kropat, J., Hong-Hermesdorf, A., Casero, D., Ent, P., Castruita, M., Pellegrini, M., … Malasarn, D. (2011). A revised mineral nutrient supplement increases biomass and growth rate in Chlamydomonas reinhardtii. *Plant J*, *66*(5), 770–780. https://doi.org/10.1111/j.1365-313X.2011.04537.x

Kropat, J., Tottey, S., Birkenbihl, R. P., Depege, N., Huijser, P., & Merchant, S. (2005). A regulator of nutritional copper signaling in Chlamydomonas is an SBP domain protein that recognizes the GTAC core of copper response element. *Proceedings of the National Academy of Sciences*, *102*(51), 18730–18735. https://doi.org/10.1073/pnas.0507693102

Kulk, G., Van De Poll, W. H., Visser, R. J. W., & Buma, A. G. J. (2013). Low nutrient availability reduces high-irradiance-induced viability loss in oceanic phytoplankton. *Limnology and Oceanography*, *58*(5), 1747–1760. https://doi.org/10.4319/lo.2013.58.5.1747

Kumar, K., Mella-Herrera, R. A., & Golden, J. W. (2010). Cyanobacterial heterocysts. *Cold Spring Harbor Perspectives in Biology*, *2*(4), a000315. https://doi.org/10.1101/cshperspect.a000315

Larsson, K. M., Logan, D. T., & Nordlund, P. (2010). Structural basis for adenosylcobalamin activation in adocbl-dependent ribonucleotide reductases. *ACS Chemical Biology*, *5*(10), 933–942. https://doi.org/10.1021/cb1000845

Lawrence, D., Fiegna, F., Behrends, V., Bundy, J. G., Phillimore, A. B., Bell, T., & Barraclough, T. G. (2012). Species interactions alter evolutionary responses to a novel environment. *PLoS Biology*, *10*(5), e1001330. https://doi.org/10.1371/journal.pbio.1001330

Lee, S. Y. (1996). High cell-density culture of Escherichia coli. *Trends in Biotechnology*, *14*(3), 98–105. https://doi.org/10.1016/0167-7799(96)80930-9

Lema, K. A., Willis, B. L., & Bourne, D. G. (2012). Corals form characteristic associations with symbiotic nitrogen-fixing bacteria. *Applied and Environmental Microbiology*, *78*(9), 3136–3144. https://doi.org/10.1128/AEM.07800-11

Letcher, P. M., Lopez, S., Schmieder, R., Lee, P. A., Behnke, C., Powell, M. J., & McBride, R. C. (2013). Characterization of Amoeboaphelidium protococcarum, an Algal Parasite New to the Cryptomycota Isolated from an Outdoor Algal Pond Used for the Production of Biofuel. *PLoS ONE*, *8*(2), e56232. https://doi.org/10.1371/journal.pone.0056232

Leung, K.-Y., Pai, Y. J., Chen, Q., Santos, C., Calvani, E., Sudiwala, S., … Greene, N. D. E. (2017). Partitioning of One-Carbon Units in Folate and Methionine Metabolism Is Essential for Neural Tube Closure. *Cell Reports*, *21*(7), 1795–1808. https://doi.org/10.1016/j.celrep.2017.10.072

Li, X., Moellering, E. R., Liu, B., Johnny, C., Fedewa, M., Sears, B. B., … Benning, C. (2012). A Galactoglycerolipid Lipase Is Required for Triacylglycerol Accumulation and Survival Following Nitrogen Deprivation in Chlamydomonas reinhardtii. *Plant Cell*, *24*(11), 4670–4686. https://doi.org/10.1105/tpc.112.105106

Lieber, C. S., & Packer, L. (2002). S-Adenosylmethionine: molecular, biological, and clinical aspects—an introduction. *The American Journal of Clinical Nutrition*, *76*(5), 1148S–1150S. https://doi.org/10.1093/ajcn/76.5.1148S

Lievers, K. J. A., Kluijtmans, L. A. J., Van Der Put, · N M J, Trijbels, F. J. M., Blom, · H J, Boers, G. H. J., … Blom, J. (2001). A second common variant in the methylenetetrahydrofolate reductase (MTHFR) gene and its relationship to MTHFR enzyme activity, homocysteine, and cardiovascular disease risk. *J Mol Med*, *79*, 522–528. https://doi.org/10.1007/s001090100253

Lively, C. M., Craddock, C., & Vrijenhoek, R. C. (1990). Red Queen hypothesis supported by parasitism in sexual and clonal fish. *Nature*, *344*(6269), 864–866. https://doi.org/10.1038/344864a0

Loizeau, K., De Brouwer, V., Gambonnet, B., Yu, A., Renou, J.-P., Van Der Straeten, D., … Ravanel, S. (2008). A genome-wide and metabolic analysis determined the adaptive response of Arabidopsis cells to folate depletion induced by methotrexate. *Plant Physiology*, *148*(4), 2083–2095. https://doi.org/10.1104/pp.108.130336

Loizeau, K., Gambonnet, B., Zhang, G.-F., Curien, G., Jabrin, S., Van Der Straeten, D., … Ravanel, S. (2007). Regulation of one-carbon metabolism in Arabidopsis: the N-terminal regulatory domain of cystathionine gamma-synthase is cleaved in response to folate starvation. *Plant Physiology*, *145*(2), 491–503. https://doi.org/10.1104/pp.107.105379

Long, J. C., & Merchant, S. S. (2008). Photo-oxidative Stress Impacts the Expression of Genes Encoding Iron Metabolism Components in Chlamydomonas †. *Photochemistry and Photobiology*, *84*(6), 1395–1403. https://doi.org/10.1111/j.1751-1097.2008.00451.x

Long, S. R. (1989). Rhizobium-legume nodulation: Life together in the underground. *Cell*, *56*(2), 203–214. https://doi.org/10.1016/0092-8674(89)90893-3

Lopez, D., Hamaji, T., Kropat, J., De Hoff, P., Morselli, M., Rubbi, L., … Pellegrini, M. (2015). Dynamic Changes in the Transcriptome and Methylome of Chlamydomonas reinhardtii throughout Its Life Cycle. *Plant Physiology*, *169*(4), 2730–2743. https://doi.org/10.1104/pp.15.00861

Lucock, M. (2004). Is folic acid the ultimate functional food component for disease prevention? *BMJ (Clinical Research Ed.)*, *328*(7433), 211–214. https://doi.org/10.1136/bmj.328.7433.211

Lutz, S., Anesio, A. M., Raiswell, R., Edwards, A., Newton, R. J., Gill, F., & Benning, L. G. (2016). The biogeography of red snow microbiomes and their role in melting arctic glaciers. *Nature Communications*, *7*, 11968. https://doi.org/10.1038/ncomms11968

Malanovic, N., Streith, I., Wolinski, H., Rechberger, G., Kohlwein, S. D., & Tehlivets, O. (2008). S-adenosyl-L-homocysteine hydrolase, key enzyme of methylation metabolism, regulates phosphatidylcholine synthesis and triacylglycerol homeostasis in yeast: Implications for homocysteine as a risk factor of atherosclerosis. *Journal of Biological Chemistry*, *283*(35), 23989–23999. https://doi.org/10.1074/jbc.M800830200

Maranger, R., Bird, D. F., & Price, N. M. (1998). Iron acquisition by photosynthetic marine phytoplankton from ingested bacteria. *Nature*, *396*(6708), 248–251. https://doi.org/10.1038/24352

Marian Cramer, B., & Myers, J. (1952). *Growth and Photosynthetic Characteristics of Euglena gracilis*. *Archiv fur Mikrobiologie* (Vol. 17). Retrieved from https://link.springer.com/content/pdf/10.1007/BF00410835.pdf

Marin, B., & Birger. (2014). Reduction to essentials: Ostreococcus, the smallest free-living eukaryote. *Perspectives in Phycology*, *1*(1), 7–10. https://doi.org/10.1127/2198-011X/2014/0011

Maroti, G., & Kondorosi, E. (2014). Nitrogen-fixing Rhizobium-legume symbiosis: are polyploidy and host peptide-governed symbiont differentiation general principles of endosymbiosis? *Frontiers in Microbiology*, *5*, 326. https://doi.org/10.3389/fmicb.2014.00326

Marsh, E. N., & Marsh, G. (1999). Coenzyme B12 (cobalamin)-dependent enzymes. *Essays in Biochemistry*, *34*, 139–154. https://doi.org/10.1042/BSE0340139

Martin, J. H., & Fitzwater, S. E. (1988). Iron deficiency limits phytoplankton growth in the north-east Pacific subarctic. *Nature*, *331*(6154), 341–343. https://doi.org/10.1038/331341a0

Martin, J. H., Fitzwater, S. E., & Gordon, R. M. (1990). Iron deficiency limits phytoplankton growth in Antarctic waters. *Global Biogeochemical Cycles*, *4*(1), 5–12. https://doi.org/10.1029/GB004i001p00005

Martin, N. C., & Goodenough, U. W. (1975). Gametic differentiation in Chlamydomonas reinhardtii. I. Production of gametes and their fine structure. *The Journal of Cell Biology*, *67*(3), 587–605. https://doi.org/10.1083/JCB.67.3.587

Martin, W., Stoebe, B., Goremykin, V., Hansmann, S., Hasegawa, M., & Kowallik, K. V. (1998). Gene transfer to the nucleus and the evolution of chloroplasts. *Nature*, *393*(6681), 162–165. https://doi.org/10.1038/30234

Mayali, X., Franks, P. J. S., & Burton, R. S. (2011). Temporal attachment dynamics by distinct bacterial taxa during a dinoflagellate bloom. *Aquatic Microbial Ecology*, *63*(2), 111–122. https://doi.org/10.3354/ame01483

McFadden, G. I. (2001). Primary and secondary endosymbiosis and the origin of plastids. *Journal of Phycology*, *37*(6), 951–959. https://doi.org/10.1046/j.1529-8817.2001.01126.x

McKay, J. A., Groom, A., Potter, C., Coneyworth, L. J., Ford, D., Mathers, J. C., & Relton, C. L. (2012). Genetic and non-genetic influences during pregnancy on infant global and site specific DNA methylation: Role for folate gene variants and vitamin B 12. *PLoS ONE*, *7*(3), 33290. https://doi.org/10.1371/journal.pone.0033290

Mcmullin, M. F., Young, P. B., Bailie, K. E. M., Savage, G. A., Lappin, T. R. J., & White, R. (2001). Homocysteine and methylmalonic acid as indicators of folate and vitamin B12 deficiency in

pregnancy. *Clinical and Laboratory Haematology*, *23*(3), 161–165. https://doi.org/10.1046/j.1365-2257.2001.00370.x

Meï, C. E., Cussac, M., Haslam, R. P., Beaudoin, F., Wong, Y.-S., Maréchal, E., & Rébeillé, F. (2016). C1 Metabolism Inhibition and Nitrogen Deprivation Trigger Triacylglycerol Accumulation in Arabidopsis thaliana Cell Cultures and Highlight a Role of NPC in Phosphatidylcholine-to-Triacylglycerol Pathway. *Frontiers in Plant Science*, *7*, 1–16. https://doi.org/10.3389/fpls.2016.02014

Melnyk, S., Pogribna, M., Pogribny, I. P., Yi, P., & James, S. J. (2000). Measurement of plasma and intracellular S-adenosylmethionine and S-adenosylhomocysteine utilizing coulometric electrochemical detection: alterations with plasma homocysteine and pyridoxal 5'-phosphate concentrations. *Clinical Chemistry*, *46*(2), 265–272. Retrieved from http://www.ncbi.nlm.nih.gov/pubmed/10657384

Meng, J., Wang, L., Wang, J., Zhao, X., Cheng, J., Yu, W., … Gong, Z. (2018). METHIONINE ADENOSYLTRANSFERASE 4 mediates DNA and histone methylation. *Plant Physiology*, *177*(2), 652–670. https://doi.org/10.1104/pp.18.00183

Mentch, S. J., & Locasale, J. W. (2016). One-carbon metabolism and epigenetics: understanding the specificity. *Annals of the New York Academy of Sciences*, *1363*(1), 91–98. https://doi.org/10.1111/nyas.12956

Merchant, S., & Bogorad, L. (1986). Regulation by copper of the expression of plastocyanin and cytochrome c552 in Chlamydomonas reinhardi. *Molecular and Cellular Biology*, *6*(2), 462–469. https://doi.org/10.1128/MCB.6.2.462.Updated

Merchant, S. S., Prochnik, S. E., Vallon, O., Harris, E. H., Karpowicz, S. J., Witman, G. B., … Zhou, K. (2007). The Chlamydomonas genome reveals the evolution of key animal and plant functions. *Science*, *318*(5848), 245–251. https://doi.org/10.1126/science.1143609

Michaelis, L., & Menten, M. L. (1913). The kinetics of invertase action. *Biochemische Zeitschrift*. https://doi.org/10.1021/bi201284u

Michod, R. E. (2006). The group covariance effect and fitness trade-offs during evolutionary transitions in individuality. *Proceedings of the National Academy of Sciences*, *103*(24), 9113–9117. https://doi.org/10.1073/pnas.0601080103

Michod, R. E. (2007). Evolution of individuality during the transition from unicellular to multicellular life. *Proceedings of the National Academy of Sciences*, *104*(Supplement 1), 8613–8618. https://doi.org/10.1073/pnas.0701489104

Miller, T. R., & Belas, R. (2006). Motility is involved in Silicibacter sp. TM1040 interaction with dinoflagellates. *Environmental Microbiology*, *8*(9), 1648–1659. https://doi.org/10.1111/j.1462-2920.2006.01071.x

Mills, M. M., Ridame, C., Davey, M., La Roche, J., & Geider, R. J. (2004). Iron and phosphorus co-limit nitrogen fixation in the eastern tropical North Atlantic. *Nature*, *429*(6989), 292–294. https://doi.org/10.1038/nature02550

Mitchell, J. G., Pearson, L., & Dillon, S. (1996). Clustering of marine bacteria in seawater enrichments. *Applied and Environmental Microbiology*, *62*(10), 3716–3721. Retrieved from http://aem.asm.org/

Mogk, A., Tomoyasu, T., Goloubinoff, P., Rüdiger, S., Röder, D., Langen, H., & Bukau, B. (1999). Identification of thermolabile Escherichia coli proteins: prevention and reversion of aggregation by DnaK and ClpB. *The EMBO Journal*, *18*(24), 6934–6949.

https://doi.org/10.1093/emboj/18.24.6934

Moldovan, M. A., Petrova, S. A., & Gelfand, M. S. (2018). Comparative genomic analysis of fungal TPP-riboswitches. *Fungal Genetics and Biology*, *114*, 34–41. https://doi.org/10.1016/J.FGB.2018.03.004

Moll, R., & Davis, B. (2017). Iron, vitamin B12 and folate. *Medicine*, *45*(4), 198–203. https://doi.org/10.1016/j.mpmed.2017.01.007

Momin, M., Jia, J., Fan, F., Li, J., Dou, J., Chen, D., … Zhang, Y. (2017). Relationship between plasma homocysteine level and lipid profiles in a community-based Chinese population. *Lipids in Health and Disease*, *16*(54), 1–7. https://doi.org/10.1186/s12944-017-0441-6

Monod, J. (1949). The Growth of Bacterial Cultures. *Annual Review of Microbiology*, *3*(1), 371–394. https://doi.org/10.1146/annurev.mi.03.100149.002103

Moon, M., Kim, C. W., Park, W.-K., Yoo, G., Choi, Y.-E., & Yang, J.-W. (2013). Mixotrophic growth with acetate or volatile fatty acids maximizes growth and lipid production in Chlamydomonas reinhardtii. *Algal Research*, *2*(4), 352–357. https://doi.org/10.1016/J.ALGAL.2013.09.003

Moore, S. J., Mayer, M. J., Biedendieck, R., Deery, E., & Warren, M. J. (2014). Towards a cell factory for vitamin B12 production in Bacillus megaterium: bypassing of the cobalamin riboswitch control elements. *New Biotechnology*, *31*(6), 553–561. https://doi.org/10.1016/J.NBT.2014.03.003

Moritz, C., Mccallum, H., Donnellan, S., & Roberts, J. D. (1991). Parasite loads in parthenogenetic and sexual lizards (Heteronotia binoei): Support for the Red Queen hypothesis. *Proceedings of the Royal Society B: Biological Sciences*, *244*(1310), 145–149. https://doi.org/10.1098/rspb.1991.0063

Morran, L. T., Schmidt, O. G., Gelarden, I. A., Parrish, R. C., & Lively, C. M. (2011). Running with the Red Queen: Host-parasite coevolution selects for biparental sex. *Science*, *333*(6039), 216–218. https://doi.org/10.1126/science.1206360

Morris, J. J. (2015). Black Queen evolution: The role of leakiness in structuring microbial communities. *Trends in Genetics*, *31*(8), 475–482. https://doi.org/10.1016/j.tig.2015.05.004

Morris, J. J., Lenski, R. E., & Zinser, E. R. (2012). The Black Queen Hypothesis : Evolution of Dependencies through adaptive gene loss. *American Society for Microbiology*, *3*(2), 1–7. https://doi.org/10.1128/mBio.00036-12.Copyright

Morris, J. J., Papoulis, S. E., & Lenski, R. E. (2014). Coexistence of evolving bacteria stabilized by a shared Black Queen function. *Evolution*, *68*(10), 2960–2971. https://doi.org/10.1111/evo.12485

Morse, D., Salois, P., Markovic, P., & Hastings, J. W. (1995). A nuclear-encoded form II RuBisCO in dinoflagellates. *Science*, *268*(5217), 1622–1624. https://doi.org/10.1126/science.7777861

Moseley, J. L., Allinger, T., Herzog, S., Hoerth, P., Wehinger, E., Merchant, S., & Hippler, M. (2002). Adaptation to Fe-deficiency requires remodeling of the photosynthetic apparatus. *The EMBO Journal*, *21*(24), 6709–6720. https://doi.org/10.1093/EMBOJ/CDF666

Moseley, J. L., Chang, C.-W., & Grossman, A. R. (2006). Genome-based approaches to understanding phosphorus deprivation responses and PSR1 control in Chlamydomonas reinhardtii. *Eukaryotic Cell*, *5*(1), 26–44. https://doi.org/10.1128/EC.5.1.26-44.2006

Msanne, J., Xu, D., Konda, A. R., Casas-Mollano, J. A., Awada, T., Cahoon, E. B., & Cerutti, H. (2012). Metabolic and gene expression changes triggered by nitrogen deprivation in the

photoautotrophically grown microalgae Chlamydomonas reinhardtii and Coccomyxa sp. C-169. *Phytochemistry*, *75*, 50–59. https://doi.org/10.1016/j.phytochem.2011.12.007

Muggia, L., Vancurova, L., Škaloud, P., Peksa, O., Wedin, M., & Grube, M. (2013). The symbiotic playground of lichen thalli - a highly flexible photobiont association in rock-inhabiting lichens. *FEMS Microbiology Ecology*, *85*(2), 313–323. https://doi.org/10.1111/1574-6941.12120

Müller, P., Li, X. P., & Niyogi, K. K. (2001). Non-photochemical quenching. A response to excess light energy. *Plant Physiology*, *125*(4), 1558–1566. Retrieved from http://www.ncbi.nlm.nih.gov/pubmed/11299337

Nahvi, A., Barrick, J. E., & Breaker, R. R. (2004). Coenzyme B12 riboswitches are widespread genetic control elements in prokaryotes. *Nucleic Acids Research*, *32*(1), 143–150. https://doi.org/10.1093/nar/gkh167

Nakayama, T., Ikegami, Y., Nakayama, T., Ishida, K., Inagaki, Y., & Inouye, I. (2011). Spheroid bodies in rhopalodiacean diatoms were derived from a single endosymbiotic cyanobacterium. *Journal of Plant Research*, *124*(1), 93–97. https://doi.org/10.1007/s10265-010-0355-0

Nakayama, T., Kamikawa, R., Tanifuji, G., Kashiyama, Y., Ohkouchi, N., Archibald, J. M., & Inagaki, Y. (2014). Complete genome of a nonphotosynthetic cyanobacterium in a diatom reveals recent adaptations to an intracellular lifestyle. *Proceedings of the National Academy of Sciences*, *111*(31), 11407–11412. https://doi.org/10.1073/pnas.1405222111

Nash, J. (1950). Equilibrium Points in n-Person Games. *Proceedings of the National Academy of Sciences*, *36*(1), 48–49. https://doi.org/https://doi.org/10.1073/pnas.36.1.48

Naumann, B., Busch, A., Allmer, J., Ostendorf, E., Zeller, M., Kirchhoff, H., & Hippler, M. (2007). Comparative quantitative proteomics to investigate the remodeling of bioenergetic pathways under iron deficiency in Chlamydomonas reinhardtii. *Proteomics*, *7*(21), 3964–3979. https://doi.org/10.1002/pmic.200700407

Nedelcu, A. M. (2009). Environmentally induced responses co-opted for reproductive altruism. *Biology Letters*, *5*(6), 805–808. https://doi.org/10.1098/rsbl.2009.0334

Neuburger, M., Rébeillé, F., Jourdain, A., Nakamura, S., & Douce, R. (1996). Mitochondria are a major site for folate and thymidylate synthesis in plants. *Journal of Biological Chemistry*, *271*(16), 9466–9472. https://doi.org/10.1074/jbc.271.16.9466

Newton, A. C., Fitt, B. D. L., Atkins, S. D., Walters, D. R., & Daniell, T. J. (2010). Pathogenesis, parasitism and mutualism in the trophic space of microbe-plant interactions. *Trends in Microbiology*, *18*(8), 365–373. https://doi.org/10.1016/j.tim.2010.06.002

Nguyen, A. V., Thomas-Hall, S. R., Malnoë, A., Timmins, M., Mussgnug, J. H., Rupprecht, J., … Schenk, P. M. (2008). Transcriptome for photobiological hydrogen production induced by sulfur deprivation in the green alga Chlamydomonas reinhardtii. *Eukaryotic Cell*, *7*(11), 1965–1979. https://doi.org/10.1128/EC.00418-07

Nichols, D., Lewis, K., Orjala, J., Mo, S., Ortenberg, R., O'Connor, P., … Epstein, S. S. (2008). Short peptide induces an "uncultivable" microorganism to grow in vitro. *Applied and Environmental Microbiology*, *74*(15), 4889–4897. https://doi.org/10.1128/AEM.00393-08

Nielsen, M. J., Rasmussen, M. R., Andersen, C. B. F., Nexø, E., & Moestrup, S. K. (2012). Vitamin B12 transport from food to the body's cells—a sophisticated, multistep pathway. *Nature Reviews Gastroenterology & Hepatology*, *9*(6), 345–354. https://doi.org/10.1038/nrgastro.2012.76

Niklas, K. J. (2014). The evolutionary-developmental origins of multicellularity. *American Journal of*

Botany, *101*(1), 6–25. https://doi.org/10.3732/ajb.1300314

Noga, A. A., Stead, L. M., Zhao, Y., Brosnan, M. E., Brosnan, J. T., & Vance, D. E. (2003). Plasma homocysteine is regulated by phospholipid methylation. *The Journal of Biological Chemistry*, *278*(8), 5952–5955. https://doi.org/10.1074/jbc.M212194200

Nowack, E. C. M., Melkonian, M., & Glöckner, G. (2008). Chromatophore Genome Sequence of Paulinella Sheds Light on Acquisition of Photosynthesis by Eukaryotes. *Current Biology*, *18*(6), 410–418. https://doi.org/10.1016/j.cub.2008.02.051

Nowack, E. C. M., Price, D. C., Bhattacharya, D., Singer, A., Melkonian, M., & Grossman, A. R. (2016). Gene transfers from diverse bacteria compensate for reductive genome evolution in the chromatophore of Paulinella chromatophora. *Proceedings of the National Academy of Sciences*, *113*(43), 12214–12219. https://doi.org/10.1073/pnas.1608016113

Nowack, E. C. M., Vogel, H., Groth, M., Grossman, A. R., Melkonian, M., & Glockner, G. (2011). Endosymbiotic Gene Transfer and Transcriptional Regulation of Transferred Genes in Paulinella chromatophora. *Molecular Biology and Evolution*, *28*(1), 407–422. https://doi.org/10.1093/molbev/msq209

Obeid, R., & Herrmann, W. (2009). Homocysteine and lipids: S-Adenosyl methionine as a key intermediate. *FEBS Letters*, *583*(8), 1215–1225. https://doi.org/10.1016/j.febslet.2009.03.038

Ohno, M., Okano, I., Watsuji, T., Kakinuma, T., Ueda, K., & Beppu, T. (1999). Establishing the Independent Culture of a Strictly Symbiotic Bacterium Symbiobacterium thermophilum from Its Supporting Bacillus Strain. *Bioscience, Biotechnology, and Biochemistry*, *63*(6), 1083–1090. https://doi.org/10.1271/bbb.63.1083

Ohwada, K. (1973). Seasonal Cycles of Vitamin B12, Thiamine and Biotin in Lake Sagami. Patterns of Their Distribution and Ecological Significance. *Internationale Revue Der Gesamten Hydrobiologie Und Hydrographie*, *58*(6), 851–871. https://doi.org/10.1002/iroh.19730580607

Ohwada, K., & Taga, N. (1972). Distribution and seasonal variation of vitamin B12, thiamine and biotin in the sea. *Marine Chemistry*, *1*(1), 61–73. https://doi.org/10.1016/0304-4203(72)90007-2

Oliveira, N. M., Niehus, R., & Foster, K. R. (2014). Evolutionary limits to cooperation in microbial communities. *Proceedings of the National Academy of Sciences*, *111*(50), 17941–17946. https://doi.org/10.1073/pnas.1412673111

Olsen, Y., Knutsen, G., & Lien, T. (1983). Characteristics of phosphorus limitation in Chlamydomonas reinhardtii (Chlorophyceae) and its palmelloids. *Journal of Phycology*, *19*(3), 313–319. https://doi.org/10.1111/j.0022-3646.1983.00313.x

Ottenhof, H. H., Ashurst, J. L., Whitney, H. M., Saldanha, S. A., Schmitzberger, F., Gweon, H. S., … Smith, A. G. (2004). Organisation of the pantothenate (vitamin B5) biosynthesis pathway in higher plants. *The Plant Journal : For Cell and Molecular Biology*, *37*(1), 61–72. Retrieved from http://www.ncbi.nlm.nih.gov/pubmed/14675432

Oulhen, N., Schulz, B. J., & Carrier, T. J. (2016). English translation of Heinrich Anton de Bary's 1878 speech, "Die Erscheinung der Symbiose" ('De la symbiose'). *Symbiosis*, *69*, 131–139. https://doi.org/10.1007/s13199-016-0409-8

Page, M. D., Allen, M. D., Kropat, J., Urzica, E. I., Karpowicz, S. J., Hsieh, S. I., … Merchant, S. S. (2012). Fe sparing and Fe recycling contribute to increased superoxide dismutase capacity in iron-starved Chlamydomonas reinhardtii. *The Plant Cell*, *24*(6), 2649–2665. https://doi.org/10.1105/tpc.112.098962

Page, M. D., Kropat, J., Hamel, P. P., & Merchant, S. S. (2009). Two Chlamydomonas CTR copper transporters with a novel cys-met motif are localized to the plasma membrane and function in copper assimilation. *The Plant Cell*, *21*(3), 928–943. https://doi.org/10.1105/tpc.108.064907

Palacios, O. A., Bashan, Y., & de-Bashan, L. E. (2014). Proven and potential involvement of vitamins in interactions of plants with plant growth-promoting bacteria—an overview. *Biology and Fertility of Soils*, *50*(3), 415–432. https://doi.org/10.1007/s00374-013-0894-3

Palenik, B., Grimwood, J., Aerts, A., & Pierre, R. (2007). The tiny eukaryote Ostreococcus provides genomic insights into the paradox of plankton speciation. *Proceedings of the National Academy of Sciences*, *104*(18), 7705–7710. https://doi.org/10.1080/03605302.2014.892128

Palmer, J. L., & Abeles, R. H. (1979). The mechanism of action of S-adenosylhomocysteinase. *The Journal of Biological Chemistry*, *254*(4), 1217–1226. Retrieved from http://www.jbc.org/

Panzeca, C., Beck, A. J., Tovar-Sanchez, A., Segovia-Zavala, J., Taylor, G. T., Gobler, C. J., & Sañudo-Wilhelmy, S. a. (2009). Distributions of dissolved vitamin B12 and Co in coastal and open-ocean environments. *Estuarine, Coastal and Shelf Science*, *85*(2), 223–230. https://doi.org/10.1016/j.ecss.2009.08.016

Panzeca, C., Tovar-Sanchez, A., Agustí, S., Reche, I., Duarte, C. M., Taylor, G. T., & Sañudo-Wilhelmy, S. A. (2006). B vitamins as regulators of phytoplankton dynamics. *Eos, Transactions American Geophysical Union*, *87*(52), 593. https://doi.org/10.1029/2006EO520001

Park, J.-J., Wang, H., Gargouri, M., Deshpande, R. R., Skepper, J. N., Holguin, F. O., … Gang, D. R. (2015). The response of *Chlamydomonas reinhardtii* to nitrogen deprivation: a systems biology analysis. *The Plant Journal*, *81*(4), 611–624. https://doi.org/10.1111/tpj.12747

Parkhill, J.-P., Maillet, G., & Cullen, J. J. (2001). Fluorescence-based maximal quantum yield for PSII as a diagnostic of nutrient stress. *Journal of Phycology*, *37*(4), 517–529. https://doi.org/10.1046/j.1529-8817.2001.037004517.x

Peaudecerf, F. J., Bunbury, F., Bhardwaj, V., Bees, M. A., Smith, A. G., Goldstein, R. E., & Croze, O. A. (2018). Microbial mutualism at a distance: The role of geometry in diffusive exchanges. *Physical Review E*, *97*(2), 22411. https://doi.org/10.1103/PhysRevE.97.022411

Pedersen, M. F., & Borum, J. (1996). Nutrient control of algal growth in estuarine waters. Nutrient limitation and the importance of nitrogen requirements... *Oceanographic Literature Review*, *142*, 261–272. https://doi.org/10.3354/meps142261

Pedersen, S., Bloch, P. L., Reeh, S., & Neidhardt, F. C. (1978). Patterns of protein synthesis in E. coli: a catalog of the amount of 140 individual proteins at different growth rates. *Cell*, *14*(1), 179–190. https://doi.org/10.1016/0092-8674(78)90312-4

Pérez-Pérez, M. E., Lemaire, S. D., & Crespo, J. L. (2012). Reactive oxygen species and autophagy in plants and algae. *Plant Physiology*, *160*(1), 156–164. https://doi.org/10.1104/pp.112.199992

Perlman, D., & Barrett, J. M. (1959). Biosynthesis of Cobalamins by cell suspensions of Propionibacteria and Streptomycetes. *Journal of Bacteriology*, *78*, 171–174. Retrieved from https://www.ncbi.nlm.nih.gov/pmc/articles/PMC290508/pdf/jbacter00493-0037.pdf

Pfaffl, M. W. (2001). A new mathematical model for relative quantification in real-time RT-PCR. *Nucleic Acids Research*, *29*(9), 2002–2007. https://doi.org/10.1093/nar/29.9.e45

Philipps, G., Happe, T., & Hemschemeier, A. (2012). Nitrogen deprivation results in photosynthetic hydrogen production in Chlamydomonas reinhardtii. *Planta*, *235*(4), 729–745. https://doi.org/10.1007/s00425-011-1537-2

Pillai, S., Behra, R., Nestler, H., Suter, M. J.-F., Sigg, L., & Schirmer, K. (2014). Linking toxicity and adaptive responses across the transcriptome, proteome, and phenotype of Chlamydomonas reinhardtii exposed to silver. *Proceedings of the National Academy of Sciences*, *111*(9), 3490–3495. https://doi.org/10.1073/pnas.1319388111

Pootakham, W., Gonzalez-Ballester, D., & Grossman, A. R. (2010). Identification and regulation of plasma membrane sulfate transporters in Chlamydomonas. *Plant Physiology*, *153*(4), 1653–1668. https://doi.org/10.1104/pp.110.157875

Prechtl, J., Kneip, C., Lockhart, P., Wenderoth, K., & Maier, U.-G. (2004). Intracellular Spheroid Bodies of Rhopalodia gibba Have Nitrogen-Fixing Apparatus of Cyanobacterial Origin. *Molecular Biology and Evolution*, *21*(8), 1477–1481. https://doi.org/10.1093/molbev/msh086

Pufulete, M., Al-Ghnaniem, R., Khushal, A., Appleby, P., Harris, N., Gout, S., … Sanders, T. A. B. (2005). Effect of folic acid supplementation on genomic DNA methylation in patients with colorectal adenoma. *Gut*, *54*(5), 648–653. https://doi.org/10.1136/gut.2004.054718

Qin, X., Li, J., Cui, Y., Liu, Z., Zhao, Z., Ge, J., … Huo, Y. (2012). MTHFR C677T and MTR A2756G polymorphisms and the homocysteine lowering efficacy of different doses of folic acid in hypertensive Chinese adults. *Nutrition Journal*, *11*(2), 1–7. https://doi.org/10.1186/1475-2891-11-2

Queller, D. C. (1997). Cooperators since life began. Book review of: The Major Transitions in Evolution, by J. Maynard Smith & E. Szathmáry. *Quarterly Review of Biology*, *72*(2), 184–188. https://doi.org/10.1086/419766

Queller, D. C., & Strassmann, J. E. (2016). Problems of multi-species organisms: endosymbionts to holobionts. *Biology and Philosophy*, *31*(6), 855–873. Retrieved from http://openscholarship.wustl.edu/bio_facpubshttp://openscholarship.wustl.edu/bio_facpubs/126

Quisel, J. D., Wykoff, D. D., & Grossman, A. R. (1996). Biochemical characterization of the extracellular phosphatases produced by phosphorus-deprived Chlamydomonas reinhardtii. *Plant Physiology*, *111*(3), 839–848. https://doi.org/10.1104/pp.111.3.839

Rampersaud, G. C., Kauwell, G. P., Hutson, A. D., Cerda, J. J., & Bailey, L. B. (2000). Genomic DNA methylation decreases in response to moderate folate depletion in elderly women. *The American Journal of Clinical Nutrition*, *72*(4), 998–1003. https://doi.org/10.1093/ajcn/72.4.998

Randaccio, L., Geremia, S., Demitri, N., Wuerges, J., Randaccio, L., Geremia, S., … Wuerges, J. (2010). Vitamin B12: Unique Metalorganic Compounds and the Most Complex Vitamins. *Molecules*, *15*(5), 3228–3259. https://doi.org/10.3390/molecules15053228

Ranocha, P., McNeil, S. D., Ziemak, M. J., Li, C., Tarczynski, M. C., & Hanson, A. D. (2001). The S-methylmethionine cycle in angiosperms: ubiquity, antiquity and activity. *The Plant Journal*, *25*(5), 575–584. https://doi.org/10.1046/j.1365-313x.2001.00988.x

Rao, D., Webb, J. S., Holmström, C., Case, R., Low, A., Steinberg, P., & Kjelleberg, S. (2007). Low densities of epiphytic bacteria from the marine alga Ulva australis inhibit settlement of fouling organisms. *Applied and Environmental Microbiology*, *73*(24), 7844–7852. https://doi.org/10.1128/AEM.01543-07

Rapoport, A., & Chammah, A. (1965). *Prisoner's dilemma: a study in conflict and cooperation*. *Prisoners dilemma a study in conflict and cooperation* (Vol. Second pri). University of Michigan Press. https://doi.org/10.3998/mpub.20269

Raux, E., Lanois, A., Levillayer, F., Warren, M. J., Brody, E., Rambach, A., & Thermes, C. (1996).

Salmonella typhimurium cobalamin (vitamin B12) biosynthetic genes: Functional studies in S. typhimurium and Escherichia coli. *Journal of Bacteriology*, *178*(3), 753–767. https://doi.org/10.1128/jb.178.3.753-767.1996

Raven, J. A. (2010). Inorganic carbon acquisition by eukaryotic algae: four current questions. *Photosynthesis Research*, *106*, 123–134. https://doi.org/10.1007/s11120-010-9563-7

Reed, M. C., Nijhout, H. F., Neuhouser, M. L., Gregory, J. F., Shane, B., James, S. J., … Ulrich, C. M. (2006). A Mathematical Model Gives Insights into Nutritional and Genetic Aspects of Folate-Mediated One-Carbon Metabolism. *The Journal of Nutrition*, *136*(10), 2653–2661. https://doi.org/10.1093/jn/136.10.2653

Reisner, A., Höller, B. M., Molin, S., & Zechner, E. L. (2006). Synergistic effects in mixed Escherichia coli biofilms: conjugative plasmid transfer drives biofilm expansion. *Journal of Bacteriology*, *188*(10), 3582–3588. https://doi.org/10.1128/JB.188.10.3582-3588.2006

Remias, D., Karsten, U., Lütz, C., & Leya, T. (2010). Physiological and morphological processes in the Alpine snow alga Chloromonas nivalis (Chlorophyceae) during cyst formation. *Protoplasma*, *243*(1–4), 73–86. https://doi.org/10.1007/s00709-010-0123-y

Remias, D., Lütz-Meindl, U., & Lütz, C. (2005). Photosynthesis, pigments and ultrastructure of the alpine snow alga Chlamydomonas nivalis. *European Journal of Phycology*, *40*(3), 259–268. https://doi.org/10.1080/09670260500202148

Remias, D., Wastian, H., Lütz, C., & Leya, T. (2013). Insights into the biology and phylogeny of Chloromonas polyptera (Chlorophyta), an alga causing orange snow in Maritime Antarctica. *Antarctic Science*, *25*(05), 648–656. https://doi.org/10.1017/S0954102013000060

Richardson, D. H. S. (1999). War in the world of lichens: Parasitism and symbiosis as exemplified by lichens and lichenicolous fungi. *Mycological Research*, *103*(6), 641–650. https://doi.org/10.1017/S0953756298008259

Rickes, E. L., Brink, N. G., Koniuszy, F. R., Wood, T. R., & Folkers, K. (1948). Crystalline Vitamin B12. *Science*, *107*(2781), 396–397. https://doi.org/10.1126/science.107.2781.396

Riekhof, W. R., Sears, B. B., & Benning, C. (2005). Annotation of genes involved in glycerolipid biosynthesis in Chlamydomonas reinhardtii: discovery of the betaine lipid synthase BTA1Cr. *Eukaryotic Cell*, *4*(2), 242–252. https://doi.org/10.1128/EC.4.2.242-252.2005

Rinta-Kanto, J. M., Sun, S., Sharma, S., Kiene, R. P., & Moran, M. A. (2012). Bacterial community transcription patterns during a marine phytoplankton bloom. *Environmental Microbiology*, *14*(1), 228–239. https://doi.org/10.1111/j.1462-2920.2011.02602.x

Road, G., Station, C., Iturriaga, R., & Sciences, E. (1986). Evidence for a protective function for secondary carotenoids of snow algae. *Journal of Phycology*, *29*(1979), 427–434. Retrieved from https://onlinelibrary.wiley.com/doi/pdf/10.1111/j.1529-8817.1993.tb00143.x

Rochaix, J.-D. (1995). Chlamydomonas reinhardtii as the Photosynthetic Yeast. *Annual Review of Genetics*, *29*(1), 209–230. https://doi.org/10.1146/annurev.genet.29.1.209

Rodionov, D. A., Vitreschak, A. G., Mironov, A. A., & Gelfand, M. S. (2003). Comparative genomics of the vitamin B12 metabolism and regulation in prokaryotes. *The Journal of Biological Chemistry*, *278*(42), 41148–41159. https://doi.org/10.1074/jbc.M305837200

Roessner, C. A., & Scott, A. I. (2006). Fine-tuning our knowledge of the anaerobic route to cobalamin (vitamin B12). *Journal of Bacteriology*, *188*(21), 7331–7334. https://doi.org/10.1128/JB.00918-06

Roje, S., Wang, H., McNeil, S. D., Raymond, R. K., Appling, D. R., Shachar-Hill, Y., … Hanson, A. D. (1999). Isolation, Characterization, and Functional Expression of cDNAs Encoding NADH-dependent Methylenetetrahydrofolate Reductase from Higher Plants. *Journal of Biological Chemistry*, *274*(51), 36089–36096. https://doi.org/10.1074/jbc.274.51.36089

Rose, N. R., & Klose, R. J. (2014). Understanding the relationship between DNA methylation and histone lysine methylation. *Biochimica et Biophysica Acta*, *1839*(12), 1362–1372. https://doi.org/10.1016/j.bbagrm.2014.02.007

Ross, M. (1952). *VITAMIN B12 assay in body fluids using Euglena gracilis*. *Journal of clinical pathology* (Vol. 5). Retrieved from https://www.ncbi.nlm.nih.gov/pmc/articles/PMC1023596/pdf/jclinpath00020-0026.pdf

Rozen, D. E., Philippe, N., Arjan de Visser, J., Lenski, R. E., & Schneider, D. (2009). Death and cannibalism in a seasonal environment facilitate bacterial coexistence. *Ecology Letters*, *12*(1), 34–44. https://doi.org/10.1111/j.1461-0248.2008.01257.x

Ruiz, F. A., Marchesini, N., Seufferheld, M., Govindjee, & Docampo, R. (2001). The polyphosphate bodies of Chlamydomonas reinhardtii possess a proton-pumping pyrophosphatase and are similar to acidocalcisomes. *The Journal of Biological Chemistry*, *276*(49), 46196–46203. https://doi.org/10.1074/jbc.M105268200

Ryther, J. H., & Dunstan, W. M. (1971). Nitrogen, phosphorus, and eutrophication in the coastal marine environment. *Science*, *171*(3975), 1008–1013. https://doi.org/10.1126/science.171.3975.1008

Sachs, J. L., & Simms, E. L. (2006). Pathways to mutualism breakdown. *Trends in Ecology & Evolution*, *21*(10), 585–592. https://doi.org/10.1016/j.tree.2006.06.018

Sachs, J. L., Skophammer, R. G., & Regus, J. U. (2011). Evolutionary transitions in bacterial symbiosis. *Proceedings of the National Academy of Sciences*, *108*(2), 10800–10807. https://doi.org/10.1073/pnas.1100304108

Sakurai, K., Mori, N., & Sato, N. (2014). Detection and characterization of phosphatidylcholine in various strains of the genus Chlamydomonas (Volvocales, Chlorophyceae). *Journal of Plant Research*, *127*(5), 641–650. https://doi.org/10.1007/s10265-014-0644-0

Sanudo-Wilhelmy, S. A., Cutter, L. S., Durazo, R., Smail, E. A., Gomez-Consarnau, L., Webb, E. A., … Karl, D. M. (2012). Multiple B-vitamin depletion in large areas of the coastal ocean. *Proceedings of the National Academy of Sciences*, *109*(35), 14041–14045. https://doi.org/10.1073/pnas.1208755109

Sañudo-Wilhelmy, S. A., Gobler, C. J., Okbamichael, M., & Taylor, G. T. (2006). Regulation of phytoplankton dynamics by vitamin B_{12}. *Geophysical Research Letters*, *33*(4), L04604. https://doi.org/10.1029/2005GL025046

Sañudo-Wilhelmy, S. a, Gómez-Consarnau, L., Suffridge, C., & Webb, E. a. (2014). The role of B vitamins in marine biogeochemistry. *Annual Review of Marine Science*, *6*, 339–367. https://doi.org/10.1146/annurev-marine-120710-100912

Sarhan, F., Houde, M., & Cheneval, J. P. (1980). The Role of Vitamin B12 Binding In the Uptake of the Vitamin By Euglena Gracilis. *The Journal of Protozoology*, *27*(2), 235–238. https://doi.org/10.1111/j.1550-7408.1980.tb04688.x

Saroussi, S. I., Wittkopp, T. M., & Grossman, A. R. (2016). The Type II NADPH Dehydrogenase Facilitates Cyclic Electron Flow, Energy-Dependent Quenching, and Chlororespiratory Metabolism during Acclimation of Chlamydomonas reinhardtii to Nitrogen Deprivation. *Plant*

Physiology, *170*(4), 1975–1988. https://doi.org/10.1104/pp.15.02014

Saroussi, S., Sanz-Luque, E., Kim, R. G., & Grossman, A. R. (2017). Nutrient scavenging and energy management: acclimation responses in nitrogen and sulfur deprived Chlamydomonas. *Current Opinion in Plant Biology*, *39*, 114–122. https://doi.org/10.1016/j.pbi.2017.06.002

Schauer, K., Rodionov, D. A., & de Reuse, H. (2008). New substrates for TonB-dependent transport: do we only see the 'tip of the iceberg'? *Trends in Biochemical Sciences*, *33*(7), 330–338. https://doi.org/10.1016/J.TIBS.2008.04.012

Scheidegger, C. (2016). As thick as three in a bed. *Molecular Ecology*, *25*(14), 3261–3263. https://doi.org/10.1111/mec.13710

Schink, B. (2002). Synergistic interactions in the microbial world. *Antonie van Leeuwenhoek, International Journal of General and Molecular Microbiology*, *81*(1–4), 257–261. https://doi.org/10.1023/A:1020579004534

Schjonsby, H. (1989). Vitamin B12 absorption and malabsorption. *Gut*, *30*, 1686–1691. https://doi.org/10.1136/gut.30.12.1686

Schmollinger, S., Mühlhaus, T., Boyle, N. R., Blaby, I. K., Casero, D., Mettler, T., … Merchant, S. S. (2014). Nitrogen-Sparing Mechanisms in Chlamydomonas Affect the Transcriptome, the Proteome, and Photosynthetic Metabolism. *The Plant Cell*, *26*(4), 1410–1435. https://doi.org/10.1105/tpc.113.122523

Schroeder, D. C., Oke, J., Hall, M., Malin, G., & Wilson, W. H. (2003). Virus succession observed during an Emiliania huxleyi bloom. *Applied and Environmental Microbiology*, *69*(5), 2484–2490. https://doi.org/10.1128/AEM.69.5.2484-2490.2003

Schroeder, D. C., Oke, J., Malin, G., & Wilson, W. H. (2002). Coccolithovirus (Phycodnaviridae): Characterisation of a new large dsDNA algal virus that infects Emiliania huxleyi. *Arch Virol*, *147*, 1685–1698. https://doi.org/10.1007/s00705-002-0841-3

Scott, J. M., & Weir, D. G. (1981). The methyl folate trap. *The Lancet*, *318*(8242), 337–340. https://doi.org/https://doi.org/10.1016/S0140-6736(81)90650-4

Selhub, J., Jacques, P. F., Rush, D., Rosenberg, I. H., & Wilson, P. W. F. (1993). Vitamin Status and Intake as Primary Determinants of Homocysteinemia in an Elderly Population. *JAMA*, *270*(22), 2693–2698. https://doi.org/10.1001/jama.1993.03510220049033

Serganov, A., & Nudler, E. (2013). A decade of riboswitches. *Cell*, *152*(1–2), 17–24. https://doi.org/10.1016/j.cell.2012.12.024

Seyedsayamdost, M. R., Case, R. J., Kolter, R., & Clardy, J. (2011). The Jekyll-and-Hyde chemistry of Phaeobacter gallaeciensis. *Nature Chemistry*, *3*(4), 331–335. https://doi.org/10.1038/nchem.1002

Shehata.E., & Kempner, E. S. (1978). Sequential changes in cell volume distribution during Vitamin B12 starvation of Euglena gracilis. *Journal of Bac*, *133*, 396–398.

Shih, P. M., & Matzke, N. J. (2013). Primary endosymbiosis events date to the later Proterozoic with cross-calibrated phylogenetic dating of duplicated ATPase proteins. *Proceedings of the National Academy of Sciences*, *110*(30), 12355–12360. https://doi.org/10.1073/pnas.1305813110

Shultis, D. D., Purdy, M. D., Banchs, C. N., & Wiener, M. C. (2006). Outer membrane active transport: Structure of the BtuB:TonB complex. *Science*, *312*(5778), 1396–1399. https://doi.org/10.1126/science.1127694

Siaut, M., Cuiné, S., Cagnon, C., Fessler, B., Nguyen, M., Carrier, P., … Peltier, G. (2011). Oil accumulation in the model green alga Chlamydomonas reinhardtii: Characterization, variability between common laboratory strains and relationship with starch reserves. *BMC Biotechnology*, *11*(1), 7. https://doi.org/10.1186/1472-6750-11-7

Smith, A. G., Croft, M. T., Moulin, M., & Webb, M. E. (2007). Plants need their vitamins too. *Current Opinion in Plant Biology*, *10*(3), 266–275. https://doi.org/10.1016/j.pbi.2007.04.009

Smith, V. H. (1983). Low Nitrogen to Phosphorus Ratios Favor Dominance by Blue-Green Algae in Lake Phytoplankton. *Science*, *221*, 669–671. https://doi.org/10.1126/science.221.4611.669

Soucy, S. M., Huang, J., & Gogarten, J. P. (2015). Horizontal gene transfer: building the web of life. *Nature Reviews Genetics*, *16*(8), 472–482. https://doi.org/10.1038/nrg3962

Stead, L. M., Brosnan, J. T., Brosnan, M. E., Vance, D. E., & Jacobs, R. L. (2006). Is it time to reevaluate methyl balance in humans? *The American Journal of Clinical Nutrition*, *83*(1), 5–10. https://doi.org/10.1093/ajcn/83.1.5

Steneck, R. S., Graham, M. H., Bourque, B. J., Corbett, D., Erlandson, J. M., Estes, J. A., & Tegner, M. J. (2002). Kelp forest ecosystems: biodiversity, stability, resilience and future. *Environmental Conservation*, *29*(04), 436–459. https://doi.org/10.1017/S0376892902000322

Stephenson, A. L., Dennis, J. S., Howe, C. J., Scott, S. A., & Smith, A. G. (2010). Influence of nitrogen-limitation regime on the production by *Chlorella vulgaris* of lipids for biodiesel feedstocks. *Biofuels*, *1*(1), 47–58. https://doi.org/10.4155/bfs.09.1

Stibal, M., Elster, J., Å AbackÃ¡, M., & KaÅ¡tovskÃ¡, K. (2007). Seasonal and diel changes in photosynthetic activity of the snow alga Chlamydomonas nivalis (Chlorophyceae) from Svalbard determined by pulse amplitude modulation fluorometry. *FEMS Microbiology Ecology*, *59*(2), 265–273. https://doi.org/10.1111/j.1574-6941.2006.00264.x

Stocker, R., Seymour, J. R., Samadani, A., Hunt, D. E., & Polz, M. F. (2008). Rapid chemotactic response enables marine bacteria to exploit ephemeral microscale nutrient patches. *Proceedings of the National Academy of Sciences*, *105*(11), 4209–4214. https://doi.org/10.1073/pnas.0709765105

Strobbe, S., & Van Der Straeten, D. (2017). Folate biofortification in food crops. *Current Opinion in Biotechnology*, *44*, 202–211. https://doi.org/10.1016/j.copbio.2016.12.003

Sujak, A., Gabrielska, J., Grudziński, W., Borc, R., Mazurek, P., & Gruszecki, W. I. (1999). Lutein and Zeaxanthin as Protectors of Lipid Membranes against Oxidative Damage: The Structural Aspects. *Archives of Biochemistry and Biophysics*, *371*(2), 301–307. https://doi.org/10.1006/ABBI.1999.1437

Sundström, B. G. (1984). Observations on Rhizosolenia clevei Ostenfeld (Bacillariophyceae) and Richelia intracellularis Schmidt (Cyanophyceae). *Botanica Marina*, *27*(8), 345–356. https://doi.org/10.1515/botm.1984.27.8.345

Sutak, R., Botebol, H., Blaiseau, P.-L., Léger, T., Bouget, F.-Y., Camadro, J.-M., & Lesuisse, E. (2012). A comparative study of iron uptake mechanisms in marine microalgae: iron binding at the cell surface is a critical step. *Plant Physiology*, *160*(4), 2271–2284. https://doi.org/10.1104/pp.112.204156

Suto, R. K., Brasch, N. E., Anderson, O. P., & Finke, R. G. (2001). Synthesis, characterization, solution stability, and x-ray crystal structure of the thiolatocobalamin γ-glutamylcysteinylcobalamin, a dipeptide analogue of glutathionylcobalamin: Insights into the enhanced Co-S bond stability of the natural product glutat. *Inorganic Chemistry*, *40*(12), 2686–2692.

https://doi.org/10.1021/ic001365n

Szathmáry, E., & Smith, J. M. (1995). The major evolutionary transitions. *Nature*, *374*(6519), 227–232. https://doi.org/10.1038/374227a0

Taga, M. E., & Walker, G. C. (2008). Pseudo-B12 joins the cofactor family. *Journal of Bacteriology*, *190*(4), 1157–1159. https://doi.org/10.1128/JB.01892-07

Taga, M. E., & Walker, G. C. (2010). Sinorhizobium meliloti requires a cobalamin-dependent ribonucleotide reductase for symbiosis with its plant host. *Molecular Plant-Microbe Interactions : MPMI*, *23*(12), 1643–1654. https://doi.org/10.1094/MPMI-07-10-0151

Taheri-Araghi, S., Bradde, S., Sauls, J. T., Hill, N. S., Levin, P. A., Paulsson, J., … Jun, S. (2015). Cell-Size Control and Homeostasis in Bacteria. *Current Biology*, *25*(3), 385–391. https://doi.org/10.1016/J.CUB.2014.12.009

Takahashi-Iñiguez, T., García-Hernandez, E., Arreguín-Espinosa, R., & Flores, M. E. (2012). Role of vitamin B12 on methylmalonyl-CoA mutase activity. *Journal of Zhejiang University. Science. B*, *13*(6), 423–437. https://doi.org/10.1631/jzus.B1100329

Takahashi, F., Okabe, Y., Nakada, T., Sekimoto, H., Ito, M., Kataoka, H., & Nozaki, H. (2007). Origins of the secondary plastids of Euglenophyta and Chlorarachniophyta as revealed by an analysis of the plastid-targeting, nuclear-encoded gene *psbO* [1]. *Journal of Phycology*, *43*(6), 1302–1309. https://doi.org/10.1111/j.1529-8817.2007.00411.x

Takahashi, H., Braby, C. E., & Grossman, A. R. (2001). Sulfur economy and cell wall biosynthesis during sulfur limitation of Chlamydomonas reinhardtii. *Plant Physiology*, *127*(2), 665–673. Retrieved from http://www.ncbi.nlm.nih.gov/pubmed/11598240

Takishita, K., Kawachi, M., Noël, M.-H., Matsumoto, T., Kakizoe, N., Watanabe, M. M., … Inagaki, Y. (2008). Origins of plastids and glyceraldehyde-3-phosphate dehydrogenase genes in the green-colored dinoflagellate Lepidodinium chlorophorum. *Gene*, *410*(1), 26–36. https://doi.org/10.1016/J.GENE.2007.11.008

Tambasco-Studart, M., Titiz, O., Raschle, T., Forster, G., Amrhein, N., & Fitzpatrick, T. B. (2005). Vitamin B6 biosynthesis in higher plants. *Proceedings of the National Academy of Sciences*, *102*(38), 13687–13692. https://doi.org/10.1073/pnas.0506228102

Tamura, M., Shimada, S., & Horiguchi, T. (2005). Galeidiniium rugatum gen. et sp. nov. (Dinophyceae), a new coccoid dinoflagellate with a diatom endosymbiont. *Journal of Phycology*, *41*(3), 658–671. https://doi.org/10.1111/j.1529-8817.2005.00085.x

Tang, Y. Z., Koch, F., & Gobler, C. J. (2010). Most harmful algal bloom species are vitamin B1 and B12 auxotrophs. *Proceedings of the National Academy of Sciences*, *107*(48), 20756–20761. https://doi.org/10.1073/pnas.1009566107

Tardy, F., & Havaux, M. (1997). Thylakoid membrane fluidity and thermostability during the operation of the xanthophyll cycle in higher-plant chloroplasts. *Biochimica et Biophysica Acta (BBA) - Biomembranes*, *1330*(2), 179–193. https://doi.org/10.1016/S0005-2736(97)00168-5

Terauchi, A. M., Peers, G., Kobayashi, M. C., Niyogi, K. K., & Merchant, S. S. (2010). Trophic status of Chlamydomonas reinhardtii influences the impact of iron deficiency on photosynthesis. *Photosynthesis Research*, *105*(1), 39–49. https://doi.org/10.1007/s11120-010-9562-8

Timm, S., Florian, A., Arrivault, S., Stitt, M., Fernie, A. R., & Bauwe, H. (2012). Glycine decarboxylase controls photosynthesis and plant growth. *FEBS Letters*, *586*, 3692–3697. https://doi.org/10.1016/j.febslet.2012.08.027

Titlyanov, E. A., Titlyanova, T. V, Leletkin, V. A., Tsukahara, J., Van Woesik, R., & Yamazato4, K. (1996). Degradation of zooxanthellae and regulation of their density in hermatypic corals. *Marine Ecology Progress Series*, *139*, 167–178. https://doi.org/10.3354/meps139167

Torrents, E., Trevisiol, C., Rotte, C., Hellman, U., Martin, W., & Reichard, P. (2006). Euglena gracilis ribonucleotide reductase: the eukaryote class II enzyme and the possible antiquity of eukaryote B12 dependence. *The Journal of Biological Chemistry*, *281*(9), 5604–5611. https://doi.org/10.1074/jbc.M512962200

Toyama, T., Kasuya, M., Hanaoka, T., Kobayashi, N., Tanaka, Y., Inoue, D., … Mori, K. (2018). Growth promotion of three microalgae, Chlamydomonas reinhardtii, Chlorella vulgaris and Euglena gracilis, by in situ indigenous bacteria in wastewater effluent. *Biotechnology for Biofuels*, *11*(1), 176. https://doi.org/10.1186/s13068-018-1174-0

Traulsen, A., & Nowak, M. A. (2006). Evolution of cooperation by multilevel selection. *Proceedings of the National Academy of Sciences*, *103*(29), 10952–10955. https://doi.org/10.1073/pnas.0602530103

Treves, H., Raanan, H., Finkel, O. M., Berkowicz, S. M., Keren, N., Shotland, Y., & Kaplan, A. (2013). A newly isolated *Chlorella* sp. from desert sand crusts exhibits a unique resistance to excess light intensity. *FEMS Microbiology Ecology*, *86*(3), 373–380. https://doi.org/10.1111/1574-6941.12162

Treves, H., Raanan, H., Kedem, I., Murik, O., Keren, N., Zer, H., … Kaplan, A. (2016). The mechanisms whereby the green alga *Chlorella ohadii* , isolated from desert soil crust, exhibits unparalleled photodamage resistance. *New Phytologist*, *210*(4), 1229–1243. https://doi.org/10.1111/nph.13870

Triantaphylidès, C., Krischke, M., Hoeberichts, F. A., Ksas, B., Gresser, G., Havaux, M., … Mueller, M. J. (2008). Singlet oxygen is the major reactive oxygen species involved in photooxidative damage to plants. *Plant Physiology*, *148*(2), 960–968. https://doi.org/10.1104/pp.108.125690

Trinh, N. B., & Laird, P. W. (2002). Thymidylate synthase: a novel genetic determinant of plasma homocysteine and folate levels. *Human Genetics*, *211*, 299–302. https://doi.org/10.1007/s00439-002-0779-2

Tsai, C.-H., Uygun, S., Roston, R., Shiu, S.-H., & Benning, C. (2017). Recovery from N Deprivation Is a Transcriptionally and Functionally Distinct State in Chlamydomonas. *Plant Physiology*, *176*, 2007–2023. https://doi.org/10.1104/pp.17.01546

Turk-Kubo, K. A., Farnelid, H. M., Shilova, I. N., Henke, B., & Zehr, J. P. (2017). Distinct ecological niches of marine symbiotic N_2 -fixing cyanobacterium *Candidatus Atelocyanobacterium thalassa* sublineages. *Journal of Phycology*, *53*(2), 451–461. https://doi.org/10.1111/jpy.12505

Turner, M. A., Yang, X., Yin, D., Kuczera, K., Borchardt, R. T., & Howell, P. L. (2000). Structure and function of S-adenosylhomocysteine hydrolase. *Cell Biochemistry and Biophysics*, *33*(2), 101–125. https://doi.org/10.1385/CBB:33:2:101

Turner, T. R., James, E. K., & Poole, P. S. (2013). The plant microbiome. *Genome Biology*, *14*, 209–219. https://doi.org/10.1186/gb-2013-14-6-209

Tyrrell, T. (1999). The relative influences of nitrogen and phosphorus on oceanic primary production. *Nature*, *400*(6744), 525–531. https://doi.org/10.1038/22941

Tyrrell, T., & Law, C. S. (1997). Low nitrate:phosphate ratios in the global ocean. *Nature*, *387*(6635), 793–796. https://doi.org/10.1038/42915

Uchiumi, T., Ohwada, T., Itakura, M., Mitsui, H., Nukui, N., Dawadi, P., … Minamisawa, K. (2004). Expression islands clustered on the symbiosis island of the Mesorhizobium loti genome. *Journal of Bacteriology*, *186*(8), 2439–2448. https://doi.org/10.1128/JB.186.8.2439-2448.2004

Uduman, N., Qi, Y., Danquah, M. K., Forde, G. M., & Hoadley, A. (2010). Dewatering of microalgal cultures: A major bottleneck to algae-based fuels. *Journal of Renewable and Sustainable Energy*, *2*(1), 012701. https://doi.org/10.1063/1.3294480

Ueland, P. M. (1982). Pharmacological and Biochemical Aspects of S-Adenosylhomocysteine and S-Adenosylhomocysteine Hydrolase. *Pharmacol. Rev.*, *34*(3), 223–253. Retrieved from http://pharmrev.aspetjournals.org/content/pharmrev/34/3/223.full.pdf

Urzica, E. I., Adler, L. N., Page, M. D., Linster, C. L., Arbing, M. A., Casero, D., … Clarke, S. G. (2012). Impact of oxidative stress on ascorbate biosynthesis in Chlamydomonas via regulation of the VTC2 gene encoding a GDP-L-galactose phosphorylase. *The Journal of Biological Chemistry*, *287*(17), 14234–14245. https://doi.org/10.1074/jbc.M112.341982

Urzica, E. I., Casero, D., Yamasaki, H., Hsieh, S. I., Adler, L. N., Karpowicz, S. J., … Merchant, S. S. (2012). Systems and trans-system level analysis identifies conserved iron deficiency responses in the plant lineage. *The Plant Cell*, *24*(10), 3921–3948. https://doi.org/10.1105/tpc.112.102491

Urzica, E. I., Vieler, A., Hong-Hermesdorf, A., Page, M. D., Casero, D., Gallaher, S. D., … Merchant, S. S. (2013). Remodeling of membrane lipids in iron-starved chlamydomonas. *Journal of Biological Chemistry*, *288*(42), 30246–30258. https://doi.org/10.1074/jbc.M113.490425

Van Bibber, M., Bradbeer, C., Clark, N., & Roth, J. R. (1999). A new class of cobalamin transport mutants (btuF) provides genetic evidence for a periplasmic binding protein in Salmonella typhimurium. *Journal of Bacteriology*, *181*(17), 5539–5541. Retrieved from http://www.ncbi.nlm.nih.gov/pubmed/10464235

Van Der Meer, S. B., Poggi, Q. F., Spada, M., Bonnefont, J. P., Ogier, H., Hubert, P., … Saudubray, J. M. (1994). Clinical outcome of long-term management of patients with vitamin B 12-unresponsive methylmalonic acidemia. *The Journal of Pediatrics*, *125*(6), 902–908. Retrieved from https://ac.els-cdn.com/S0022347605820050/1-s2.0-S0022347605820050-main.pdf?_tid=b494b448-025c-4d3a-b4e8-3ed13c117196&acdnat=1535998367_2d16f663be2d550383e33c90ed646520

van Kapel, J., Spijkers, L. J. M., Lindemans, J., & Abels, J. (1983). Improved distribution analysis of cobalamins and cobalamin analogues in human plasma in which the use of thiol-blocking agents is a prerequisite. *Clinica Chimica Acta*, *131*(3), 211–224. https://doi.org/10.1016/0009-8981(83)90090-6

Van Valen, L. (1973). A new Evolutionary Law. *Evolutionary Theory*, *1*, 1–30. https://doi.org/10.1038/344864a0

Vasconcelos, C. V., Pereira, F. T., Duarte, E. A. A., de Oliveira, T. A. S., Peixoto, N., & Carvalho, D. D. C. (2018). Physiological and Molecular Characterization of Cephaleuros virescens Occurring in Mango Trees. *The Plant Pathology Journal*, *34*(3), 157–162. https://doi.org/10.5423/PPJ.OA.09.2017.0194

Villareal, T. A. (1990). Laboratory Culture and Preliminary Characterization of the Nitrogen-Fixing Rhizosolenia-Richelia Symbiosis. *Marine Ecology*, *11*(2), 117–132. https://doi.org/10.1111/j.1439-0485.1990.tb00233.x

Vineis, P., Chuang, S.-C., Vaissière, T., Cuenin, C., Ricceri, F., Genair-EPIC Collaborators, … Herceg, Z.

(2011). DNA methylation changes associated with cancer risk factors and blood levels of vitamin metabolites in a prospective study. *Epigenetics*, *6*(2), 195–201. Retrieved from http://www.ncbi.nlm.nih.gov/pubmed/20978370

Visram, M., Radulovic, M., Steiner, S., Malanovic, N., Eichmann, T. O., Wolinski, H., … Tehlivets, O. (2018). Homocysteine regulates fatty acid and lipid metabolism in yeast. *The Journal of Biological Chemistry*, *293*(15), 5544–5555. https://doi.org/10.1074/jbc.M117.809236

Vítová, M., Bišová, K., Hlavová, M., Kawano, S., Zachleder, V., & Čížková, M. (2011). Chlamydomonas reinhardtii: duration of its cell cycle and phases at growth rates affected by temperature. *Planta*, *234*(3), 599–608. https://doi.org/10.1007/s00425-011-1427-7

Wagner-Döbler, I., Ballhausen, B., Berger, M., Brinkhoff, T., Buchholz, I., Bunk, B., … Simon, M. (2010). The complete genome sequence of the algal symbiont Dinoroseobacter shibae: a hitchhiker's guide to life in the sea. *The ISME Journal*, *4*(1), 61–77. https://doi.org/10.1038/ismej.2009.94

Wald, D. S., Law, M., & Morris, J. K. (2002). Homocysteine and cardiovascular disease: evidence on causality from a meta-analysis. *BMJ (Clinical Research Ed.)*, *325*(7374), 1202. https://doi.org/10.1136/BMJ.325.7374.1202

Wang, H., Tomasch, J., Michael, V., Bhuju, S., Jarek, M., Petersen, J., & Wagner-Döbler, I. (2015). Identification of Genetic Modules Mediating the Jekyll and Hyde Interaction of Dinoroseobacter shibae with the Dinoflagellate Prorocentrum minimum. *Frontiers in Microbiology*, *6*, 1262. https://doi.org/10.3389/fmicb.2015.01262

Wang, J. X., Lee, E. R., Morales, D. R., Lim, J., & Breaker, R. R. (2008). Riboswitches that Sense S-adenosylhomocysteine and Activate Genes Involved in Coenzyme Recycling. *Molecular Cell*, *29*(6), 691–702. https://doi.org/10.1016/j.molcel.2008.01.012

Warren, M. J., Raux, E., Schubert, H. L., & Escalante-Semerena, J. C. (2002). The biosynthesis of adenosylcobalamin (vitamin B12). *Natural Product Reports*, *19*(4), 390–412. https://doi.org/10.1039/b108967f

Wase, N., Black, P. N., Stanley, B. A., & Dirusso, C. C. (2014). Integrated Quantitative Analysis of Nitrogen Stress Response in Chlamydomonas reinhardtii Using Metabolite and Protein Profiling. *Journal of Proteome Research*, *13*, 1373–1396. https://doi.org/10.1021/pr400952z

Watanabe, F., Takenaka, S., Kittaka-Katsura, H., Ebara, S., & Miyamoto, E. (2002). Characterization and Bioavailability of Vitamin B12-Compounds from Edible Algae. *J Nutr Sci Vitaminoi*, *48*, 325–331.

Waterborg, J. H., Robertson, A. J., Tatar, D. L., Borza, C. M., & Davie, J. R. (1995). Histones of Chlamydomonas reinhardtii (Synthesis, Acetylation, and Methylation). *Plant Physiology*, *109*(2), 393–407. https://doi.org/10.1104/pp.109.2.393

Waterland, R. A. (2006). Assessing the Effects of High Methionine Intake on DNA Methylation. *The Journal of Nutrition*, *136*(6), 1706S–1710S. https://doi.org/10.1093/jn/136.6.1706S

Watkin, D., & Rosenblatt, D. S. (1989). Functional methionine synthase deficiency (cblE and cblG): Clinical and biochemical heterogeneity. *American Journal of Medical Genetics*, *34*(3), 427–434. https://doi.org/10.1002/ajmg.1320340320

Wellburn, A. R. (1994). The Spectral Determination of Chlorophylls a and b, as well as Total Carotenoids, Using Various Solvents with Spectrophotometers of Different Resolution. *Journal of Plant Physiology*, *144*(3), 307–313. https://doi.org/10.1016/S0176-1617(11)81192-2

West, S. A., Fisher, R. M., Gardner, A., & Kiers, E. T. (2015). Major evolutionary transitions in individuality. *Proceedings of the National Academy of Sciences*, *112*(33), 10112–10119. https://doi.org/10.1073/pnas.1421402112

Westhoek, A., Field, E., Rehling, F., Mulley, G., Webb, I., Poole, P. S., & Turnbull, L. A. (2017). Policing the legume-Rhizobium symbiosis: a critical test of partner choice. *Scientific Reports*, *7*(1), 1419. https://doi.org/10.1038/s41598-017-01634-2

Wheatley, C. (2007). The return of the Scarlet Pimpernel: cobalamin in inflammation II - cobalamins can both selectively promote all three nitric oxide synthases (NOS), particularly iNOS and eNOS, and, as needed, selectively inhibit iNOS and nNOS. *Journal of Nutritional & Environmental Medicine*, *16*(3–4), 181–211. https://doi.org/10.1080/10520290701791839

White, S., Anandraj, A., & Bux, F. (2011). PAM fluorometry as a tool to assess microalgal nutrient stress and monitor cellular neutral lipids. *Bioresource Technology*, *102*(2), 1675–1682. https://doi.org/10.1016/j.biortech.2010.09.097

Whitehead, L. F. (2003). Metabolite comparisons and the identity of nutrients translocated from symbiotic algae to an animal host. *Journal of Experimental Biology*, *206*(18), 3149–3157. https://doi.org/10.1242/jeb.00539

Whitman, W. B., Coleman, D. C., & Wiebe, W. J. (1998). Prokaryotes: The unseen majority. *Proceedings of the National Academy of Sciences*, *95*(12), 6578–6583. https://doi.org/10.1073/pnas.95.12.6578

Whitney, S. M., Shaw, D. C., & Yellowlees, D. (1995). Evidence that some dinoflagellates contain a ribulose-1,5-bisphosphate carboxylase/oxygenase related to that of the alpha-proteobacteria. *Proceedings. Biological Sciences*, *259*(1356), 271–275. https://doi.org/10.1098/rspb.1995.0040

Wolf, Y. I., & Koonin, E. V. (2013). Genome reduction as the dominant mode of evolution. *BioEssays : News and Reviews in Molecular, Cellular and Developmental Biology*, *35*(9), 829–837. https://doi.org/10.1002/bies.201300037

Wong, P. P., & Burris, R. H. (1972). Nature of oxygen inhibition of nitrogenase from Azotobacter vinelandii. *Proceedings of the National Academy of Sciences*, *69*(3), 672–675. https://doi.org/10.1073/pnas.69.3.672

Woodward, R. B. (1973). The total synthesis of vitamin B12. *Pure and Applied Chemistry*, *33*(1), 145–177. https://doi.org/10.1351/pac197333010145

Wright, S. (1945). Tempo and Mode in Evolution: A Critical Review. *Ecology*, *26*(4), 415–419. https://doi.org/10.2307/1931666

Wu, K., Atkinson, I. J., Cossins, E. A., & King, J. (1993). Methotrexate Resistance in Datura innoxia (Uptake and Metabolism of Methotrexate in Wild-Type and Resistant Cell Lines). *Plant Physiology*, *101*(2), 477–483. https://doi.org/10.1104/pp.101.2.477

Wykoff, D. D., Davies, J. P., Melis, A., & Grossman, A. R. (1998). The Regulation of Photosynthetic Electron Transport during Nutrient Deprivation in Chlamydomonas reinhardtii. *Plant Physiology*, *117*(1), 129–139. https://doi.org/10.1104/pp.117.1.129

Wykoff, D. D., Grossman, A. R., Weeks, D. P., Usuda, H., & Shimogawara, K. (1999). Psr1, a nuclear localized protein that regulates phosphorus metabolism in Chlamydomonas. *Proceedings of the National Academy of Sciences*, *96*(26), 15336–15341. https://doi.org/10.1073/pnas.96.26.15336

Xia, L., Cregan, A. G., Berben, L. A., & Brasch, N. E. (2004). Studies on the formation of

glutathionylcobalamin: Any free intracellular aquacobalamin is likely to be rapidly and irreversibly converted to glutathionylcobalamin. *Inorganic Chemistry*, *43*(21), 6848–6857. https://doi.org/10.1021/ic040022c

Xie, B., Bishop, S., Stessman, D., Wright, D., Spalding, M. H., & Halverson, L. J. (2013). Chlamydomonas reinhardtii thermal tolerance enhancement mediated by a mutualistic interaction with vitamin B12-producing bacteria. *The ISME Journal*, *7*(8), 1544–1555. https://doi.org/10.1038/ismej.2013.43

Yallop, M. L., Anesio, A. M., Perkins, R. G., Cook, J., Telling, J., Fagan, D., … Roberts, N. W. (2012). Photophysiology and albedo-changing potential of the ice algal community on the surface of the Greenland ice sheet. *The ISME Journal*, *6*(12), 2302–2313. https://doi.org/10.1038/ismej.2012.107

Yamada, K., Strahler, J. R., Andrews, P. C., & Matthews, R. G. (2005). Regulation of human methylenetetrahydrofolate reductase by phosphorylation. *Proceedings of the National Academy of Sciences*, *102*(30), 10454–10459. https://doi.org/https://doi.org/10.1073/pnas.0504786102

Yamamura, N. (1993). Verical transmission and evolution of mutualism from parasitism. *Theoretical Population Biology*, *44*, 95–109. https://doi.org/10.1006/tpbi.1993.1020

Yee, L., & Blanch, H. W. (1993). Defined media optimization for growth of recombinant Escherichia coli X90. *Biotechnology and Bioengineering*, *41*(2), 221–230. https://doi.org/10.1002/bit.260410208

Yi, P., Melnyk, S., Pogribna, M., Pogribny, I. P., Hine, R. J., & James, S. J. (2000). Increase in plasma homocysteine associated with parallel increases in plasma S-adenosylhomocysteine and lymphocyte DNA hypomethylation. *Journal of Biological Chemistry*, *275*(38), 29318–29323. https://doi.org/10.1074/jbc.M002725200

Yildiz, F. H., Davies, J. P., & Grossman, A. R. (1994). Characterization of Sulfate Transport in Chlamydomonas reinhardtii during Sulfur-Limited and Sulfur-Sufficient Growth. *Plant Physiology*, *104*(3), 981–987. https://doi.org/10.1104/pp.104.3.981

Yoon, H. S., Hackett, J. D., Ciniglia, C., Pinto, G., & Bhattacharya, D. (2004). A Molecular Timeline for the Origin of Photosynthetic Eukaryotes. *Molecular Biology and Evolution*, *21*(5), 809–818. https://doi.org/10.1093/molbev/msh075

Záhonová, K., Füssy, Z., Oborník, M., Eliáš, M., & Yurchenko, V. (2016). RuBisCO in Non-Photosynthetic Alga Euglena longa: Divergent Features, Transcriptomic Analysis and Regulation of Complex Formation. *PLOS ONE*, *11*(7), e0158790. https://doi.org/10.1371/journal.pone.0158790

Zelezniak, A., Andrejev, S., Ponomarova, O., Mende, D. R., Bork, P., & Patil, K. R. (2015). Metabolic dependencies drive species co-occurrence in diverse microbial communities. *Proceedings of the National Academy of Sciences*, *112*(20), 6449–6454. https://doi.org/10.1073/pnas.1421834112

Zhang, Y., Rodionov, D. A., Gelfand, M. S., & Gladyshev, V. N. (2009). Comparative genomic analyses of nickel, cobalt and vitamin B12 utilization. *BMC Genomics*, *10*(78), 1–26. https://doi.org/10.1186/1471-2164-10-78

Zhang, Z., Shrager, J., Jain, M., Chang, C.-W., Vallon, O., & Grossman, A. R. (2004). Insights into the survival of Chlamydomonas reinhardtii during sulfur starvation based on microarray analysis of gene expression. *Eukaryotic Cell*, *3*(5), 1331–1348. https://doi.org/10.1128/EC.3.5.1331-1348.2004

Zhou, H.-R., Zhang, F.-F., Ma, Z.-Y., Huang, H.-W., Jiang, L., Cai, T., … He, X.-J. (2013). Folate Polyglutamylation Is Involved in Chromatin Silencing by Maintaining Global DNA Methylation and Histone H3K9 Dimethylation in Arabidopsis C W. *The Plant Cell*, *25*, 2545–2559. https://doi.org/10.1105/tpc.113.114678

Zuelzer, W. W., & Ogden, F. N. (1946). Megaloblastic anemia in infancy. *American Journal of Diseases of Children*, *71*(3), 211. https://doi.org/10.1001/archpedi.1946.02020260002001

7. Appendices

7.1 Media

Media	**Volume/Mass**
TAP media	**1000ml (autoclaved)**
Beijernick salts	25ml
Tris-acetic acid	10ml
Phosphate solution	1ml
$CoCl_2$ ($1mgml^{-1}$)	1ml
EDTA-Na_2(25mM)	1ml
$(NH_4)_6Mo_7O_{24}$ (28.5uM)	1ml
Zn.EDTA	1ml
Mn.EDTA	1ml
Fe.EDTA	1ml
Cu.EDTA	1ml
HCl (glacial)	To pH 7.0
LB media	**1000ml (autoclaved)**
diH_2O	1000ml
Tryptone	10g
Yeast extract	5g
NaCl	5g
TY media	**1000ml (autoclaved)**
diH_2O	1000ml
Tryptone	5g
Yeast extract	3g
$CaCl_2.2H_2O$	0.875g
Tris minimal medium	**1000ml (autoclaved)**
Beijernick salts	25ml
Tris.Cl	20ml
Phosphate solution	1ml
CoCl2 ($1mgml^{-1}$)	1ml
EDTA-Na2(25mM)	1ml
$(NH_4)_6Mo_7O_{24}$ (28.5uM)	1ml
Zn.EDTA	1ml
Mn.EDTA	1ml

Fe.EDTA	1ml
Cu.EDTA	1ml
HCl (glacial)	To pH 7.0

2*M9 media	**250ml (Filter-sterilised)**
10*M9 salts	50ml
20% glucose	10ml
1M $MgSO_4$	1ml
L-cysteine (5mg/ml)	5ml
0.1M $CaCl_2$	0.5ml
H_2O	183.5ml

M9 agar	**250ml**
10 x M9 salts	25ml
20% glucose	5ml
1 M $MgSO_4$	0.5ml
0.1 M $CaCl_2$	0.25ml
L-cysteine (5 mg/ml)	2.5 ml (prepare fresh)
L-methionine (5 mg/ml)	2.5 ml
2% bacto-agar	214.25ml (autoclaved)

Beijernick salts	**1000ml (Autoclaved)**
diH_2O	1000ml
NH_4Cl	15g
$MgSO_4$.7H2O	4g
$CaCl_2$.2H_2O	2g

Tris.Cl	**1000ml (Autoclaved)**
diH_2O	900ml
Tris	121g
HCl (1M)	To pH 7.2
diH_2O	To 1000ml

Tris-acetic acid	**500ml (Autoclaved)**
diH_2O	450ml
Acetic acid (glacial)	50ml
Tris	121g

Phosphate solution	**100ml (Autoclaved)**
diH_2O	100ml

K_2HPO_4	28.8g
KH_2PO_4	14.4g

10*M9 salts	**500ml (Autoclaved)**
Na_2HPO_4-$7H_2O$	64g
KH_2PO_4	15g
NH_4Cl	5g
NaCl	2.5g
diH_2O	500ml

EDTA-NA_2 (125mM)	**250ml (Autoclaved)**
EDTA-NA_2	13.959g
diH2O	200ml, then titrate to pH 8.0 with KOH and bring volume to 250ml.

EDTA-NA_2 (25mM)	**250ml (Autoclaved)**
EDTA-NA_2 (125mM)	50ml
diH2O	200ml

$(NH_4)_6Mo_7O_{24}$ (28.5uM)	**250ml (Autoclaved)**
$(NH_4)_6Mo_7O_{24}$	8.8mg
diH_2O	250ml

Na_2SeO_3 (0.1mM)	**250ml (Autoclaved)**
Na_2SeO_3	4.3mg
diH_2O	250ml

Zn.EDTA	**250ml (Autoclaved)**
$ZnSO_4 \cdot 7H_2O$	0.18g
EDTA-NA_2 (125mM)	5.5ml
diH_2O	244.5ml

Mn.EDTA	**250ml (Autoclaved)**
$MnCl_2 \cdot 4H_2O$	0.297g
EDTA-NA_2 (125mM)	12ml
diH_2O	238ml

Fe.EDTA	**250ml (Autoclaved)**
$FeCl_3 \cdot 6H_2O$	1.35g (Add after fully dissolving EDTA-Na_2 and Na_2CO_3 in water)
EDTA-Na_2	2.05g
Na_2CO_3	0.58g

diH_2O	250ml

Cu.EDTA	**250ml (Autoclaved)**
$CuCl_2 \cdot 2H_2O$	85mg
EDTA-NA_2 (125mM)	4ml
diH_2O	244ml

7.2 qPCR primers

Gene name	**Primer Sequence**		**Product size/bp**
	Forward primer	**Reverse primer**	
ACTIN	AGAAGGACTCGTACGTTGGC	TGAAGAAGGTGTGGTGCCAG	129
APX1	GCTGCAACCCCATTTCTGTG	CCAGAGCAATAGCCAGACCC	156
BTA1	GGCTGGAAGAATGTCCAGGT	TTGGGACAGGTACGAGCAAG	150
CBA1	ATCCTCAACGTGCTGGACC	GCTGAAGCCCACGAACTTG	144
CYCA1	CCAGCCTTCCATTCCGCTT	CGAGTCCACGTCAATCCAGG	109
DMC1	ATAGTGTTCCGTTGCTGGCTG	AGCTCTGCCTCGTACTTAGC	101
DMT1	GCCTGCACTATAAGACGGGT	CTTCTCCGCGTCCACATACA	116
EEF1	GGGTGTCAGTTCCTTTTGCG	GACGATGGACAGATGCTCCT	122
FAP24	AATCCTCAACGTGCTGGAC	CGCTGAAGCCCACGAAC	146
FTL1	GGCTTCGTGGTGACAGAGG	CACGTTCTCGGTGGTGTAGT	198
GPX5	TGGCGAACCCCGAGTTTTAC	TTGCTAGCCACGTTCACGAT	109
GSTS1	TCATTCTCCCTACCGGCTGA	GGTTGGAGAGCGACACGTAA	184
H2B	TAAATGCGCTCAGAGGCTGG	ATCTACACTGGTTCCTCGCC	151
IFT25	CAGGACAAGCCAGACCAGTT	ACCGACACGCGGTTGAC	164
LHCA1	GCTACGGCAACTGGTACGAT	CATGGCAACGAACTCGAAGG	119
LHCA2	TACAAGAAGACCGGCGAGAC	GAGAGCAGAAGCCCAGGAAC	136
LHCBM1	TCCATGTTCGGCTTCTTCGT	AAACCGCTCAGACCTGCATC	184
METC	GGCTACTACGTGGACCTCATC	CAGCCCAAACCAGGCGTA	192
METE	CCGCTACAGCCAGACTTCA	GTGACAGCGACACGAACGT	118
METH	GGCGACGACTACAGCTACATC	CCCTGGTACTTGACCTTGAGC	158
METM	TCAAAGGTTGCCTGCGAGAC	GAAGCCAATCTCCTTGCACAC	123
MSD3	GGCTTACCACTGGCTTACGA	GACAATCTCCGACAGCGACA	156
MTHFD	GCGTGCGTATGCATCTTGAG	GCCCTTTCGTTTCCATGTCC	108
MTHFR	GTACATCAGGAAGCAGCACGG	TCCACGTCGTAAAACAGCTGC	189
PGK1	ACCTGAACGTGCCTCTTGAC	GTCAGGCGGTACTTGTCCTC	166
PRMT1	CTGGGACAATGTGTACGGCT	TGGTGCTGATGTCCACTGAC	134
RACK1	CGTCTGTGGGACCTGAACAC	GCTCGCCAATGGTGTACTTG	172
RLS1	GAAAGGCTCTTGGTCAAGCC	CGCTACATCATTGGCAACACC	196
RPL10A	GTGATGTGAAGCACTGCGAG	TTGATGACGGAGTCCGAAGC	148
SAH1	CGCACCATTGTGTCGGAGAT	ATGATGTCCTTGTTGCCGGT	134

SEBP1	TGGATGCACGTCAAGGAGAC	ATGATCTGGAACACGTCGGG	173
SET3	AGGTGTTCATGACGGAGAGC	GTGTGCGAAGAAGTCGAGGT	164
SHMT1	AGAACTTCGTGTCTGCCTCG	TCCAGGTGGAATGCCTTCAG	160
SHMT2	AGTACTCGGAGCAGGTTGTG	ACAGGATGAGGTGGTTGTCG	105
SHMT3	GTCGACCCGGAGATTAGTGC	CGACCCTCGGAGTACTTGTT	146
THIC	AAGGCGCGGTTTGAGTTCC	CACATGGAGCAGAAGTGGGC	128
TOC1	CGCACCCTTGCTTTTGGGTA	GCCGTCTATAATCCACAACGC	105
TUB1	CAAGGGCCACTACACCGAG	CAGAGAGTGGCAAACCTGGA	112
TYMS	ATGCACACCGACTACACAGG	GAACTGGCAGAACATGTGGC	159
UBQ	GAAACGGCCACAAGTTGGAC	CGCATATTTGCTGGGAACCG	136
VTC2	ACTGCTGTCTCTGCTGCTAAAG	ACTGAGACACGTCGTACCTGAA	139